Cryogenic Machining of Titanium Alloy

Shokrani Chaharsooghi, Alborz

Award date:
2014

Awarding institution:
University of Bath

Cryogenic Machining of Titanium Alloy

Alborz Shokrani Chaharsooghi

A thesis submitted for the degree of Doctor of Philosophy

University of Bath

Department of Mechanical Engineering

April 2014

Dedicated to my parents, Parvaneh and Mansour

Acknowledgements

There are a number of people without whom, this research would have not been possible and to whom I am deeply indebted.

First and foremost, I would like to express my sincerest gratitude to my 'Boss', Prof Stephen T Newman whom without his kind supports, professional supervision and friendship, I would not have been where I am now. I was fortunate to be introduced to Prof Newman at the University of Bath in 2009, who gave me an opportunity to follow my dreams through reality. He taught me not to settle for 'good enough' but to thrive for higher standards both in life and research.

I would also wish to extend my sincere appreciation to Dr Vimal Dhokia who walked me through the world of research and through his guidance, help and support this research has been completed.

I would also like express my appreciation to Prof Geoff McFarland and Mr Mark Buckingham of Renishaw Plc who trusted me on carrying out this research and provided me with financial and technical support throughout the research.

I would also like to extend my gratitude to various academics, industrialists and technicians who helped me during the experimental aspects of this research. This includes but is not limited to Prof Chris Bowen, Dr John Mitchels, Dr Pishi, Mr Darren Lingard, Mr Joseph Flynn, Mrs Clare Ball, Mr Andrew Green and Mr David Wood.

Last but not least, I owe my deepest gratitude to my mum and dad, Parvaneh and Mansour, who have always been by my side and supported me throughout the 23 years of my studies.

Abstract

Materials which are both lighter and stronger have faced an increased demand over the past decades to fulfil the requirements across a range of industrial applications. More specifically, demands for titanium alloys have increased significantly due to its high strength to weight ratio which is particularly attractive for increasing fuel efficiency in aircrafts and cars and is also used in biomedical implants.

Despite the increasing demand for titanium made products, machining titanium alloys remains a significant challenge. High material strength and hardness lead to excessive heat generation at the cutting zone which accumulates and results in high cutting temperatures due to the poor thermal conductivity. The high cutting temperatures together with inherent material properties of titanium are responsible for short tool life and poor surface finish. Despite the environmental and health drawbacks, a generous amount of cutting fluids is commonly used to control the cutting temperature in machining titanium alloys. However, conventional cutting fluids evaporate at high cutting temperatures which isolate the cutting zone by forming a vapour cushion resulting in further increases in cutting temperatures.

This research investigates the effects of cryogenic cooling on machinability of Ti-6Al-4V alloy in CNC milling as compared to conventional dry and wet machining environments. Two literature reviews were conducted and a methodology has been developed and implemented consisting of three experimental stages of i) design and manufacture of a cryogenic cooling system, ii) comparative study of cryogenic cooling with dry and wet machining and iii) optimisation of cutting parameters for cryogenic machining.

The major contribution of this research can be summarised as design, realisation and assessment of a novel cryogenic cooling system for CNC milling, termed cryogenic shower, which is retrofitable to an existing CNC machining centre. In addition, the research provides a thorough study on the effects of cryogenic cooling on machinability of Ti-6Al-4V alloy in comparison with dry and wet machining. The studies range from power consumption and tool wear through to surface topography and surface integrity. Furthermore, the optimum cutting parameters for cryogenic machining are identified.

The research demonstrates that using the cryogenic shower has significantly improved machinability of Ti-6Al-4V through realisation of higher material removal rates, reduced tool wear and improved surface finish, surface topography and surface integrity.

Contents list

List of Abbreviations

Abbreviation	Definition
2D	2 dimensional
3D	3 dimensional
AISI	American Iron and Steel Institute
ANOVA	Analysis of Variance
AWPC	Average White Pixel Concentration
BCBN	Binderless Cubic Boron Nitride
BEI	Backscatter Electron Image
BS	British Standard
BUE	Built Up Edge
C	Cryogenic
CAD	Computer Aided Design
CAE	Computer Aided Engineering
CAM	Computer Aided Manufacturing
CBN	Cubic Boron Nitride
CCD	Central composite design
CFD	Computational Fluid Dynamics
CLs	Coolant-Lubricants
CNC	Computer Numerical Control
CO2	Carbon Dioxide
Co-Cr	Cobal-Chromium
CoF	Coeficient of Friction
CVD	Chemical Vapor Deposition
D	Dry
DF	Degree of Freedom
DoE	Design of Experiment
EC/V	Energy consumption per unit volume of removed material
ECM	Electro-chemical Machining
EDM	Electro-discharge Machining
EDS	Energy-dispersive X-ray spectroscopy
EDS	Energy-dispersive X-ray spectroscopy
EDX	Energy-dispersive X-ray
EVA	Ethylene-vinyl acetate
Exp	Experiment
FCCCD	Face Centred Central Composite Design
FEA	Finite Element Analysis
FEM	Finite Element Method
HDPE	High-density polyethylene
HRC	Hardness Rockwell C
HSE	Health and Safety Executive
HSS	High Speed Steel
IBM	Ion Beam Machining
ID	Identification
IDEF	Integrated Definition

IGES	Initial Graphics Exchange Specification
ISO	International Organization for Standardization
K	Kelvin
LBM	Laser Beam Machining
LCO_2	Liquid Carbon Dioxide
lf	Load force
Lhe	Liquid Helium
LN_2	Liquid Nitrogen
LSC	Large secondary carbide
MDF	Medium Density Fibreboard
MQL	Minimum Quantity Lubricant
MS	Mean Square
N_2	Nitrogen
NiTiNOL	Nickel Titanium Naval Ordnance Laboratory
No.	Number
PA	Polyamide
PC	Primary Carbides
PC/V	Power consumption per unit volume of removed material
PCBN	Polycrystalline Cubic Boron Nitride
PCD	Polycrystalline Diamond
PDMS	Poly-dimethyl-siloxane
PMMA	Polymethyl methacrylate
PTFE	Polytetrafluoroethylene
PVD	Physical Vapor Deposition
R^2	Coeficient of determination
Ra	Arithmetic surface roughness
RBSN	Reaction Bonded Silicon Nitride
Rq	root-mean-square deviation surface roughness
RSM	Response Surface Method
Rz	ten point height of irregularity surface roughness
SA	Simulated Annealing
SCD	Single Crystal Diamond
SEI	Scanning Electron Image
SEM	Scanning Electron Microscope
SN	Signal to Noise
SS	Sum of Squares
SSC	Small secondary carbide
TiAlN	Titanium Aluminium Nitride
UHMW	Ultra-high molecular polyethylene
VH	Vickers Hardness
W	Wet
WATCH	The Working Group on Action to Control Chemicals
WC	Tungsten Carbide

List of Figures

List of tables

Chapter 1

Introduction

Material cutting is one of the dominant parts of shaping materials into the final product. Machining operations, such as milling, turning and drilling, present a major proportion of material cutting operations. In machining operations, a cutting tool is used to remove material from a workpiece in the form of cutting chips by plastic deformation. This process consists of mechanical and thermal forces being induced into both cutting tool and workpiece. Some of the advanced materials, such as titanium and nickel alloys, possess high cutting forces and temperature during machining operations which have resulted in them being generally termed difficult-to-machine materials, as opposed to easy-to-machine materials such as aluminium alloys and medium carbon steels.

It is well recognised that using cutting fluids is one of the most common methods to regulate the cutting temperature by removing excessive heat generated during machining operations. In addition, cutting fluids can lubricate the cutting zone and reduce friction. As a result, lower mechanical stress will be induced on the cutting tool and the heat generated due to friction will be reduced. However, cutting fluids, also known as metal cutting fluids, are known to be dangerous substances for both the environment and human health. This has resulted in overgrowing concerns and generation of different government rules regulating the use, maintenance and disposal of cutting fluids.

A report by HSE WATCH committee (2007) identified a priority to the health issues as a result of respiratory exposure to cutting fluids and raised concerns with regards to the heavy contamination of cutting fluids with bacteria, endotoxin and other allergens. It has been estimated that more than 50,000 shop floor workers in the UK and 1,200,000 workers in the USA are exposed to cutting fluids that are prone to occupational respiratory and skin disease (WATCH-Commitee, 2007, Mirer, 2010, Meza et al., 2013).

Since using cutting fluids is generally considered to be a beneficial technique for improving machinability, there are, on the contrary, evidence to suggest it cannot be extended to machining advanced materials. There are reports (Astakhov, 2006) stating that at high cutting temperatures in machining advanced alloys such as titanium and nickel alloys, cutting fluids evaporate in contact with hot surfaces. The vaporised cutting fluid forms a hot vapour cushion around the hot surfaces and isolates the cutting zone. Thus, the generated heat accumulates at the cutting zone resulting in further increases in the cutting temperature (Astakhov, 2006). This generated heat is expected to be dissipated through the workpiece, cutting chips and cutting tool. However, some advanced materials such as

nickel, titanium and cobalt-chromium alloys possess relatively poor heat conductivity. Therefore, the generated heat cannot be dissipated effectively through the workpiece and cutting chips. High cutting temperatures weaken the cutting tool material and result in short tool life and poor surface finish. In addition, high temperatures facilitate chemical reaction between the tool material and workpiece resulting in diffusion, smearing, welding and galling (Hong et al., 2001). A report (Kara, 2009) estimated that more than 94,500,000 cutting tools are used in the UK annually and since domestic production cannot meet the demand, there is a potentially large saving which could be made through improved tool life.

Using liquefied gases (e.g. liquid nitrogen and carbon dioxide) as a coolant is a technique to control the cutting temperature. This technique is termed cryogenic machining and has attracted significant attention from researchers globally (Yildiz and Nalbant, 2008). In this method, a super cold liquid gas is used to freeze the workpiece material and/or cutting tool in order to modify their material properties and control the cutting temperature. There are a number of reports on the effects of cryogenic cooling on machinability of different materials (Yildiz and Nalbant, 2008). Since different materials react differently at low temperatures, different approaches are required for different materials and machining operations.

Advanced materials, arguably, have always been one of the key factors for advances in technology. For instance, aerospace engines require materials which can withstand higher temperatures, are stronger and weigh less. Biomedical implants, on the other hand, need materials which are stiffer, more wear resistant and biocompatible. Such advanced materials are inherently more difficult to manufacturer due to their specific material properties.

Titanium and its alloys is one of the most attractive materials across different industries due to its high strength to weight ratio. The demand for titanium has increased by an 87% from 2005 to 2010 (Seong et al., 2009) and is expected to grow by 4.6% per year through to 2018 (Roskill, 2013). Whilst aerospace industries account for almost 50% of the global consumption of titanium metal, the demand for titanium is increasing significantly across other industries such as medical, chemical processes, sporting goods, jewellery and architecture. In medical industries alone, it is believed that more than 1000 tonnes of titanium alloys are used for medical implants annually.

The Ti-6Al-4V titanium alloy is one of the most used titanium alloys. It has been reported that Ti-6Al-4V forms more than 50% of the titanium alloys used globally where more than 80% of it is used in medical and aerospace industries (Boyer et al., 1994). Whilst the annual production of titanium has increased significantly in recent years (Roskill, 2013), the machining of titanium and particularly Ti-6Al-4V has remained the bottleneck in manufacturing of titanium products. Therefore, this research is focused on cryogenic CNC milling of Ti-6Al-4V alloy.

The organisation of the chapters presented in this thesis is such that initially, two sets of literature review have been conducted. As shown in figure 1.1, these chapters form the second and third chapters of this thesis. The aim of the first review in chapter 2 is to identify different difficult-to-machine materials and the material properties which have made them difficult to cut. In addition, different cutting fluids and the problems associated with their usage in machining operations are reviewed. Based on this section, it has been found that using conventional coolants is neither economical nor environmentally friendly. Thus different techniques to eliminate or reduce the use of cutting fluids in machining have been also reviewed.

The second review, presented in chapter 3 is an overview of different studies on using cryogenic cooling in material cutting operations. The use of cryogenic cooling in material cutting is divided into two main sections, namely cryogenic processing and cryogenic cooling. The effect of cryogenic processing on the material properties and tool life of different tool materials has also been reviewed as part of chapter 3. In addition, the techniques used by other researchers for cryogenic cooling during material cutting operations and their effect on the machinability of different tool-workpiece materials, has been studied thoroughly. Furthermore, the research gaps in cryogenic processing and machining have been identified based on workpiece materials and machining operations. This research gaps have been presented to the funding body of this research and end milling of Ti-6Al-4V titanium alloy using solid carbide tools has been selected as the major focus of this research.

Based on the findings from the literature, scope of the research, aims and objectives have been identified and are presented in chapter 4. The methodology which has been used to achieve the aim and objectives of this research is detailed in chapter 5. In the experimental phase of this research, the procedure of designing, making and developing a cryogenic

cooling system for end milling operations is envisaged in chapter 6. Following the methodology, a set of machining experiments has been designed and conducted in order to identify the effects of cryogenic cooling as compared to traditional dry and wet machining. This has been presented in chapter 7 as shown in figure 1.1. The collected data in chapter 7 has been used to design and conduct a set of machining experiments to enable the optimisation of cutting parameters for cryogenic end milling of Ti-6Al-4V alloy which is provided in chapter 8. The experimental and analytical activities conducted for this research are critically discussed in chapter 9. Chapter 10 concludes this research and identifies the research areas for further investigation.

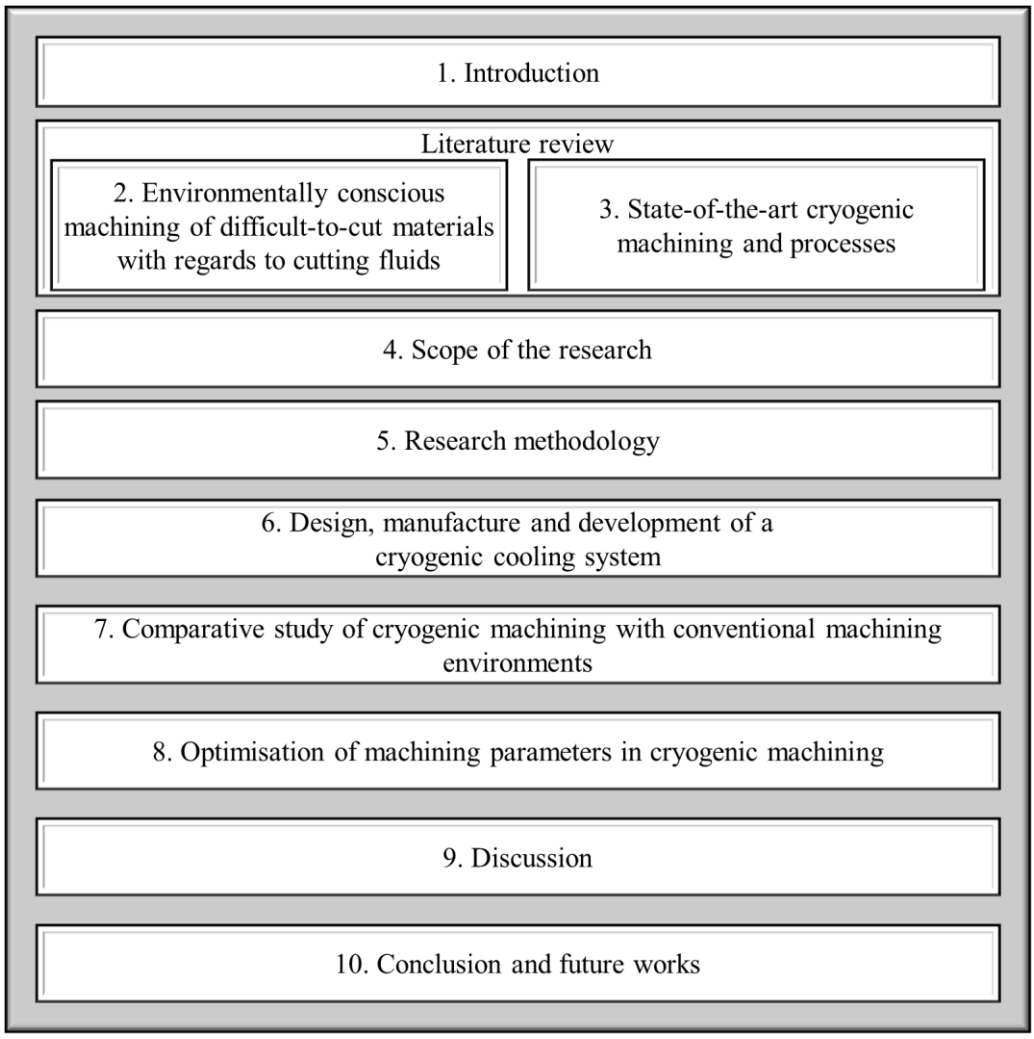

Figure 1.1 Structure of the thesis chapters

Note: Renishaw Plc is the funding body of this research and is referred to as 'the funding body of this research' throughout this thesis.

Note: The companies and product names mentioned in this thesis are trademarks or registered trademarks of various companies.

Chapter 2*

Environmentally conscious machining of difficult-to-machine materials with regards to cutting fluids

*This chapter is an updated version of Shokrani et al., 2012b

2.1. Introduction

Material cutting also known as machining is one of the most used techniques for producing different components. In machining processes a cutting tool removes material from a workpiece of a less resistant material. The removed material called chip or swarf slides on the tool face and leaves the workpiece material. As a result of this process the cutting tool would be subjected to high normal and shear stresses (Aggarwal et al., 2008). Figure 2.1 shows a schematic view of a typical cutting operation also known as the single shear plane model. Although from the modelling point of view this model is a matter of debate and suffers from a lack of accuracy (Astakhov, 2006) it provides sufficient information required for this study. As shown in figure 2.1, the chip formation is categorised into two zones, namely primary and secondary shear zones. In the primary shear zone, the material is being cut by elasto-plastic deformation. The majority of the energy used for cutting in this section is transformed into heat. At the secondary shear zone the produced chip slides on the rake face of the cutting tool resulting in high frictional force and heat. In addition to these zones, sliding of the tool flank face on the machined surface at the tertiary deformation zone generates friction and heat and could cause flank wear on the flank face (Childs et al., 2000, Abukhshim et al., 2006). Furthermore, friction and heat on the rake face could result in chipping and crater wear leading to tool failure.

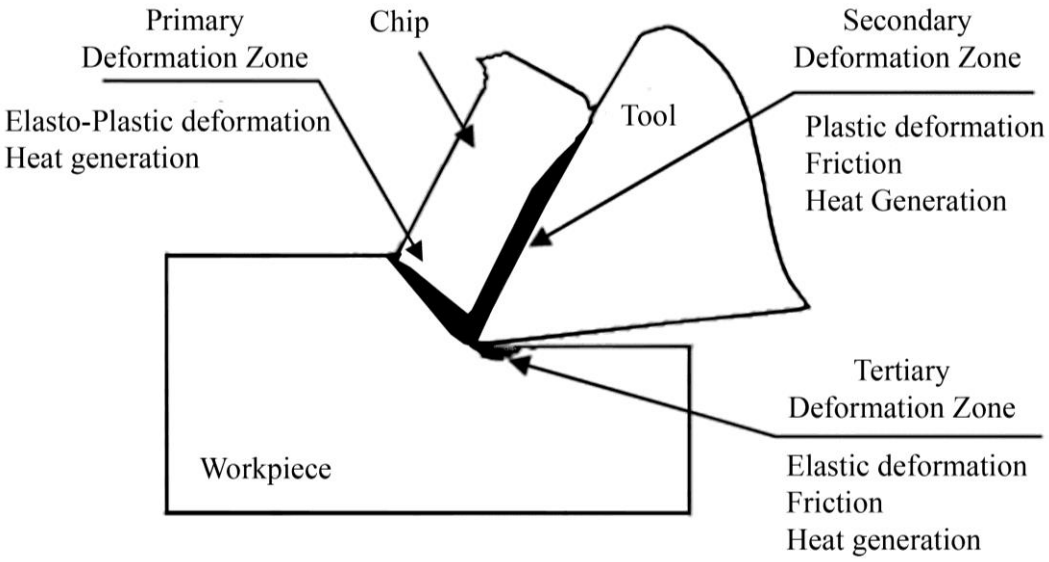

Figure 2.1 Schematic view of the cutting zone and chip formation (Abukhshim et al., 2006)

Machining advanced engineering materials is usually associated with high machining costs and low productivity. This is due to the excessive generation of heat at the cutting zone and difficulties in heat dissipation due to relatively low heat conductivity of these materials. High material hardness and strength together with high temperatures at the cutting zone could result in excessive tool wear and thus short tool life and poor surface quality. Most components produced from advanced materials such as titanium and nickel based alloys have high buy-to-fly ratio as most of them are made to be used in aerospace, engine and gas turbine industries (Sun et al., 2010).

2.2. Difficult-to-machine material

Titanium and nickel based alloys are readily regarded as difficult-to-machine or hard-to-cut materials. Commonly, wider categories of materials defined as difficult-to-machine are super-alloys and refractory metals which are consisted of titanium, nickel, steel, molybdenum, rhenium, tungsten, cobalt, tantalum, niobium, chromium, etc. alloys (Olofson, 1961). However, materials which are hard to machine are not limited to these alloys and also consist of structural ceramics, composites, polymers and magnesium alloys.

Difficult-to-machine materials are referred to the materials which during machining operations produce excessive tool wear, heat and/or cutting forces, difficulties in chip formation and/or poor surface quality. One of the important phenomena in machining difficult-to-machine materials is excessive generation of heat at the cutting zone resulting in very high cutting temperature. In this section hard-to-cut materials are reviewed and their characteristics, which make them difficult to machine are identified.

2.2.1. Titanium alloys

Titanium is the fourth most abundant structural metal in the earth's crust (Choragudi et al., 2010). While pure titanium is soft and does not have significant mechanical properties, alloyed titanium exhibits mechanical and thermal characteristics close to that of nickel alloys. Moreover, the density of titanium is half of nickel and closer to that of aluminium with considerably higher fatigue resistance (Jaffery and Mativenga, 2008).

Titanium and its alloys are attractive materials in many engineering fields such as aerospace, vehicles, engines and gas turbines, nuclear, biomedical, etc. This is mainly due to their superior mechanical and physical properties such as: high strength to weight ratio, high yield stress, very high creep and corrosion resistivity, high toughness, high wear

resistance and good biocompatibility (Ulutan and Ozel, 2011, Choragudi et al., 2010, Ohkubo et al., 2006, Watanabe et al., 2000). In addition, titanium alloys are low dense materials which maintain their hardness and strength at very high temperatures. Titanium poses the highest strength to weight ratio between all common metals up to 550˚C (Pittalà and Monno, 2011). However, its application is limited to 400˚C as it can ignite and cause serious problems during operation (Jaffery and Mativenga, 2008). These properties in conjunction with high chemical reactivity, low thermal conductivity, high specific heat and high strain hardening (work hardening) have made machining of titanium alloys extremely difficult, which is often associated with low productivity and very short tool life (Zhang et al., 2009, Jaffery and Mativenga, 2008). It has been reported that economical machining of titanium alloys is limited to 30 m/min and 60 m/min using High Speed Steel (HSS) and tungsten carbide tools respectively due to high tool wear (Rahman et al., 2003b, Komanduri and Von Turkovich, 1981). In machining titanium alloys, due to low thermal conductivity of the material the generated heat during machining cannot be conducted through the workpiece and chips effectively. Hence the generated heat should be dissipated through the cutting tool and cooling media. Conventional coolants fail to penetrate into the cutting zone as they are vaporised before reaching the tool-chip contact area. This could result in very high localised temperature at the cutting zone and thermal stress at the cutting edge (Abele and Fröhlich, 2008, Paul and Chattopadhyay, 2006). As titanium alloys maintain their strength even at very high temperatures, increases in the cutting temperature is not beneficiary for machining these materials where the cutting tools suffer from heat softening.

Titanium is also chemically reactive to all known cutting tool materials. This reactivity increases at elevated temperatures, resulting in adhesion and diffusion wear accompanied with formation of BUE, smearing, chipping and galling (Paul and Chattopadhyay, 2006, Abele and Fröhlich, 2008, Ghani et al., 2013). While cutting forces in machining titanium alloys is comparable with that of steels, very high pressure on the cutting edge is contributed as an inherent characteristic of machining titanium. This is attributed to very small tool-chip contact area close to the cutting edge rather than high cutting forces (Choragudi et al., 2010, Dearnley and Grearson, 1986). This high localised mechanical stress together with thermal stress induced from rubbing the chips on the chip-tool contact area lead to crater wear on the tool rake face adjacent to the cutting edge. The presence of

the crater wear has the potential to weaken the cutting edge and result in catastrophic tool failure.

Titanium machining is characterised by the production of serrated or saw-tooth chips. This is attributed to the localised adiabatic shear bending at the primary shear zone where the material suffers from an intense shear rate. It is due to the high dynamic shear strength of titanium and high chip-tool interface temperature. Formation of serrated chips results in machining instability, force fluctuations and thus chatter which can lead to chipping on the cutting edge (Pittalà and Monno, 2011, Ezugwu et al., 2003, Paul and Chattopadhyay, 2006, Ginting and Nouari, 2006).

Properties which have made titanium alloys hard to machine could be summarised as follows (Jaffery and Mativenga, 2008, Ezugwu, 2005, Ezugwu et al., 2003, Choragudi et al., 2010, Donachie, 2000, Nath et al., 2014, Ghani et al., 2013):

- Low thermal conductivity and high thermal capacity
- High chemical reactivity with all known tool materials
- High strain hardening due to their austenitic matrix
- Low elastic modulus; workpiece deflection due to cutting forces causing chatter and vibration
- Springing and chatter
- Small tool chip contact area
- Tendency to adhesion and forming BUE
- High dynamic shear strength

2.2.2. Nickel based alloys

The advantages of nickel-based alloys over titanium alloys have made them another attractive material for aerospace, gas turbine and nuclear industries. Nickel based alloys have very broad operational temperature which makes them more attractive than titanium alloys at extreme temperatures. For example nickel alloy Inconel® 718 has high fatigue endurance up to 700˚C (Alauddin et al., 1996, Wang et al., 2003) while Udimet® 720 nickel-based alloy has a service temperature of up to 982˚C for long exposure times (Truesdale and Shin, 2009). Nickel exhibits superior hot strength and hardness and is very temperature resistance. It maintains its chemical and mechanical properties at elevated temperatures and is highly resistant to creep and corrosion (Khidhir and Mohamed, 2011). Other unique properties of Ni-based alloys can be defined as: high thermal fatigue

resistivity, high erosion resistivity, resistance to thermal shock and high melting temperature (Ulutan and Ozel, 2011, Ezugwu et al., 2003, Alauddin et al., 1998). It has been reported (Miller, 1996) that 50% of the materials used in aerospace industries are nickel based alloys.

Due to the high strength of nickel alloys, very high temperatures and forces are produced during cutting operations. As nickel has a very low heat conductivity, the generated heat cannot be effectively dispersed through the workpiece and chips. Conventional cutting fluids cannot penetrate the chip-tool interface and reach the highest temperature zone especially at high cutting speeds. They tend to evaporate at high temperatures and form a high temperature blanket over the cutting zone which results in further increase in the temperature (Sun et al., 2010).

Drastic increases in the cutting temperature lead to excessive tool wear and low surface quality of the machined part. In addition, the hardness of the nickel alloys increases with increases in the temperature below 650˚C. This is due to the presence of γ′ participates in the material which is also responsible for the material work hardening. For instance, the hardness of Inconel® 718 increases by temperature up to 650˚C as shown in figure 2.2 (Liao et al., 2008). Thus, increases in the cutting temperature under 650˚C do not help to soften the material and improve machinability. Furthermore, nickel is chemically reactive to most cutting tool materials.

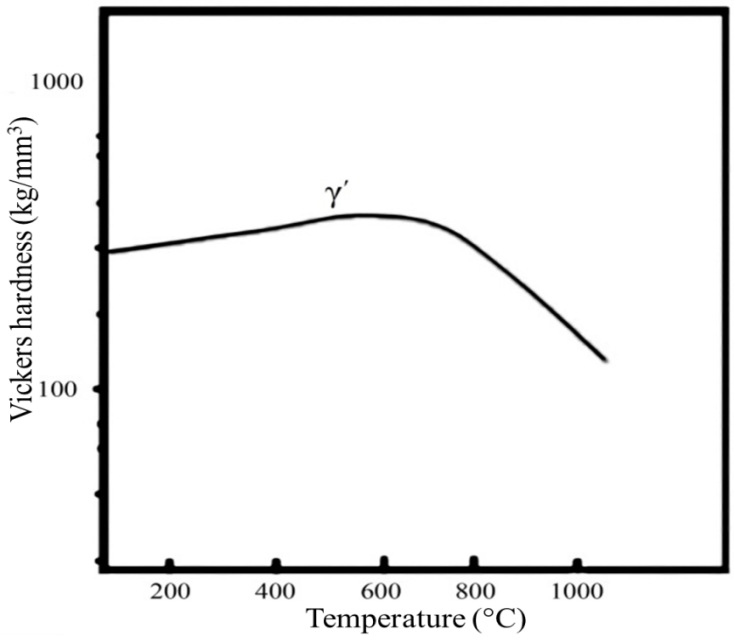

Figure 2.2 Relation between temperature and Vickers hardness of Inconel® 718 (Liao et al., 2008)

High temperature at the cutting edge together with increased chemical reactivity at elevated temperatures results in very low tool life. Attrition and crater wear on the rake face and flank wear are the dominant tool failure modes in machining nickel based alloys. Diffusion, adhesion and formation of BUE on the rake face cause attrition (notching), alteration and crater wear while abrasion is dominant on the rake face. Abrasion wear is mainly attributed to the presence of super hard carbide particles such as TiC, CrC, MoC, NbC, FeC, WC, MC, $M_{23}C_6$, etc. in the microstructure of the material (Kaya et al., 2011, Devillez et al., 2007, Krain et al., 2007, Sharman et al., 2001, Ezugwu et al., 2003).

The high temperature produced during machining not only shortens tool life and reduces the surface quality but could also alter the microstructure of the material and induce residual stress, micro cracks and micro-hardness variations through the formation of white layer. These machining induced problems are identified as affecting the service life of the machined component and particularly its fatigue resistivity (Dudzinski, 2004).

Another machining induced problem in cutting nickel based alloys is subsurface metallurgical damage due to the work hardening tendency of the material as a response to the cutting forces (Sharman et al., 2001). Hence, machining nickel based alloys traditionally is associated with low cutting speeds, poor surface and subsurface quality, short tool life and thus high machining costs (Leshock and Kim, 2001). Krain et al. (2007) studied the effects of cutting parameters in end milling Inconel® 718 nickel alloy. They found that adhesion and attrition were the dominant tool wear mechanisms resulting in the formation of BUE and notching. It is attributed to the high temperature and pressure at the cutting zone and chemical affinity of the workpiece material to the WC tool. Umbrello (2013) studied the effects of cutting speed and feed rate in dry machining on surface integrity of Inconel® 718 and concluded that at high cutting speeds and low feed rates, good surface finish comparable to grinding can be achieved.

The properties responsible for making nickel based alloys difficult to machine have been classified by the author and summarised based on a number of references (Ezugwu et al., 2003, Alauddin et al., 1998, Dudzinski, 2004, Machado et al., 1998, Wang et al., 2003, Umbrello, 2013) as:

- High shear strength
- High hot strength and hardness
- High strain hardening

- Low thermal conductivity and high heat capacity result in high temperature at cutting zone up to 1200˚C
- High chemical reactivity to most tool materials
- Adhesion and Welding tendency to the cutting tool and formation of BUE
- Very high cutting forces due to the material strength which may result in vibration
- Presence of hard carbide particles in the microstructure which encourage abrasive wear
- Small tool-chip contact area result in high thermal and mechanical stress close to the cutting edge
- Production of long continuous chips which exacerbates the machined surface chip disposal and hinders the machining in unmanned operations.

2.2.3. Difficult-to-machine ferrous alloys

Iron based difficult-to-machine materials have been classified by the author into three categories, low-carbon ductile steels, stainless steels and hardened steels. While in general the machining of steels is considered easy to moderate, some steel alloys exhibit characteristics which make them difficult to machine.

i) Low-carbon ductile steels: The major problem in machining ductile low carbon steel materials such as AISI 1008 steel is chip formation. Production of long continuous curled chips can scratch the machined surface, jam the automatic machine tool and cause unnecessary machine down time. In addition, low carbon steels tend to adhere and produce BUE on the cutting tool which may affect the cutting forces, tool life and surface finish of the machined part (Hong et al., 1999). While conventional cutting fluids are extremely effective in extending tool life and preventing adhesion in machining low-carbon steels, they cannot help chip formation. In addition, cutting fluids are considered as health and environmentally hazardous substances and using them in machining operations should be minimised. In order to improve the chip breakability, employing chip breaker mechanisms and cutting tools with integrated chip breakers is widely accepted. However, in machining ductile materials, the effect of chip breakers is limited to the increased plastic deformation at the second shear zone and cannot actually break the chips. As most steel materials are highly temperature dependant, Hong et al. (Hong et al., 1999) suggested using cryogenic coolant to freeze the chips in machining AISI 1008 low carbon steel. At cryogenic

temperatures the material transforms to a brittle state and resulting in enhanced chip breakability.

ii) Stainless steels: Another very difficult to cut material is stainless steel which is widely used in chemical, aerospace, automotive and food processing industries. This is due to high strength, high fracture toughness, high fatigue and corrosion resistivity as compared to plain carbon steels. Low thermal conductivity together with high strength and high heat capacity has made stainless steel a difficult-to-machine material. High material strength requires high cutting energy resulting in high heat generation during machining. Similar to titanium and nickel alloys, in machining stainless steels the generated heat cannot effectively be transferred into the workpiece and chips due to low thermal conductivity of the material. Thus, the generated heat during machining operation is concentrated at the cutting zone and produce high cutting zone temperatures. High temperatures at the cutting zone increase the thermally induced tool wear such as diffusion and chemical reaction between the tool and workpiece materials. In addition, stainless steels tend to adhere to the cutting tools and form BUE. This increases the machining instability and thus chipping on the cutting edge. The work hardening capability of stainless steel together with its mentioned mechanical and thermal properties results in severe tool wear and low surface quality of the machined surface (Nalbant and Yildiz, 2011, Endrino et al., 2006, Korkut et al., 2004, Fernández-Abia et al., 2011, Paro et al., 2001, Dolinšek, 2003, Naves et al., 2013). Generally the difficulties in machining stainless steel are attributed to low thermal conductivity, work hardening and poor chip breakability, which characterise the machining of stainless steels together with short tool life and poor surface quality, resulting in low productivity and high machining costs.

iii) Hardened steels: The third category of difficult-to-machine ferrous alloys is hardened steels. The term hard-machining and particularly hard-turning is referred to the machining (typically milling and turning) of steels with hardness beyond 45HRC (Thiele and Melkote, 1999). This technique is introduced as an alternative to the expensive and low productive grinding operations of heat treated steel components which can contribute up to 90% of the final cost of a machined part. Hard machining eliminates the requirements for grinding and second heat treatment, hence reducing the manufacturing cost. Hard-machining owes its existence to advances in machining operation and cutting tool materials such as ceramics with high hot hardness, toughness and chemical stability which have

made machining hardened steels possible (Rech and Moisan, 2003, Dogra et al., 2010). Tool failure modes in hard machining are (Grzesik and Zalisz, 2008, Ghosh et al., 2003):

- Superficial plastic deformation of the cutting edge due to high workpiece hardness;
- Dissolution/diffusion between tool and workpiece materials due to high cutting temperatures attributed to high cutting energy requirements;
- Formation of BUE due to high temperatures and chemical welding tendency of ferrous materials
- Non-uniform flank wear result in unpredictable catastrophic tool failure

2.2.4. Other materials

In addition to titanium, nickel and ferrous alloys, there are some other materials which are classified as difficult-to-machine materials. Structural ceramics, tantalum, elastomeric materials, composites, etc. are also known as difficult-to-machine due to exhibition of one or more following properties:

- High hardness
- High strength
- Ductility
- Toughness
- Low thermal conductivity

These characteristics can result in poor machinability of the material. If any combination of the following characteristics exists in machining a material, it will be considered as a difficult to machine material:

- Short tool life
- Poor surface quality
- Poor geometrical accuracy
- Poor chip formation

Due to the extremely difficult machining of some of these materials and specific application of them, there are very limited studies on the machining of most of these materials. For instance components made of NITINOL® nickel-titanium alloy, Stellite® and Vitallium® Co-Cr alloys, molybdenum alloys and tungsten alloys are usually manufactured by casting and sintering techniques or machined by non-traditional

techniques such as electro-discharge machining (EDM), electro-chemical machining (ECM), laser beam machining (LBM) or ion beam machining (IBM), etc. (Jia et al., 2010).

I. Composites

Machining composites is usually different to homogeneous materials due to their inhomogeneous and anisotropic nature. This is attributed to the presence of usually tough and flexible reinforcement fibres in a brittle matrix (Tsao and Hocheng, 2004, Lasri et al., 2011). It has been reported (Koplev et al., 1983, Davim, 2013) that cutting mechanisms and chip formation in machining composites consist of a series of material fractures. This cutting condition can result in sever surface quality issues such as delamination, burning, fibre pull-out, uncut fibres, high surface roughness and high dimensional deviation (Bhattacharyya and Horrigan, 1998).

Difficult-to-machine composites are not limited to the synthetic fibre/matrix materials and also cover metal matrix composites such as 356Al/SiC particulate metal matrix composite (Lin et al., 2001). These new engineered materials usually have a metal matrix of aluminium, titanium or magnesium reinforced with silicon carbide or alumina. The presence of hard abrasive particulates such as SiC or Al_2O_3, which are harder than WC tools can cause severe tool wear (Davim, 2002, El-Gallab and Sklad, 1998). It is clear that machining these composites involves problems associated with their matrix material together with other enhanced properties as an advantage of their particulates, such as higher strength, higher abrasion resistance, higher toughness, etc.

II. Ceramics

Advanced engineering structural ceramics such as reaction bonded silicon nitride (RBSN) is another attractive engineering material due to its comprehensive properties. It has high hot strength, even at 1400˚C, high thermal shock resistivity, low thermal expansion and is considered as an inert material (Wang et al., 1996). High strength together with poor thermal conductivity of the material can result in high temperatures at the cutting zone.

Due to very high hot hardness of the RBSN, the generated heat cannot help soften the material and subsequently cannot improve its machinability. Thus, generated heat at the cutting zone results in tool material softening and plastic deformation of the edge. To machine RBSN the cutting tool should be highly wear resistant, tough and thermally stable. RBSN is more wear resistant than conventional cutting tool materials such as HSS,

tungsten carbide and even ceramics. Thus, the only appropriate tool material to machine RBSN is made of diamond or polycrystalline boron nitride (PCBN). However, diamond is not thermally stable and transforms to graphite at elevated temperatures (Wang et al., 1996). Thus, Wang et al. (1996) suggested that the most appropriate cutting tool material for machining RBSN is PCBN due to its high toughness, hot hardness, wear resistivity and thermal stability.

III. Elastomers

Elastomeric materials such as polymers and rubbers are another difficult-to-machine group of materials but are significantly different in nature in terms of machinability compared to previously discussed materials. The elastomeric components are usually produced by injection moulding and not manufactured by cutting processes. They have a very low elastic modulus accompanied with a high percentage of elongation before fracture which results in elastic deformation against the cutting forces, hence preventing the cutting tool from machining the material. Low thermal conductivity results in high temperatures at the cutting edge where the material tends to adhere to the cutting tool. Unlike previously stated materials, adhesion in machining elastomers does not affect the tool life but it exacerbates the cutting operation and the surface finish. These properties together with high energy absorption capacity and low stiffness have made these materials hard or even impossible to machine in conventional environmental conditions (Shih et al., 2004a, Shih et al., 2004b, Mishima et al., 2010, Kakinuma et al., 2008, Dhokia et al., 2011). In addition, traditional machining techniques cannot assure the surface quality and geometrical accuracy of the components and the results are usually not comparable with injection moulded parts.

IV. Magnesium alloys

Magnesium, cobalt-chromium, titanium, nickel alloys and stainless steels are the most used materials for medical implants. While machinability of stainless steels, titanium and nickel alloys were reviewed in the previous sections, this section is focused on the machinability of the magnesium and cobalt-chromium alloys, although there are very limited studies on the machining of these materials.

Magnesium is known as the lightest structural metal with high strength-to-weight ratio and corrosion resistance (Chen and Alpas, 2000). Due to its low density, good ductility, cast-ability, damping behaviour etc. magnesium is very attractive to aerospace and automobile

industries (Froes et al., 1998). In addition, it has been reported (Denkena et al., 2005, Witte et al., 2005, Staiger et al., 2006) that magnesium has the potential to be employed as bio-degradable temporary implants.

Due to low cutting forces, good surface finish, well-formed chips and long tool life, magnesium is considered as one of the easiest structural materials to machine (Denkena et al., 2005, Gariboldi, 2003). Magnesium is a highly inflammable material and the risk of ignition increases when temperatures exceed above 450°C, close to the material's melting point (650°C) (Weinert et al., 2004). Magnesium is able to burn in different atmospheres such as nitrogen, carbon dioxide and water even in the absence of oxygen. As a result controlling the cutting temperature is extremely crucial during machining in order to prevent ignition.

The presence of inflammable magnesium chips close to the machining zone further increase the fire hazards on the shop floor (Weinert et al., 2004). Weinert et al. (2004) noted that removing the chips from the workspace of the machine tool during the cutting operation is very important. As the chips contain up to 90% of the heat generated at the cutting zone, fast and reliable removal of the chips can significantly reduce the risk of fire and potential damages to the workpiece as well as the machine tool.

Using cutting fluids in order to control the temperature at the cutting zone is limited to neutral mineral oils as magnesium reacts with water-based cutting fluids and produces highly explosive hydrogen gas (Denkena et al., 2005, Polmear, 1994). Therefore, machining magnesium alloys is usually conducted under dry conditions (Polmear, 1994). This can result in limited productivity as the cutting temperature has to be controlled through precise selection of the cutting parameters e.g. cutting speed and feed rates. Another problem in dry cutting of magnesium alloys is the formation of BUE on the tool which results in an increase in the cutting forces and poor surface finish (Gariboldi, 2003).

V. Cobalt chromium alloys

Another type of alloy which is considered extremely difficult to machine is Cobalt-Chromium alloys such as Stellite and Vitallium. The main material properties of these alloys are high strength, high hardness, high biocompatibility, high creep resistance and high corrosion and wear resistance superior to that of titanium based alloys (Song et al., 2010, Bagci and Aykut, 2006, Ohmori et al., 2006). These properties have made them

appropriate candidates for medical implants, aero-engine, nuclear and gas turbine components (Aykut et al., 2007). Similar to other refractory metal alloys, machinability of cobalt-chromium alloys suffers from work hardening and poor thermal conductivity of the material, resulting in low tool life and poor surface quality (Song et al., 2010). Due to the poor machinability of the Co-Cr alloys, most components made of these alloys are produced by different casting, sintering or unconventional machining techniques such as EDM, LBM, etc. (Jia et al., 2010). This has led to low productivity and high manufacturing costs of the Co-Cr alloy components and especially medical implants such as hip and dental implants.

2.2.5. Cutting tool materials in machining difficult-to-machine materials

It has been mentioned that the main problems in machining difficult-to-cut materials are very high temperature at the cutting zone, presence of abrasive carbide particles, chemical reactivity between the tool and workpiece materials and high hot strength and hardness of the workpiece materials. Thus, the required properties of the desired cutting tool have been recognised by a number of references (Dudzinski, 2004, Ezugwu, 2005, Rahman et al., 2003b) as:

- High hot hardness
- High strength and toughness
- High chemical and thermal stability
- High wear resistance
- High thermal shock resistance
- High thermal conductivity to reduce the thermal gradient
- High compressive tensile and shear stress

The effect of temperature in machining has been known for several decades. A major portion of the machining energy transforms into heat at the cutting zone (Astakhov, 2006). The generated heat at the cutting zone can soften the workpiece materials and result in lower cutting forces and longer tool life. However, in machining difficult-to-machine materials the cutting temperature plays a critical role as it is much higher than that of carbon steels. The generated heat in machining difficult-to-cut materials may not only soften the workpiece material but could also reduce the strength and hardness of the cutting tools. It could also increase the chemical reactivity of the materials and cause excessive thermal and chemical tool wear.

It is known that cutting speed has a significant bearing on cutting temperature and thus cutting forces. Hence, increased cutting speed and cutting temperature can result in lower cutting forces and longer tool life (Kalyankumar and Choudhury, 2008, Liao et al., 2008, Astakhov, 2006). For instance, cutting forces in machining Inconel® 718 reduce significantly at cutting temperatures above 750˚C due to significant reduction in its strength and hardness (Leshock and Kim, 2001). In order to benefit from workpiece material softening at elevated temperatures, the cutting tool should withstand high thermal and mechanical stresses and be chemically stable at elevated temperatures.

In order to quantify the performance of different cutting tools in machining, their hot hardness and wear resistant could be used. The specific wear resistance of materials can be calculated from (Evans and Marshall, 1980):

$$W_R = K_{IC}^{-1/2} E^{-4/5} H^{-5/8}$$

Where W_R is wear resistance, K_{IC} is fracture toughness (MPa $m^{1/2}$), E is the Young's modulus (MPa) and H is the material hardness in MPa. The wear resistance of five common tool materials is provided in table 2.1. In addition to the wear resistance, the hardness of cutting tool materials at different temperatures is presented in figure 2.3.

Carbide tools are one of the most used tools in machining difficult-to-cut materials due to their performance and price. It has been reported that 75%-85% of carbide tools used in industry are coated (Sharman et al., 2001, Astakhov, 2006). While the coatings revolutionised the life span of cutting tools, the extent of their effectiveness differ across different manufacturers (Astakhov, 2006). Most common tool wear mechanisms in machining difficult-to-machine materials with carbide tools regardless of their coating are, adhesion, diffusion and abrasion.

Tool material	**Wear resistance (mm^3/Nm)**
White ceramic (Al_2O_3)	0.76
Black ceramic (Al_2O_3-TiC)	0.79
Tungsten carbide	0.92
PCBN	2.01
PCD	2.99

Table 2.1 Wear resistance of different tool materials (Wang et al., 1996)

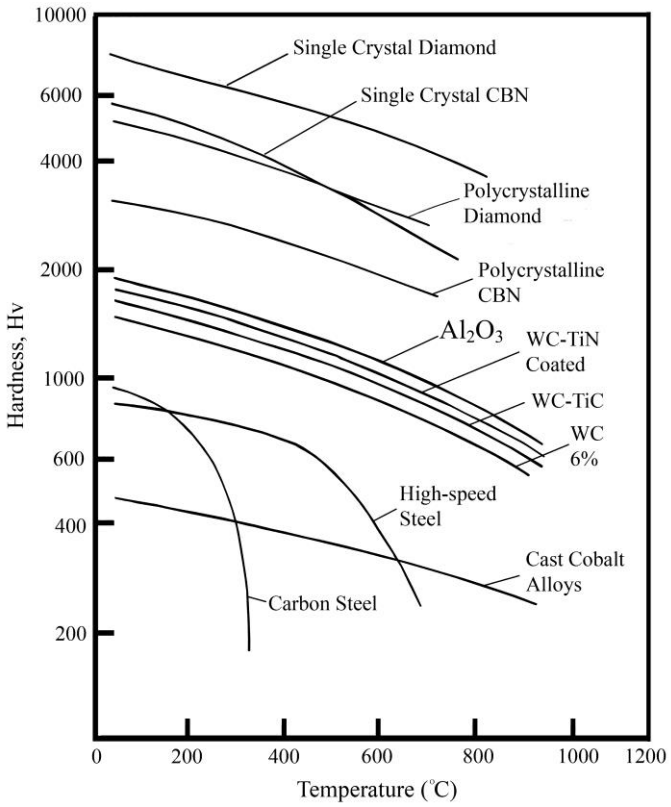

Figure 2.3 Tool materials hardness at different temperatures (Sreejith and Ngoi, 2000)

Different coatings have been introduced in order to improve the cutting tools performance. Figure 2.4 illustrates the major types of coatings used in industries. While the effect of coatings is still mysterious in machining difficult-to-cut materials, generally coated tool materials perform better than uncoated carbide tools. On the contrary, Hong et al. (2001b) complained the effectiveness of coatings in machining titanium as Al_2O_3 reduces the heat conductivity of the cutting tool and TiC and TiN are reactive to the workpiece material.

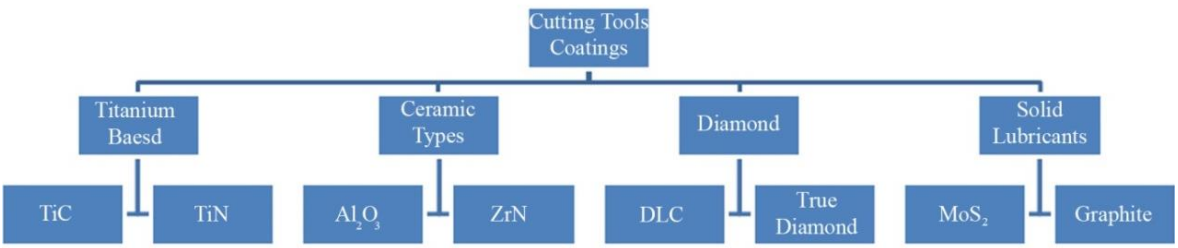

Figure 2.4 Basic categories of cutting tools coatings and some examples of each category

Excessive research has been conducted to investigate and compare different coatings in machining difficult-to-machine materials (Krain et al., 2007, Kustas et al., 1997, Sharman et al., 2001, López de Lacalle et al., 2000, Bian et al., 2014, Kaladhar et al., 2012). Coatings form a barrier between the cutting tool and workpiece materials preventing the tool material from being exposed. This reduces the diffusion rate and lowers the chemically and thermally induced tool wears such as adhesion and oxidation.

Coatings can also enhance the cutting tools performance by altering the friction coefficient, increasing hot hardness, resulting in lower abrasion rate (Ezugwu et al., 2003). Krain et al.(2007) empirically compared the performance of chemical vaporised deposition (CVD) TiN/Al_2O_3/TiCN and physical vaporised deposition (PVD) TiN/TiCN coated WC tools in milling Inconel® 718. The researchers found that the PVD coated tool outperformed the CVD coating in less aggressive (lower cutting speed, feed rate and immersion rate) cutting conditions. Although the CVD coated tool performed better than the PVD coated tools in more aggressive conditions. It has been attributed to the presence of the Al_2O_3 coating layer on the material, which acted as a thermal barrier that preventing carbides from being exposed (Krain et al., 2007). López de Lacalle et al. (2000) studied different types of coatings in drilling titanium and nickel based alloys and concluded that generally TiAlN coated carbide drills are the most appropriate tools for drilling Ti-6Al-4V and Inconel® 718 alloys.

Ceramic tools are considered as an attractive alternative to carbide tools in machining ferrous alloys (Sarma and Dixit, 2007). However, they are not recommended for machining titanium alloys due to the chemical reactivity between ceramic tools and titanium, low toughness and poor thermal conductivity which causes excessive tool wear at high cutting temperatures (Rahman et al., 2003b).

Ceramic tools exhibit high hardness but are very sensitive to mechanical and thermal shock (Ezugwu, 2005). The addition of titanium particles and reinforcement with silicon carbide fibres have improved the shock resistance and fracture toughness of the alumina tools which have made them potential alternative for carbide tools in machining nickel based alloys (Liao et al., 2008).

Machining with ceramic tools is usually conducted under a dry condition. It is because ceramic tools are sensitive to thermal shock and have low fracture toughness. The presence of moisture further reduces the fracture toughness of the tool and facilitates crack

propagation resulting in excessive notching and catastrophic tool failure (Jayal et al., 2010). The addition of TiB_2 to the ceramic tool material provides a self-lubricating effect which could lower the forces and improve the tool life in machining carbon steels (Jianxin et al., 2005). At high cutting temperature the TiB_2 grains react with oxygen and form a low friction oxide layer between the cutting tool and chips/workpiece surface. The oxidation process requires high temperature, thus at low cutting speeds oxidation does not take place. The tool wear mechanism at low speed machining of carbon steel material with alumina-titanium boride ceramic tool is reported to be abrasive and adhesive whilst at high speeds it transforms into oxidation (Jianxin et al., 2005). It should be noted that in machining nickel alloys with alumina ceramic tools the tool wear mechanism is notching and attrition while it is diffusion and adhesion in machining titanium (Liao et al., 2008, Ezugwu et al., 2005).

According to table 2.1 and figure 2.3 cubic boron nitride (CBN) and diamond based tools demonstrate the highest wear resistance and hot hardness among common tool materials. These properties have made them the most appropriate candidates for machining difficult-to-cut materials. Similar to other tool materials boron nitride particles and carbon particles of CBN and diamond tools respectively are chemically reactive with titanium and nickel which cause serious diffusion wear (Liao et al., 2008). CBN tools are conventionally produced from CBN powder in conjunction with a binder material. Thus, the mechanical and thermal properties of CBN tools are highly dependent on the type and quality of the binder material which could be metallic or ceramic (Wang, 2005). For instance while CBN is not reactive to ferrous materials, cobalt binder of the cutting tool may chemically react with the workpiece and result in diffusion wear (Liu et al., 2002).

Another type of the CBN tool is binderless CBN (BCBN) which does not have a binder material and so the problems associated with binder materials are eliminated. While the boron nitride component is reactive with titanium and nickel, BCBN tools perform much better than conventional CBN tools in machining titanium alloys (Wang, 2005). The cutting speed when machining titanium with CBN tools can be as high as 220 m/min, which is much higher than that for carbide tools (60 m/min) (Rahman et al., 2003b).

While diamond tools have the highest wear resistance and hot hardness, they are unstable at temperatures above 700˚C (Abele and Schramm, 2008). At high cutting temperature different types of tribochemical and tribothermal mechanisms can affect the diamond tools

life. The main tool failure mechanisms in machining with diamond tools are defined by Evans and Bryan (1991) as:

- Adhesion and formation of BUE
- Abrasion by micro cleavage, edge chipping and fatigue fracture
- Graphitisation at high temperatures (1800°C in vacuum or inert gas, 1100°C in presence of oxygen and above 1000°C in presence of iron)
- Oxidation at 900°C to 1000°C
- Dissolution and diffusion into the workpiece material
- Catalysed Graphitisation

Despite these problems, polycrystalline diamond (PCD) tools has been reported to be the best candidate for machining titanium alloys credited to their low solubility to titanium, high hot hardness and low tool wear (Nabhani, 2001, Rahman et al., 2003b).

2.3. Coolants and lubricants (CLs)

Shaw (1986) defines that one of the main issues that affects machinability is the heat generated during machining. Cutting fluids have been used in machining for decades in order to increase the machinability through lubricating the contact areas between rake face and chips, flank face and machined surface and reducing the friction induced heat and removing the generated heat from the cutting zone as a result of severe plastic deformation through conduction and evaporation (Aggarwal et al., 2008, Astakhov, 2006).

Based on the first law of metal cutting developed by Makarow, the highest machinability is achievable at a critical cutting temperature known as optimal cutting temperature (θ_{opt}) which is the temperature that the highest ratio of the cutting tool hardness over workpiece hardness can be achieved (Astakhov, 2006). θ_{opt} is independent of the cutting parameters and machining condition and is based on the material properties of the tool and workpiece materials. Astakhov (2006) noted that by increasing the cutting temperature close to θ_{opt}, machinability increases. Although, further increases in cutting temperature beyond θ_{opt} exacerbate the machining condition. Using cutting fluids is one of the most widely adopted techniques to maintain the cutting temperature below the optimal cutting temperature while other techniques such as pre-heating, plasma and ion-beam heating are common to increase the cutting temperature to that of θ_{opt} (Astakhov, 2006). The cooling effect of cutting fluids increases tool life by maintaining temperature below the thermal softening temperature of

the tool material and decreasing the thermally induced tool wear such as diffusion and adhesion. In addition, the lubrication effect of the cutting fluids could reduce the mechanical wears such as abrasion on the rake face (Dudzinski, 2004). In contrast, decreases in the workpiece temperature in certain conditions could increase the material hardness therefore increasing cutting forces, power consumption and reducing tool life (El Baradie, 1996). Other effects of cutting fluids are flushing chips away and preventing the machined surface and cutting tool from corroding (Oberg et al., 2004). Maintaining the cutting edge for longer and reducing the heat and friction in machining operations can also lead to improved surface characteristics of the machined parts.

Proper selection of cutting fluids is particularly important as it could affect the tool life, cutting forces, power consumption, machining accuracy, surface integrity etc. For instance, cutting fluids with a greater lubrication effect are usually employed in severe machining operations such as low speed machining and machining difficult-to-machine materials. However, coolants are more favourable in high speed machining with low cutting forces and high temperatures (Oberg et al., 2004). Despite the significant effects of cutting fluids in machining, the selection of the type and delivery system of the cutting fluids are usually based on the recommendations of cutting fluid suppliers and machine tool manufacturers which are not necessarily aware of the machining conditions (Astakhov, 2006).

Substances used in machining for cooling and/or lubrication can be defined as cutting fluids, gas-based coolants/lubricants and solid lubricants (Trent and Wright, 2000). Different approaches have been used in order to classify the cutting fluids due to their wide varying characteristics. One of the widely accepted characteristics of the cutting fluids is their miscibility in water. Thus, it has been used widely in order to categorise the cutting fluids into water-soluble (Water-miscible) cutting fluids and non-water-soluble – also known as oil-based - cutting fluids (El Baradie, 1996, Grzesik, 2008, Oberg et al., 2004). In addition, gas-based CLs can also be defined as liquefied gases and gas-form CLs.

2.3.1. Water miscible cutting fluids

As it was mentioned before (section 2.3), one of the effects of cutting fluids is to remove generated heat at the cutting zone by conduction. Thus, the desired cutting fluid used particularly for cooling should have high thermal conductivity and specific heat (El Baradie, 1996). Specifically, water is the most favourable coolant fluid with this characteristics accompanied with low cost. However water is corrosive to ferrous materials

specifically used in expensive machine tools (Astakhov, 2006). In addition, water has low lubrication effectiveness and tends to wash lubricants used on the sliding and rotating surfaces therefore increasing the machine wear. To overcome these problems and enhance the lubrication properties of water-based cutting fluids, different additives have been added to water (Oberg et al., 2004).

Water miscible cutting fluids are categorised into soluble oil, synthetic and semi-synthetic fluids. Soluble oils consist of a mineral oil accompanied with emulsifiers which allow the oil to be dispersed into the water (Grzesik, 2008). The soluble oils have lubrication and corrosion prevention characteristics of mineral oils together with the cooling effect of water. Synthetic fluids are mineral oil free cutting fluids which contains inorganic or organic chemical solutions in order to provide: 1) water softening; 2) corrosion prevention; 3) lubrication; 4) reduction of surface tension and 5) blending.

Synthetic CLs are water-based and contain synthetic water-soluble lubricants, high pressure additives, corrosion inhibitors, biocides, surfactants and defoamer. Synthetic fluids are generally considered as coolants with low lubrication characteristics and are particularly used for low force operations. This poor lubrication characteristic is the major drawback of these CLs which has limited the use of synthetic CLs in industries (El Baradie, 1996, Astakhov, 2006). Semi-synthetic cutting fluids contain both mineral oils and chemical additives and have both characteristics of soluble oil and synthetic fluids. They are considered of better lubricants when compared to synthetic fluids and are cleaner and more effective in rust prevention than soluble oils.

One of the main problems associated with maintenance of the water miscible fluids is the bacteria and fungi growth in the fluid lowering the fluids service life and increases health hazards. To control the bacteria growth in the cutting fluids, humectants, germicide and bactericide additives may be used (El Baradie, 1996).

2.3.2. Oil-based or neat-oil cutting fluids

Oil-based fluids are other alternative coolant fluids widely used in most machining operations. They are usually mineral oils which often contains some additives such as other kinds of lubricants and extreme pressure compounds in order to enhance their applications (Grzesik, 2008). This type of cutting fluid is used to lubricate the tool-chip interface and thus reduce the friction and friction induced heat at the cutting zone. Reduction in friction

can result in lower cutting forces, crater wear on the tool rake face and other types of thermally induced tool wear in certain machining conditions. The application of oil-based fluids also lubricate the moving parts of the machine tool and reduces the corrosion/oxidation on the machined surface and machine tool (El Baradie, 1996).

The oil-based cutting fluids are classified into two basic categories namely, naphthenic mineral oils and paraffinic mineral oils. The characteristics of these mineral oils are usually enhanced through the addition of fatty lubricants, extreme pressure additives such as chlorine, sulphates and phosphates, friction modifiers, viscosity index modifiers, odorants, thickness modifiers and polar additives (Astakhov, 2006). While straight oils provide good lubrication, anti-seizure characteristics and corrosion protection, they cannot maintain their characteristics at higher load and temperatures and make mist and smoke. Thus, the application of straight oils is limited to low duty machining of easy-to-cut metals eg. aluminium, magnesium, brass, low carbon steels, etc. In contrary, compounded mineral oils chemically react with machining surface at high machining pressures and temperatures which makes them favourable for low speed heavy duty machining operations such as threading, broaching, tapping gear hobbing, etc. (El Baradie, 1996, Oberg et al., 2004, Astakhov, 2006). This leads to formations of lubricating films between sliding surfaces leading to reductions in friction. It is noteworthy that this chemical reaction should not result in surface degradation. For instance, the presence of chlorine additives in cutting fluids used in machining titanium alloys can cause corrosion on the machined surface and affect the service life of the machined component (Donachie, 2000).

2.3.3. Gas-based coolant-lubricants (CLs)

Gas-based CLs generally refers to the substances that at room temperature are in gas form, however in machining applications they are used in the form of either gas or cooled-pressured fluids. Main gas-based CLs are air, nitrogen, argon, helium or carbon dioxide. The gas-based CLs might be used in conjunction with traditional cutting fluids in the form of mist or droplets to enhance their lubrication capability.

The most broadly known usage of gases as coolants is in dry cutting where air is being used in order to cool the tool and workpiece (El Baradie, 1996). However, gases are poor thermal conductors and have low cooling capacity. Different approaches have been used in order to increase the cooling capability of gas-based CLs namely: compressing, cooling and liquefying. Compressed gas-based CLs are especially attractive where traditional

cooling techniques fail to penetrate the chip-tool interface, such as heavy duty cutting conditions.

Brandao et al. (2008) compared the effect of three different gas-based cooling techniques of dry, compressed air and chilled air on the heat flow through the workpiece during end milling of die steels. The researchers found that the thermal energy transferred to the workpiece reduced by using compressed air and chilled air as compared to dry cutting. In addition, the lowest thermally induced dimensional variations in the workpiece is achieved when using compressed air for cooling.

Gaseous coolants are also beneficial when liquid coolants cannot be applied. In machining medium density fibreboard (MDF) applying chilled air as cutting coolant improves the tool life while not affecting the cutting forces and power consumption. Application of chilled air removes the heat generated at cutting zone effectively and resulted in lower chemical reaction of cobalt binders and tungsten carbide grains of the tool with workpiece material (Gisip et al., 2009).

Hong et al. (2001b) investigated the effects of different methods of using liquid nitrogen (LN2) as a cutting fluid on tool life when turning Ti-6Al-4V titanium alloy. They found that by applying LN2 on the rake and flank face of the uncoated carbide tool, the tool life could be improved by up to 3.3 times by reducing the thermally induced tool wear and reducing the chemical reactivity of the workpiece material. Other research (Hong, 2006) studied the effect of LN2 on the friction coefficient through the disk-pin sliding test. It has been observed that LN2 can reduce the friction coefficient by changing the material frictional behaviour due to ultra-low temperatures. In addition, it has been proved that LN2 itself is a good lubricant and can reduce the friction coefficient between sliding surfaces. It should be noted that the lowest friction coefficient obtained when freezing the sliding parts together with spraying LN2 between sliding surfaces. This is attributed to formation of a fluid/gas cushion between the tool/workpiece surfaces which results in better lubrication and lower friction coefficient (Dhananchezian and Kumar, 2011).

Adding a small amount of lubricant could reduce the cutting temperature and cutting forces. It has been observed that by spraying micro-drops of bio-degradable oil in air the tool flank wear has been reduced by up to 44% in high speed milling of low carbon steels. Application of oil spray into the machining zone also reduces the cutting temperature and forces (López de Lacalle et al., 2006).

Gaseous CLs such as CO_2, argon, nitrogen and helium also provide an inert environment which could prevent the cutting tool and machined surface from oxidation at high cutting temperatures.

2.3.4. Economical, environmental and health issues associated with coolants and lubricants

It has been reported that more than 240,000 tonnes of water-miscible cutting fluids are consumed in the UK annually and more than 50,000 workers are exposed to cutting fluids (WATCH-Commitee, 2007). In the United States, it is approximated that yearly, 100 million gallons of cutting fluids are consumed whilst the number of exposed workers reaches 1.2 million. The annual consumption of cutting fluids has been reported to be equal to 71bn Japanese Yen in Japan where 42bn Yen is the disposal cost (Feng and Hattori, 2000, Mirer, 2010, Meza et al., 2013). In 1994, the cutting fluids consumption in manufacturing industries in Germany was estimated to be 75,491 tons which 28,415 tonnes of it was water-miscible cutting fluids (Klocke and Eisenblätter, 1997). The reports indicated that almost 38 million tonnes of cutting fluids were consumed in 2005 globally and it was expected to be increased by 1.2% over the following decade (Sharma and Sidhu, 2014). It is estimated that the costs associated with cutting fluids are about 16% of the total manufacturing costs (Byrne and Scholta, 1993) while in machining difficult-to-machine materials they reach 20%-30% (Pusavec et al., 2010). This is much higher than the tooling costs which are about 2-4% of the total manufacturing cost (Klocke and Eisenblätter, 1997).

The associated costs with cutting fluids is not only limited to their purchase and preparation but also include the maintenance and disposal costs. Disposal costs of the cutting fluids can be up to two or four times their purchase price in the United States and Europe respectively (Hong and Zhao, 1999). This is mainly due to the fact that most cutting fluids are not naturally bio-degradable and require expensive treatments prior to disposal (Hong and Zhao, 1999). This issue has been supported through the introduction of restricted environmentally conscious regulations such as the Control of Substances Hazardous to Health (COSHH) essentials for machining with metalworking fluids in the UK (COSHH, 2011), the technical code of practice for hazardous substances (TRGS) in Germany and the Decree 259/1998 of 29 of September in Spain (López de Lacalle et al., 2006). It is noteworthy that 155million litres of used cutting fluids are estimated to be

discharged into the environment yearly only in the United States (Hong and Broomer, 2000).

Cutting fluids require regular maintenance in order to control their optimum characteristics. They are a rich environment for growth of bacteria and fungi. Presence of bacteria in the cutting fluids could split the emulsion and reduce the lubricity of the fluids. They could also change the PH of the cutting fluid and increase the risk of corrosion on the machine tool and workpiece. In addition, they could be especially dangerous for the workers on the shop floor (Hong and Broomer, 2000). To control the bacterial growth in cutting fluids different kinds of bactericides, humectants and germicides are currently in use in industries. Although studies revealed that while PH of cutting fluids exceeds 10, some bacteria known as extremophiles could live and grow in such extreme environments (Karadzic et al., 2004). Even in the presence of bactericides it has been proved that some bacteria such as Pseudomonas could survive (Mattsby-Baltzer et al., 1989). The presence of the bacteria is not limited to the cutting fluids and microbial masses and particularly endotoxin have been evident at the shop floor atmosphere. This increases the importance of controlling the bacterial growth in metal working fluids.

While chemical additives are necessary to control the bacterial growth in cutting fluids, they are accounted as hazardous substances for both the environment and workers health. Discharge of cutting fluids containing biocides could affect the natural decomposition process and some municipalities prohibited the disposal of biocides into the sewage systems (Hong and Broomer, 2000). It has been argued that antimicrobials and biocides are used to maintain the cutting fluids functionality rather than protect the workers. Many of the available biocides release formaldehyde which is a potential carcinogen. Similarly, the International Agency for Research on Cancer reported that mineral oil used in metal workings is carcinogenic and exposure to it could result in occupational skin cancer (Peter et al., 1996). On the other hand, non-formaldehyde releasing biocides are very dangerous for health and highly corrosive to the skin (Hong and Broomer, 2000).

In addition to biocides, there are many other chemicals in the cutting fluids which are considered hazardous to the environment and health. Chlorinated and sulphurised additives in extreme pressure cutting fluids chemically react with metallic surfaces resulting in formation of a low friction protective film between the sliding surfaces. However, they are considered as toxic substances for workers health as well as the environment (Hong, 2006).

Chlorinated paraffin in extreme pressure cutting fluids changes by heat and pressure to dioxin which is a toxic substance. The existence of chlorine in cutting fluids also increases the disposal costs by a factor of 7 due to restricted environmental regulations (Feng and Hattori, 2000).

Cutting fluids in machining operations could be vaporised and atomised due to high pressure and temperature and form cutting fluids mist. As a result, the airborne particles of cutting fluids could be easily inhaled by workers causing different kinds of lung diseases ranging from mild respiratory problems to asthma and several types of cancers. The effect of aerosols of the cutting fluids on the workers' health is not limited to the lung disease and could also increase the risk of esophagus, stomach, pancreas, prostate, colon and rectum cancers.

Some manufacturers use cutting fluids in order to reduce the machining solid dust. However, it has been found that wet machining could produce 12-80 times more airborne particulate matter than dry cutting (Sutherland et al., 2000). In addition, airborne particles produced at wet machining are much smaller than that of dry cutting. Smaller particles could remain suspended longer in the working area and are easier to inhale. They are also more likely to pass the larynx and penetrate into the conducting airways and bronchial part of the lungs. Skin exposure to the cutting fluids could also cause skin dermatitis. In Finland in 1993, registered cases on occupational dermatoses formed the fourth most common work place disease after musculoskeletal disease, hearing loss and disease caused by asbestos and counted as 16% of all registered occupational diseases (Koh and Goh, 1998). Some types of allergens in the water-miscible oils are coconut diethanolamide, tertiary-butylhy-droquinone, alkanolamine borates, oleyl alcohol, bronopol, etc. cutting fluids induced dermatitis ranges from ugly rashes to malignant cancer (Hong and Zhao, 1999).

In contrast to the conventional cutting fluids, gaseous CLs are relatively cleaner and more environmentally friendly. Nevertheless, they are generally known to be more expensive alternatives than cutting fluids which require additional equipment which normally are not provided with machine tools (Kopac, 2009). In addition, gas-based CLs cannot circulate in the machine tool and thus they are not reusable in the system as they vaporise after application (Kim et al., 2001, Hong et al., 2001a). This on the other hand eliminates the disposal costs and cost associated with cleaning the parts, machining chips and machine tools (Dogra et al., 2010).

While nitrogen is lighter than air and can be dispersed into the atmosphere, when using CO_2 as coolant, there is a requirement for ventilation over the machining zone. This is due to the fact that CO_2 is heavier than air and accumulates at the shop floor increasing the risk of oxygen depletion (Hong, 2001). To conclude, while gas-based CLs are considered to be more environmentally friendly solution for machining operations, there is not any gas-based and particularly cryogenic system which is economical and practical enough to replace current conventional techniques (Hong et al., 2001b).

2.4. Environmentally conscious machining

As mentioned previously using cutting fluids in the cutting operations becomes a major problem due to the associated economical, environmental and health problems. The best approach to eliminate the effects of cutting fluids is to eliminate their usage completely which is known as dry cutting (Klocke and Eisenblätter, 1997). However, dry cutting is not applicable in all machining operations mainly due to excessive tool wear or low surface quality. In order to improve machinability a minimum quantity lubricant (MQL) could be penetrated into the cutting zone. Although MQL reduces the CLs consumption, it still uses them in the form of mist or droplets which increases health hazards for the workers (Sreejith and Ngoi, 2000). Another alternative is to use a cryogenic coolant in order to dissipate the generated heat at the cutting zone and enhance the machinability through the changes in cutting tool/workpiece material properties. In this section different issues and achievements to eliminate or reduce the consumption of cutting fluids in machining are reviewed through three different methods, namely 1) Dry machining; 2) MQL and 3) Cryogenic Machining.

2.4.1. Dry cutting

Dry machining is considered as the best approach to eliminate the use of cutting fluids in manufacturing enterprises and thus reduce the machining costs and ecological hazards (Klocke and Eisenblätter, 1997, Rivero et al., 2006) Weinert et al. (2004) identified the benefits of adopting dry machining which are shown in figure 2.5. It is known that employing cutting fluids can improve tool life, prevent built up edges (BUE) from forming on the cutting tool and reduce the cutting forces and surface roughness. On the contrary, in dry machining friction and cutting temperature could be more than that of wet machining. These could reduce the tool life, reduce the surface quality and cause thermally induced geometrical deviations in the machined part. However, this is not the case for all materials

and machining operations and dry cutting shows positive effects such as lower thermal shock and improved tool life in some cases (Sreejith and Ngoi, 2000, Klocke and Eisenblätter, 1997).

Techniques employed by researchers to compensate the effects of the elimination of cutting fluids in machining could be categorised into i) indirect heat dissipation and ii) improving cutting tools properties by introducing better tool materials, coatings or tool geometries. This has led to the introduction of advanced tool materials such as Cubic Boron Nitride (CBN), Polycrystalline Cubic Boron Nitride (PCBN), Polycrystalline Diamond (PCD), cermets, ceramics and different kinds of coatings.

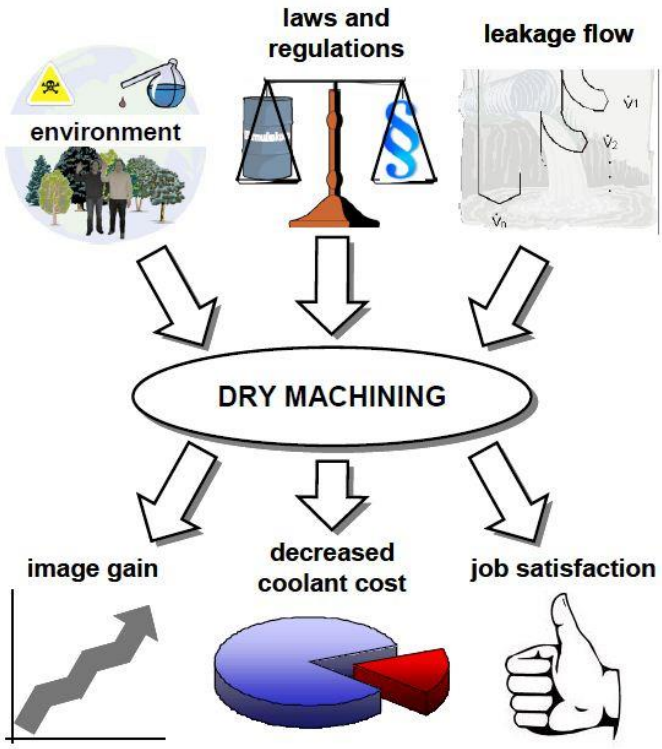

Figure 2.5 Benefits of adopting dry machining (Weinert et al., 2004)

It is known that an increase in cutting speed results in higher cutting temperature. Higher cutting temperatures could reduce the workpiece material strength and thus result in lower cutting forces. Although, high temperatures can also reduce the hardness of the cutting tools and result in excessive tool wear. In addition, higher temperatures at the cutting zone increase the risks of adhesion and diffusion wear due to the higher chemical reactivity of the workpiece and cutting tool materials at higher temperatures. Lenz et al.(1976. In: Klocke and Eisenblätter, 1997) studied the effects of cutting speeds on tool wear of uncoated tungsten carbide tools in machining carbon steels. Investigations revealed that at

low cutting speeds the dominant flank wear mechanism is abrasion which changes to adhesion at higher cutting speeds. Further increases in the cutting speed changes the dominant wear mechanism to diffusion. Thus an increase in the cutting speed to a certain point could result in lower flank wear by changing the wear mechanism from abrasion to adhesion.

Tool wear and the failure mechanisms of different tool materials were investigated by Dearnley and Grearson (1986) during turning Ti-6Al-4V alloy. Their experimental studies revealed that the main tool failure mechanism was diffusion on the rake face resulting in excessive crater wear. This is attributed to high and localised temperature at the chip-tool contact on the rake face and high chemical reactivity of the workpiece material. CBN tools performed better than other ceramic and carbide tools by showing a lower and smoother tool wear. In addition, studies showed that the straight grade carbide tools with finer grain size pose lower tool wear than that with larger grain size or steel grade.

Ginting and Nouari (2006) investigated the applicability of dry end milling of Titanium alloy Ti 6242S with uncoated alloyed carbide tools. They used an uncoated tungsten carbide with cobalt binders alloyed with 20.7 wt% of (Ti/Ta/Nb)C. The investigations were limited to the study of chip formations, tool wear, cutting temperature and surface finish of the machined part. Observation of the worn tools after machining under the scanning electron microscope (SEM) revealed that localised flank wear was the dominant tool failure mode. Brittle fracture of the cutting edge accompanied with localised flank wear was reported to be the second most observed tool failure mode.

In contrary to the observations of Dearnley and Grearson (1986) in the study by Ginting and Nouari (2006) the tool did not suffer from excessive crater wear. This could be explained by the fact that in continuous machining such as turning, temperature at the cutting zone is much higher than that of intermittent cutting operations. This high temperature facilitates the adhesion of the chip to the rake face of the cutting tool. The adhered material is then torn off by the flow of the chips. In addition, at high temperatures the cutting tool material diffuses into the chips at the tool-chip interface. Thus abrasion and diffusion due to high cutting temperature are responsible for crater wear on the rake face of the cutting tool in turning (Ginting and Nouari, 2006). The researchers (Ginting and Nouari, 2006) concluded that uncoated alloyed carbide tools with properties as specified before are suitable for dry end milling of titanium alloys with the following machining

parameters: cutting speed > 150 m/min, feed rate = 0.15 mm/tooth, 2 mm of axial depth of cut and 8.8 mm radial depth of cut. These machining parameters result in 11.3min tool life and 0.61µm surface roughness. In addition, experimental investigations proved that FEA could effectively model the dry end milling operations.

Krain et al. (2007) studied the effects of machining parameters in end milling operation of Inconel® 718 nickel based alloy in order to gain higher productivity through optimising the material removal rate. Generally, adhesion and attrition was found to be the main tool wear mechanism due to high cutting pressure and chemical reactivity of the tool and workpiece materials. Low thermal conductivity of Inconel® 718 leads to high local temperature at the cutting zone which facilitates the wear mechanisms. At high cutting temperatures the workpiece material is adhered to the tool and forms a BUE on the flank face. Experiments revealed that immersion rate (percentage of radial depth of cut) controls the effect of feed rate on the tool life and material removal rate. While higher immersion rate reduces the machining time, it was found that optimum material removal rate was achieved at immersion rates of 25% and 50%.

As mentioned previously one of the requirements to move toward dry cutting is enhanced cutting tools. In this regard tool coating is considered as a technique to apply the characteristics of several materials on the surfaces of the cutting tools. These nanostructured materials may enhance the characteristics of the cutting tool by providing different properties such as higher hardness, higher strength, higher Young's modulus, higher wear resistance, higher fracture toughness, higher chemical stability and reduced frictional behaviour (Kustas et al., 1997). In addition to machining parameters, Krain et al.(2007) compared the tool life of two different types of coatings in machining Inconel® 718. Empirical evaluations illustrated that PVD TiN/TiCN coated tungsten carbide tool performed better at less aggressive cutting conditions. At more aggressive cutting conditions CVD TiN/Al_2O_3/TiCN coated carbide tool outperformed the PVD coated tool. This is mainly attributed to the existence of a thermal barrier of Al_2O_3 which prevents the tungsten-carbide particles to be exposed (Krain et al., 2007).

Generally, coated tools perform better than uncoated tools in dry machining through the three mechanisms of i) increasing the tool hardness; ii) preventing the tool material to be exposed; iii) reducing the friction coefficient. In another experiment (Kustas et al., 1997) the effect of multi-layer solid lubricant (MoS_2/Mo) coated high speed steel (HSS) drill

tools was compared with an uncoated drill in machining Ti-6Al-4V workpiece material. The uncoated drill was tangled into the workpiece as a result of constant increase in torque during machining. On the other hand, 33% reduction in the cutting torque was observed when using the coated drill with no evidence of catastrophic fracture or seizure.

It has been studied (Nabhani, 2001) that PCD (SYNDITE) tools outperform PCBN (AMBORITE) and CVD TiN/TiCN/TiC triple coated carbide tools in dry turning of Ti48 titanium alloy. This is mainly attributed to the chemical reaction between carbon substrates of the tool material and titanium and formation of a TiC layer. This TiC layer protects the cutting tool from abrasion and reduces the diffusion rate increasing tool life. It could be concluded that chemical reactions between tool and workpiece materials could increase the tool life by the formation of a protective layer.

Liu et al.(2002) investigated the effect of adding aluminium to pearlitic cast iron on its machinability with CBN tools. They found that addition of Al could result in the formation of a harder protective layer of aluminium oxide on the tool surface. This layer protects the cutting tool from abrasive wear and makes it possible to increase the cutting speed up to 4500 m/min. In most cases the lower tool wear also reduces the cutting forces and surface roughness as the cutting edge remains sharp for a longer period. It is noteworthy to mention that in machining titanium alloys, generally the dominant tool wear mechanism is adhesion and diffusion on the rake face and adhesion and abrasion on the flank face (Zhang et al., 2009, Nabhani, 2001). Excessive crater and flank wear could weaken the cutting edge resulting in plastic deformation and even premature tool failure. Another characteristic associated with machining titanium alloys is that crater wear is usually narrow and formed closely to the cutting edge, which is due to a small contact area between tool and chip (Zhang et al., 2009).

It is known that an increase in the cutting temperature can soften the workpiece material and ease the cutting operation. Studies (Liao et al., 2008, Wang, 2005) show that higher cutting speed results in higher cutting temperature which could lower the cutting forces and increase the tool life. However in machining high chemically active materials such as titanium and nickel based alloys high temperatures at the cutting zone is critical. High cutting temperatures increase the chemical reactivity of the tool/workpiece material resulting in excessive tool wear, due to adhesion, diffusion and attrition. Also, while these materials maintain their hardness even at high temperatures, the tools may fail by material

softening. Specifically the hardness of Inconel® 718 increases with increase in temperature up to 650˚C. In other words, an increase in the cutting speed when the cutting zone temperature is lower than 650˚C, increases the material hardness and results in more difficult machining condition (Liao et al., 2008). Further increases in the cutting speed and thus cutting temperatures above 650˚C lead to lower material hardness and cutting forces resulting in chips changing from segmented to continuous. However, cutting temperatures higher than 1100˚C would lead the cutting tool to suffer from heat softening. For instance in end milling Inconel® 718 with a K10 grade of carbide tool it has been observed that increasing the cutting speed up to 113.1 m/min resulted in lower cutting forces and tool wear. Further increase in the cutting speed has led to the welding of chips to the cutting tool retarding the chip flow and increasing the cutting forces (Liao et al., 2008).

One of the problems in machining with CBN tools is the chemical reaction between binder and workpiece material which reduces the tool strength. It is more obvious in machining ferrous alloys where boron nitride particles are not chemically active with ferrous particles. Studies (Liu et al., 2002) on the CBN tools with different binder materials in machining ferrous alloys show that CBN tools with TiC or Cobalt binders perform better than their counterparts with TiN and TiCN binders. On the other hand, in machining titanium alloys CBN particles are highly reactive with the workpiece material at high cutting temperatures.

Experiments (Wang, 2005) in machining Ti-6Al-4V with binderless CBN (BCBN) tools revealed that the highest material removal rate and tool life could be achieved through combining high cutting speed and low feed rate and depth of cut. High cutting speed increases the cutting temperature and reduces the workpiece material strength where BCBN could maintain its hardness. Dominant tool wear in this condition is adhesion and diffusion of the workpiece material into the flank face resulting in non-uniform flank wear. Unlike what was reported (Zhang et al., 2009, Nabhani, 2001) about the tool wear when using CBN or carbide tools, the crater is not significant on the BCBN tool and does not affect tool life (Wang, 2005).

Another technique in enhancing the properties of conventional cutting tools is cryogenic treatment (Stewart, 2004, Yong et al., 2006, Koneshlou et al., 2011, Li et al., 2010). The hardness and wear resistance of the metals which contain retained austenite could be improved by this technique (Sreeramareddy et al., 2009). As cryogenic treatment affects the whole material properties, unlike coating it preserves its properties after re-sharpening

or regrinding (Dasilva et al., 2006). Sreeramareddy et al.(2009) reported that cryogenic treatments increased the thermal conductivity and reduced the tool wear of multilayer coated carbide tool as compared to non-treated tools. Increased thermal conductivity resulted in lower temperature and better heat dissipation capability of the tool. This reduces the thermally induced tool wears such as adhesion and diffusion. It should be noted that while cryogenic treatment reduced the hardness of the material at the room temperature, it increased the hot hardness of the tool material (Sreeramareddy et al., 2009).

In machining operations the major portion of energy used transforms into heat. In the absence of cutting fluids in dry machining the generated heat should be dissipated by conduction through the chips, workpiece and cutting tool. An alternative to enhancing the heat conduction is indirect cooling of the cutting tool and/or workpiece by using heat pipes (Noorul Haq and Tamizharasan, 2005, Jen et al., 2002), coolant through tools (Jen et al., 2002, Rozzi et al., 2011), cooling the workpiece (Uehara and Kumagai, 1968, Uehara and Kumagai, 1970, Tsai and Hocheng, 1998), etc.

Jen et al.(2002) investigated the feasibility of manufacturing and using heat pipes with coolant fluid through the heat pipe for HSS drills. FEM analysis and experimental investigations illustrated that this method has the potential to reduce the cutting temperature up to 50%. However, the application of this method is limited due to geometrical restrictions of cutting tools and manufacturing difficulties. Empirical studies (Noorul Haq and Tamizharasan, 2005) also revealed that using a brass heat pipe integrated tool holder in turning engine crank pins with CBN tool can reduce the cutting temperature by 25˚C. This is equal to a 5% reduction in the cutting zone temperature which resulted in up to 9% reduction in the tool flank wear.

2.4.2. Minimum quantity lubricant (MQL)

Minimum Quantity Lubricant (MQL) or near dry machining is another alternative to conventional flood coolant. It also provides an alternative for machining operations which dry machining is not applicable especially where machining efficiency and/or high surface quality are of more interest (Dhar et al., 2006). Based on the recommendations by Klocke et al. (2004) table 2.2 provides a comparative application of MQL and dry machining for some materials in different machining operations. MQL is referred to as the application of a small amount of cutting fluid (10 to 100 ml/h) mixed with compressed air to form an aerosol (Sharma et al., 2009). This mixture is then penetrated to the cutting zone in order to

lubricate the chip-tool contact area and reduce the temperature. Boundary lubrication on the contact surfaces results in a lower friction coefficient whilst heat transformation is mainly in the form vaporisation at the cutting zone and conduction through the flow of the air. Evaporation of the CL at the cutting zone eliminates the requirements for maintenance, circulation and disposal of the cutting fluid and the associated costs (Sharma et al., 2009, Sales et al., 2009).

Today, there are many companies involved in the production of sophisticated MQL systems for machining operations. UNIST Inc. claimed that its first MQL system named uni-MIST® was designed and patented in 1957 at Grand Rapids, Michigan based on the concept of low volume and low pressure lubrication (UNIST, 2012). Further developments of the system have resulted in the current cutting edge MQL facilities of through-the-tool cooling systems, MQL flow control systems, atomisers, etc. Other major companies in the area of MQL are Accu-Lube, Bielomatik GmbH, MAG, Menzel Metallchemie GmbH.

Most of the commercial products available in the market consist of five main parts namely, air compressor, CL container, tubings, flow control system and spray nozzles. Generally, in all MQL systems, the coolant and pressured air are mixed together and a controlled flow of the mixture is delivered through the tubings and nozzle into the cutting point. The nozzle could be external or internal which is also known as a through-the-tool cooling/lubricating system. Figure 2.6 provides a schematic view of a typical MQL system developed for turning operations while figure 2.7 demonstrates a through the tool MQL cooling system for face-milling operations.

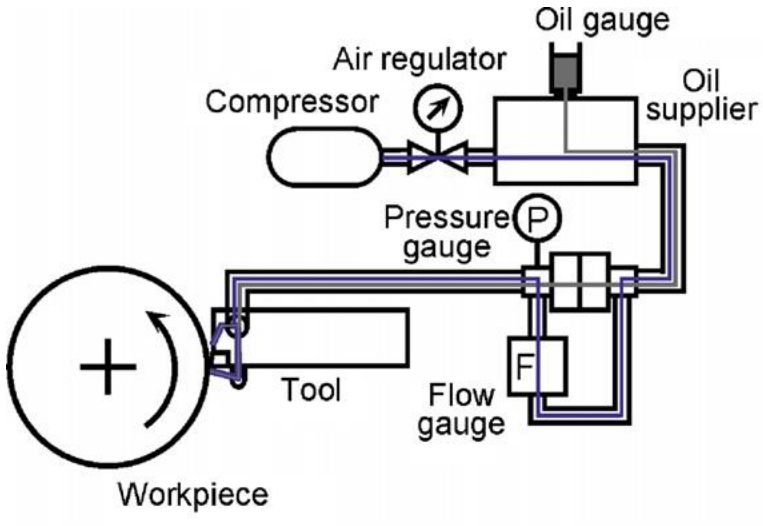

Figure 2.6 Schematic view of the components of a MQL system developed by Kamata and Obikawa (2007)

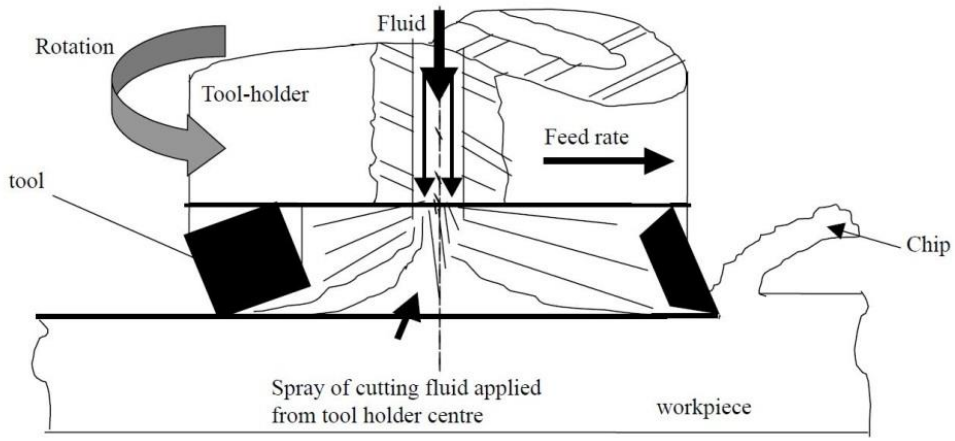

Figure 2.7 Schematic view of a through-the-tool MQL cooling system designed by Sales et al. (2009) for face-milling

As mentioned previously, MQL is introduced where dry cutting is not applicable and flood cooling is not desirable. Machining ductile materials is one of these cases where high cutting temperature increases the tendency of adhesion between the cutting tool and workpiece materials. The high cutting temperature in the case of ductile materials is mainly due to large plastic deformation at the primary cutting zone and high friction coefficient at the second shear zone between the chips and rake face.

This high temperature increases the adhesion of the chip material to the cutting tool resulting in the formation of BUE. The presence of BUE on the cutting tool in most cases not only reduces the tool life but also worsens the machined surface quality (López de Lacalle et al., 2006). For instance, dry machining of aluminium alloy parts is specifically critical. Heat generated during machining transforms into the workpiece due to its high thermal conductivity. Changes in the workpiece temperature during machining could cause thermal deformation and/or geometrical deviations. Aluminium alloys also tend to adhere to the cutting tool and form BUE. This affects the surface finish of the machined part as well as tool life, cutting forces and power consumption (Rivero et al., 2006). Studies on the application of MQL in drilling aluminium alloys showed that it could drastically increase the tool life up to 8 times (Klocke and Eisenblätter, 1997).

In high speed milling of A380 wrought aluminium, applying a very small amount (0.06 ml/hr) of biodegradable oil in the form of micro droplets in the flow of compressed air can reduce the tool wear and eliminate the BUE. Experiments (López de Lacalle et al., 2006) showed that 0.04 ml/hr to 0.06 ml/hr of lubricant if sprayed in a suitable area could reduce

the tool wear by up to 40% as compared to conventional emulsion cooling. This amount of lubricant is much lower than stated in most other studies (Dhar et al., 2006, Sharma et al., 2009) and as the difference between tool life at 0.04 ml/hr and 0.06 ml/hr MQL is not significant 0.04 ml/hr is more desirable as lower amounts of lubricant are used. The technique described by López de Lacalle et al. (2006) not only enhanced the tool life but also reduced the consumption of cutting fluids by 95%.

Yuan et al. (2011) studied the effect of air temperature in MQL milling of Ti-6Al-4V alloy. They used 20 ml/hr of synthetic ester oil in the flow of air at different temperatures of 0˚C, -15˚C, -30˚C and -45˚C compared to MQL at the room temperature, dry and flood cooling. Formation of BUE was observed under dry, wet, MQL at room temperature and MQL at 0˚C. They noticed that the workpiece material became harder at very low air temperatures of -30°C and -45°C which resulted in higher cutting forces as compared to that of dry machining. The longest tool life and lowest surface roughness were achieved under a MQL environment with an air temperature of -15˚C. Application of MQL at -15˚C increased the tool life by the factor of three by eliminating the formation of BUE on the cutting tool while not affecting the workpiece material hardness.

Modifying cutting tools and tool holders is a method widely used to deliver cutting fluids to the desired point of cutting e.g. tool tip, rake face and/or flank face (Li and Liang, 2006, Li and Liang, 2007, Kamata and Obikawa, 2007, Sharma et al., 2009). Specifically in MQL turning operations these modification is used to focus the flow of the air on the rake and/or flank face of the cutting tools. Sharma et al. (2009) reported that MQL flank face cooling has resulted in longer tool life and lower surface roughness in comparison with dry and MQL rake face. It is because the cutting fluid cannot reach the tool-chip interface when it is sprayed on the rake face (Sharma et al., 2009).

In machining AISI 1045 steel, it was found (Li and Liang, 2006) that application of MQL does not have a significant effect on the cutting zone temperature. It is because the coolant is penetrated between the flank and machine interface which is far away from the highest temperature zone at the cutting edge. Study of the cutting forces (Li and Liang, 2007) showed that spraying the coolant on the flank wear reduced the cutting forces significantly. It illustrated that in machining AISI 1045 steel with uncoated carbide tools the effect of penetrating a small amount of cutting fluid with compressed air is more lubricating rather than cooling. On the contrary, Kamata and Obikawa (Kamata and Obikawa, 2007) pointed

that in machining Inconel® 718 the cooling effect is more significant than lubrication. It has been found that changing the lubricant carrier gas from air to argon reduces the tool life to that of dry cutting or even lower. This is attributed to the lower heat conductivity, specific heat and lubricating capability of argon in comparison with air. Kamata and Obikawa (2007) investigated the effect of MQL in turning Inconel® 718 with carbide tools with different coatings. It was found that while the longest tool life was achieved by TiCN/Al2O3/TiN coated tool, the lowest surface roughness was produced by the TiN/AlN coated tool. This could be explained by uniform wear and an increase in the radius of curvature of the worn edge of TiN/AlN coated tool.

As mentioned before, the MQL method is considered as a lubricating method rather than cooling. This poor cooling capability limits the effectiveness of MQL in machining difficult-to-machine materials such as titanium and nickel based alloys where excessive heat generation is the main problem (Su et al., 2007).

Material / Process	Aluminium		Steel		Cast Iron
	Cast alloys	Wrought alloy	High alloyed bearing steel	Free cutting, quenched and tempered steel	GG20 to GG70
Drilling	MQL	MQL	MQL	MQL/DRY	MQL/DRY
Reaming	MQL	MQL	MQL	MQL	MQL
Tapping	MQL	MQL	MQL	MQL	MQL
Thread forming	MQL	MQL	MQL	MQL	MQL
Deep hole drilling	MQL	MQL		MQL	MQL
Milling	MQL/DRY	MQL	DRY	DRY	DRY
Turning	MQL/DRY	MQL/DRY	DRY	DRY	DRY
Gear milling			DRY	DRY	DRY
Sawing	MQL	MQL	MQL	MQL	MQL
Broaching			MQL	DRY	DRY

Table 2.2 Application areas of dry and MQL for some types of materials (Klocke et al., 2004)

2.4.3. Cryogenic machining

Cryogenic machining is a term referred to machining operations conducted at very low temperatures typically lower than 120˚K (Timmerhaus and Reed, 2007). Although, there are some references where the cryogenic term is used for higher temperatures (Yalcin et al., 2009, Yuan et al., 2011). In cryogenic machining a super cold medium, usually liquefied gases, is directed into the cutting zone in order to reduce the cutting zone temperature and cool down the tool and/or workpiece. The cryogen medium absorbs the heat from the cutting zone and evaporates into the atmosphere. As most cryogenic coolants

used in machining operations such as liquid nitrogen and liquid helium are made from air, they are not considered as pollutants for the atmosphere. Nitrogen in particular is an inert gas which forms 78% of the atmosphere and is lighter than air. As a result it is dispersed into the atmosphere and does not harm the workers on the shop floor. On the contrary carbon dioxide is considered as an air pollutant, however it has been suggested (De Chiffre et al., 2007) that liquid carbon dioxide could be produced from the exhaust gases of power plants thus not forcing additional contamination to the atmosphere. It is noteworthy that carbon dioxide is heavier than air and could cause CO_2 accumulation and oxygen deficiency problems on the shop floor (Hong, 2001).

Cryogenic machining is usually accompanied with changes in the properties of the workpiece and/or cutting tool materials, as a result of lowering the temperature. Ultra-low temperatures could increase the strength and hardness, and lower the elongation percentage and fracture toughness of materials. Cryogenic cooling could be beneficial for machining materials which at room temperature have large elongation to fracture percentage, low elastic modulus and are very ductile such as elastomers (Shih et al., 2004a, Kakinuma et al., 2008, Mishima et al., 2010). In addition, increases in the hardness of the cutting tool materials could enhance their wear resistance and improve the tool life (Zhao and Hong, 1992, Hong and Zhao, 1999). The cooling effect of the cryogens are particularly interesting in machining difficult-to-machine materials that suffer from excessive tool wear mainly due to high cutting temperatures such as titanium and nickel based alloys. Common cryogenic coolants used in machining operations are liquid nitrogen (LN2), liquid carbon dioxide (LCO_2), solid carbon dioxide (dry ice), liquid helium and air (usually temperatures above -50˚C).

Spraying cryogenic coolant at the cutting zone could reduce the chip-tool interface temperature and thus reduce the chemical reaction between the cutting tool and chips (Hong and Ding, 2001a, Bermingham et al., 2011b). This reduces the adhesion and diffusion wear of the cutting tool hence increase the tool life (Bermingham et al., 2011a). Elimination of BUE as a result of lower temperature could also increase the surface finish of the machined part (Hong et al., 2001a, Hong and Ding, 2001a, Abele and Schramm, 2008). Lower chemical reactivity also makes it possible to machine materials with cutting tools which are highly reactive at high temperatures. For instance, machining ferrous materials with diamond tools usually results in high tool wear due to chemical reaction between steel and carbon particles of diamond tools and graphitisation. Machining at

-196˚C using LN2 reduces both chemically and thermally induced tool wear in machining stainless steel components and significantly increases the tool life (Evans and Bryan, 1991). Similarly spraying LN2 at the cutting zone reduces the chemical reactivity and thermally induced tool wear between a titanium alloy workpiece and carbide tools (Wang and Rajurkar, 2000, Ke et al., 2009, Hong, 2001). For instance, as shown in figure 2.8, Venugopal et al. (Venugopal et al., 2007) reported that applying LN2 as a coolant in turning Ti-6Al-4V alloy resulted in 77% and 66% reduction in crater and flank wear respectively as compared to dry machining.

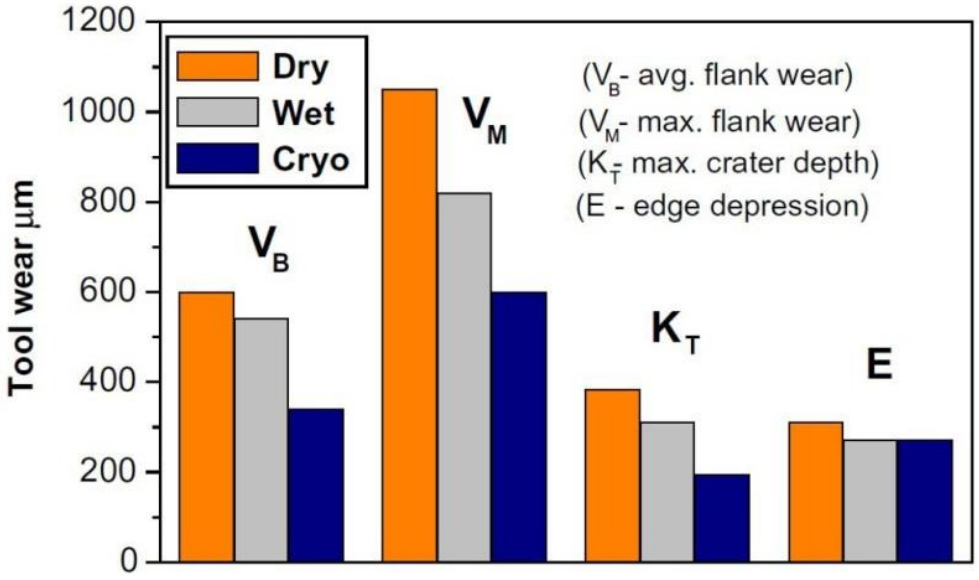

Figure 2.8 Comparison of tool wear in turning Ti-6Al-4V alloy with carbide tools under different machining environments (Venugopal et al., 2007)

Cryogenic cutting environment could also increase the strength and hardness of the workpiece material hence increasing the cutting forces (Hong and Zhao, 1999). Higher cutting forces could reduce the tool life, increase vibration and chatter and thus surface roughness. This flourishes the importance of the cooling strategy for machining different workpiece/tool material pairs as they might react differently to the low temperatures (Zhao and Hong, 1992).

Application of cryogenic coolants specifically LN2 could drastically increase the tool life and allow higher speeds (Bermingham et al., 2011b, Abele and Schramm, 2008, Pusavec and Kopac, 2009, Pusavec et al., 2010). It has been proven (Hong, 2006) that some cryogenic coolants such as LN2 do not only act as a coolant but has good lubrication characteristics. LN2 could be penetrated between the tool-chip interface and produce a gas/liquid cushion which reduces the friction at second shear zone (Hong et al., 2002,

Dhananchezian and Kumar, 2011). Very low temperature also increases the surface hardness of the sliding materials which could alter the coefficient of friction and friction forces resulting in enhanced machining condition (Hong, 2006, Hong et al., 2001a).

Air Products Inc. and MAG IAS LLC are two pioneering companies in the area of cryogenic machining. ICEFLY® is the first commercial equipment developed by Air Products for cryogenic turning which delivers liquid nitrogen into the cutting zone. The MAG cryogenic milling system delivers liquid nitrogen through the CNC milling machine tool's spindle to the cutting zone. The latter has been recently approved by the US government to be used in the production line of the Lockheed Martin's F-35 Lightning II stealth fighter (Lockheed Martin Co., 2011).

2.4.4. Air cooling

Employing chilled and compressed air for cooling in machining operations is a relatively new technique which has attracted many researchers (Brandao et al., 2008, Gisip et al., 2009, Kim et al., 2001, Liu and Kevinchou, 2007, Su et al., 2006, Sun et al., 2010, Yalcin et al., 2009). As in this technique the cooling media is air, it could be defined as the cleanest and most environmentally friendly method of cooling in cutting operations. Most studies (Yalcin et al., 2009, Sun et al., 2010, Su et al., 2007) indicated that using chilled air as coolant in machining resulted in longer tool life. The effect of chilled air on the surface finish is highly dependent on the machining parameters. In general it could be claimed that air cooling produces lower surface roughness than dry cutting. However, the produced surface roughness is higher than that made by MQL or emulsion coolant (Rahman et al., 2003a, Su et al., 2007, Yuan et al., 2011).

Liu and Kevinchou (2007) studied the effects of chilled air produced by a vortex tube in turning A390 aluminium with an uncoated WC tool. Studies showed that at the cutting speed of 300 m/min and feed rate of 0.055 mm/rev chilled air reduced the flank wear by 20%. In addition, the cooling system was found to be effective in reducing the tool-chip contact temperature up to 7%. Furthermore, employing chilled air as a coolant reduced the cutting forces during the operation mainly due to reductions in adhesion and BUE at the cutting edge. However, it should be noted that the effectiveness of the system on the tool life is highly dependent on the process parameters. It could be explained by the fact that in machining A390 aluminium the main tool wear mechanism is abrasion by hard and abrasive silicon particles in the material structure which is not a thermally controlled

parameter. Rahman et al. (2003a) reported that in end milling AISI P-20 steel with uncoated WC tool machining at -30°C produced lower surface roughness than flood cooling only at higher feed rates. Whilst at the feed rate of 0.01 mm/tooth chilled air cooling produced the highest surface finish, increase in the feed rate reduced the surface finish where at the feed rate of 0.02 mm/tooth chilled air resulted in the lowest surface roughness irrespective of the cutting speed.

Kim et al. (2001) declared that while using chilled air increased the tool life up to 3.5 in machining hardened steel with TiAlN coated WC, no significant changes has been observed in machining Inconel® 718 at high cutting speeds. Although at low cutting speeds the tool machined 2.2m of the workpiece material using chilled air compared to 1.4m in dry machining. This could be explained by poor thermal conductivity of air where at high cutting speeds the generated heat surpasses the cooling effect of the chilled air. A similar effect was observed by Sun et al. (2010) where they used cryogenically cooled air and compressed air in turning Ti-6Al-4V. They also found that while chilled air cooling increased the cutting forces, the average cutting forces reduced in comparison with dry machining due to reduction in the tool wear. They reported that in dry machining cutting forces along the x, y and z axes increased by 54%, 41%, 23% respectively, while it was 30%, 16% and 6% for compressed air and 17%, 7%, 4% for cryogenically cooled air. However, studies revealed that this is not the case in milling operations. In drilling CFRP, Nor Khairusshima et al. (2013) found that using chilled air at -10°C can significantly reduce the tool wear as compared to machining at ambient temperature. They reported that the improvement was more significant at higher cutting speed and feed rates.

In order to improve the cooling effect of MQL some researchers (Su et al., 2007, Su et al., 2006, Yuan et al., 2011) have integrated chilled air and MQL. Yuan et al. (2011) stated that by using chilled MQL the tool life increased by a factor of three in machining Ti-6Al-4V using uncoated WC cutting tool. In addition, they noted that the best results in terms of tool life and surface roughness was achieved by using MQL at the temperature of -15°C compared to dry, wet, MQL at 0°C, -30°C and -45°C. Su et al. (2007) declared that chilled MQL produced lower surface roughness as compared to chilled air and dry conditions in machining Inconel® 718 using TiAlN coated WC tool. They found that the dominant tool wear mode regardless of cutting environment was nose wear. Thus, the enhancement in the surface roughness was attributed to the increase in the tool wear resistance by using chilled MQL. They reported that respectively 78% and 124% increase in the tool life has been

achieved by using chilled air and chilled MQL in comparison with dry cutting. Yalcin et al. (2009) stated that dry machining of ductile materials is not favourable as it does not provide acceptable tool life and surface finish. They recommended chilled air as an environmentally friendly and cheap alternative to conventional flood cooling.

2.5. Critique and research gaps

In this section the findings of the review of difficult-to-machine materials and their properties together with coolants commonly used in material cutting operations are critiqued. In addition, the problems associated with the use of conventional coolants and different techniques to reduce or eliminate the use of conventional cutting fluids in material cutting are discussed. Furthermore, the areas which require more study and investigation are identified.

2.5.1. Difficult-to-machine materials

Review of the literature on the machining of hard-to-cut materials revealed that there is no standardised format to categorise difficult-to-machine materials and their definition is still vague. Based on findings in the literature the author has classified the difficult-to-machine materials into three categories namely: hard materials, ductile materials and non-homogeneous materials. This classification and its sub-categories are demonstrated in figure 2.9. While advances in the metallurgy of engineering alloys have led to an improved service life of the components, they have resulted in difficulties in their machinability. The main properties to consider these materials as hard to machine, are high hardness and strength together with poor thermal conductivity which can result in short tool life, low productivity and poor surface quality (Jaffery and Mativenga, 2008, Zhang et al., 2009, Ezugwu et al., 2003, Ghani et al., 2013). On the other hand another category of materials such as polymers and low carbon steels which are considered to be difficult-to-machine exhibit high ductility and elongation percentage. The main problems in machining these materials are the chip formation, geometrical accuracy and surface quality of the machined components (Hong and Ding, 2001b, Hong et al., 1999, Kakinuma et al., 2008). Composites are also known as difficult-to-machine materials due to short tool life and/or poor surface quality. This is mainly attributed to the fact that composites are made of a combination of different materials with different properties which are neither homogenous nor chemically combined. Thus, defining the cutting parameters to deal with the

characteristics of all materials, individually within a composite material and the whole composite together is very difficult.

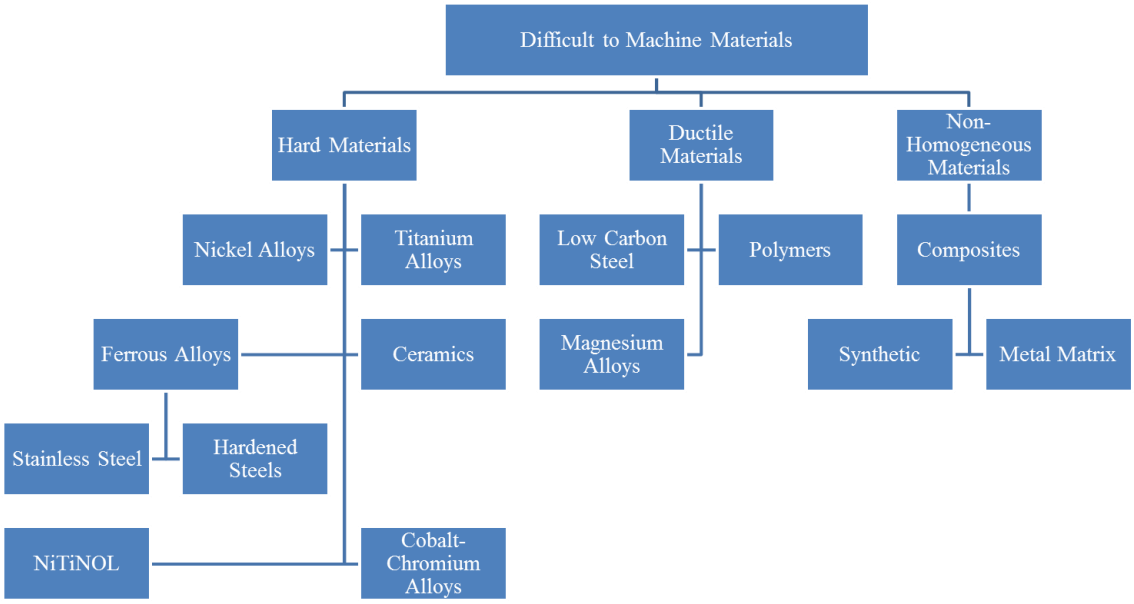

Figure 2.9 Classification of the difficult-to-machine materials

2.5.2. Coolants and environmentally conscious machining

Using cutting fluids is a traditional approach for reducing the temperature and friction at the cutting zone (Aggarwal et al., 2008). Astakhov (2006) identified that a systematic method is required to quantify and compare the performance of different cutting fluids in machining. Despite the wide usage of cutting fluids in industry to the best of the author's knowledge there is not any standard format to classify the cutting fluids and their usage. Due to the presence of dangerous constituents such as chlorine and microbial growth in the cutting fluids, they are considered as hazardous substances for the workers' health and environment. In addition, extending governmental and environmental regulations have limited the usage and increased the costs associated with cutting fluids (Feng and Hattori, 2000, Klocke and Eisenblätter, 1997, López de Lacalle et al., 2006, Hong and Broomer, 2000). Another approach to improve the tool life and surface quality of the machined surface is to control the cutting parameters and specifically the cutting speed. However, this method fails to satisfy the today competitive manufacturing market requirements for higher productivity at higher quality and lower prices.

The best approach to reduce the usage and costs of using cutting fluids is to not use them at all (Klocke and Eisenblätter, 1997, Sreejith and Ngoi, 2000). However dry cutting fails to produce desired tool life and surface finish in some cases. Due to the excessive generation of heat at the cutting zone and direct relation between the cutting speed and cutting temperature, dry cutting has a limited available cutting speed based on the cutting tool and workpiece materials. In order to realise the dry machining, improved cutting tool materials and further studies on the cutting parameters is inevitable. However, most advanced cutting tools are very expensive which can result in higher machining costs.

MQL is introduced to reduce the heat generation at the cutting zone by lubricating the cutting zone by delivering lubricants just at the required point (Sharma et al., 2009, Dhar et al., 2006). While MQL is an effective way to lubricate the cutting zone, reduce the heat generation, extend the cutting speed limits and reduce the usage of the cutting fluids, it is not an effective cooling method (Li and Liang, 2007, Su et al., 2007). This is the case especially in machining engineering alloys where the temperature at the cutting zone could reach the melting point of the workpiece materials (Su et al., 2007). In addition, the main environmental problem in MQL is the fact that cutting fluids are still in use. Using air as coolant has been studied for several years. However it is known that air has poor thermal conductivity and cooling capability. Thus, some researchers used chilled air to cool the cutting zone although the effect of the chilled air on the machinability is not consistent and is highly dependent on the cutting parameters and tool-material pairing (Kim et al., 2001, Liu and Kevinchou, 2007, Rahman et al., 2003a).

Using liquefied gases and specially LN2 is also suggested as an approach to eliminate the use of cutting fluids in the machining operations while improving the general machinability. Using cryogenic LN2 is acknowledged as an effective technique to improve the tool life (Bermingham et al., 2011b). However the literature has revealed that the effects of cryogenic cooling are not consistent for all tool-workpiece material pairs and cryogenic cooling techniques. The main reason behind this is that cryogenic temperatures change the properties of the tool and workpiece materials but to a different extent. Thus different workpiece-tool material pairs should be studied individually and the appropriate cryogenic cooling technique should be defined for them. Figure 2.10 illustrates different environmentally conscious machining techniques which have successfully reduced or eliminated the use of conventional cutting fluids in material cutting operations.

It has been found that none of the above mentioned techniques could be mentioned as a general method to be used for all tool-piece material pair. Indeed at the current stage each of the techniques has benefits and disadvantages.

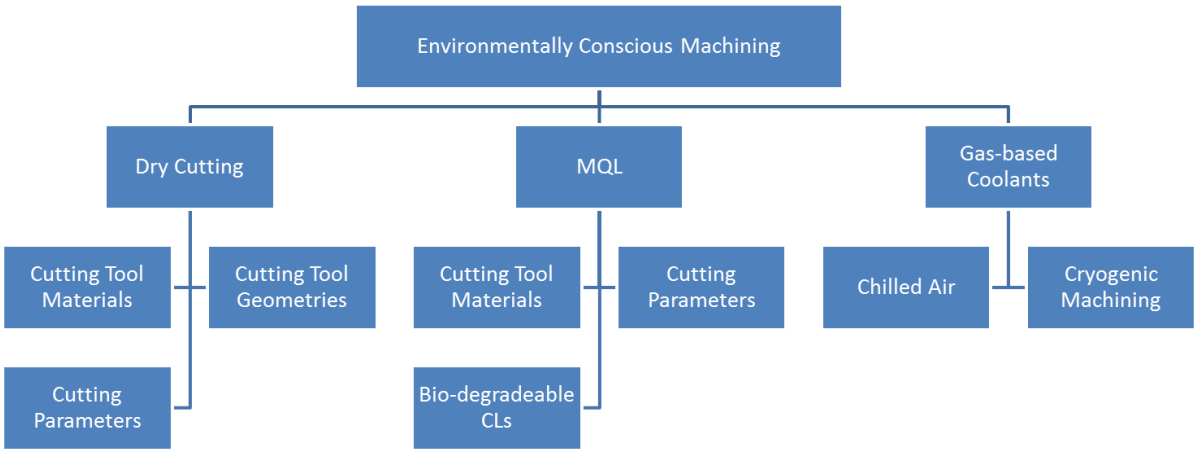

Figure 2.10 Classification of different environmentally conscious machining techniques

2.6. Summary

In this chapter materials which are generally known as difficult-to-machine have been reviewed and classified into three major categories namely, hard materials, ductile materials and non-homogeneous materials. Furthermore the material properties which make these types of materials difficult to machine have also been identified. In general, the materials which have one or more of the machining characteristics bulleted below, could be defined as difficult-to-machine, however these criterion need to be quantified.

- High cutting temperature;
- Short tool life;
- Poor surface quality;
- Poor geometrical accuracy;
- Poor chip formation.

Though, as a result of this review it has been found that the area of difficult-to-machine materials is still vague and requires further research.

Different types of coolant/lubricants currently in use in machining industries were reviewed and the drawbacks of using conventional cutting fluids were defined. The major drawbacks are the environmental and health impacts with the costs associated with their

use, maintenance and disposal. It has been found that no standard exist to classify the cutting fluids and their usage criteria.

Different machining techniques used to reduce or eliminate the use of conventional cutting fluids in material cutting have also been reviewed in this chapter. The most common machining techniques to reduce or eliminate the use of conventional cutting fluids were identified as

- Dry machining,
- Minimum quantity lubricant (MQL),
- Chilled air, and
- Cryogenic machining.

Due to the difficulties in machining difficult-to-machine materials, none of the above techniques have been found to be a complete alternative for cutting fluids. As a result, further research on cooling techniques, cutting tool materials, cutting parameters and tool geometries has been identified as essential and has potential to provide significant advantages.

Chapter 3*

State-of-the-art cryogenic machining and processing

*This chapter is an updated version of Shokrani et al., 2013

3.1. Introduction

Generally the term cryogenics refers to the science of very low temperatures. Though, this is not specifically defined and can be referred to the temperatures lower than 120°K, the boiling point of air (Timmerhaus and Reed, 2007) or 100°K (Karassik et al., 2008). Typical cryogens are usually in the form of liquid gases and can be defined as liquid nitrogen (LN_2), oxygen, helium (LHe), methane, ethane and argon. However, in machining, sometimes temperatures higher than 100°K are also considered by some authors as cryogenics e.g. cryogenic machining using liquid and/or solid carbon dioxide (Abele and Schramm, 2008, De Chiffre et al., 2007, Machai and Biermann, 2011) and even chilled air at lower temperatures (Tsai and Hocheng, 1998, Yalcin et al., 2009).

The efforts on liquefying permanent gases goes back to the mid-18th century and the development of the first two thermodynamic laws, followed by liquefaction of oxygen (1877), nitrogen, hydrogen and finally helium in 1908 (Kalia, 2009, Timmerhaus and Reed, 2007, Dhokia, 2009). The word "cryogenic" was first used by Heike Kamerlingh Onnes in 1894 as an adjective in the title of his paper "On the cryogenic laboratory at Leiden and on the production of very low temperatures" (Timmerhaus and Reed, 2007).

The early industrial usage of cryogenic technology was limited to the use of liquid oxygen particularly in oxygen-acetylene welding and oxygen furnaces for steel production. The first usage of liquid oxygen for rockets fuels was reported in 1926 in combination with gasoline, followed by the development of alcohol-oxygen fuelled German V-2 rocket during Second World War (Timmerhaus and Reed, 2007, Edwards, 2003). The studies continued in the United States which led to the development of the Redstone rocket which was first launched in 1953. The successful launch of liquid parahydrogen-oxygen fuelled rockets and the development of thermonuclear bomb and further expansions of the space programmes in the United States led to rapid growth in gas liquefaction industries in the 1950's (Timmerhaus and Reed, 2007).

The application of cryogenic cooling in machining can be categorised into cryogenic processing of the cutting tools and cryogenic machining. The earliest use of a cryogen as a cutting fluid is reported by Reitz (1919) who used carbon dioxide in cutting operations. In cryogenic machining the cryogen medium is introduced into the cutting operation as a coolant in order to change the material properties and/or dissipate the heat generated at the

cutting zone. Cryogenic processing also known as cryo-processing is an extended heat treatment process in a heat treatment cycle and has been acknowledged since 1937 as enhancing tool material properties (Dasilva et al., 2006). In this chapter these two categories of cryogenic manufacturing are reviewed and discussed. In addition, the cryogenic machining technique is studied from different points of view, namely machinability and workpiece material.

This chapter has been published in Shokrani et al. 2013 and updated to include latest publications in the area of cryogenic machining.

3.2. Cryogenic processing of cutting tools

Cryogenic processing is defined as an extended quench process in the conventional heat treatment cycle. The advantages of cold processing have been known for centuries (Busch, 1969). In order to age and improve the stability and wear resistance of watch parts, Swiss watch makers would leave components in cold climates of the Alps for months (Kamody, 1999, Busch, 1969). While cryogenic processing can improve the properties and specially the wear resistance of all materials which contain retained austenite at the room temperature, (Sreeramareddy et al., 2009) the focus of the current chapter is on the cutting tool materials used in machining operations.

3.2.1. Steel-based cutting tools

The first application of cryogenic treatment on the tool materials is reported by Gulyaev (1937) which exposed high speed steel (HSS) cutting tool to the -80°C to -100°C temperatures for 30 to 60 minutes.

Retained austenite is a soft and ductile allotrope of iron which is unstable at room temperature. Under particular circumstances such as high temperature and pressure during cutting operation, it is likely to transform into martensite which can result in the propagation of micro-cracks. Existence of retained austenite in the cutting tools can result in the rapid tool wear and chipping on the cutting edge (Harris, 1970). Traditional quenching converts the majority of the austenite into martensite, though some percentage of the austenite will be retained in the material structure. This is attributed to the fact that the final martensite transformation temperature of eutectoid steel is -50°C, while traditional quenching is limited to the room temperature (Dasilva et al., 2006).

A typical cryogenic process in a traditional heat treatment cycle is as follows:

(1) Slow cooling to the LN_2 or LHe temperature
(2) Soaking in the LN_2 or LHe for a reasonable time
(3) Slow heating to the room temperature

This shows a general cryogenic cycle which is usually executed just after conventional quench processes. However, a single process or even heat treatment cycle cannot be recommended for all tool materials. Each cutting tool should be studied separately based on the cutting process requirements for hardness, toughness and wear resistance of the cutting tool (Gill et al., 2009). The cooling and heating rate to and from cryogenic temperature is particularly important as it can result in thermal shock, material deformation and propagation of micro-cracks. It is evident that some changes happen in the material properties when it is cooling down (ramp down) and when heated to the room temperature (ramp up) (Kalia, 2009). The cooling rate is defined as the third most significant parameter affecting the mechanical properties of steels. In addition to the cooling/heating rate the soaking time is another important parameter of the cryogenic treatment. This is due to the slower atomic movements at very low temperatures. Generally the entire cryogenic process including ramp down and ramp up takes approximately 36 to 72 hours depending on the work material and weight (Kalia, 2009).

Dasilva et al. (2006) reported that cryogenic treatment did not affect the hardness, micro-hardness and wear resistance of HSS tool materials, but reduced the wear resistance of TiN coated HSS milling tools. Though, cryogenic treatment increased the HSS drill tool life from 65% to 343% until catastrophic fracture. Ramji et al. (2010) cryogenically treated HSS drill bits and monitored the thrust force and torque as indicators of the tool wear in machining grey cast iron. They found that cryogenic treatment is an effective method to increase the wear resistance of the cutting tool and enhance the surface quality of the holes. Similar results have been reported by Firouzdor et al. (2008) in dry drilling of carbon steel. They reported that cryogenic processing can improve the HSS tool life by up to 126%. In addition, they studied the effect of tempering after the cryogenic process and revealed that it has the potential to improve tool life by 49% as compared to the non-tempered cryogenically treated tools (Firouzdor et al., 2008). Leskovsek et al. (2006) studied the effect of tempering temperature and cryogenic treatment on the M2 HSS tool wear

resistance and reported that generally cryogenic treatment improves the HSS tool wear resistance. It should be noted that in this study tempering temperature also affected the wear resistance of the tools significantly. The lowest tool wear was reported for the tools tempered at 600°C regardless of cryogenic treatment. Among the tools tempered at 600°C, the cryogenically treated tool performed slightly better than its counterpart which was only tempered. Molinari et al. (2001) studied the effect of different cryogenic treatment cycles (table 3.1) on the wear resistance of M2 HSS tool material. As shown in table 3.1, in contrast to the results obtained by Firouszor et al. (2008) and Leskovsek et al. (2006) the specimen which was not tempered after cryogenic treatment (B) showed the highest wear resistance. The researchers attributed the improvements to an increase in the material hardness due to cryogenic treatment and concluded that the highest improvements could be achieved if cryogenic treatments were carried out on the quenched and tempered steel (Molinari et al., 2001).

Specimen	Treatment	Wear rate ($g/m \times 10^{-6}$)
A	Quench + Temper + Temper	3.7
B	Quench + Temper + Temper + Cryogenic	1.8
C	Quench + Cryogenic + Temper	2.2
D	Quench + Cryogenic + Temper + Temper	2.4

Table 3.1 Cryogenic treatment cycle and wear rate of M2 HSS tool material (Molinari et al., 2001)

3.2.2. Tungsten carbide tools

Compared to tool steel materials, there is a very limited number of investigations on the effects of cryogenic treatment on the performance of tungsten carbide tools. Seah et al. (2003) performed a series of experiments in order to investigate the effect of cold and cryogenic treatments on the performance of uncoated tungsten carbide inserts in single point turning of ASSAB 760 carbon steel. They reported that at different cutting speeds, the cold and cryogenically treated inserts have shown more wear resistance than their untreated and quenched counterparts. In addition, it has been found that cold and cryogenic treatment have significantly improved the resistance of the cutting inserts to chipping which was more significant at higher cutting speeds. In another study, Young et al. (2006) cooled a set of uncoated WC inserts at a rate of 0.28°C/min (0.5°F/min) to -184.5°C (-300°F) where the inserts were kept for 24 hours and then heated to the room temperature at a rate of 0.28°C/min (0.5°F/min). Their experimentation consisted of a series of face milling operations at different cutting speeds where other machining parameters were kept

constant using cryo-processed and non-treated inserts. They found that while generally cryo-processed inserts performed better than their non-treated counterparts, the effect of cryogenic treatment on the tool life was more significant in wet machining as opposed to dry machining.

Sreemaredy et al. (2009) investigated the effect of cryo-processing on the performance of multi-layer coated WC inserts in turning operations by studying tool wear, cutting forces and surface finish of the machined parts. They reported that cryo-processing significantly reduced the flank wear of the inserts as compared to non-treated inserts resulting in lower cutting forces and surface roughness.

These studies suggest that cryogenic treatment of carbide tools has the potential to improve the productivity and quality through improved wear resistance and surface finish. Despite these achievements, the number of studies in this area is very limited and further investigations on the performance and micro-structure of the cryo-treated WC tools is inevitable.

3.2.3. Improvement theories of cryogenic processing

While cryogenic treatment is widely acknowledged by researchers as a technique to improve wear resistance and hardness of cutting tool materials, the underlying reason for these improvements are still unclear. There are several theories to explain the enhancement of the tool materials subjected to cryogenic processing, although none of them can completely explain the reason (Gill et al., 2011).

3.2.3.1. Austenite transformation

The first theory to explain the improvements in cutting tools subjected to the cryogenic treatment is the transformation of retained austenite in the material structure into the harder martensite allotrope (Preciado et al., 2006). It has been confirmed by X-ray diffraction that cryogenic treatment transforms almost all retained austenite into the martensite. It has been reported (Dasilva et al., 2006, Leskovsek et al., 2006) that the volume fraction of retained austenite in HSS material reduced from almost 25% to nearly 0% by cryogenic treatment. On the contrary, Molinari et al. (2001) compared the retained austenite percentage of two specimens (A and B in table 3.1) subjected to different heat treatment cycles. X-ray diffraction analysis revealed that both samples contain lower than 2% retained austenite

while sample B was harder and more wear resistant. Therefore, in this case transformation of residual austenite cannot explain the enhancements in the material properties of M2 tool steel.

3.2.3.2. Carbide precipitation and refinement

Another theory is that cryogenic treatment enhances the precipitation of carbide particles into the martensite matrix. This also results in lower internal stress in the treated material. In addition, it has been reported that cryogenic treatment refines the carbide particles and produces a more homogeneous carbide distribution in the material structure which may result in improved tool life (Firouzdor et al., 2008, Dasilva et al., 2006). Das et al. (2007) classified the carbide particles in the material into primary carbides (PC), large secondary carbides (LSC) and small secondary carbides (SSC). They found that the amount of LSC is significantly lower in cryogenically treated (Quench-Cryogenic-Temper (QCT)) samples than conventionally treated (Quench-Temper (QT)) samples (figure 3.1). In addition, as it is shown in figure 3.1, SSCs in the QCT samples were more uniformly distributed and finer. Furthermore, Energy-Dispersive X-ray (EDX) spectroscopy showed that cryogenic treatment produces secondary carbides which are richer in alloying elements.

Moreover the chemical composition of LSC and SSC in the QCT samples was found to be similar, while in QT samples LSCs were richer in alloying elements as compared to SSCs.

It should be noted that generally these mechanisms (carbide precipitation and refinement) require further tempering after the cryogenic treatment to be performed and cannot explain the improvements in the non-tempered cryogenically treated materials as discussed by (Molinari et al., 2001).

3.2.3.3. Formation of μ phase in the material microstructure

Unlike ferrous materials, no martensite phase exists in tungsten carbide tools, therefore another mechanism should explain any improvements (Yong et al., 2006). Stewart (2004) attributed the improvements to the change in the formation of cobalt binders as tungsten carbide crystal is a stable structure in the carbide tools. This could explain the tool life improvement by enhancement in the cobalt binder micro-structure where more cobalt binder is retained during the machining operation. Seah et al. (2003) classified the microstructure of tungsten carbide tools into four categories namely:

- α phase: tungsten carbide particles
- β phase: cobalt binders
- μ phase: multiple carbides of tungsten and at least one other binder metal (e.g. Ti, Fe, etc.)
- γ phase: carbide of cubic lattice

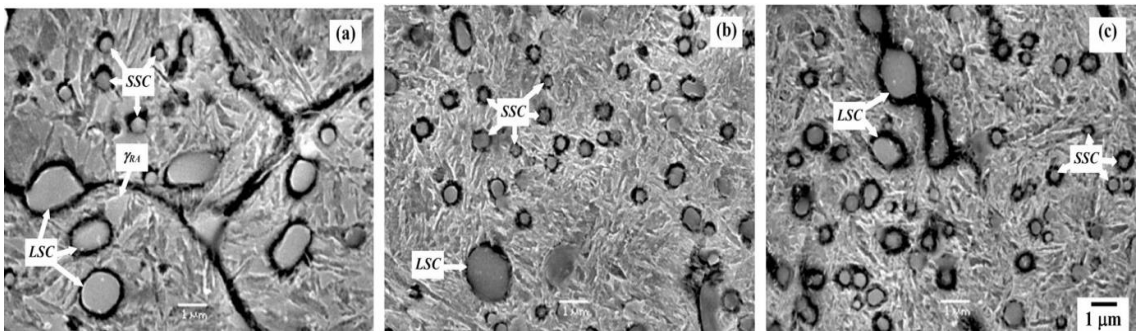

Figure 3.1 SEM images of microstructure of a) Quenched and tempered, b) quenched, cryo-treated for 36hrs and tempered, c) quenched, cryo-treated for 84hrs and tempered (Das et al. 2007).

Electron microscopy of the microstructure of the material revealed that the cryogenic treatment does not affect α and β phases of the material. Investigations between treated and non-treated specimens revealed that no μ phase existed in non-treated tools while the μ phase appeared after the material was subjected to the cryogenic process. Consequently, changes in the material properties could be attributed to the formation of μ phase in the material microstructure. The presence of μ phase in the material is known to decrease the fracture toughness. On the contrary, as μ phase is harder than the rest of the material, it enhances the wear resistance of the cutting tool. Therefore, the growth of μ phase through the material should be controlled so as to reach the optimum hardness while not affecting the fracture toughness (Seah et al., 2003). Despite the fact that cryogenic processing can change the material properties of cutting tools, there is not any solid evidence to explain the changes in material properties subjected to cryogenic temperatures (Gill et al., 2009).

3.3. Cryogenic machining

Cryogenic machining is a term to describe the use of super cold liquefied gases as coolant in material cutting operations. The aim of this section is to review the effects of cryogenic cooling on the material behaviour during machining and on machinability parameters such as tool life, cutting temperature, surface integrity, etc.

3.3.1. Material behaviours at cryogenic temperatures

It has been known that a large proportion of the power consumed for material cutting transforms into heat at the cutting zone (Trent and Wright, 2000). This is particularly important in machining difficult-to-cut heat resistant materials such as nickel and titanium alloys, where the thermal conductivity of the workpiece material is very low resulting in very high temperatures at the cutting zone (Hong et al., 1993, Kitagawa et al., 1997, Arunachalam and Mannan, 2000). High temperatures at the cutting zone can affect the tool life, surface finish and geometrical accuracy of the machined part. One approach to dissipate the heat generated during machining is through cryogenic cooling. Cooling the cutting zone by using a cryogen not only cools the cutting zone but could also change the workpiece/cutting tool material properties. Generally, the hardness, modulus of elasticity and strength of materials increase at the cryogenic temperatures. Nevertheless, the effect of cryogenic temperatures on the physical properties, fracture toughness and ductility is not consistent for all materials (Zhao and Hong, 1992). Therefore, the study of material behaviour at cryogenic temperatures is an important parameter for defining the suitable cooling approach for machining.

The effect of cryogenic temperatures on the material properties of some materials have been studied by Zhao and Hong (1992) and Hong and Zhao (1999) in order to identify the most appropriate cryogenic cooling techniques. Their studies are summarised as follows:

Soft, low strength, ductile materials such as low carbon steels are usually considered difficult-to-machine due to their welding tendency and difficulties in chip formation. Low carbon steels have a unique ductility to brittleness temperature similar to the glass transition temperature in polymers. At temperatures lower than this temperature, ductility and toughness of the material reduces significantly which favours the machinability. In addition, cryogenic temperatures reduce the welding tendency of the material and reduce the formation of Built Up Edge (BUE). An increase in brittleness not only enhances the chip breakability but also reduces the cutting forces. Hence, it could be concluded that cryogenic cooling of the workpiece is the favourable cooling technique to enhance machinability (Hong and Zhao, 1999). A similar mechanism could be expected for polymer materials. Polymers have a distinctive glass transition temperature in which the polymers transform into a glassy state at the temperatures below it (Kakinuma et al., 2008).

This is attributed to the high thermal dependant material properties of polymeric materials. Reduction in the temperature increases the hardness and Young's modulus of the material drastically (Hübner et al., 1998). Hardness of some polymers at different temperatures is provided in table 3.2.

Another group of materials which react differently at cryogenic temperatures are high carbon steels. The strength and hardness of these materials increase drastically through the reduction in temperature. The hardness of AISI 52100 steel increases from 19HRc at room temperature to about 33HRc at -196°C. In addition, the material strength increases drastically from ambient to the LN_2 temperature while the reduction in toughness is not noticeable. Thus, it is clear that cooling the workpiece material is not favourable as it increases the material hardness and strength while it does not improve the machinability (Hong and Zhao, 1999, Zhao and Hong, 1992).

Temperature	293°K	77°K
Material	Hardness (MPa)	
PA 101	150	750
PTFE	33	450
UHMW	48	520
HDPE	62	550

Table 3.2 Hardness of some polymeric materials at room and cryogenic temperatures (Hübner et al., 1998)

Two other materials which were studied by the researchers are A390 cast aluminium and Ti-6Al-4V titanium alloy. The hardness of Ti-6Al-4V increases from 32HRc at ambient temperature to 42HRc at the LN_2 temperature while the material maintains its toughness and ductility to a large extent even at cryogenic temperatures. A390 cast aluminium is brittle in nature and has low impact strength due to the high silicon content in the material structure. Low toughness and ductility are two favourable characteristics for machining operations, though the presence of hard silicon particles results in poor machinability and abrasive wear. Cryogenic cooling of such materials could worsen machinability by increasing micro-hardness of the material.

Reduction in the temperature reduces the thermal conductivity of most materials including Ti-6Al-4V and Inconel® 718. This could exacerbate the conductive heat dissipation from the cutting zone at cryogenic temperatures (Marquardt et al., 2002). In addition, lowering the temperature lowers the significant heat capacity of the materials which could result in

unpredictable behaviour of the material subjected to cryogenic temperature during the cutting operation.

Based on the stated material behaviours at cryogenic temperatures it is clear that no single approach can be defined for cryogenic machining. Furthermore, it cannot be concluded that cryogenic machining is beneficial for machining all materials.

3.3.2. Tribological behaviour of materials at cryogenic temperatures and lubrication effects of liquid nitrogen

One of the parameters that affect tool life, cutting forces and surface finish of machined parts is the coefficient of friction (CoF) between the cutting tool and the workpiece material. Two main sliding zones in machining materials can be defined as sliding between the chips and the tool rake face resulting in abrasion and crater wear in the rake face and sliding between the machined surface and flank face leading to abrasive flank wear. In this section the effects of low temperatures on the tribological behaviour of the sliding materials and the lubrication effect of liquid nitrogen are investigated.

3.3.2.1. Tribological behaviour of materials at cryogenic temperatures

Generally, it is expected that cryogenic temperature changes the tribological behaviour of the sliding surfaces by increasing surface hardness and reducing the interface temperature. Though, it is not the case for all sliding pairs and is highly dependent on the sliding pair's coating and substrate materials (Ostrovskaya et al., 2001).

El-Tayeb et al. (2009) developed an apparatus to study the effect of spraying LN_2 into the sliding zone on the CoF between tungsten carbide wheel and two types of titanium pins made of Ti-5Al-4V-0.6Mo-0.4Fe (Ti54) and Ti-6Al-4V. It has been found that spraying LN_2 can reduce the CoF between carbide wheel and Ti54 pin up to 35% as compared to dry sliding. However, for the Ti-6Al-4V and tungsten carbide sliding pair LN_2 spray increased the CoF. This effect has been reported to be more significant at higher load and longer sliding time where spraying LN_2 has resulted in up to a 20% increase in the CoF.

As shown in figure 3.2, Hong (2006) developed an apparatus similar to pin-on-disk to study the effect of different cryogenic cooling techniques on CoF including (i) freezing tool specimen, (ii) freezing workpiece sample disk, (iii) freezing tool specimen and

workpiece disk simultaneously, (iv) spraying LN_2 into the sliding zone and (v) freezing the tool specimen and spraying LN_2 into the sliding zone simultaneously. A schematic view of the tests is provided in figure 3.3. In contrary to the previous study by El-Tayeb et al. (2009), Hong (2006) reported that cryogenic cooling of the Ti-6Al-4V and/or uncoated tungsten carbide sliding pair (concepts i, ii and iii) reduced the CoF significantly. This effect increased when both parts were cooled simultaneously (concept iii). On the contrary, Cournon et al. (2014) reported that neither gaseous nor liquid nitrogen are capable of altering the CoF when Ti-6Al-4V and WC pair are sliding. However, it stated that LN_2 can significantly reduce the CoF for Inconel® 718 and WC pair.

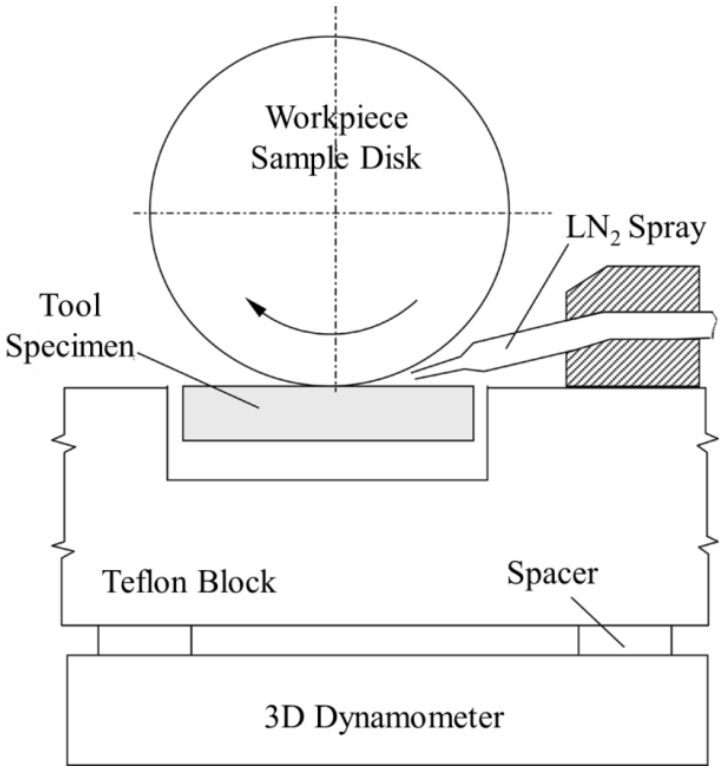

Figure 3.2 A schematic view of an apparatus similar to pin-on-disk developed by Hong (2006) for studying the tribological behaviour of materials at cryogenic temperatures and lubrication effect of LN_2

Further studies (Hong, 2006, Hong et al., 2002) on the effect of cryogenic temperatures on the tribological behaviour of materials revealed that cryogenic cooling alters the material properties and surface hardness resulting in lower CoF. Nevertheless, this effect is highly dependent on the sliding materials. For instance, cryogenic cooling reduces the CoF between AISI 1018 steel-uncoated tungsten carbide and Ti-6Al-4V-uncoated tungsten carbide pairs while it increases the CoF when AISI 1018 and Ti-6Al-4V disks are sliding on a CVD (TiN,TiCN,TiC) triple coated carbide tool specimen. This is also the case for an

AISI 1018 specimen sliding on a disk of the same material (Hong, 2006). Where cryogenically cooled AISI 1018 steel or Ti-6Al-4V sample is sliding against a solid lubricant CVD triple coated tungsten carbide disk, increases in the load resulted in lower CoF which could be explained by increased temperature at the sliding zone. Higher sliding temperatures could surpass the cooling effect of cryogen media and activate the solid lubricant hence reducing the CoF. Under this condition the sliding nature becomes closer to that of dry sliding at room temperature. The reduction rate of the effective shear strength with the decrease in temperature of some metallic materials is lower than the reduction rate of their yield stress. The CoF of these metals could be altered by reduction in the interfacial temperature by properly applied cryogenic cooling (Hong et al., 2002).

Cryogenic temperature changes the material properties of the polymeric materials such as polytetrafluoroethylene (PTFE) and polyamide 6. Hübner et al. (1998) stated that changes in the polymeric material properties due to cryogenic temperature results in reductions in frictional forces when sliding against a steel disk.

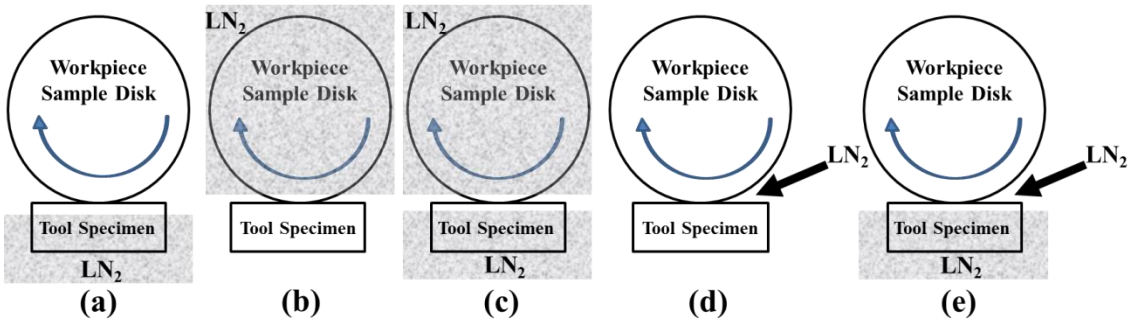

Figure 3.3 Different cooling techniques studied by Hong (2006) to investigate the lubrication mechanism of LN_2 and tribological behaviour of materials at cryogenic temperatures. (a) Freezing tool specimen; (b) freezing workpiece disk specimen; (c) freezing tool and workpiece specimens simultaneously; (d) spraying LN2 into the sliding zone and (e) freezing the tool specimen and spraying LN2 into the sliding zone simultaneously.

3.3.2.2. Lubrication effects of liquid nitrogen

In addition to the effects of low temperatures on the tribological behaviour of materials, Hong (2006) also studied the effect of spraying LN_2 between the sliding surfaces using a device similar to pin-on-disk test (figures 3.2, 3.3a and 3.3b). As a result of the studies, the researcher stated that LN_2 forms a lubrication film between the sliding surfaces resulting in lower CoF. He also stated that unlike cryogenic cooling, the lubricating effect of LN_2 is independent of sliding materials and can reduce the CoF effectively. For instance, in the

case of sliding against solid lubricant coated carbide where cryogenic cooling increased the CoF, penetrating LN_2 between the sliding surfaces reduces the CoF as compared to dry sliding. In another pin-on-disk set of experimentation, El-Tayeb et al. (2010) also reported that LN_2 forms a boundary film between the sliding surfaces which reduces the wear and CoF. However, Hong et al. (2002) argued that in machining operations, LN_2 cannot provide a boundary lubrication similar to conventional lubricants. LN_2 evaporates quickly at the cutting zone and it is very difficult to keep it between the sliding surfaces. Therefore, the lubrication effect of LN_2 is attributed to the formation of a hydraulic cushion of LN_2 between the sliding surfaces provided by the spraying pressure which carries a portion of normal loads (Hong et al., 2002, Hong et al., 2001a). This could explain the increase in the CoF as a result of increases in the normal load where the LN_2 is squeezed from the contact area or cannot be penetrated into it due to low spraying pressure. Jun (2005) developed three models based on force component projection, geometrical relationship and vector manipulation in order to evaluate the machining forces and calculate the normal and friction forces in turning. The results are then used to specify the CoF at the cutting zone. He used the models to investigate the lubrication effect of LN_2 sprayed on the rake and flank faces of WC cutting insert in machining Ti-6Al-4V and AISI 1018 steel. Empirical and computational investigations indicated that applying LN_2 significantly reduced the CoF in the machining of steel and titanium materials. It was found theoretically that spraying LN_2 into the cutting zone could reduce the CoF by 0.3 and 0.4 for Ti-6Al-4V and AISI 1018 steel respectively. Although in practice, the cooling mechanism reduced the CoF by 0.27 in machining Ti-6Al-4V and 0.35 for the AISI 1018. In addition, it was found that LN_2 spraying is more effective at high cutting speeds in machining AISI 1018. This is due to increases in the material hardness due to low temperatures at lower speeds which surpasses the lubrication effect of LN_2.

Hong et al. (2002) summarised the effects of spraying LN_2 between the sliding surfaces as:

- Changes in the material properties of sliding pairs;
- Formation of a liquid/gas film between the sliding surfaces reducing the contact area resulting in lower friction forces;
- Reduction in interfacial temperature resulting in the modification of the sliding surfaces by reducing the chemical reactivity and welding tendency;

- Increasing the surface hardness of the sliding materials and reducing the tendency of CoF to be increased over time.

3.3.3. Cryogenic cooling techniques in machining operations

Different techniques have been adopted in order to apply the cooling effect of cryogenic media into the cutting process. These techniques can be classified into workpiece cooling, cutting zone and/or chip cooling and indirect cutting tool cooling (Yildiz and Nalbant, 2008) or the combination of these techniques. Though, defining a clear border between these techniques is not applicable due to the complex nature of the cutting process especially in intermittent operations. In addition each technique consists of some subcategories which are further discussed in following sections.

3.3.3.1. Cutting zone cooling

One of the most widely researched methods of using cryogenic coolants is spraying the cooling media into the cutting zone or the tool-chip contact area. Different approaches have been implemented to penetrate the coolant media into the cutting zone. The main objective of this technique is to dissipate the heat generated during the cutting operation, cool down the cutting tool, enhance the cutting tool properties and alter the CoF, while preventing alterations in the workpiece material properties.

Cryogenic cooling of the cutting tool reduces the chemical reactivity of the tool material resulting in lower adhesion and diffusion wear. Bermingham et al. (2011a) reported that while cryogenic cooling is not capable of reducing cutting temperature to a point that prevents diffusion and attrition wears, it significantly reduces the wear rate and extends the tool life. At cryogenic temperatures the cutting tools become harder, thus lower abrasive wear is expected. Lower tool wear means that the cutting edge can literally remain intact for a longer time resulting in improved surface roughness as compared to dry machining.

In order to spray the cryogen into the cutting zone two approaches are common namely: 1) using an external nozzle and 2) modifying the cutting tool or tool holder. As the cryogen cannot be circulated in the machine tool, economical consumption of the cryogen is very important. Hence, the most economical approach is to bring and penetrate it at the exact point where it is required (Hong and Ding, 2001a).

Axer (1954) modified a carbide tool by drilling a hole in the flank face of the tool to spray cryogen into the cutting zone. Hong (1999) integrated a chip breaker and a cryogenic nozzle and developed an innovative LN_2 spraying device for turning applications. As shown in figure 3.4, the device was designed to spray LN_2 on the rake face and/or flank face of the cutting tool. The chip breaker helps to raise the chips and let the LN_2 penetrate into the tool-chip contact area effectively. Experimental investigations (Hong and Ding, 2001a) revealed that the most effective approach is spraying the cryogen simultaneously on both the flank and rake face to cover both flank and crater wear zones. They also found that the effect of cooling the rake face is more significant than the flank face. Bermingham et al. (2011a) noted that in turning of Ti-6Al-4V alloy, spraying LN_2 simultaneously on the rake and flank faces and the nose of the tool yields to the highest tool life improvement as compared to other cooling methods. Dhananchezian and Kumar (2011) modified an ISO K10 CNMG 120408 MP1-KC 5010 carbide insert. Dhar et al. (2002b), Venugopal et al. (2007b, 2007a) and Kenda et al. (2011) used a set of external nozzles to impinge LN_2 along the main and auxiliary cutting edges of carbide inserts. The objective of their nozzles was to cover the rake and flank face of the cutting tool by LN_2 and penetrate the cryogen into the chip-tool contact area. While LN_2 could reach close the cutting zone and reduce the cutting temperature, it failed to penetrate into the chip-tool contact zone. Machai and Biermann (2011) modified the clamping jaw of the cutting insert and delivered liquid carbon dioxide (LCO_2) to the cutting zone through two holes in the clamping jaw. It has been reported that the CO_2 stream has failed to reach the tool-chip contact area and reduce the chemical affinity of the titanium alloy workpiece.

For milling operations, Nalbant and Yildiz (2011) designed an external jet system to spray LN_2 into the tool-workpiece interface. They reported that the system cooled the cutting tool and the workpiece together and resulted in over hardening of the workpiece material. Biermann and Heilmann (2010) designed two delivery systems for face milling operations in order to reduce burr size in machining aluminium alloy workpiece. The first system was stationary in relation to the workpiece, while the second system consisted of five nozzles placed around the face mill cutting tool and was fixed in accordance to the feed motion of the cutting tool. Experiments illustrated that smaller burrs can be achieved by using the second cooling system.

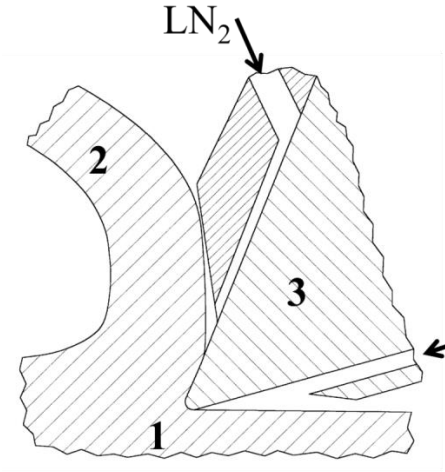

Figure 3.4 Cryogenic cooling device for turning operations with integrated chip breaker designed and patented by Hong (1999). 1- workpiece, 2- chip, 3- cutting tool.

3.3.3.2. Workpiece cooling

Cryogenic cooling of the workpiece material before or during the cutting operation is one of the most widely used cryogenic machining techniques. The main objective of this technique is to change the material properties of the workpiece in order to enhance machinability. To cool the workpiece two methods are commonly used, namely cryogenic bath and/or cryogenic spray. In cryogenic bath cooling the workpiece is usually submerged in a cryogen, while in workpiece cooling with spray jets the cryogen is sprayed onto the workpiece during machining and just before the cutting operation.

Uehara and Kumagai (1968, 1970) developed two approaches for cooling the workpiece during turning operations. The first concept (Uehara and Kumagai, 1968) was to inject LN_2 into the workpiece through a copper tube placed in the main spindle of a lathe machine. The second system (Uehara and Kumagai, 1970) consisted of two copper tubes with holes facing the workpiece material acting as spraying nozzles. LN_2 was sprayed through the holes on the workpiece surface before the cutting zone. Ahmed et al. (2007) modified a PSBNR 2525 M12 standard turning tool holder to deliver LN_2 close to the cutting edge. The discharged nitrogen is sprayed onto the chips to increase chips embrittlement. Increased brittleness enhances chip formation for ductile materials which normally produce continuous chips in cutting operations.

Mishima et al. (2010), Kakinuma et al. (2008, 2012) and Dhokia et al. (2010) developed fixturing solutions for freezing elastomer workpieces of different materials and keep their

temperature below the glass transition temperature during machining operations. The glass transition temperature is a characteristic of polymer materials where the material transforms into a rigid and stiff glassy state (Kakinuma et al., 2008, Dhokia et al., 2010). This transition allows the material to withstand the cutting forces and make the machining operation possible. Kakinuma et al. (2008) cryogenically cooled a poly-dimethyl-siloxane (PDMS) workpiece using a specially designed fixture which contained LN_2 as a cooling media. They stated that cryogenic machining enhanced the machinability of PDMS drastically, however super cold temperature resulted in geometrical inaccuracies in the machined part. Truesdale and Shin (2009) used a nozzle to spray LN_2 for face milling Udimet 720 nickel based alloy. The nozzle was designed to pre-cool the workpiece just before the cutting operation without affecting the cutting tool.

3.3.3.3. Indirect cooling

In this technique the heat generated during machining is dissipated by conduction through the cutting tool. Traditional indirect cooling of the cutting tool also known as heat pipe consists of three sections namely evaporation, adiabatic and condensation. The heat generated at the cutting zone transforms into the evaporation section by conduction and evaporates the cooling fluid. The vaporised fluid is then transferred to the condensation section through the adiabatic unit. The vapour is then cooled and liquefied in the condensation section (Noorul Haq and Tamizharasan, 2005, Jen et al., 2002). In indirect cryogenic cooling of the cutting zone, there is no requirement for the adiabatic and condensation units, as the cryogen media does not require cooling and evaporates to the atmosphere after absorbing the heat.

The cryogen coolant is delivered to a chamber designed over or beneath the cutting tool. The cryogen absorbs the generated heat at the cutting zone through conduction and evaporates. The evaporated cryogen is then released to the atmosphere through the outlet of the chamber. The main objective of this technique is to freeze the cutting tool without direct contact between the cryogen and the cutting zone or workpiece.

Wang et al. (1996) designed a tool cap placed over the cutting tool so as to concentrate LN_2 over the cutting tool's back face. An identical design was used (Wang et al., 2003) for plasma assisted machining of Inconel® 718, while similar method was employed by Dandekar et al. (2010) for hybrid laser assisted turning of Ti-6Al-4V titanium alloy. The

laser beam was used to heat and soften the workpiece material while LN_2 was employed to freeze the cutting tool. Rozzi et al. (2011) designed a heat exchanger for a modified turning tool holder. The heat exchanger was placed under the cutting tool to transfer the heat from cutting tool to the LN_2 inside the heat exchanger. Ahmed et al. (2007) modified a PSBNR 2525 M12 standard turning tool holder to deliver LN_2 beneath the cutting tool. In their system, the LN_2 absorbed heat from cutting tool, evaporated and then released into the atmosphere away from the workpiece so as to prevent cooling of the workpiece resulting in hardening.

In this technique the cryogen is not in direct contact with the workpiece, therefor the negative effects of cooling the workpiece, such as geometrical deviations and increase in material strength and hardness could be eliminated (Wang and Rajurkar, 2000). However, the effectiveness of the technique is highly dependent to the cutting tool material properties.

3.3.4. Effects of cryogenic cooling from machinability point of view

In this section the effect of cryogenic cooling on the cutting forces, cutting temperature, tool life and surface integrity is reviewed.

3.3.4.1. Effect of cryogenic cooling on cutting forces

As clarified in previous sections, the application of cryogenic media in the machining operations can increase the hardness and strength of workpiece/cutting tool materials, change the material toughness, CoF, reduce the chemical reactivity and welding tendency of the workpiece/tool materials etc. The effect of using cryogenic coolant on the cutting forces and power consumption is highly dependent on the tool/workpiece material and cooling technique. Indeed, it cannot generally be concluded that cryogenic cooling can result in reductions or increases in cutting forces.

Aggarwal et al. (2009) studied the cutting parameters of turning operations of AISI P-20 steel using TiN coated tungsten carbide tools in order to optimise the turning cutting forces. They found that the environment is one of the most significant parameters for cutting forces. Despite the 10% increase in the material hardness at the cryogenic temperature, they concluded that the cryogenic environment is desirable in order to achieve the lowest cutting forces (Aggarwal et al., 2009). A similar conclusion was drawn for

optimisation of power consumption, where the cryogenic environment was found to be the most significant parameter (Aggarwal et al., 2008b). Spraying LN_2 on the crater and flank faces of uncoated carbide tools has been reported by Paul and Chattopadhyay (2006) showing significant reductions in cutting forces when machining different steels, namely AISI 1040, AISI 1060, AISI E4340C, AISI 4140 and AISI 4320. Similarly it has been stated (Dhar et al., 2002a, Dhar et al., 2002d) that cryogenic turning resulted in significant reductions in cutting forces in machining AISI 1040 and AISI 4320 steels as compared with dry machining. Jainbajranglal and Chattopadhyay (1984) attributed reductions in cutting forces in machining carbon steel materials to the transformation of chip formation into brittle fracture and reduction in the formation of BUE on the cutting edge.

In contrary to these papers, it has been indicated (Dhananchezian et al., 2009) that the application of LN_2 to the rake face of the cutting tool in machining AISI 1040 and 6061-T6 aluminium increased the cutting forces by 15% and 10% respectively. Hong and Ding (2001b) declared that the application of the cryogen increased the cutting forces by 8% in turning AISI 1008 low carbon steel with an uncoated tungsten carbide tool. This could be attributed to the different cooling techniques used by the researchers. For instance, Dhar et al. (2002a) modified a carbide insert in order to inject LN_2 into the cutting zone while the Hong and Ding's (2001b) concept was to cool the rake face together with the chips so as to enhance chip breakability. Jun (2005) experimentally studied the effect of material hardening on the cutting forces in turning AISI 1018 steel. He found that applications of LN_2 at higher speeds could reduce cutting forces, while at lower cutting speeds the lubrication effect is surpassed by an increase in the material hardness. Therefore, the researcher concluded that to obtain the lubrication effect of LN_2 it should be penetrated into the chip-tool interface. It is noteworthy to mention that one of the problems in investigating the lubricating effect from cutting forces is that other affecting parameters, such as material properties of sliding pairs and tool-chip contact area are being neglected. For instance, in this paper the lubrication effect has been attributed to the changes in the material properties and not to the lubrication effect of the LN_2 itself. However, in order to understand the real mechanism of reduction in the CoF, further studies considering other involving parameters are required.

In machining AISI 202 stainless steel it has been reported (Kalyankumar and Choudhury, 2008) that spraying LN_2 on the cutting edge reduced the cutting forces by up to 14.83% in

comparison with dry machining. Nalbant and Yildiz (2011) used an external nozzle to spray LN_2 into the tool-chip interface in milling AISI 304 stainless steel. They stated that the cryogenic temperature resulted in excessive increases in the workpiece material hardness. Applying LN_2 increased the cutting forces by 6.5%, 5.6% and 3.3% along the X, Y and Z axes respectively. It also increased the spindle torque by 7.9%. In addition, further studies on the effect of cooling the workpiece by LN_2 in turning AISI 304 stainless steel illustrated that cryogenic cooling of the workpiece is not favourable as it leads to drastic increases in material hardness and thus cutting forces (Uehara and Kumagai, 1968, Uehara and Kumagai, 1970).

Dhananchezian and Kumar (2011) reported that in turning Ti-6Al-4V with a modified PVD TiAlN coated carbide tool, application of cryogenic coolant on the rake face reduced the main cutting force and feed force by 38% and 39% respectively as compared to wet machining. Bermingham et al. (2011b) studied the effect of cryogenic cooling of the rake and flank faces of a WNMG 120408 MF1 WC carbide tool with an integrated chip breaker in turning Ti-6Al-4V material. LN_2 was delivered through the tool holder to the rake face and an external nozzle was used to spray LN_2 on to the flank face. Experimental measurements of the cutting forces revealed that this technique reduced the main cutting force and increased the thrust force, whereas this did not change the feed force significantly, regardless of the cutting parameters. Similarly, it has been reported that in turning Ti-5Al-4V-0.6Mo-0.4Fe titanium alloy, using LN_2 as coolant results in a reduction in all cuuting forces (Yap et al., 2013). Ke et al. (2009) stated that the application of cryogenic cooling in high speed milling (HSM) of Ti-6Al-4V by TiAlN coated carbide tool resulted in 32.7% reduction in the cutting force. It has been attributed to the enhanced chip flow and reduction in BUE and tool wear (Ke et al., 2009). In turning Ti-10V-2Fe-3Al alloy with TiAlN-TiN coated carbide with CNMG 120404 geometry the application of LCO_2 reduced the main cutting and feed forces while formation of CO_2 snow on the surface resulted in higher radial forces as compared to emulsion cooling (Machai and Biermann, 2011). Hong et al. (2001a) studied the effect of different cryogenic cooling concepts on the cutting forces in turning Ti-6Al-4V workpiece using uncoated WC cutting tools. The cooling concepts were spraying LN_2 on the i) rake face, ii) flank face and iii) rake and flank face simultaneously. The researchers concluded that cryogenic machining regardless of cooling technique increases the thrust and main cutting forces, while reducing

the feed force. Experiments showed that spraying LN_2, simultaneously on flank and rake face resulted in the highest increase in cutting forces as compared to the other two techniques. Hence, it was found that extra cooling of the workpiece resulted in increased cutting forces. In addition, the reduction in the feed force was attributed to the lubrication effect of LN_2. However, the conclusion of this study is in contrast with previously stated research in machining Ti-6Al-4V titanium alloy.

Wang et al. (2002) indirectly cooled a H13 carbide insert with cobalt binders in turning tantalum. They found that up to 60% reduction in cutting forces can be achieved using this technique. Wang et al. (2003) used a similar cryogenic cooling technique for plasma-enhanced hybrid turning of Inconel® 718. A plasma beam was employed in order to heat and soften the workpiece material just before cutting. In addition, a cooling cap was placed on the silicon carbide whisker reinforced alumina ceramic cutting insert so as to cool the cutting tool using LN_2. The technique resulted in a 30%-50% reduction in cutting forces as compared to conventional dry machining. They attributed the enhancements to 1) the lower workpiece material hardness and strength due to plasma heating and 2) increase in the cutting tool material strength and hardness due to cryogenic cooling. In machining Udimet 720 nickel based alloy, Truesdale and Shin (2009) suggested that cryogenic conventional-milling is more favourable than cryogenic down-milling and dry machining as lower cutting forces are produced in this method. Interestingly while cryogenic cooling of the workpiece reduces the cutting forces in conventional-milling, it yields to higher cutting forces in down-milling as compared to dry machining.

As discussed above, it has been found that the cooling approach and workpiece material are two important phenomena that affect the cutting forces. Similar cooling techniques could yield different results in machining different materials. In addition, different results could be obtained by different cooling techniques in machining similar materials.

3.3.4.2. Effect of cryogenic cooling on cutting temperature

Cutting temperature is an important phenomenon in machining operations, which affect tool life, power consumption, cutting forces, surface finish and geometrical accuracy of machined parts. It is more important in machining difficult-to-machine materials where the thermal conductivity of the workpiece material is very low. The generated heat at the

cutting zone cannot be effectively dissipated through the workpiece or chips. This would result in very high localised temperatures at the cutting zone and the tool rake face.

The main application of coolants is to reduce the cutting temperature through conduction. However, at very high cutting temperatures the conventional cutting fluids evaporate before reaching the cutting zone and fail to penetrate into the tool/chip interface. Evaporation of the cutting fluids in contact with hot surfaces results in the formation of a hot vapour cushion at the cutting zone and over the hot surfaces which exacerbates the conduction and further increases the cutting zone temperature (Abele and Fröhlich, 2008, Astakhov, 2006).

It is known and empirically proved that an increase in the cutting speed increases the cutting temperature (Schulz and Moriwaki, 1992, Astakhov, 2006). Higher cutting temperatures could soften the workpiece material which together with other phenomena could improve machinability (Wang, 2005, Truesdale and Shin, 2009, Kalyankumar and Choudhury, 2008). Yet, this effect is not limited to the workpiece material and could also soften the cutting tool material. In addition, it increases the chemical reactivity between the workpiece and cutting tool materials and deteriorates adhesion and formation of BUE. Consequently, it is important to control the temperature at the cutting zone by reducing the heat generation and/or heat dissipation for instance, by proper selection of the cutting parameters (Dhar and Kamruzzaman, 2007). This is more important in the case of difficult-to-machine materials, such as titanium and nickel alloys where the workpiece material maintains most of its mechanical properties at elevated temperatures. On the other hand, controlling the cutting temperatures in order to extend the tool life has resulted in very low productivity.

Using cryogenic media particularly LN_2 as coolant in different machining operations has been reported as an effective method to reduce cutting temperatures (Dhananchezian et al., 2009, Dhar et al., 2002d, Benfredj et al., 2006, Hong and Ding, 2001a). Dhar et al. (2002d) investigated the effect of cryogenic cooling in turning steel with WC tools. In order to estimate the cutting zone temperature they simplified the problem to a 2-dimensional model of orthogonal machining. In addition, four boundary conditions were defined as room temperature, constant temperature which was set to the LN_2 temperature around the cutting zone, thermally insulated zone and convective heat transfer boundary zone.

Computational FEA was conducted using NISA FEA software (2011) and revealed that the model tends to overestimate the results in comparison with measured values using a tool-work thermocouple with an average of 5.4% deviation. Based on the computational and empirical investigations it has been found that cryogenic machining significantly reduces the tool-chip interface temperature. It is attributed to improved heat conduction, reduction in tool-chip contact length and improved chip breakability as a result of spraying LN_2 into the cutting zone (Dhar et al., 2002d).

In machining aluminium 6061-T6, a reduction in the cutting temperature up to 39% has been reported as a result of spraying LN_2 onto the rake face of an uncoated WC tool (Dhananchezian et al., 2009). Wang et al. (1996) used a thermocouple placed in 2×1mm distance from the cutting edge, while Uehara and Kumagai (1968) employed the tool-chip thermocouple method to measure the cutting zone temperature. While both of them failed to measure the actual cutting temperature, the measured results show the effect of LN_2 cooling on the cutting zone temperature. The researchers (Uehara and Kumagai, 1968, Wang et al., 1996) concluded that the application of LN_2 resulted in reduction in the cutting zone temperature.

In end milling hardened AISI H13 die steel Ravi and Kumar (2011) reported that spraying LN_2 into the cutting zone could reduce the cutting temperature by 57%. Hong and Ding (2001a) measured the cutting temperature in turning Ti-6Al-4V using uncoated WC insert under different cutting environments. They ranked the machining environments in terms of effectiveness (highest cutting temperature to the lowest) as: i) dry cutting; ii) indirect cryogenic cooling; iii) emulsion coolant; iv) cryogenic cooling of flank face; v) cryogenic cooling of rake face and vi) simultaneous cryogenic cooling of flank and rake faces. Ben Fredj et al. (2006), Fredj and Sidhom (2006) and Paul and Chattopadhyay (1996a) reported that injecting LN_2 into the tool-workpiece interface in grinding steels reduced the grinding zone temperature significantly. Fredj and Sidhom (2006) indicated that reductions in the grinding zone temperature resulted in improvements in the fatigue life and surface integrity of the ground AISI 304 stainless steel part.

From the literature (Benfredj et al., 2006, Paul and Chattopadhyay, 1996a, Paul and Chattopadhyay, 2006, Uehara and Kumagai, 1970, Uehara and Kumagai, 1968, Ghosh et al., 2003, Wang and Rajurkar, 1997, Truesdale and Shin, 2009, Dutra Xavier et al., 2011,

Ravi and Kumar, 2011) it can be found that regardless of cooling technique using LN_2 as cryogen is an effective method to dissipate and reduce the chip-tool interface temperature which could lead to a reduction in thermally induced tool wear mechanisms.

3.3.4.3. Effect of cryogenic cooling on tool life

It is clear that cryogenic coolant, in particular LN_2 increases tool life by reducing the chemical reactivity of the workpiece material with the cutting tool and also by increasing the cutting tool hardness (Bermingham et al., 2011b). The Taylor equation is one of the well-known equations in tool life prediction.

Taylor Equation: $VT^n = C$

Where V is cutting speed in m/min, T is tool life in min and n and C are machining constants which are related to depth of cut, feed, workpiece and tool material (Taylor, 1907)

Based on the Taylor equation, it is clear that the tool life is highly influenced by the cutting speed and thus cutting temperature. Evans and Bryan (1991) indicated that in single point diamond turning of stainless steel graphitisation and dissolution are two dominant tool wear mechanisms. This is mainly attributed to the affinity of carbon to ferrous materials. They reported that by indirect cooling of the cutting tool using LN_2, the tool wear reduced significantly where no wear could be detected at 400X magnification after machining 1000 mm^2 of 440V steel. On the contrary, machining with the diamond tool was stopped due to excessive wear when machining a similar area in dry environment. Pahlitzsch (1953) reported that using LCO_2 and LN_2 resulted in 150% and 240% respectively longer tool life as compared to dry cutting. He attributed the improvements to the exclusion of the oxygen from the cutting zone as a result of applying inert carbon dioxide or nitrogen.

In turning Inconel® 718, Kaynak (2014) reported that using a cryogenic nozzle can significantly reduce the flank and crater wear growth rate as compared to dry and MQL. Ahmed et al. (2007) compared the tool life in dry cutting with two cryogenic cooling techniques. At the cutting speed of 250 m/min, cooling the cutting tool and chips (concept 1) resulted in a 30 times improvement in tool life as compared to dry cutting. By only cooling the cutting tool and releasing the nitrogen gas away from the cutting zone (concept 2) the tool life increased even further. At the cutting speed of 450m/min the tool in concept

2 performed 13 times longer than concept 1. This was explained by over hardening of the workpiece material in concept 1, where the nitrogen gas was released towards the chips as well as the workpiece.

It has been reported (Hong and Ding, 2001a) that simultaneous spraying of LN_2 on the rake and flank faces of the cutting tool can reduce chemical reactivity of Ti-6Al-4V to the WC cutting tool. The diffusion rate of the workpiece material to the cutting tool could be controlled significantly and resulted in increased tool life. It should be noted that diffusion is one of the dominant wear mechanisms in machining titanium alloys as titanium is chemically reactive to all known tool materials (Hong and Ding, 2001a, Paul and Chattopadhyay, 2006). Similarly, Klocke et al. (2012) reported that cryogenic cooling using LN_2 or CO_2 has significantly improved the tool life of cemented carbide tools in turning Ti-6Al-4V material. The researchers attributed the 5 times improvement in tool life when using LN_2 as compared to conventional flood coolant to the improved heat conduction resulting in lower cutting temperatures.

Khan and Ahmed (2008) modified a tool holder to cool the cutting tool through a chamber under the cutting insert and spray a cryogen media onto the cutting edge. By cooling the TiCN coated WC cutting tool using LN_2, a 4 times improvement in comparison with conventional emulsion coolant was achieved in turning AISI 304 stainless steel. AISI 304 stainless steel is particularly interesting as it retains its ductility even at cryogenic temperatures while its hardness increases significantly. Thus, Khan and Ahmed (2008) successfully increased the hardness of the carbide tool, while the workpiece material remained intact. The dominant tool wear mechanism in machining AISI 304 stainless steel with WC tool was abrasion and attrition on the flank face and abrasion and diffusion on the rake face resulting in crater wear. Cryogenic cooling has been observed to effectively reduce the diffusion and abrasion and increase the tool material hardness. Strano et al. (2013) reported that cryogenic cooling has resulted in more than 40% increase in tool life in turning Ti-6Al-4V. They used a modified tool holder and cutting tool which sprayed LN_2 over both flank and rake faces of the cutting tool.

Hong and Broomer (2000) compared the tool lives in machining AISI 304 stainless steel in different cooling techniques, namely state-of-the-art emulsion coolant through the tool holder, LN_2 flood, cooling the rake face along the Z-axis (rake Z), cooling the rake face

along the X and Z axes (rake X and rake Z), cooling the rake face along the Z and X axes together with flank face and rake X and Z axes with LN_2. The experiments showed that the lowest tool wear is achieved by spraying LN_2 along the Z-axis to the rake face. Using this method, up to 67% and 43% increase in tool life could be expected at 3.8m/sec and 3.4m/sec cutting speeds respectively in comparison with emulsion cooling. Indirect cryogenic cooling of the TiAlN coated WC tool in machining AISI 416 stainless steel resulted in a 10 times increase in tool life. The application of LN_2 in turning AISI 202 stainless steel with PVD TiN coated WC tool reduced the flank wear by 37%. This is attributed to the reduction in the cutting zone temperature preventing the tool material from softening (Kalyankumar and Choudhury, 2008).

Ghosh et al. (2003) declared that spraying two-phase gas/liquid droplets of LN_2 on the rake face of TiN coated WC tool doubled the tool life in machining AISI A2 tool steel as compared to wet machining. Machai and Biermann (2011) reported a two times increase in tool life of (Ti-Al)N-TiN coated WC tool in machining Ti-10V-2Fe-3Al titanium alloy as a result of using LCO_2 at the cutting zone in comparison with conventional emulsion cooling. These improvements are also supported by studies conducted by Venugopal et al. (2007b, 2007a) in cryogenic turning of Ti-6Al-4V with uncoated WC tool. The studies indicated that cryogenic cooling reduced the tool crater and flank wear by 77% and 66% respectively as compared to dry machining. This resulted in up to a 240% and 71% increased tool life in comparison with dry machining and emulsion cooling respectively.

Bermingham et al. (2011b) stated that by injecting LN_2 on the flank and rake face of WC tools in machining Ti-6Al-4V, a 43% to 58% improvement in the tool life could be achieved although the improvement is lower than in previous studies. They found that the main tool failure mode regardless of cutting environment was crater wear which was confined to the nose or distributed along the rake and nose in high and low feed rates respectively. In dry turning of the AISI 52100 steel the PCBN tool failed prematurely prior to 300µm flank wear due to nose fracture (Ghosh et al., 2003). It has been proven that spraying LN_2 on the rake face during the operation prevents nose fracturing (Ghosh et al., 2003, Dutra Xavier et al., 2011) and resulted in up to a 65 times improvement in tool life by limiting flank wear to 250µm (Dutra Xavier et al., 2011).

In machining Inconel® 718, Kopac (2009) integrated MQL and cryogenic machining by spraying LN_2 on the flank face and an oil-mist onto the rake face. The technique yielded a significant reduction in both crater and flank wear resulting in longer tool life as compared with dry and MQL machining. The dominant tool failure mechanism regardless of cooling technique was crater wear leading to catastrophic tool failure (Kopac, 2009). Pusavec et al. (2010) reported that by employing LN_2 cooling in turning Inconel® 718 with TiAlN coated WC tools, machining time could be reduced by up to 63% as a result of the increase in tool wear resistance and thus cutting speed. Longer tool life means that the cutting nose will literally remain intact for a longer time.

3.3.4.4. Effect of cryogenic cooling on surface integrity

Surface integrity is one of the most important parameters in assessing the performance, quality and reliability of a machined part throughout its service life (Ulutan and Ozel, 2011, Kenda et al., 2011). As shown in figure 3.5, surface integrity defines the mechanical, metallurgical and topological properties of a machined surface. Residual stress and surface roughness are two important parameters of surface integrity in machining and considerable research (Ulutan and Ozel, 2011, Thiele and Melkote, 1999, Pusavec et al., 2011, Zurecki et al., 2003, Paul and Chattopadhyay, 1996b, Umbrello et al., 2012) has been conducted on the study of the effect of machining parameters and machining environments on residual stress and surface finish.

Many researchers have reported that using cryogenic coolant in the cutting process has resulted in a reduction in the surface roughness and tensile residual stress of the machined surfaces. Bhattacharyya and Horrigan (1998) studied the effect of cryogenic cooling in drilling Kevlar composites with HSS drills. The application of LN_2 improved surface integrity of the drilled holes regardless of the tool geometry by reducing the surface roughness and geometrical deviations.

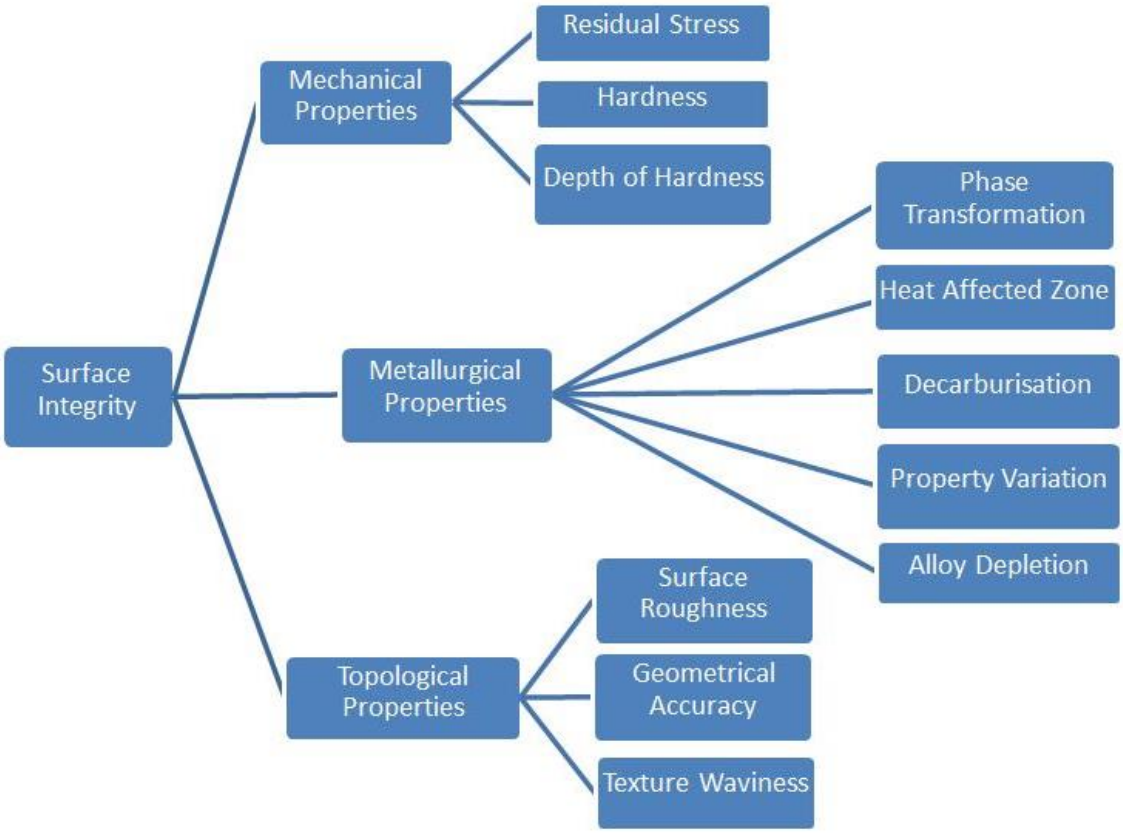

Figure 3.5 Surface integrity sub groups and parameters
(Ulutan and Ozel, 2011, Zurecki et al., 2003, Pusavec et al., 2011)

Application of LN_2 as coolant has been found to reduce surface roughness by 59% and 32% in comparison with dry and wet environments in grinding AISI 316 stainless steel (Manimaran et al., 2014). Biermann and Heilmann (2010) used CO_2 snow to cool the aluminium alloy workpiece surface during face milling by a PCD cutting tools. It was found that this technique could result in a reduction in the surface roughness and burr size of the machined surface as compared to dry machining and compressed air cooling.

In cryogenic machining of different steels namely, AISI 4037, AISI 1040, AISI E4340, AISI 4041 and AISI C60 increased life and wear resistance of the cutting tools is one of the main reasons for improved surface finish. It is also responsible for reduction in the geometrical deviation as the cutting tool remains intact for a longer time during machining (Dhar et al., 2006b, Dhar and Kamruzzaman, 2007, Dhar et al., 2002b, Dhar et al., 2002c, Dhar et al., 2006a).

Porous tungsten components for dispenser cathode manufacture are traditionally machined by using polymeric or copper infiltrant. These infiltrants act as a support for the pore

structure and lubricant (Tarter et al., 2008). Tarter et al. (2008) and Pusavec (2012) reported that using LN_2 as coolant media in turning porous tungsten not only enhanced machinability by improving the tool life and surface finish, but also eliminates the requirement for infiltrant material. In addition, Pusavec (2012) noted that using cryogenic cooling not only improve the surface finish but also prevents smearing on the machined surface and produce less porosity on the machined surface as compared to conventional techniques.

Ke et al. (2009) noted that by using LN_2 as coolant in high speed milling of Ti-6Al-4V with TiAlN coated WC tool, a 93.7% reduction in the surface roughness was achieved. Venugopal et al. (2003) noted that cryogenic cooling is an effective method to reduce the material re-deposition to the machined surface which can happen in dry turning of titanium alloys.

Pusavec et al. (2011) investigated the surface quality of machined Inconel® 718 under different environments, namely cryogenic LN_2, MQL, dry, integrated LN_2 spray and MQL. They ranked the cutting environments based on their effectiveness on the surface finish (from best to the worst) as: integrated LN_2 and MQL, LN_2, MQL. The highest surface roughness was produced as a result of dry cutting. Wang et al. (1996) found that in machining reaction bonded silicon nitride using LN_2 to cool the PCBN cutting tool led to a 84% reduction in the surface roughness. By using a similar cooling technique, surface roughness of a tantalum workpiece reduced by 40% in comparison with dry machining (Wang et al., 2002). By integrating plasma heating and LN_2 cooling in hybrid turning of Inconel® 718 using an SiC whisker reinforced alumina ceramic tool, Wang et al. (2003) enhanced the surface finish by 250% as compared to conventional dry machining.

Zurecki et al. (2004) studied the effect of cryogenic machining on surface integrity of heat treated and non-heat treated FN-0208 powder metallurgy steels with different densities. The hardness of the heat treated samples was higher than the non-treated samples. The samples were either machined conventionally by a low-content PCBN tool under flood coolant or by a TiN coated Al2O3-TiC black ceramic tool with LN_2 coolant. Investigations revealed that the cryogenically machined samples with lower hardness (non-treated) regardless of their density have a lower surface roughness than PCBN flood machined samples. Although in the case of heat treated samples, cryogenic machining with black

ceramic tools has failed to improve the surface finish in comparison with conventional PCBN turning. In general, except for surface roughness, LN_2 cooling with ceramic tool improved the surface integrity by producing harder and denser surface, while in flood cooling the surface hardness was reduced after the cutting operation. This is attributed to the local tempering of the material at the cutting zone due to the high cutting temperature.

Formation of white layers is a thermo-mechanical defect which can occur during machining and is correlated to the materials true hardness (Zurecki et al., 2004). It is attributed to the dissolution of low alloy carbide particles into the austenitic matrix of the workpiece material, where catastrophic shear takes place as the operating mechanism resulting in carbide refinement (Zurecki et al., 2003). Zurecki et al. (2004) found that there is a relation between the cutting forces and formation of the white layer. They identified that white layer forms when the value of R in the below equation becomes larger than 1.5.

$$R = \frac{(F_f{}^2 + F_n{}^2)^{\frac{1}{2}}}{F_c}$$

Where F_f is feed force, F_n is normal force and F_c is tangential force (Zurecki et al., 2004).

It has been found that an increase in the feed rate increases the depth and extent of the white layer. In addition, this could be controlled by monitoring the cutting zone temperature (Zurecki et al., 2003). Applying LN_2 as cooling media showed promising results in reducing the thickness of the white layer in machining AISI 52100 steel with 60HRc (Zurecki et al., 2003, Umbrello et al., 2011, Umbrello et al., 2012). Interestingly Dutra Xavier et al. (2011) reported that LN_2 coolant eliminated the white layer in machining AISI 52100 with 62HRc. Furthermore, other studies (Zurecki et al., 2003) indicated that while at lower feed rates alumina tools produced thinner white layers, at higher feed rates PCBN tools outperformed alumina tools. This could be explained by the low thermal conductivity of alumina in comparison with PCBN revealing the importance of contact temperature on the thickness of the white layer.

Unlike AISI 52100, the existence of white layer is claimed to improve the corrosion resistance of AZ31 magnesium alloy (Jawahir et al., 2011, Yang et al., 2011). Cryogenic burnishing of AZ31 Mg alloy and Co-Cr-Mo alloy resulted in finer grains on the burnished surface of the specimen as well as a thicker white layer and hardness resulting in higher

corrosion resistance, compared to traditionally ground surfaces (Pu et al., 2011c, Yang et al., 2011). Similarly, in turning processes, cryogenic cooling led to formation of a white layer on the machined surface of the AZ31 Mg alloy workpiece with a 60% increase in the hardness when compared to dry machining (Pu et al., 2010, Pu et al., 2011b, Pu et al., 2011a).

In contrary to previously stated studies, LN_2 precooling of the workpiece in turning AISI 1020, AISI 304 (18-8) stainless steel and 99.99% pure titanium has been reported (Uehara and Kumagai, 1968) to exacerbate the surface finish as compared with dry machined surfaces. In addition, Ahmed et al. (2007) stated that direct cryogenic cooling of the AISI 4340 steel workpiece together with the cutting tool resulted in higher surface roughness compared to dry machined samples.

Scanning Electron Microscopy (SEM) images of the cryogenically ground surfaces revealed that the cryogenic temperature reduced the sliding and enhanced material removal by shearing and ploughing (Benfredj et al., 2006). Ben Fredj et al. (2006) demonstrated that pouring LN_2 into the grinding zone when machining AISI 304 stainless steel could result in a 40% reduction in the surface roughness. Their study (Benfredj et al., 2006) also indicated that cryogenic grinding produced 180MPa and 215MPa lower parallel and perpendicular residual stresses than wet grinding. These enhancements resulted in improved corrosion resistance and fatigue life of the ground surface (Benfredj and Sidhom, 2006). Paul and Chattopadhyay (1995) noted that grinding zone temperature plays an important role in controlling the residual stress. They found that LN_2 is an effective coolant in comparison with emulsion for reducing the grinding zone temperature and thus controlling residual stresses.

3.3.5. Effect of cryogenic machining with respect to the workpiece material

It is known that using cryogen as a cooling media in machining could improve machinability by increasing tool life, reducing cutting zone temperatures, improving surface finish, etc. Though, as discussed above, the effect of cryogenic cooling on machining operations is highly dependent on the tool/workpiece material pair. The aim of this section is to review the studies in cryogenic machining from the workpiece material point of view. This will help to find the appropriate requirements for a specific material type. The majority of studies in cryogenic machining have concentrated on ferrous

materials, polymers and super alloys including titanium and nickel based alloys. In this section materials are classified into steels, super alloys, composites, polymers and other materials.

3.3.5.1. Machining ferrous materials

A large body of research has been conducted on studying the effects of different cryogenic cooling methods on the machinability of different types of ferrous alloys. Chip formation and BUE are two phenomena which has made low carbon steels hard to machine, while excessive heat generation, short tool life and poor surface quality are usually associated with machining high carbon steels.

I. Low carbon steels

Hong and Zhao (1999) and Hong and Ding (2001b) reported that cryogenic cooling of chips and the cutting zone in turning low carbon steels results in enhanced chip breakability and elimination of the BUE. Cryogenic temperatures increase the hardness, strength and reduce the fracture toughness and elongation percentage of the carbon steels. This ductility to brittleness transition is a distinctive characteristic of low carbon steels which in cryogenic machining enhances machinability. In machining AISI 1020 low carbon steel, studies by Uehara and Kumagai (1968, 1970) indicated that cryogenic cooling of the workpiece regardless of the cooling technique enhanced the chip breakability and eliminated BUE. In addition, they found that cryogenic cooling of the workpiece reduced the cutting forces and the flank wear width resulted in longer tool life. Despite improvements in the tool life and chip breakability, cooling the workpiece exacerbated the surface quality as compared to dry machining (Uehara and Kumagai, 1968). Studies (Hong et al., 1999, Hong and Ding, 2001b) revealed that cryogenic spraying on the chips and rake face of the cutting tool improved chip breakability and tool life. In addition, it resulted in an 8% increase in the cutting forces and a reduction in the surface roughness. It has been noted (Hong et al., 1999) that at high cutting speeds the heat generated at the cutting zone surpassed the cooling effect of LN_2,therefore its effectiveness in chip breakability was reduced. At low and medium cutting speeds LN_2 effectively cooled the chips below their embrittlement temperature resulting in satisfactory chip breaking. In order to benefit from the lubrication effect of LN_2 in machining AISI 1018, Jun (2005) recommended that the cutting operation should be conducted at high speeds. He

noted that at low cutting speeds, the cooling effect of LN_2 could result in over hardening of the workpiece material and thus increase the cutting forces, surpassing the lubrication effect.

II. Medium and high carbon, die and high speed steels

Aggarwal et al. (2009, 2008a, 2008b) studied the effect of spraying LN_2 into the cutting zone in machining AISI P-20 medium carbon steel. They stated that despite the 10% increase in the material hardness, machinability improved by decreasing the radial and feed forces and power consumption. Rahman et al. (2003) investigated the effect of chilled air at -23°C in end milling AISI P-20 steel. Investigations revealed that the effectiveness of the cooling method is highly dependent on the cutting parameters. For instance, while the lowest tool flank wear was achieved at low feed rates and cutting speeds, it produced higher surface roughness as compared to conventional flood cooling. In addition, chilled air was found to be only beneficial in terms of improved surface finish at higher feed rates (0.02 mm/tooth) while at lower feeds, flood coolant was superior.

Brinksmeier and Glabe (2001) reported that cryogenic cooling doubled the tool life of single crystal diamond (SCD) tools as compared to dry cutting in turning AISI 1045 steel. In order to study the effect of inert environments on tool wear, the experiment was repeated under an argon atmosphere and showed that machining in an inert atmosphere does not have any advantages over machining in air. Thus, the improvements in LN_2 cryogenic machining was credited to the super cold machining environment. Other research (Dhananchezian et al., 2009) indicated that cryogenic turning of AISI 1045 produced higher cutting forces than conventional dry machining when using multi-layer coated WC tools. While cryogenic machining increased cutting forces, it reduced the chip thickness by 15% resulting in up to a 30% increase in the shear angle improving machinability.

Dhar and Kamruzzaman (2007) and Dhar et al. (2002a, 2002b, 2002c, 2002d, 2006b) studied the effect of spraying LN_2 on the rake and flank faces along the auxiliary edges of the cutting tool on machinability of different types of steels including AISI 1040, AISI 1060, AISI 4037, AISI 4041, AISI 4320 and AISI 4340. The researchers reported that in general, cryogenic cooling resulted in reduced cutting zone temperature, longer tool life, reduced cutting forces, improved surface finish and lower geometrical deviation. Yet, the

two latter improvements were mainly attributed to the reduction in tool wear rather than cryogenic temperature.

It has been noted (Hong and Zhao, 1999) that increases in the carbon content in steels up to 0.24% improves machinability by increasing brittleness enhancing chip formation. However, carbon content beyond 0.24wt% results in high material strength and produces large amounts of carbide particles which are responsible for abrasive wear. In addition high carbon steels do not show temperature embrittlement characteristics (Uehara and Kumagai, 1968). Hence, the cryogenic temperatures fail to enhance machinability as hardness and strength increases sharply by lowering the temperature, while the fracture toughness and elongation percentage reduces gradually (Hong and Zhao, 1999). Zhao and Hong (1992) recommended that the most appropriate method to cryogenically machine high carbon steels is to inject the cryogen media into the cutting zone rather than cooling the workpiece. Paul et al. (2001) reported that spraying LN_2 into the cutting zone resulted in a 2.5 times increase in the uncoated WC tool life in turning AISI 1060 steel in comparison with emulsion machining.

Ghosh et al. (2003) examined the machinability of AISI 52100 steel under cryogenic and dry environments in turning with TiN coated Al2O3 cutting tool. It has been observed that under cryogenic conditions, the cutting tool lasted twice as long as its counterpart in dry cutting. In addition, the researchers noted that cryogenic cooling produced a uniform and predictable wear making it easier to predict tool life. Furthermore, cryogenic machining makes it possible to machine components with surface roughness lower than 0.38µm with a flank wear limit of 0.6mm. Dutra Xavier et al. (2011) stated that spraying LN_2 into the cutting zone in machining AISI 52100 bearing steel improved tool life significantly and reduced the chip-tool contact area by 26%. In addition, they noted that spraying LN_2 did not affect the surface roughness and also extinguished the formation of the white layer on the machined surface. Investigations by Zurecki et al. (2004) revealed that cryogenic cooling improves the machinability of powder metallurgy steel using TiN coated alumina cutting tools. In this study cryogenic machining improved tool life by a factor of 5 and considerably reduced plastic deformation and smearing on the machined surface. In addition, LN_2 cooling retained the surface hardness of the component, while in dry cutting it reduced after machining as a result of local tempering due to the high cutting temperature. Crater wear on the rake and abrasion on the flank faces was defined as the

main tool wear mechanisms in cryogenic turning of metallurgy powder steel with 32HRc hardness.

III. Stainless steels

The main problem in machining stainless steels such as AISI 304 and AISI 316 is their high material strength, high toughness and low thermal conductivity. In addition, lowering their temperature increases their strength and hardness significantly, while gradually reducing their fracture toughness. Hence, cooling the material hinders overall machinability (Uehara and Kumagai, 1968, Uehara and Kumagai, 1970). Due to these characteristics, Hong and Broomer (2000) suggested cooling the cutting zone in order to improve machinability. An uncoated WC cutting tool was used to machine AISI 304 workpieces. Cryogenic cooling of the cutting zone exhibited up to 67% longer tool life than wet machining. In addition, the cryogenically cooled cutting tool could withstand higher cutting speeds of 3.82m/sec, where its counterpart under dry and wet conditions failed by catastrophic fracture. Kalyan Kumar and Choudhury (2008) demonstrated a 14.8% and 37.39% reduction in the cutting forces and tool flank wear by using LN_2 in turning AISI 202 stainless steel with PVD TiN coated WC tool. Hong and Broomer (2000) reported that in machining AISI 304 stainless steel, spraying LN_2 into the cutting zone increased tool life by 67%. In addition, they found that cryogenic cooling is more favourable at high cutting speeds, while emulsion cooling performs better at lower cutting speeds. Similar conclusions were drawn by Khan and Ahmed (2008) and Khan et al. (2010) where cryogenic cooling resulted in up to a four times improvement in the TiCN coated WC tool. Nalbant and Yildiz (2011) used an external nozzle to inject LN_2 into the cutting tool in milling AISI 304 stainless steel with uncoated carbide tools. They reported that cryogenic cooling resulted in increased cutting forces and spindle torque, but did not change the tool failure mechanism as compared to dry cutting. They concluded that cryogenic machining does not show significant advantages over dry machining.

3.3.5.2. Machining special alloys

The majority of studies in cryogenic machining of special alloys have concentrated on titanium and nickel alloys. Theses alloys exhibit distinctive characteristics making the machining of these materials relatively difficult. These alloys are chemically reactive to most known tool materials. Very low thermal conductivity results in extremely high

temperatures at the cutting zone. By considering the high thermal stability and hardness of the material, increased cutting temperatures do not help workpiece material softening. High temperatures at the cutting zone have led to sever tool wear and short tool life.

I. Titanium alloys

Using cryogens as a cooling media in the machining of titanium alloys has been studied for several years. Uehara and Kumagai (1968, 1970) investigated the effect of cryogenic cooling of the workpiece in the machinability of 99.99% pure titanium. They reported that cryogenic cooling extended tool life (Uehara and Kumagai, 1970), but increased cutting forces and reduced surface finish (Uehara and Kumagai, 1968). Ti-6Al-4V can maintain a large portion of its ductility and toughness at low temperatures and does not exhibit low temperature embrittlement. Accordingly, Hong and Zhao (1999) suggested that freezing cutting tool is more favourable than freezing the workpiece. However, considering the chemical reactivity of titanium, the researchers pointed that cooling the workpiece in addition to the cutting tool can be beneficial by reducing chemical reactivity between the workpiece and tool materials. In addition, freezing the cutting tool enhances the mechanical properties and chemical stability of the cutting tool material whilst it can reduce the friction at cutting Zone.

For their experiments, Hong and Zhao (1999) used a nozzle spraying LN_2 into the cutting zone to reduce cutting temperatures, while preventing over hardening of the workpiece material. The researchers reported that five times improvement in tool life has been achieved using this system. It has been reported that spraying LN_2 into the cutting zone reduces the cutting temperature significantly as compared to dry and wet machining (Dhananchezian and Kumar, 2011, Hong and Ding, 2001a).

Hong and Ding (2001a) empirically investigated the effectiveness of different LN_2 cooling methods in terms of reducing the tool-chip contact temperature. The cooling approaches were then ranked in terms of effectiveness (best to worst) as i) simultaneous LN_2 cooling of rake and flank faces, ii) LN_2 cooling of rake face, iii) LN_2 cooling of flank face and iv) indirect LN_2 cooling of the cutting tool (Hong and Ding, 2001a). It is noteworthy to mention that in their experiments, emulsion cooling performed better than indirect cryogenic cooling. A similar order has been observed (Hong et al., 2001b) when tool life was of interest.

Machai and Biermann (2011) used LCO_2 to cool the cutting zone in machining Ti-10V-2Fe-3Al alloy using (TiAl)N-TiN coated WC tool with CNMG 120404 geometry. They reported that using LCO_2 reduced flank wear geometries and resulted in a two times improvement in tool life. In high speed milling of Ti-6Al-4V, Ke et al. (2009) reported that cryogenic cooling of the cutting zone using LN_2 is an effective method to reduce the BUE and prevent the adhesion of chips to the machined surface. In their experiments, cryogenic cooling resulted in a 93.7% reduction in the surface roughness and a 32.7% reduction in cutting forces.

Bermingham et al. (2011b) investigated the determination of optimal cutting parameters in cryogenic turning of Ti-6Al-4V alloy using Seco WNMG 120408 MF1 tungsten carbide tool. The main tool failure mode regardless of the cutting environment was crater wear, either limited to the tool nose at high feed rates or distributed along the rake and nose at low feed rates. Based on the cutting parameters the application of LN_2 into the cutting zone resulted in a 43% to 58% improvement in tool life. The biggest improvement in tool life was achieved at high feed rates and low depths of cut. Low feed and high depth of cut yielded the longest tool life. The researchers concluded that controlling heat generation by precise selection of cutting parameters is more important than heat dissipation through the application of LN_2. A study (Islam et al., 2013) showed that using LN_2 as coolant has significant effect in improving radial accuracy of turned Ti-6Al-4V parts. The report attributed the improvements to reduction in tool wear resulting in higher radial accuracy.

Pusavec and Kopac (2009) reported that by using LN_2 as a coolant, the cutting tool could withstand higher cutting speeds as compared to dry and emulsion cutting. Venugopal et al. (2003) studied the effects of TiB_2 coating on the machinability of Ti-5Al-5Mo-2Sn-V alloy under dry and cryogenic conditions. They reported that while cryogenic cooling generally improved machinability, TiB_2 coating is not appropriate for machining titanium alloys as it cannot withstand the fluctuating cutting forces and cutting temperatures. Based on their studies, despite the higher costs of LN_2 in comparison with emulsion and dry machining, cryogenic machining can reduce machining costs by up to 70%.

Based on the studies in cryogenic machining of titanium alloys it can be found that regardless of the cooling technique, cryogenic coolant exhibits promising improvements in

tool life. However, in order to enhance the surface finish in the machining zone the best approach is to penetrate the cryogen into the cutting zone.

II. Nickel based alloys

The majority of studies in machining nickel based alloys have concentrated on Inconel® 718. This is due to the high usage of this material in the hot regions of aerospace engines and gas turbines where other materials cannot withstand high temperatures. Wang and Rajurkar (2000) studied the effect of cryogenic cooling of the cutting tool through a cap placed over the cutting insert. Cryogenic cooling in machining Inconel® 718 improved the surface finish and reduced tool flank wear significantly. Flank wear was 0.85mm after a 62mm cutting length in dry cutting, whereas cryogenic cooling produced 0.6mm flank wear after 110mm of cutting. While the researchers did not conduct comparable measurements, the results showed the effectiveness of cryogenic cooling on tool life. Pusavec et al. (2011) reported that spraying LN_2 into the cutting zone enhances the surface integrity of the Inconel® 718 component. The enhancements were defined as lower surface roughness, increased surface and sub-surface hardness, higher compressive residual stresses and a thicker residual stress affected zone. In addition, by applying LN_2 into the cutting zone higher cutting speeds become available resulting in up to a 63% reduction in the machining time (Pusavec et al., 2010).

Wang et al. (2003) integrated plasma heating of the workpiece and LN_2 cooling of the cutting tool in turning of Inconel® 718 with silicon carbide whisker-reinforced Al2O3. In this technique the workpiece was heated by a plasma beam and softened just before the cutting operation. In addition, the hardness and strength of the cutting tool was increased due to the cryogenic temperature. Wang et al. (2003) noted that this technique has led to 250% reduction in the surface roughness and 156% longer tool life in comparison to conventional dry cutting. Studies showed that in plasma enhanced machining the cutting tool suffered from excessive flank wear as compared to dry machining due to higher cutting temperatures. Cryogenic cooling of the cutting tool in plasma enhanced machining increased tool life up to 170%. This study indicates that plasma enhanced machining is not an effective method for machining Inconel® 718. This could be explained by Inconel® 718's very low thermal conductivity, where plasma heating increases the cutting temperature drastically resulting in thermally induced tool failure. It was reported that

cryogenic plasma enhanced turning, produced 30%-50% less cutting forces than conventional dry machining. This is attributed to (i) lower material hardness and strength due to plasma heating (ii) higher tool hardness and wear resistance resulted in lower friction and tool wear.

Truesdale and Shin (2009) noticed that smearing and plucking are two main surface defects that affect the performance life of components made from Udimet 720 nickel based alloys. The researchers found that in wet milling an increase in the feed rate and cutting speed can result in increased plucking and smearing respectively. Accordingly, machining Udimet 720 is associated with very conservative cutting parameters and high machining costs. They reported that under cryogenic cooling at 120m/min, similar surface quality was produced as 10m/min in dry cutting. Despite reductions in the tool life and 84% increase in tool change cost, cryogenic cooling of the workpiece resulted in a 90% reduction in the total machining cost through an 1100% increase in the cutting speed. Similarly in CNC milling of Inconel® 718, Shokrani et al. (Shokrani et al., 2012) reported that while cryogenic cooling has failed to improve tool life, significant (33%) reduction in surface roughness has been achieved. The main tool failure mechanism in their study was reported to be chipping and catastrophic failure of cutting edge, thus they recommended that further studies on machining parameters and cutting tool geometry is required.

3.3.5.3. Aluminium composites and alloys

Studies on the cryogenic machining of aluminium alloys are very limited. This could be explained by the fact that generally aluminium alloys are considered as easy to cut materials. However, it should be noted that in order to step into the more environmentally friendly machining techniques aluminium should be particularly considered, due to the increased use of aluminium components in different aspects of life and industry. In addition, aluminium is highly thermally dependant and produces many difficulties in dry machining.

Dhananchezian et al. (2009) studied the impact of injecting LN_2 into the cutting zone in turning 6061-T6 aluminium alloy using uncoated WC cutting tools. They noted that while cryogenic machining produced 10% higher cutting forces than emulsion cooling, it reduced cutting temperature by up to 39% as compared to emulsion cooling. In addition, it resulted in a 25% reduction in the chip thickness and a 30% increase in the shear angle. It

can be concluded that despite the increase in the cutting forces, cryogenic cooling improved the machinability of 6061-T6 aluminium alloy. In another study, Dhokia et al. (2012a) reported that spraying LN_2 over the machining surface in CNC milling of 6061-T6 aluminium surface roughness has been reduced by as much as 50% as opposed to conventional dry and wet conditions whilst chip re-deposition and BUE was eliminated. Biermann and Heilmann (2010) studied the effect of CO_2 snow cryogenic cooling on the surface roughness and burr size of aluminium 6068-T6 face-milled surface. They investigated two cryogenic cooling concepts namely (i) stationary cooling of the exit edges and (ii) cooling nozzles moving with feed rate. Empirical studies revealed that the surface roughness of the machined surfaces under a cryogenic environment is significantly lower than dry and compressed air cooled environments. It should be noted that while the smallest burr size was produced using the first concept, the second concept produced the lowest surface roughness. The researchers noticed that the effectiveness of the stationary cooling method is limited to simple shapes and cannot be utilised for complex shapes consisting of several edges. They concluded that the best method to reduce the burr size and surface roughness in machining complex shapes is to use a cooling device which moves with the cutting tool and is fixed with respect to the feed motion of the tool.

Another type of aluminium based materials subjected to cryogenic machining are aluminium alloys or aluminium matrix composites containing silicon particles. The presence of silicon phase/particles in the material structure of aluminium alloys/composites increases the wear resistance, hardness and strength of the material. Although the presence of hard and abrasive silicon carbide particles, which are harder than WC tools has resulted in excessive tool wear (Hong and Zhao, 1999, Tanaka and Akasawa, 1999, Liu and Kevinchou, 2007, El-Gallab and Sklad, 1998, Davim, 2002). Hong and Zhao (1999) argued that cryogenic cooling of A390 aluminium workpiece could increase material strength and hardness of the abrasive silicon phase. They recommended freezing the cutting tool in order to enhance wear resistance and hardness of the tool material. Liu and Kevinchou (2007) used a vortex tube to produce chilled air for turning of A390. They found that while chilled air cooling generally increases tool life, the effectiveness of the system is highly process parameter dependant. For instance, while chilled air cooling at a cutting speed of 5mm/sec reduced the flank wear by up to 20%, the improvements at the higher and lower cutting speeds is not significant. This can be explained by the poor

thermal conductivity and low cooling capacity of air. Lin et al. (2001) studied the effect of cryogenic cooling, SiC content and heat treatment in the machinability of 356Al/SiC metal matrix composite. They reported that an increase in the SiC content in the material increases the flank wear rate, while the applications of cryogenic coolant on the PCD cutting tool material regardless of the silicon content and heat treatment improved surface finish and tool life.

3.3.5.4. Polymers

The main application of cryogenic cooling in machining of polymers is to freeze the workpiece material so as to enhance machinability. This is attributed to the distinctive ductile to brittle characteristic change of polymers at low temperatures known as glass transition temperature. Cryogenic temperature reduces the ductility and elongation percentage of the material, thus enabling it to withstand the cutting forces without deformation. Dhokia et al. (2010) used LN_2 to freeze ethylene-vinyl acetate (EVA) for milling sculptured surfaces such as shoe insoles. They noted that by freezing the workpiece it becomes possible to machine a single personalised shoe insole which is traditionally manufactured by expensive and time consuming injection moulding. Kakinuma et al. (2008) designed a special fixture to cool PDMS workpieces for manufacturing micro-fluidic chips. Micro fluidic chips are usually manufactured through photolithography and a micro-moulding process. Cryogenic freezing of the material has made it possible to machine micro-fluidic chips by a micro-milling operation. However, tool run out and material shrinkage at ultralow temperatures result in geometrical deviations. Kakinuma et al. (2008) found that the desired surface roughness could be achieved by selecting a high spindle speed (20000rpm), low feed rate (1mm/min) and low depth of cut (10µm). Mishima et al. (2010) suggested that in cryogenic machining of PDMS, dimensional inaccuracies can be compensated by considering the thermal shrinkage of the material. They also successfully deformed and then froze the workpiece in order to manufacture different shapes such as bent holes and channel grooves with different shapes. The pictorial process of machining a bent hole with pre-deformed material using cryogenic freezing is shown in figure 3.6.

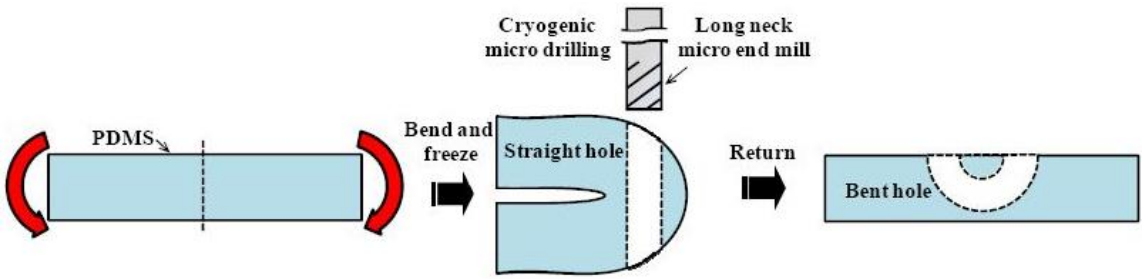

Figure 3.6 Pre-deformed bent hole manufacturing process using LN_2 cryogenic freezing (Mishima et al., 2010)

3.3.5.5. Ceramics

Most of the cryogenic machining experiments on the ceramics have concentrated on machining reaction-bonded silicon nitride Si_3N_4 (RBSN). This material exhibits high wear resistance, high strength together with poor thermal conductivity even at high temperatures. These characteristics can result in high temperature concentration at the cutting zone. As RSBN has very high hot hardness, elevated temperatures fail to soften the material and enhance the material cutting process. In contrary, most cutting tools fail at elevated temperatures and suffer from heat softening (Wang et al., 1996, Wang and Rajurkar, 2000). The wear resistance of the RBSN is higher than most cutting tool materials. Based on the studies by Wang et al. (1996) only diamond and PCBN tools have wear resistance higher than RBSN. However, diamond is unstable at high cutting temperatures. By cooling the cutting tool using LN_2, it has been reported (Wang et al., 1996, Wang and Rajurkar, 2000, Wang and Rajurkar, 1997) that significant improvement in tool life can be achieved. Investigations on the tool wear mechanism revealed that while LN_2 cooling eliminated the chipping and fracture on the cutting edge as seen in dry cutting, the main tool failure mode regardless of cooling method was flank wear (Wang et al., 1996). In addition, it has been found that among different types of PCBN tools, CBN50 exhibited the longest tool life followed by VC722 and VC734 in decreasing order (Wang and Rajurkar, 2000). Cryogenic cooling also enhanced the average surface roughness by 84% along a 40mm length of cut. It is clear that in this case the surface roughness is highly affected by tool wear, as for the same length of cut the flank wear of the tool in dry cutting was 5 times bigger than that of cryogenic machining (Wang et al., 1996). As a result, it cannot be concluded that the enhancements in the surface roughness is directly due to cryogenic cooling.

3.4. Critique and research gaps

The application of cryogenics in material cutting processes can be classified into: i) Cryo-processing of the cutting tools and ii) Cryogenic Machining. These categories with related areas of study and research requirements are illustrated in figure 3.7. In this section these categories are critiqued and the areas of investigation are defined.

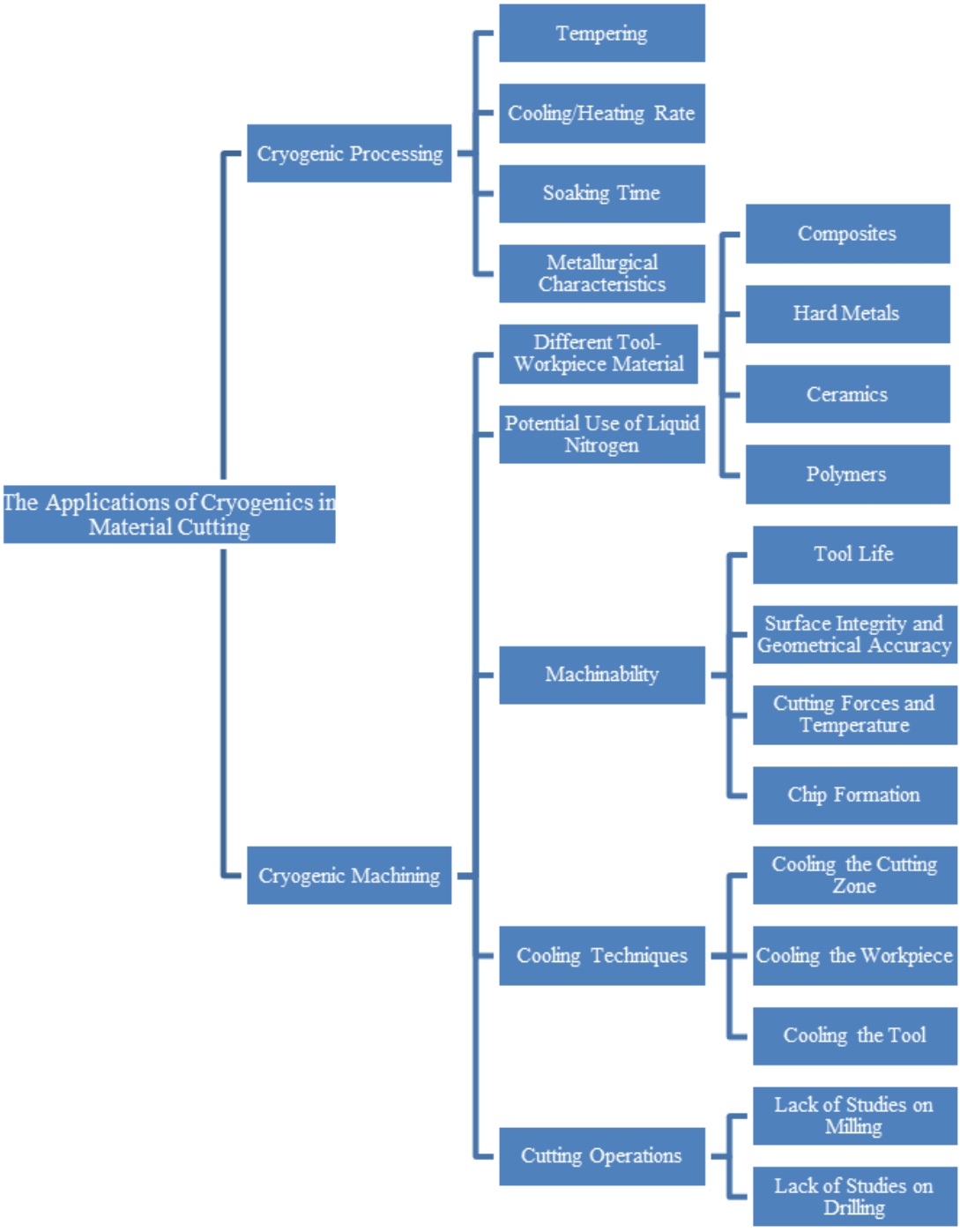

Figure 3.7 Areas of study and classification of the applications of cryogenics in material cutting

3.4.1. Cryogenic processing

Based on the literature, cryogenic treatment of the cutting tools is found to be an effective method for enhancing the strength, hardness and wear resistance of HSS and WC cutting tools. However, while retained austenite transformation and carbide precipitation are defined by researchers as the main reasons behind the improvements of the cryogenically treated HSS tools, it failed to explain the improvements of the treated WC tools. Thus, it can be stated that the factors for explaining improvements in cryogenically treated cutting tools are still unclear and requires further studies on the metallurgy and microstructure of the treated materials.

It is known that some changes in the material microstructure happen in cooling to and heating from cryogenic temperature as well as when the material is soaked into the cryogen (Kalia, 2009). Though, the optimum cooling and heating rates and the soaking time is still unclear. The literature showed that tempering before and after the cryogenic treatment can affect the effectiveness of the treatment process to differing extents. Although the effects were in contrast among different studies such as: (Firouzdor et al., 2008, Molinari et al., 2001, Leskovsek et al., 2006). Thus, further studies are required to understand, clarify and define the effects of tempering and tempering temperature on the performance of the cutting tools.

The review of the literature showed that all studies on the cryogenic treatment of the cutting tools are concentrated on HSS and WC tools and there is no report on the effect of cryogenic treatment on the performance of other cutting tool materials.

3.4.2. Cryogenic machining

As shown in figure 3.8, while the studies on cryogenic machining date back to the early 20th century and were preceded by the mid-20th, when the first liquid gas fuelled rockets were launched, the majority of the studies have been conducted during years 2000 onwards.

Despite the long history of cryogenic machining, its advantages over dry and flood cooling and the introduction of some commercial cryogenic machining equipment (MAG, 2012, Air-Products, 2011), this technique is not popular among industrialists. This could be

explained by the fact that most studies in this area have concentrated on the turning of steel materials using LN_2, as illustrated in figure 3.9.

Unlike conventional cutting fluids, cryogens cannot be cycled in the machine tool and reused in the cutting operations therefore economical use of the cryogen is very important. The most economical approach for cryogenic machining is to deliver the cryogen to the exact point. Another step towards realising the use of cryogenic machining in industry is to extend its application into other cutting operations, such as milling and drilling, using more common materials such as aluminium alloys.

As mentioned before and illustrated in figure 3.9, majority of studies on the cryogenic machining of hard metals have concentrated on turning operations. It is true that turning is one of the most common operations in any manufacturing process, though milling operations are more significant in mainstream CNC manufacturing.

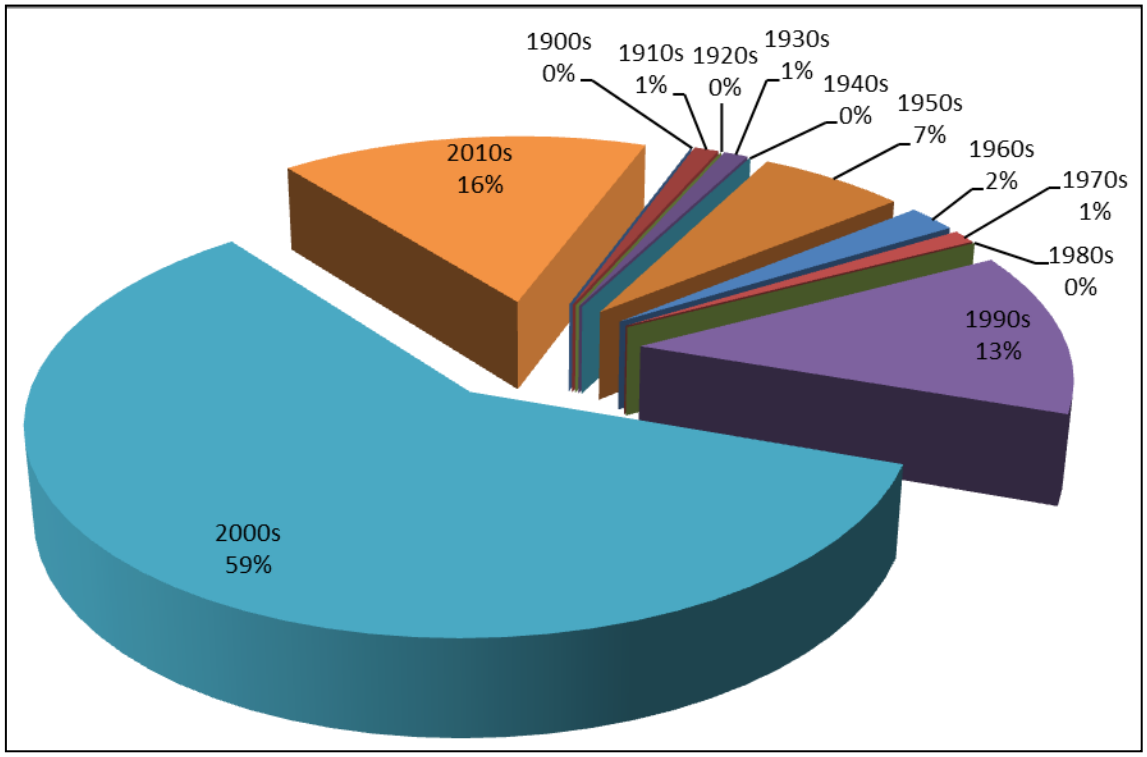

Figure 3.8 Distribution of the total 109 collected papers on cryogenic machining based on the publication year

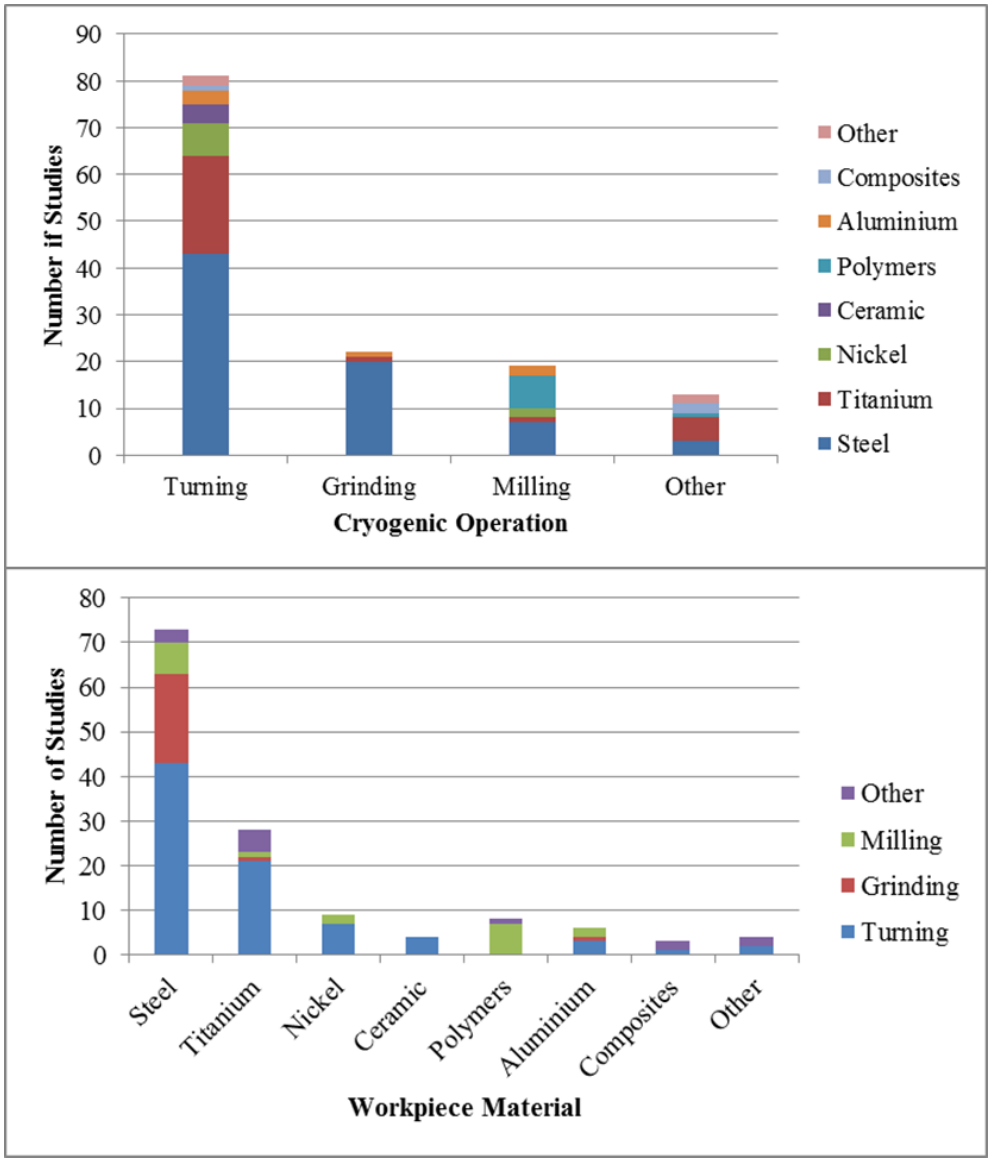

Figure 3.9 Distribution of the collected studies on cryogenic machining based on the workpiece materials and cutting operations

In addition, except studies by Bhattacharyya and Horrigan (1998) on drilling Kevlar composites, Ke at al. (2009) on helical high speed milling of holes and Dhokia et al. (2012b) on drilling carbon fibre composites, to the best of the author's knowledge, there is no study on the effect of cryogenic cooling in drilling operations. This is mainly due to the difficulties of gaining access to the cutting tool and modification in drilling and milling as compared to turning where the cutting tool can be modified or an external nozzle can be focused on the cutting zone more easily. Compared to single point turning, milling inherently is an intermittent operation with increased degrees of freedom enabling significantly more complex parts to be machined (Dhokia, 2009). Thus, focusing an

external nozzles or modifying the cutting tool is relatively more complex and could consist of changes in the design of the machine tool. These technical issues together with cost implications of the CNC machining centres and unwillingness of industry to adapt new systems are responsible for the lack of knowledge, slow improvements and adoption of cryogenic machining.

Most researchers in cryogenic machining have used LN_2 as the cryogen in their experiments. The main benefits of LN_2 over other liquid gases can be defined as follows. Nitrogen is a colourless, odourless and inert gas which forms 78% of the air. Nitrogen is lighter than air so it disperses into the atmosphere easily so reduces the requirements for extra ventilation at the shop floor. LN_2 is a relatively cheap liquid gas with a boiling temperature, much lower than LCO_2 with proven lubrication capabilities, which in machining is accompanied with reductions in tool-chip contact length resulting in lower cutting forces.

In machining hard materials where the tool life and surface quality is of interest, most researchers have used an external nozzle or modified cutting tool/tool holder to inject the cryogen into the cutting zone.

In machining ductile materials and polymers, the main goal of using cryogens is to make the workpiece material brittle so as to enhance the chip formation and cutting operations. In such cases, for ductile materials such as low carbon steels Hong et al. (1999) suggested focusing the cryogen nozzle onto the chip to make it brittle and enhance chip breakability. Although in machining polymers, where the workpiece material deforms due to cutting forces, the workpiece should be frozen in order to enhance machinability (Dhokia et al., 2010). It should be noted that in this case the workpiece material should be soaked in a cryogen bath. There is no study on the effect of freezing the cutting point rather than the whole material in machining polymers in order to reduce cryogen consumption.

As shown in figure 3.9 the extent of the workpiece materials used for the cryogenic machining research is very limited and is mostly concentrated on turning steel materials. Among the 5 studies on cryogenic milling of steel workpieces, only Nalbant and Yildiz (2011) used LN_2 for machining AISI 304 stainless steel.

There is a significant lack of research on the cryogenic machining of composite materials. The only notable studies in cryogenic machining of synthetic composites has been conducted by Bhattacharyya and Horrigan (1998) and Dhokia et al. (2012b) where substantial improvements in machinability have been reported. Although, in the study by Bhattacharyya and Horrigon (1998) due to the use of a new cutting tool together with cryogenic coolant and lack of methodical experimental design the underlying reasoning behind the improvements has remained unclear.

In comparison with steels, machining titanium alloys is very critical. This is due to the chemical affinity of titanium to all known cutting tool materials together with high cutting zone temperatures, high material strength and poor thermal conductivity. These characteristics have resulted in poor machinability of the material together with high machining costs and low productivity. As a result, industry tends to use more advanced cutting tools to increase productivity and reduce the tool change costs as the main application of titanium alloys is for components used in aerospace and gas turbine industries with high buy-to-fly ratios resulting in substantial machining costs (Sun et al., 2010).

Despite the advantages of cryogenic cooling in machining titanium alloys, there is very limited research on different cryogenic cutting operations (figure 3.9). For instance, while 22.4% of the research in cryogenic machining has focused on titanium alloys, only 1 paper is focused on cryogenic milling operations.

Nickel alloys with mechanical and thermal properties superior to titanium alloys is another machining challenge for manufacturing industries. Similar to studies on machining titanium alloys, most researchers have stated that cryogenic cooling enhances the machinability of nickel alloys and reduces machining cost significantly. However, only 6.5% of the studies on cryogenic machining have concentrated on machining nickel alloys with only two experiment on the milling of Udimet 720 (Truesdale and Shin, 2009) and Inconel® 718 (Shokrani et al., 2012). Truesdale and Shin (2009) reported that while cryogenic cooling of the workpiece reduced the tool life, increased productivity can reduce total machining cost by up to 90%. Thus, there is a significant further area of study on the effects of cryogenic cooling on the machinability and machining cost of nickel alloys.

There are a very limited number of studies on cryogenic machining of other materials such as tantalum, cobalt-chrome alloys, polymers, WC-Co composites, aluminium alloys and structural ceramics. Cryogenic milling of polymers is defined as the most suitable method for machining personalised or modified products and prototypes as an alternative to expensive and time consuming processes such as moulding, micro-moulding and photolithography. Despite successful application of cryogenic milling of polymers, the research in this area is very limited and all papers are published after the year 2000. It is noteworthy to mention that the optimal cutting parameters in this technique are still unclear and the workpiece materials are very restricted. This is a significant research area related to defining the optimal cutting parameters and their effects on the machinability of different polymer materials.

From the cutting tool material point of view, as illustrated in figure 3.10, 68% of the cutting tools used in cryogenic machining studies are WC. Almost one third of these were coated carbide tools with different coatings and coating methods namely, PVD and PCD. Based on the review in the section 3.4.3 most of the studies stated that cryogenic cooling resulted in longer tool life when machining different materials. Though, while carbide tools are significantly cheaper than more advanced tools such as CBN, PCBN, PCD, SCD etc., there are limited studies on comparative cost implications of using cheaper options in cryogenic machining compared to advanced cutting tools in conventional environments.

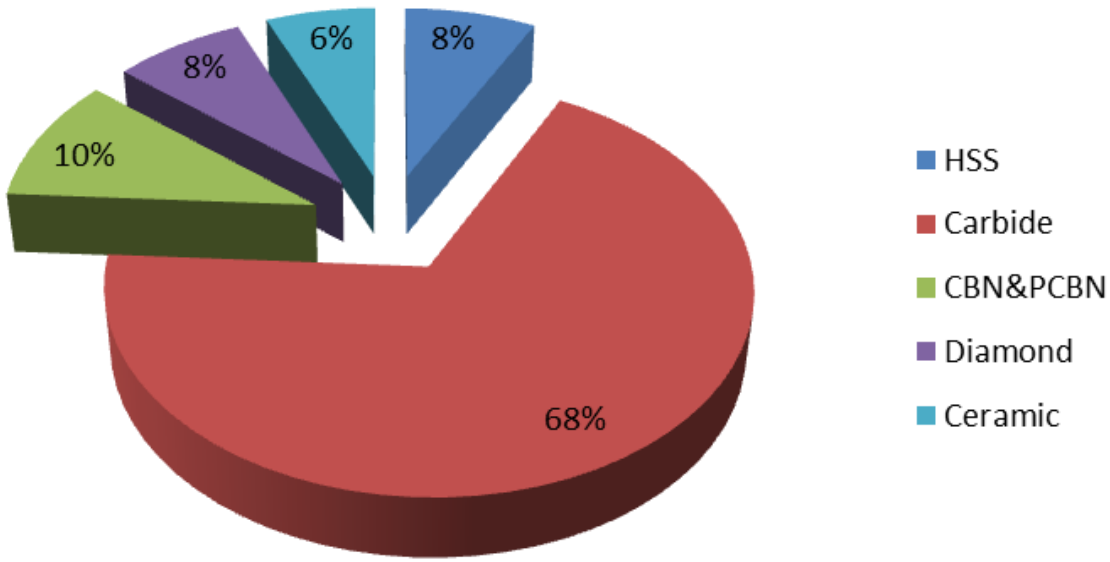

Figure 3.10 Distribution of the cutting tool materials used in the studies in cryogenic machining

3.5. Summary

This chapter reviewed the application of cryogenics in machining processes. In general, cryogenics in machining operations was classified into two categories of (i) cryogenic processing and (ii) cryogenic machining. Cryogenic processing was identified as an extended heat treatment process in a typical heat treatment cycle. Most studies in this area are concentrated on the cryo-processing of HSS cutting tools and also carbide tools. Different theories to explain the effects of cryo-processing on the material structure of the cutting tool materials were identified and are listed below:

- Austenite transformation
- Carbide precipitation
- Formation of the μ phase in the material microstructure

Nevertheless, none of the above theories can completely explain the changes in performance of the treated tools and further research is required.

In cryogenic machining, a cryogen is used to cool the workpiece material and/or cutting tool during the cutting operation. The cooling technique is highly dependent on the workpiece-tool materials. For instance, while workpiece cooling is suggested for ductile materials, cooling the cutting zone or cutting tool is recommended more for harder materials. In majority of cases, researchers have reported that cryogenic cooling has positively impacted on the machinability of different materials in terms of tool life and surface finish. Though, as mentioned in section 3.4.2, most studies in cryogenic machining have concentrated on turning operations for steel and titanium alloys. Hence, the authors conclude that further research in cryogenic machining using other machining operations such as milling and drilling with different tool-workpiece materials is essential.

Chapter 4

Scope of the research

4.1. Introduction

Based on the literature described in chapters 2 and 3, there are a number of materials which are generally known as difficult-to-machine materials. This is mainly due to a series of obstacles that machinists have to overcome during machining operations. These problems vary from short tool life and high machining forces to poor surface integrity and changes in microstructure of the machined products during machining processes. Generally, it is believed that using a generous amount of cutting fluids improves the machinability by removing excessive heat generation and lubricating the cutting zone during machining (Bermingham et al., 2011). However, as outlined in chapter 2, it has been found that there exists a number of environmental and health issues associated with the use of conventional oil-based cutting fluids.

Using liquefied gases such as nitrogen and carbon dioxide as lubricants, also known as cryogenic cooling, is a method that is widely believed to enhance the machinability of difficult-to-machine materials. As outlined in section 3.4.2, it has been recognised that most of these studies are concentrated on turning operations. Thus, despite the existence of cryogenic milling centres such as MAG Inc. (MAG, 2012), it was found that there is a significant research gap in cryogenic milling operations. In addition, from the literature, Ti-6Al-4V titanium alloy was found to be the most used titanium alloy due to its vast use in aerospace and medical implant applications.

This chapter outlines the scope of this research and consists of the aims and objectives and the areas of investigation.

4.2. Aims and objectives

The aim of this research is to design a cryogenic cooling system for CNC end milling of Ti-6Al-4V alloy and to evaluate and identify the effects of cryogenic cooling on the machinability of Ti-6Al-4V alloy in comparison to traditional dry and wet cooling.

In achieving this aim, the main objectives of this research are provided as follows:

i. To critically study the state-of-the-art in machining difficult-to-machine materials with regards to cutting fluids.
ii. To provide an in-depth understanding of cryogenic machining

iii. To design, manufacture and test a cryogenic cooling system which is adaptable to current CNC milling centres.
iv. To compare and evaluate the effects of cryogenic cooling on machinability of Ti-6Al-4V alloy with conventional machining environments, namely dry and wet.
v. To define a series of experiments to enable optimisation of the machining parameters for cryogenic milling of Ti-6Al-4V.

4.3. Scope of the research

According to the aims and objective of the research, the following areas of investigation are identified.

4.3.1. Design of a cryogenic cooling system for CNC milling

Based on the findings in the literature, a cryogenic cooling system is to be specified and designed which will be transferable to a wide majority of the currently available CNC milling machine tools. A set of concepts will be designed and the most appropriate design will be selected according to the literature and available resources. In the embodiment design stage, additional computer aided tools will be used to model, analyse and enhance the selected concept. A prototype of the system will be made and the system will then be used for some initial machining trials. Based on the findings from modelling and experimental trials, the embodiment design will be updated and a finalised design will be generated. The finalised design will then be manufactured and the system requirements will be procured in order to provide a cryogenic cooling system.

4.3.2. Comparative study of the effects of cryogenic machining

In order to understand the effects of cryogenic cooling on the machinability of Ti-6Al-4V alloy, it is important to compare the machining results with the current practice e.g. dry and wet machining which are commonly used in industry. A DoE will be used to define the affecting parameters and order of machining trials. Furthermore, statistical analysis tools will be employed to study the effects of cryogenic cooling as compared to conventional dry and wet machining environments. This set of studies will include macroscopic and microscopic analysis of tool wear and surface roughness together with power consumption of the machine tool.

4.3.3. Optimisation of machining parameters for cryogenic machining

The data collected for comparative study will be used to develop a new DoE for optimisation. A set of machining experiments will be conducted according to the DoE in order to enable optimisation of machining parameters for cryogenic milling of Ti-6Al-4V aiming to reduce surface roughness and tool wear. A series of mathematical and statistical techniques such as ANOVA, regression and RSM will be considered for the analysis.

4.4. Research boundaries

Material cutting is a broad area consisting of different operations, cutting tool/workpiece materials and machining environments. Considering the available resources and in order to narrow the research and focus the efforts in a timely manner, a series of boundaries has been defined. As shown in figure 4.1 and reflected in the aim, this research is limited to the study of the effects of cryogenic cooling using liquid nitrogen in CNC end milling of Ti-6Al-4V titanium alloy.

As outlined in chapter 3, among all available cryogens, LN_2 and CO_2 are the more desirable cryogens for machining due to their cost and availability. For this research, LN_2 was selected for cryogenic cooling as it has higher thermal conductivity and lower temperature than CO_2. In addition, it forms almost 80% of the air which reduces the environmental and health risks associated with its use.

MQL, dry and wet machining techniques have been identified in the literature (chapter 2 and 3) as the most common techniques for machining difficult-to-machine materials and more specifically titanium. However, due to the limited resources, dry and wet machining has been selected as base environments for comparative study. Furthermore, the major aim of using MQL is to reduce the cutting fluid consumption and not specifically improving the machinability (Ezugwu, 2005, Rahim and Sasahara, 2011).

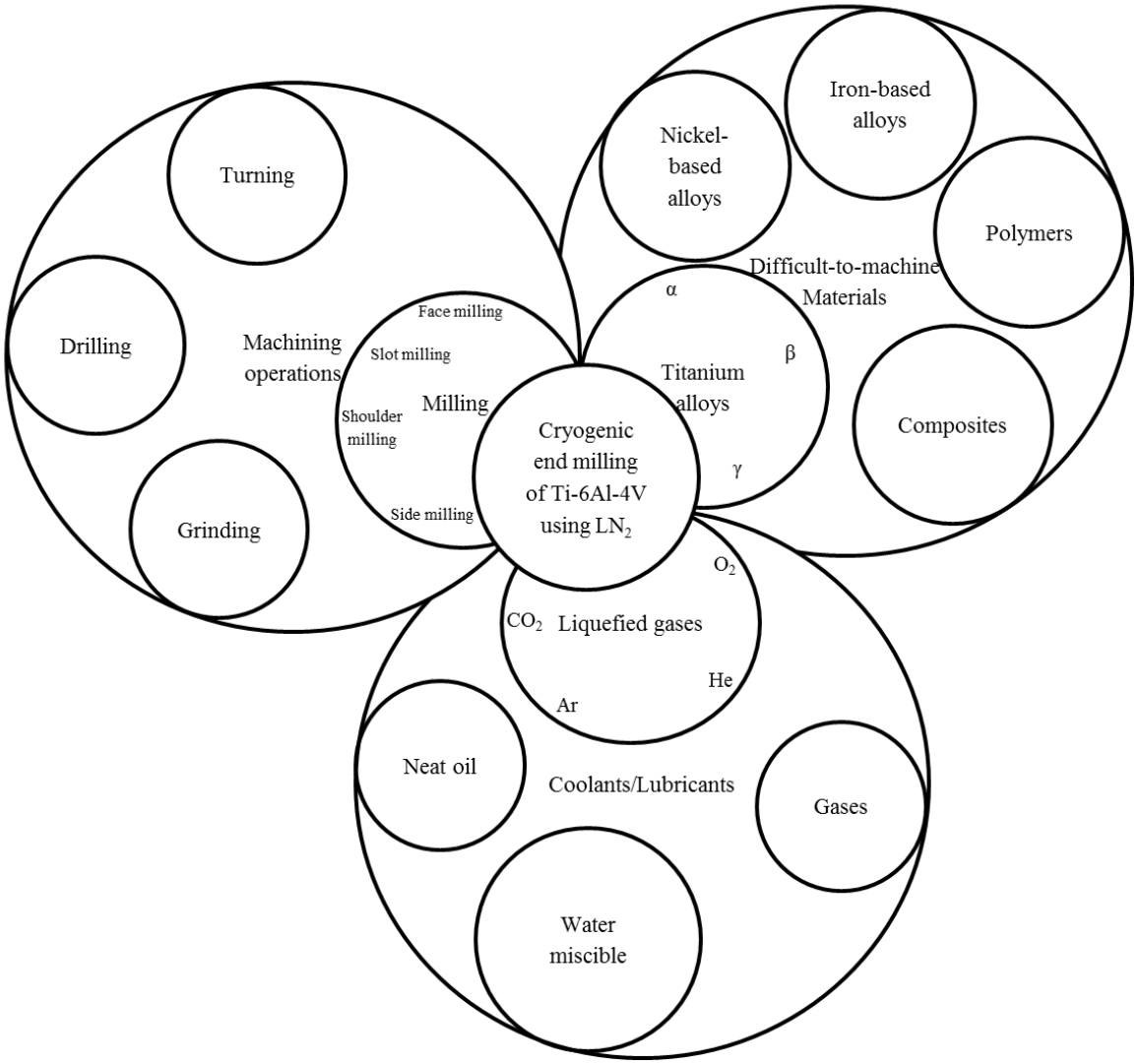

Figure 4.1 Graphical presentation of the boundaries of research

Chapter 5

Research methodology

5.1. Introduction

This chapter explains the methodology that is followed to achieve the aims and objectives of this research based on the scope outlined in section 4.3.

5.2. Overview of the research methodology

The experimental methodology of this research is developed based on the IDEF0 diagram shown in figure 5.1 which presents the overall inputs and outputs of this research together with the required resources and controlling parameters. Furthermore, as illustrated in figure 5.2, the major activities to be executed for this research are identified and a second level IDEF0 diagram of these activities is generated. Together with the relationships of the activities, this diagram provides an overview of the inputs, facilities and control parameters which are used at different stages of this research. As demonstrated in figure 5.2, the experimental methodology is divided into three major activities, namely (i) design and manufacture of a cryogenic cooling system, (ii) comparative study and (iii) optimisation of cutting parameters. Each section is explained thoroughly as follows. In the first stage, a cryogenic cooling system is designed and manufactured. The cooling system is then used in the second stage to compare the effects of cryogenic cooling with other machining environments, namely dry and wet. In the third stage, the result of the comparative study is used to design and conduct a series of machining experiments aiming to optimise the cutting parameters.

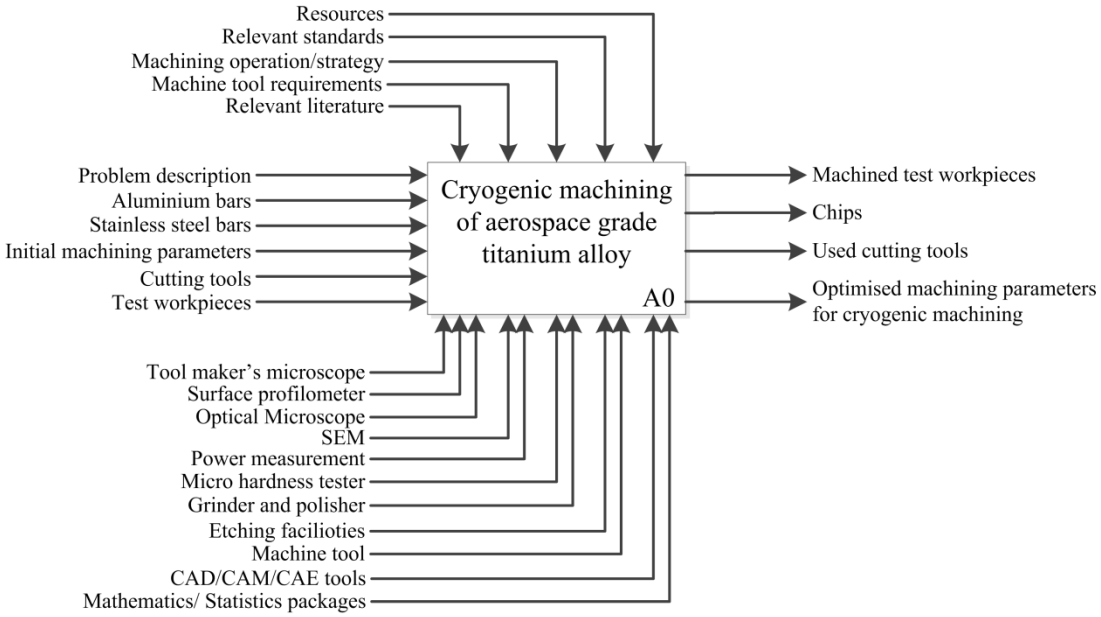

Figure 5.1 IDEF0 diagram of the overall research

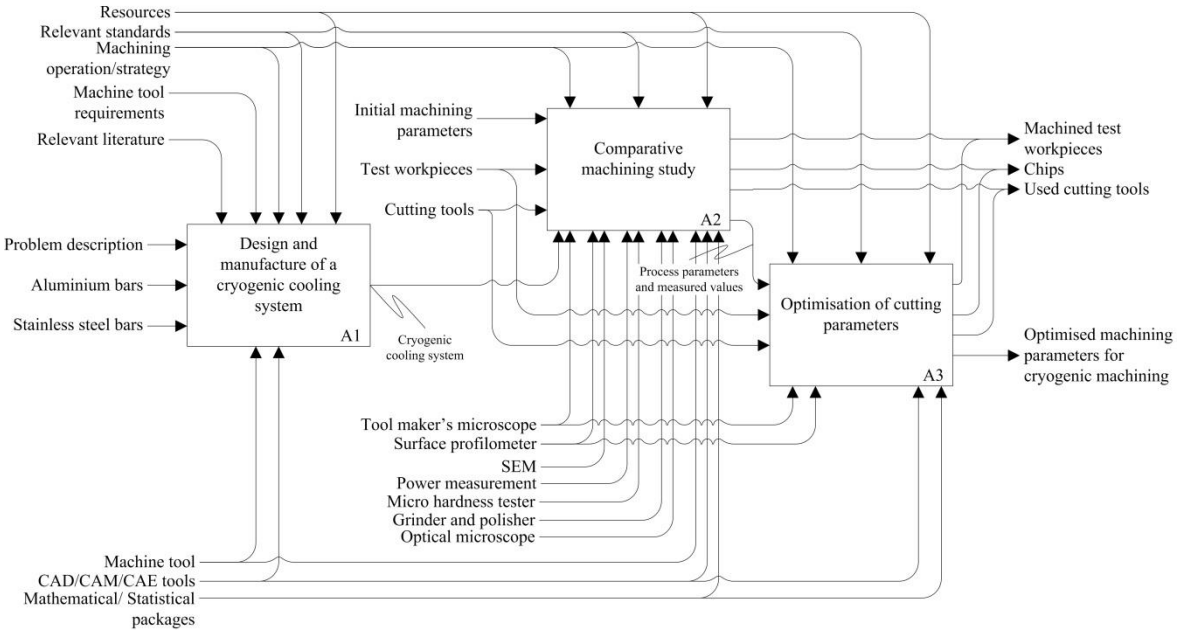

Figure 5.2 IDEF0 representation of the research methodology

5.3. Design, manufacturing and development of a cryogenic cooling system

In order to design a cryogenic cooling nozzle, a systematic design method utilising Pahl and Beitz technique (Pahl et al., 2007) is used. The initial knowledge for developing a cryogenic cooling system has been derived from the literature in section 3.3.3 and 3.3.5. As shown in figure 5.3, this stage of the research is separated into five parts starting with defining the problem to be addressed by design. The findings of the literature, available resources, machine tools' and process' requirements and limitations have been used to define the specifications required for the ideal cryogenic cooling system. A set of conceptual designs are generated and then evaluated using appropriate score sheets and the best concept is selected for further development. After selecting the most appropriate design, a 3D CAD model of the design is generated for computer modelling. This process is illustrated in figure 5.3.

The initial cryogenic cooling system design is then simulated using Ansys® Fluent® (Ansys, 2013) to model the flow of LN_2 inside the system. The simulation provides the pressure and velocity of LN_2 throughout the system. This data is then used to optimise the initial design. The procedure is repeated until satisfactory results are obtained and the final design is selected. As shown in figure 5.4, following the computer modelling stage, a prototype of the selected design is manufactured. In addition, other parts of the system

such as valves, electronics, etc., are procured from a variety of cryogenic equipment specialist suppliers.

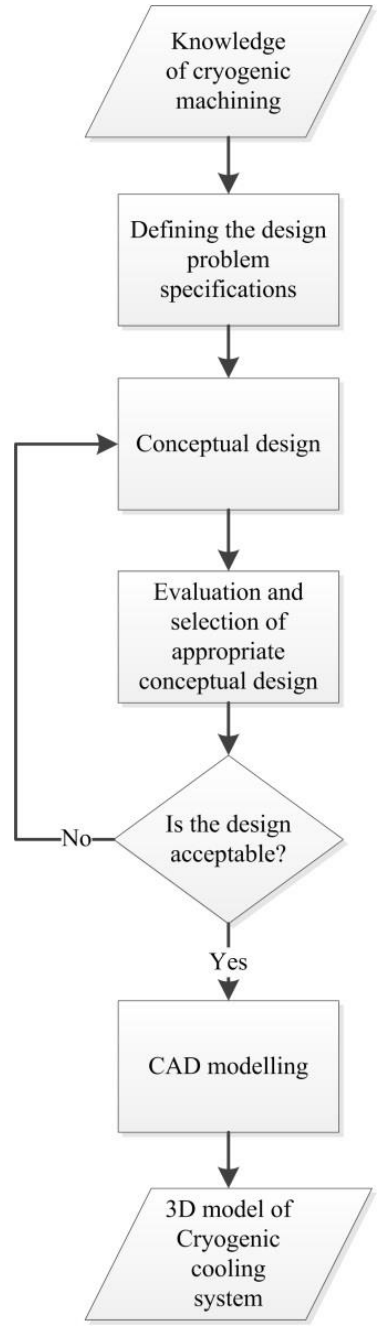

Figure 5.3 Process flowchart for conceptual design and evaluation of a cryogenic cooling nozzle

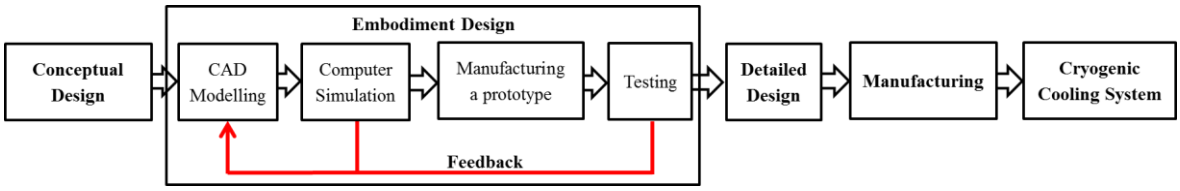

Figure 5.4 Illustration of the design, manufacturing and development of a cryogenic cooling system

When the cryogenic cooling system is prepared and developed, it has to be tested on a selected CNC milling centre. This consists of machining trials and high speed filming of the machining process. For the initial machining trials, tool wear, surface roughness and power consumption are monitored and compared to that of conventional machining techniques. The observations during machining trials and high speed film of the operation are recorded and used for updating the design. The finalised design is then developed and manufactured and used for the comparative study.

5.4. Comparative study

At this stage, the effects of different machining environments, namely dry, wet and cryogenic on the desired machinability metrics are compared. The desired machinability metrics for this research has been identified to be surface roughness and tool wear/tool life. In addition, power and energy consumption of the machine tool, chip formation and surface integrity of the machined parts are also examined. Based on the literature, it has been found that machining environment changes the material properties of the workpiece/cutting tool materials (Hong and Zhao, 1999). Thus, it is a valid argument to assume that the machining parameters need to be adjusted to obtain the optimum results for each individual machining environment. However, at this stage of the research, the optimum cutting parameters are still unknown. Therefore, the machining experiments need to be conducted with different combinations of cutting parameters. As shown in figure 5.5, a set of machining trials are conducted to identify the maximum and minimum values of cutting parameters that the cutting tools last for a minimum of 150mm machining length (1 pass). These values are used to conduct machining experiments. A DoE is implemented to generate a combination of different machining parameters whilst minimising the number of required experiments. As shown in figure 5.5, a series of machining experiments are conducted based on the DoE and different machinability metrics such as surface roughness and tool wear are collected for each experiment. Statistical analysis techniques are used to identify the effects of cryogenic cooling as compared to conventional machining environments. Based on the statistical analysis and other qualitative parameters such as surface topography and microstructure, the best machining environment is then identified. In order to reduce the random errors induced by practitioner, a procedure is followed for both machining and data collection activities which are described in detail in chapter 7 following the instructions provided in BS ISO 5725-1 (1994) and BS ISO 5725-3 (1994).

These procedures are followed for all machining and measurement experiments throughout this research.

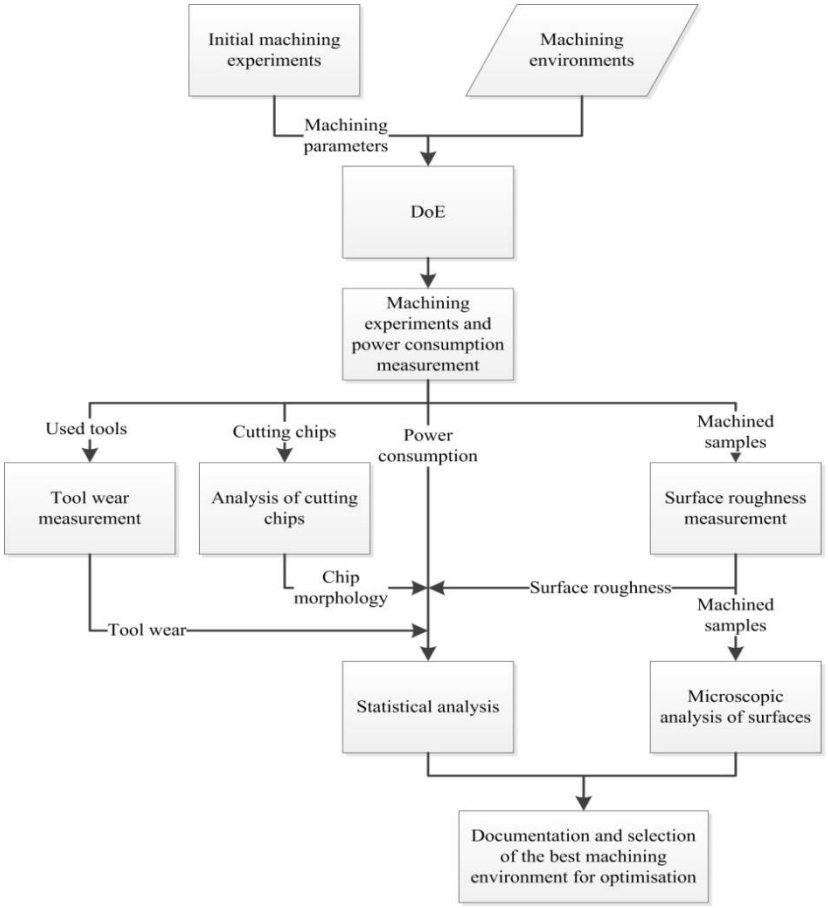

Figure 5.5 Illustration of procedure of conducting comparative study

5.5. Optimisation of machining parameters for cryogenic machining

As mentioned previously, the machining environment and thus temperature affects the material properties of both workpiece and cutting tool materials. As a result, the cutting parameters are required to be optimised in order to achieve improved machinability. The goal of this stage is to identify the best combination of machining parameters for cryogenic machining of titanium. The data collected from the comparative study are used to design a new set of experiments for optimisation and a set of machining experiments are conducted accordingly. Pareto ANOVA is used to identify the significance level of each cutting parameter on surface roughness and tool wear. In addition, regression modelling and RSM are performed on the collected data in order to identify the optimum level of desired machinability metrics. The funding body for this research indicated a maximum surface roughness Ra of 0.8μm with minimum tool wear as the desired objective for optimisation.

Chapter 6

Design, manufacture and development of a cryogenic cooling system

6.1. Introduction

In this chapter the activities conducted to design and finalise a cryogenic cooling system for CNC end milling of Ti-6Al-4V are explained. Following the methodology, the knowledge gathered from the literature reviews was used as a starting point for the design. According to the literature, the material strength and hardness of titanium increases sharply by lowering the temperature whilst it maintains most of it toughness. Hong and Zhao (1999) suggested that the best approach for machining titanium is to spray a small amount of LN_2 into the cutting zone whilst freezing the workpiece to a limited extent. In this technique, LN_2 helps to reduce the temperature at the cutting zone, whilst freezing the workpiece and cutting tool materials will help reduce their chemical reactivity.

The design stage is divided into two main sections namely cryogenic delivery system (section 6.2) and cryogenic cooling nozzle (section 6.3). The cryogenic delivery system includes all the equipment and facilities which are outsourced and are assembled which includes the LN_2 storage, valves and measurement gauges. The cryogenic cooling nozzle is specially designed and manufactured by the author for the specific requirements of this research.

Following the methodology disclosed in section 5.3, the specifications of the problem have been defined and explained in section 6.3.1. Based on the explanation and findings of the literature three concepts were designed and are presented in section 6.3.2 and the constraints and limitations of the design were identified. Based on these requirements and limitations the concepts were scored and ranked thus the most appropriate design was selected based on the ranking. The selected design was then simulated using Ansys® Fluent® (Ansys, 2013) (section 6.3.3.1). Based on the findings of the simulation, the initial design was updated and a prototype of the nozzle was manufactured. A series of machining trials were conducted to test and identify the effectiveness of the prototype. The findings were then used to improve the initial design. The detailed sketches of the final design were generated and the nozzle was manufactured which are detailed in section 6.4.

The results of the machining trials have been published in Shokrani et al., 2012c, Shokrani et al., 2012d.

6.2. Design and development of a cryogenic delivery system

This section explains the activities related to the selection of the components for delivery of LN_2 to the nozzle which are designed and manufactured for cryogenic machining. The system which was developed by Dhokia (2009) for machining elastomer materials was used as a basis for this research. As shown in figure 6.1, this system consists of a 180 litre self-pressurised cryogenic Dewar, a pressure gauge, a globe valve, a solenoid shut off valve and a vacuum jacketed hosing for delivery of LN2 with minimum loss due to evaporation. The specifications of the cryogenic Dewar are provided in table 6.1.

6

Figure 6.1 Cryogenic cooling system developed by Dhokia (2009) for cryogenic machining of elastomers

Manufacturer	Statebourne Cryogenics Ltd
Product name	Cryostor 180
Capacity	180 lit
Weight (empty)	124 kg
Weight (full LN_2)	269 kg
Maximum allowable working pressure	3 bar
Maximum flow rate	20 lit/min
Safety equipment	Adjustable relief valve and burst disk

Table 6.1 Specifications of cryogenic Dewar used for this research

In order to provide precise control on the flow rate of LN_2, a cryogenic flow control valve and a Coriolis mass flow meter have been integrated into the original system. The flow meter was specifically selected for this process and was calibrated prior to use. Table 6.2 provides the specifications of the flow meter. In addition, a quick release coupling was ordered and specifically manufactured research to permit easy connection/disconnection of the cryogenic cooling nozzle from the hosing. The coupling is made from AISI 316L stainless steel and fitted with Kel-F and PTFE seals. For extra safety reasons, the coupling is designed so as the flow is only permitted when the coupler and nipple halves are connected. These facilities, namely flow control valve, flow meter and quick release coupling have been integrated into Dhokia's (2009) cryogenic cooling system design. Figure 6.2 illustrates a pictorial presentation of the final cryogenic delivery system.

Manufacturer	Emerson Electric Co.
Sensor Type	Micro Motion® Elite® flow meter
Sensor model	CMF050M319NQEMEZZZ
Transmitter model	1700R12AEMEZZZ
Wetted material	316L stainless steel
Fluid	Liquid Nitrogen
Mass flow accuracy	0.1%
Pressure drop at operating flow	0.09004bar
Working temperature	-240°C to 427°C
Working pressure	Vacuum to 413 bar

Table 6.2 Technical data of Micro Motion® Elite® flow meter

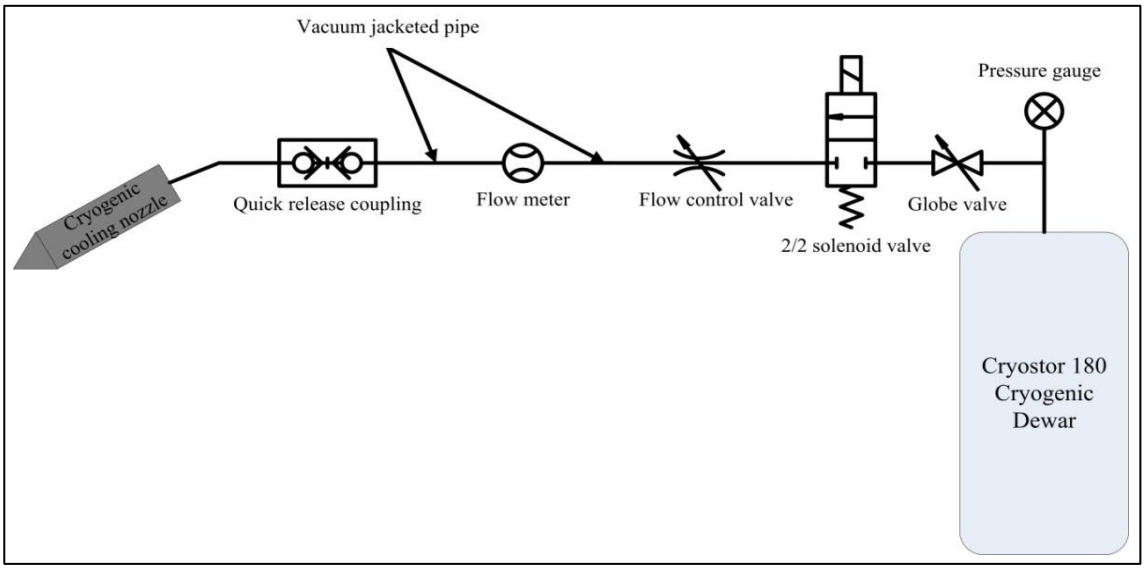

Figure 6.2 Design of the cryogenic delivery system

6.3. Design, manufacture and test of the cryogenic cooling nozzle

In this section, the activities conducted in order to design and manufacture a cryogenic cooling nozzle for CNC milling are described.

6.3.1. Specifications of the problem

A cryogenic cooling nozzle is required to spray liquid nitrogen onto the contact zone between cutting tool and workpiece. The aim is to dissipate generated heat at the cutting zone due to plastic deformation at the cutting zone during chip formation (primary deformation zone) and friction between the chips and tool's rake face (secondary deformation zone) and machined surface and tool's flank face (tertiary deformation zone) as shown in figure 6.3. In addition, as explained in section 2.3, one of the aims of using cutting fluids is chip removal thus, it is desired that the LN_2 flow also blows the chips away from the cutting zone. Furthermore, the design is required to retrofit into the available CNC machining centres.

6.3.2. Conceptual design of a cryogenic cooling nozzle

In this section, three solutions (concepts) are provided to address the problem specified in section 6.3.1. Furthermore, based on the process requirements and findings of the literature, design constraints are identified and used for scoring each concept. The concept ranked highest was then selected as the most appropriate solution to the problem and thus was used for embodiment design.

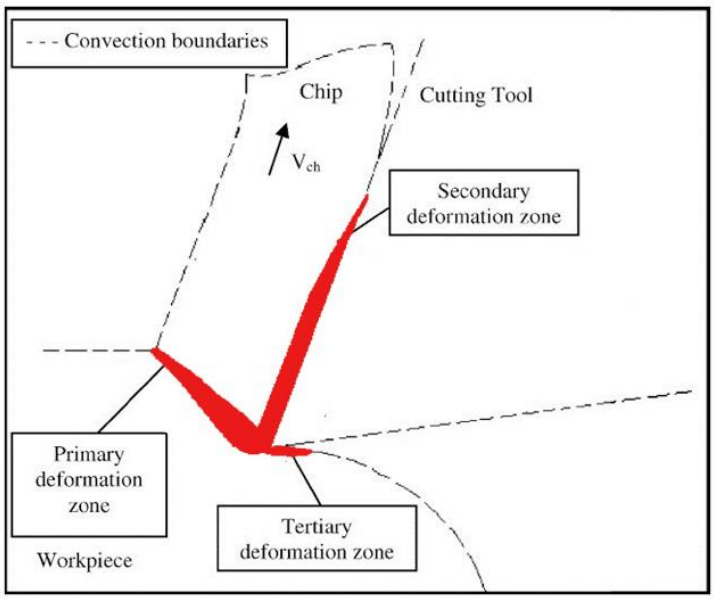

Figure 6.3 Simplified model of cutting zone in machining operations such as turning and milling

6.3.2.1. Conceptual designs

Based on the design constraints three concepts were generated for further investigations. These concepts are explained as follows:

I. Concept 1: External Nozzle

As shown in figure 6.4, in this design the coolant delivery nozzle commonly used for flood cooling and MQL is replaced with a cryogenic cooling nozzle after some modifications. In this approach a single nozzle targets the cutting tool from a set distance.

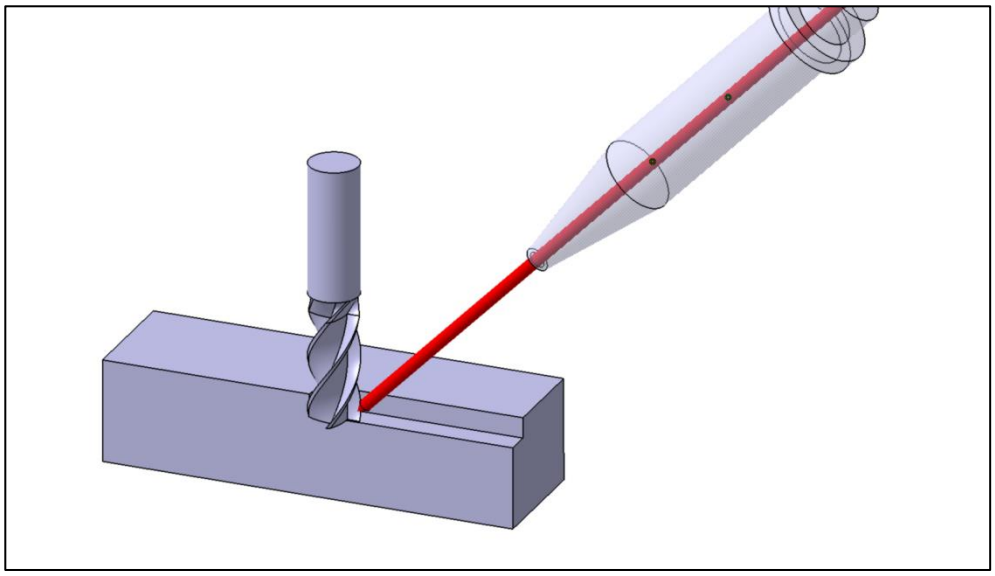

Figure 6.4 Pictorial illustration of 1st concept for cryogenic cooling using a single external nozzle (the flow of cryogen inside the nozzle is shown in red)

II. Concept 2: Cryogenic Shower

In this concept, the nozzle forms a cryogenic curtain around the cutting tool and aims to deliver LN_2 to the cutting zone along the cutting tools' axis and directly through the flutes. This concept is visualised in figure 6.5. In the figure, the nozzle is shown transparent and the cryogen flow is highlighted in red.

III. Concept 3: Through the Spindle Cooling

In this concept, LN_2 will be delivered through the tool holder and cutting tool to the cutting zone by the means of holes embedded within the cutting tool. This concept has a series of holes which are designed so that cryogen is sprayed along the rake face of the cutting tool. Figure 6.6 illustrates this concept and the cryogen flow is shown in red whilst the tool is transparent.

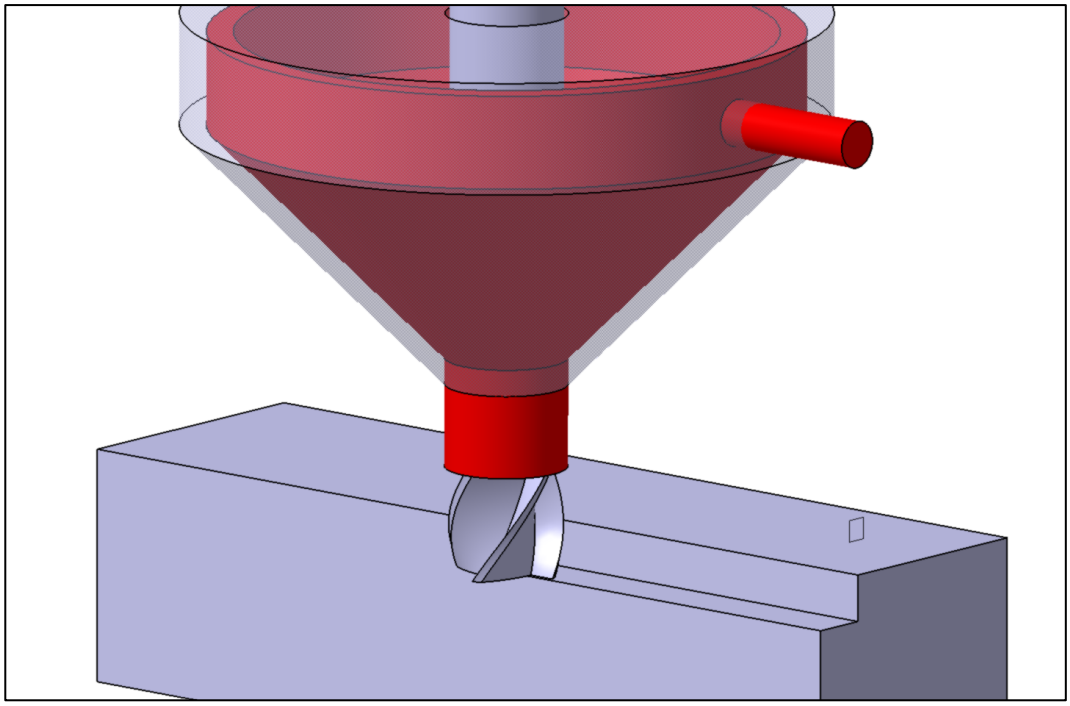

Figure 6.5 Pictorial illustration of the second concept for cryogenic cooling by providing a cryogen shower around the cutting tool (the flow of cryogen inside the nozzle is shown in red)

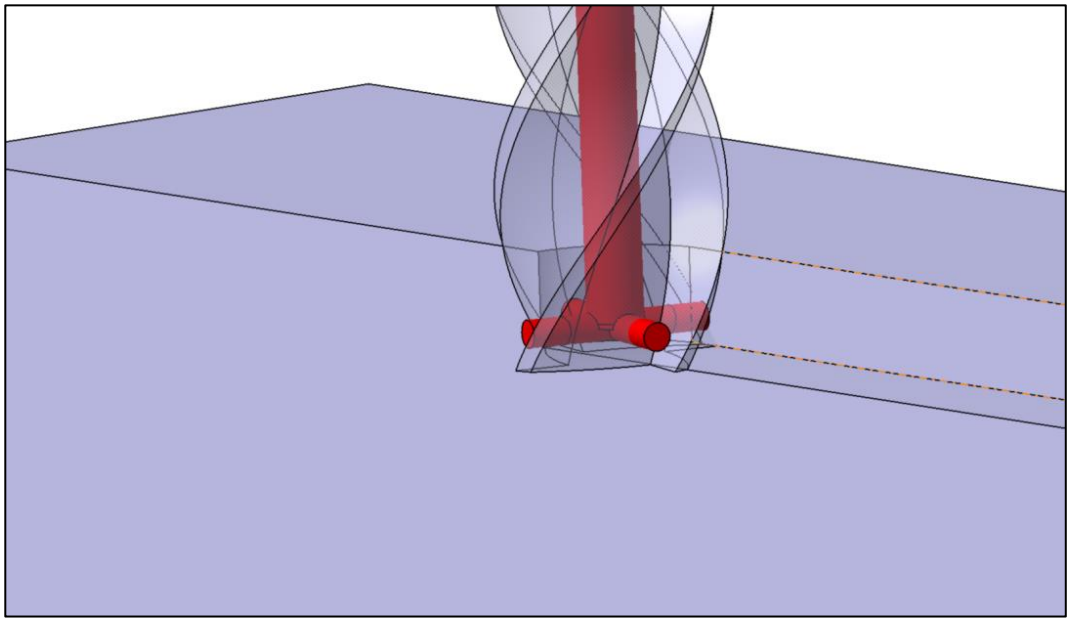

Figure 6.6 Pictorial illustration of the third concept for cryogenic cooling by through the spindle cooling (the flow of cryogen inside the nozzle is shown in red)

6.3.2.2. Design constraints

Following the findings from the literature, end milling process, machine tool and available resources, a series of constraints have been identified for the design of the cryogenic cooling system. These constraints can be summarised as follows:

(i) The cryogenic cooling system should deliver a controlled amount of LN_2 into the cutting zone;
(ii) The cryogenic cooling system should not over cool the workpiece and the machine tool;
(iii) The cryogenic cooling system should retrofit into most conventional CNC milling centres;
(iv) The cryogenic cooling system should be able to deliver LN_2 to the cutting zone, irrespective of the machining direction and mode;
(v) The cryogenic cooling system should be economically justifiable in order to be developed and manufactured;
(vi) The cryogenic cooling system should be able to be manufactured according to available resources;
(vii) The cryogenic cooling system should be easy to use.

In addition to these, the available resources such as technical expertise and facilities considered in the design stage.

6.3.2.3. Conceptual design selection

Based on the design constraints, a weighting table was generated and the concepts presented in the previous section were ranked for each criterion accordingly (table 6.3). Since the aim of cryogenic cooling is to deliver a small amount of a cryogen into the cutting zone, the system should be able to target the cutting zone without extra adjustments. As the first concept is mounted externally, it requires extra adjustment to deliver a stream of LN_2 into the cutting zone. In contrast, the second and third concept are secured on the machine tool's spindle and do not require extra adjustments. As the through the tool concept is implemented into the cutting tool, it has a higher score than the second concept. Similarly, in the first concept, more LN_2 is required to compensate for the distance and lack of accuracy, thus the likelihood of over-cooling the workpiece is very high. Both second and third concepts cover a ring around the cutting tool thus they are also

likely to over-cool the workpiece where it is not necessary. However, as the cryogen is delivered to the point, the chances of over-cooling are less than the first concept. As the first two concepts are extra attachments, they are easy to retrofit to different machine tools whilst in the third concept changing the spindle system of the machine tool is inevitable and potentially costly. Unlike single-point cutting, in milling operations, the position of the cutting zone changes according to the relative movement of cutting tool to workpiece. Therefore, the cryogenic nozzle should be able to target the cutting zone according to the relative movement of the tool and workpiece. Considering this, the first concept can only target one side of the tool unless an actuator moves the nozzle according to the position of the cutting zone which adds to the complexity of the system. Both second and third concepts cover the complete periphery of the cutting tool, thus wherever the cutting zone is, it is covered by the cryogen flow.

As shown in table 6.3, the second concept was ranked highest (scored lower) and thus it is selected as the most appropriate concept for the cryogenic cooling nozzle in terms of the design requirements, constraints and available resources.

Design constraints and requirements	**Ranking**		
	Concept 1	**Concept 2**	**Concept 3**
Ease of targeting the cutting zone	3	2	1
Not over-cooling the workpiece	3	2	1
Retrofit-ability into different machine tools	1	1	3
Compatibility with machining direction	3	1	1
Cost	1	2	3
Ease of manufacturing	1	2	3
Ease of use	3	1	1
Total Score	15	11	13

Table 6.3 Score sheet for selecting the best concept for cryogenic cooling in CNC milling applications

6.3.3. Embodiment design

As explained in the previous section, the most viable concept to meet the requirements of this research has been found to be the cryogenic shower concept (concept 2). One of the requirements of this nozzle is to provide a uniform flow of LN_2 around the cutting tool. In order to achieve this, LN_2 will go through a chamber inside the nozzle after passing through the inlet. This chamber is connected to an internal nozzle by the means of three internal inlets. The inlets provide a more uniform flow of LN_2 around the cutting tool. This is shown in figure 6.7.

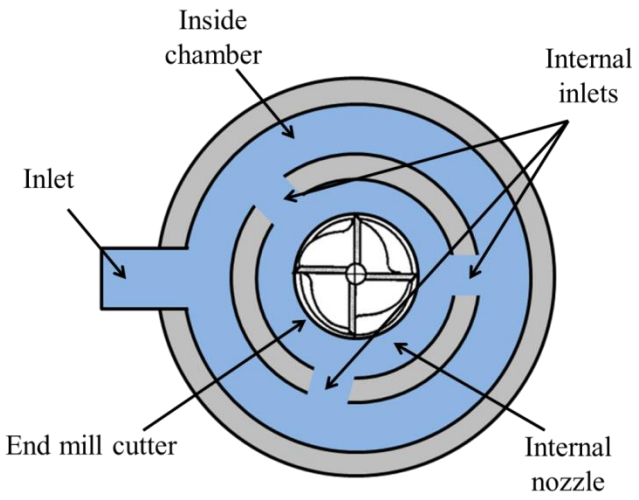

Figure 6.7 Pictorial presentation of details of the cryogenic shower nozzle

As shown in the cross sectional view of the nozzle (figure 6.8), the internal nozzle is tilted 60° downward, thus most of LN_2 will be targeted towards the cutting zone.

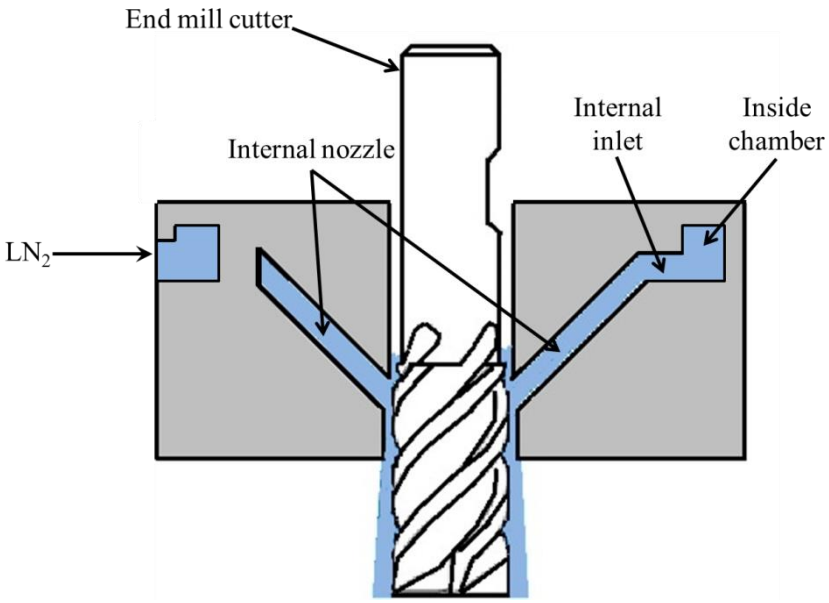

Figure 6.8 Cross section presentation of the cryogenic shower nozzle

In order to make the manufacturing of the nozzle possible, the design was divided into four parts requiring assembly to form the final cryogenic shower nozzle. As shown in figure 6.9, the inlet, chamber and internal inlets are embedded in the base (1) and there is a bore in the centre where the internal nozzle can be placed. Two parts, namely internal nozzle down (2) and internal nozzle up (3) forms the required tilt for the internal nozzle towards the centre of the nozzle and a cap (4) secures the assembly together allowing the LN_2 to travel through the nozzle without escape.

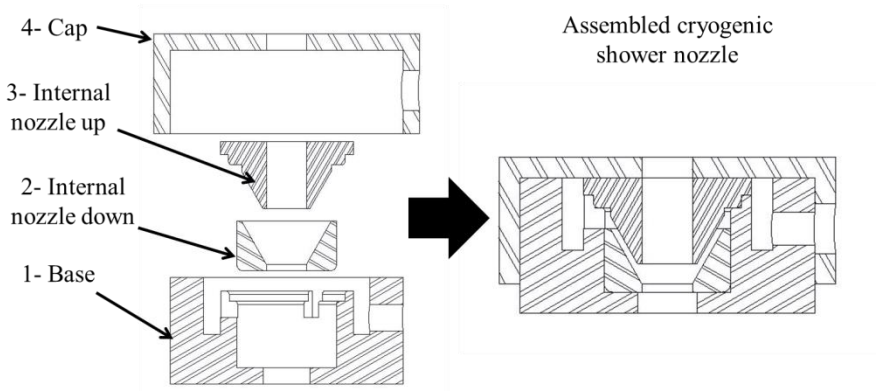

Figure 6.9 Presentation of different parts of cryogenic shower nozzle

As the cutting tool passes through the centre of the nozzle, the diameter of the hole in the centre of the nozzle dictates the tool size. A common mid-range 12mm diameter end mill cutter was selected as the baseline tool size for this research. These tools represent a standard size and are typically used in machining. Therefore, the dimensions are to be decided for a 12mm end mill cutter whilst considering minimising the size of the nozzle where possible. This initial design has been modelled in a CAD system to be used for CFD modelling.

6.3.3.1. Computational fluid dynamic modelling and analysis

In order to model the flow of LN_2 inside the nozzle, a 3D enclosure of the nozzle was generated in a CAD programme to be directly used for CFD analysis in Ansys® Fluent® (Ansys, 2013). An enclosure is a boundary or space which indicates the presence of a system for a fluid to flow in a CFD programme. Figure 6.10 shows the enclosure of the cryogenic shower nozzle assuming the existence of a 12mm end mill cutter in the centre of the nozzle.

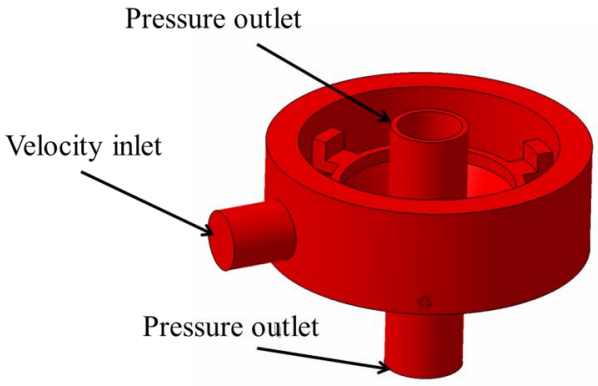

Figure 6.10 Cryogenic shower nozzle's enclosure

Whilst meshing is a very important parameter in finite element analysis, due to the limited number of elements in Ansys® Fluent® student licence (Ansys, 2013), a selective meshing regime was implemented. A finer mesh with higher concentration was used for more critical areas whilst a coarser mesh was used for areas with lower importance. The element size used for meshing ranges from 0.1mm to 0.02mm. Figure 6.11 illustrates the mesh used for the CFD analysis.

For simulation purposes, the inlet of the nozzle was defined as the velocity inlet and the two sides of the cutting tool on top and bottom of the nozzle were defined as pressure outlets as illustrated in figure 6.10. The properties of LN_2 which were used for simulation are provided in table 6.4 and were given to Ansys® Fluent® (Ansys, 2013) as an input. The software provides two options of pressure-based and density-based solver types. For this problem, the pressure-based solver was selected based on the assumption that the density of the fluid remains constant during the process as LN_2 is not compressed at the relatively low pressure of 1 bar used in this research. In addition, a K-epsilon turbulent model was activated to model the turbulence inside the nozzle. It is noteworthy to mention that the constants for the K-epsilon model and the turbulence intensity requires experimental measurement and are usually defined practically which is out of the scope of this research. Thus, for this problem and in the absence of experimental measurements, the turbulence intensity of low turbulent systems has been selected whilst realisable K-epsilon model constants are used.

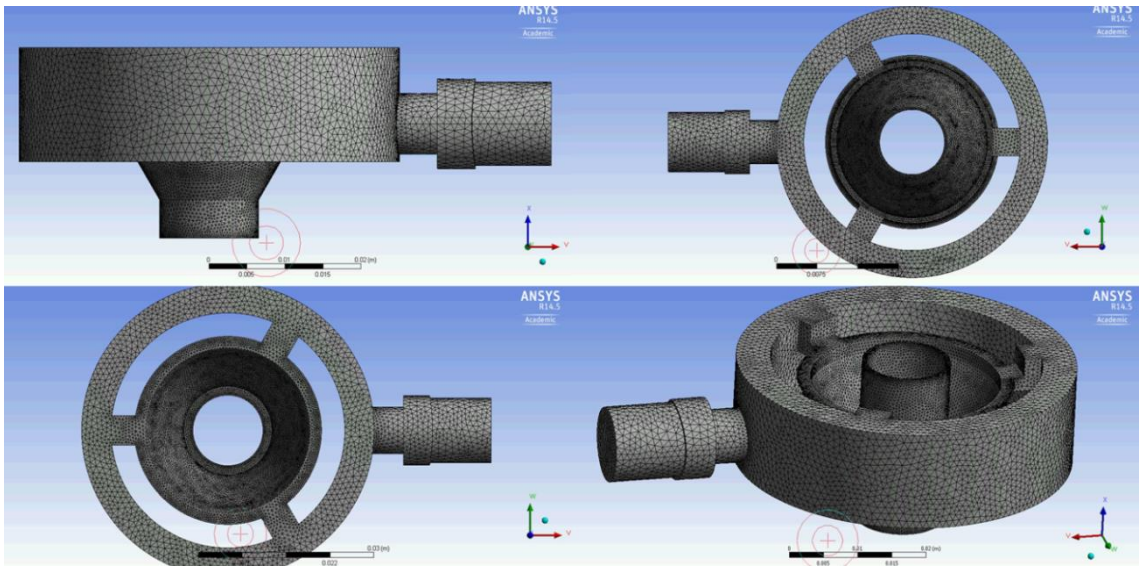

Figure 6.11 Digital representation of the mesh used for CFD analysis

Input pressure		1 bar
Input flow rate		20 lit/min
Inlet's hydraulic diameter D_H		11.8
Outlet's Hydraulic diameter		0.25
Density of LN_2		806.08 kgm^{-3}
Viscosity		0.00016065 $kgm^{-1}s^{-1}$
Temperature		-197°C
Turbulence intensity		5%
Realisable K-epsilon model constants	$C_{1\epsilon}$	1.44
	$C_{2\epsilon}$	1.9
	C_{μ}	0.09
	σ_K	1.0
	σ_ϵ	1.2

Table 6.4 Input parameters of LN_2 for CFD analysis

The simulation was run for 500 iterations and stopped where the residual errors became less than 10^{-4} and converged as shown in figure 6.12.

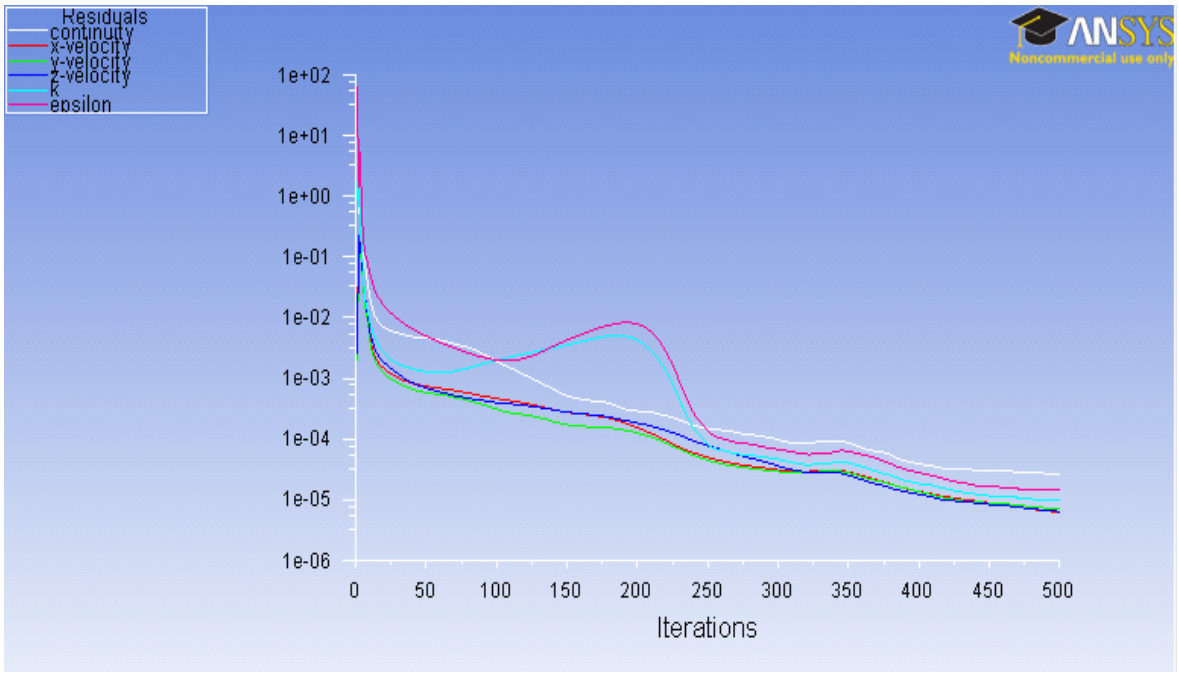

Figure 6.12 Graph of residuals for CFD simulation of cryogenic shower nozzle

Figure 6.13 shows the velocity vectors of LN_2 inside the nozzle and depicts that the maximum velocity of 16.82 m/sec inside the nozzle. The simulation revealed that the form of internal inlets requires slight modification and proved that quite a uniform flow of LN_2 can be expected at the outlet. In addition, it showed that the majority of LN_2 flows downward towards the cutting zone.

In order to improve the flow at the internal inlets, fillets radii was used in the corners of the internal inlets. This modification is shown in figure 6.14. In addition, from the manufacturing point of view, it has been found that the base and internal nozzle down (figure 6.9) can be integrated and make one part (integrated body) reducing the number of parts for the nozzle to three.

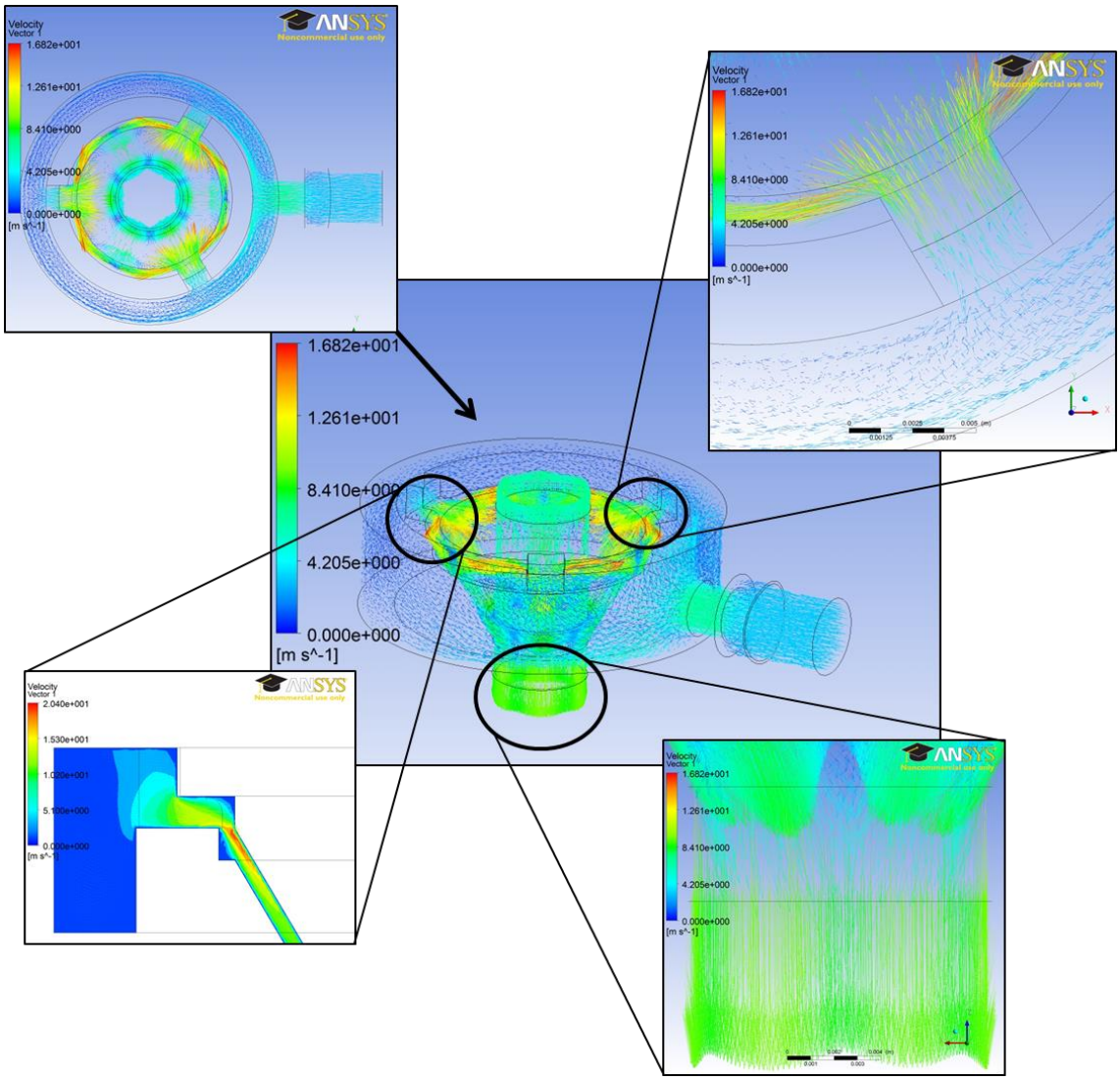

Figure 6.13 Presentation of velocity of LN_2 when passing through the nozzle

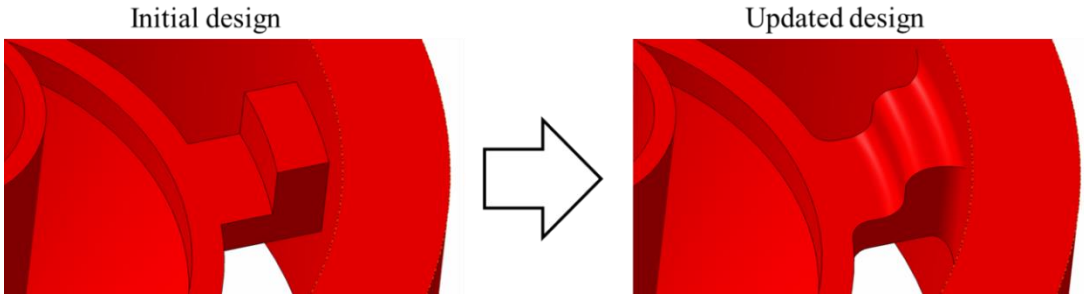

Figure 6.14 Updated enclosure as a result of modified design of internal nozzles

6.3.3.2. Embodiment design for clamping the nozzle onto the machine tool's spindle

In order to secure the nozzle in the correct position around the tool, a simple clamping system was designed. The system consists of a C shaped ring placed around the spindle and a disk which holds the nozzle at the required distance from the spindle. The C ring and the disk are held together by means of three threaded bars. A pictorial view of the clamping system is shown in figure 6.15.

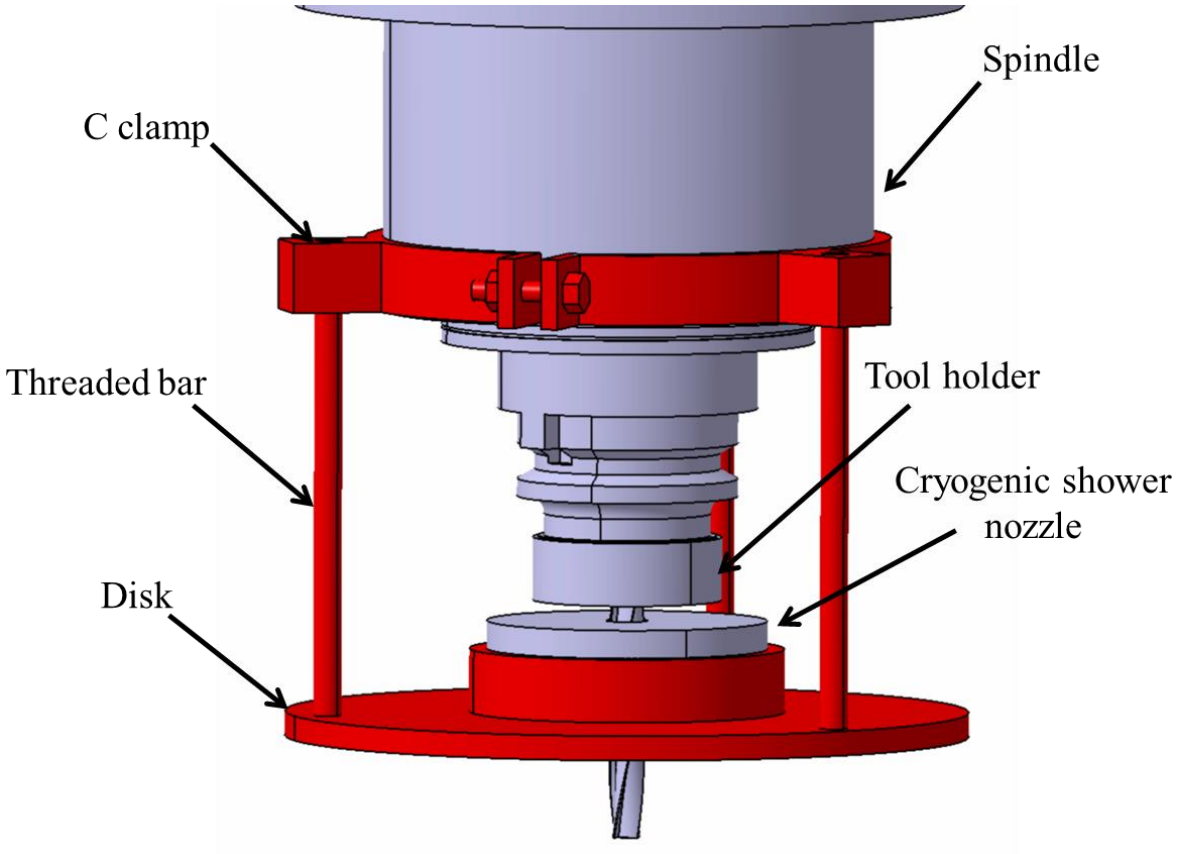

Figure 6.15 Clamping system for cryogenic shower nozzle

6.3.3.3. Manufacturing drawing and making the prototype

A standard commercial vertical CNC milling centre, namely Bridgeport 610 XP^2 was selected as a platform to carry out the machining trials.

Due to the costs and ease of machining, it was decided to machine the prototype out of free cutting aluminium 6061. Figure 6.16 shows the final assembly of the first prototype of the cryogenic shower nozzle mounted on the spindle of the Bridgeport machine tool.

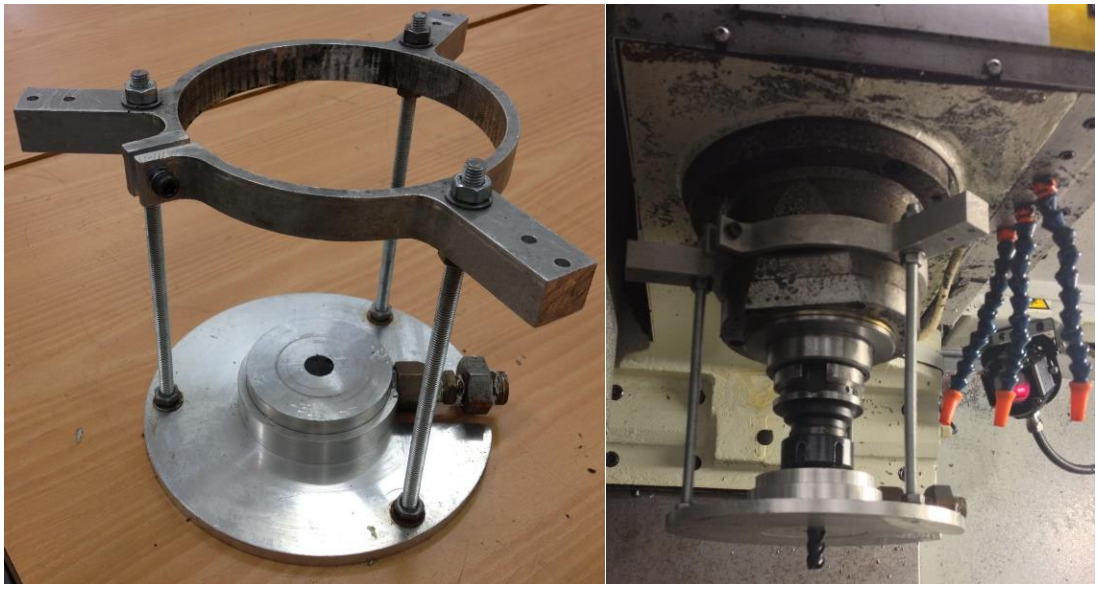

Figure 6.16 The cryogenic shower nozzle and clamping system prototypes mounted on the Bridgeport VMC 610 XP^2 vertical milling centre

6.3.3.4. High speed filming of the working nozzle

In order to observe the flow of LN_2 upon its exist from the nozzle, an ®Olympus iSpeed high speed video camera was used to film the nozzle as the spindle rotated at 5000 rpm. The camera was set to capture 4000 frames per second at the resolution of 546x684 pixels. Slow motion analysis of the system revealed that LN_2 flows downward through the flutes of the cutting tool covering the rake face of the tool. In addition, a spray of LN_2 forms a curtain around the tool and covers the flank face of the tool. Figure 6.17 shows a range of images taken by high speed camera whist the red circle shows the flow of LN_2.

6.3.3.5. Cryogenic machining trials

In order to test the cryogenic shower nozzle and identify its effectiveness, strengths and weaknesses, two sets of machining trials have been designed and conducted. Two types of commercial end mill cutters were used for machining trials. The trials consisted of side milling of Ti-6Al-4V blocks using different machining environments. The cutting parameters, namely cutting speed, feed rate and depth of cut were selected according to the tool manufacturer's recommendation. Three machinability indexes of surface roughness, tool wear and power consumption were monitored to identify the effects of cryogenic cooling using the designed cryogenic shower nozzle in comparison with conventional machining environments of dry and wet.

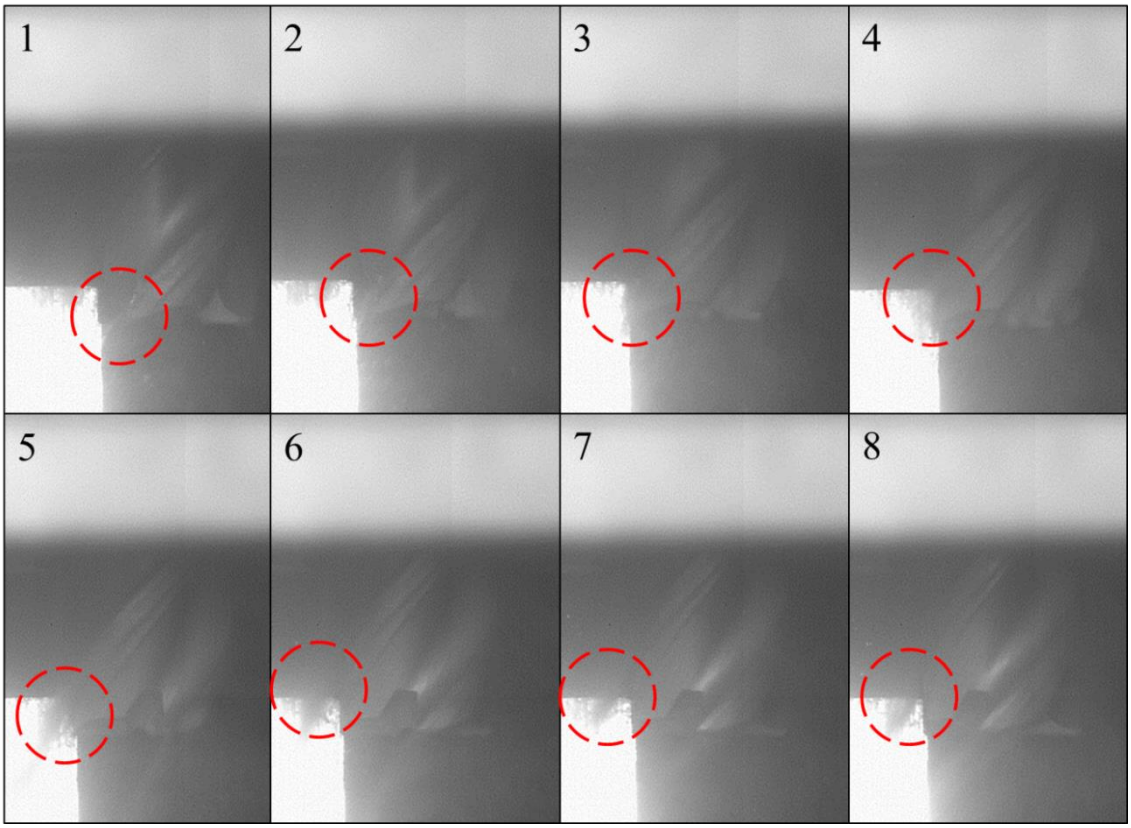

Figure 6.17 High speed images of cutting tool whilst LN_2 is being sprayed using cryogenic shower nozzle

I. First machining trial

I.1 Design of experiments

As mentioned previously, a one-factor-at-a-time experimental design approach was implemented for comparing the effects of cryogenic cooling with dry machining in conventional end milling operation. The single factor of the experiments is defined as being the machining environment or cooling system at two levels, namely, dry and cryogenic. Other machining parameters including cutting speed, chip load, immersion rate (radial depth of cut), depth of cut and machining strategy (straight line slots) were kept constant during the trials. The machining parameters used in this investigation are provided in table 6.5. The selected monitoring parameters were surface roughness (Ra), power consumption (W) and tool wear (mm). The cutting tool used for this experiment was a WNT general purpose uncoated solid carbide end mill with a 12° rake angle, a 45° helix angle and sharp precision ground edges.

Cutting Tool	Uncoated solid carbide end mill
Tool Diameter	10mm
Cutting Speed	30m/min
Chip Load	0.15mm/tooth
Immersion Rate	50%
Depth of Cut	1mm

Table 6.5 Cutting parameters used for the first machining trial

I.2. Results and discussions for the first machining trial

Two machining trials under cryogenic and dry conditions with similar cutting parameters were conducted. From these machining trials, the machined surfaces were evaluated for arithmetic surface roughness (Ra) following the instructions provided by BS EN ISO 4288-1998, using a Taylor Hobson's Talysurf® contact surface roughness tester. The surface roughness was measured at 20 points for each sample and the mean of the measured values was calculated to present the average Ra of each surface. Figure 6.18, illustrates the measured values of Ra for each surface and as can be observed, the comparison of the surface roughness values suggests that cryogenic cooling has significantly improved the surface finish. In fact, the reduction in surface finish from an average of 1.85µm in dry machining to 0.82 in cryogenic cooling has resulted in a 2-fold improvement in surface finish before tool failure. As shown in figure 6.18, the initial start point of the machining path for both experiments has a high surface roughness which can be attributed to the instability of the cutting tool at the start of the cutting operation. Another notable point in both dry and cryogenic surface roughness graphs is the increasing trend starting at the length of 55mm which is attributed to the fracture of the cutting edge resulting in higher surface roughness.

In addition to surface roughness, power consumption of the CNC milling machine was monitored during the cutting operation using a Hioki 3169-20 power measurement instrument attached to the main power line of the machine tool. The instrument has a reported accuracy of 0.5% and was setup to measure the power consumption of the machine tool at 1-second time intervals. The power consumption of the CNC machine tool for an identical machining path was measured in three different conditions. In order to provide a base line for the power consumption of the machine tool, power consumption was measured based on the DoE tool path without any cutting material. The same process was repeated while cutting Ti-6Al-4V alloy under dry and cryogenic conditions.

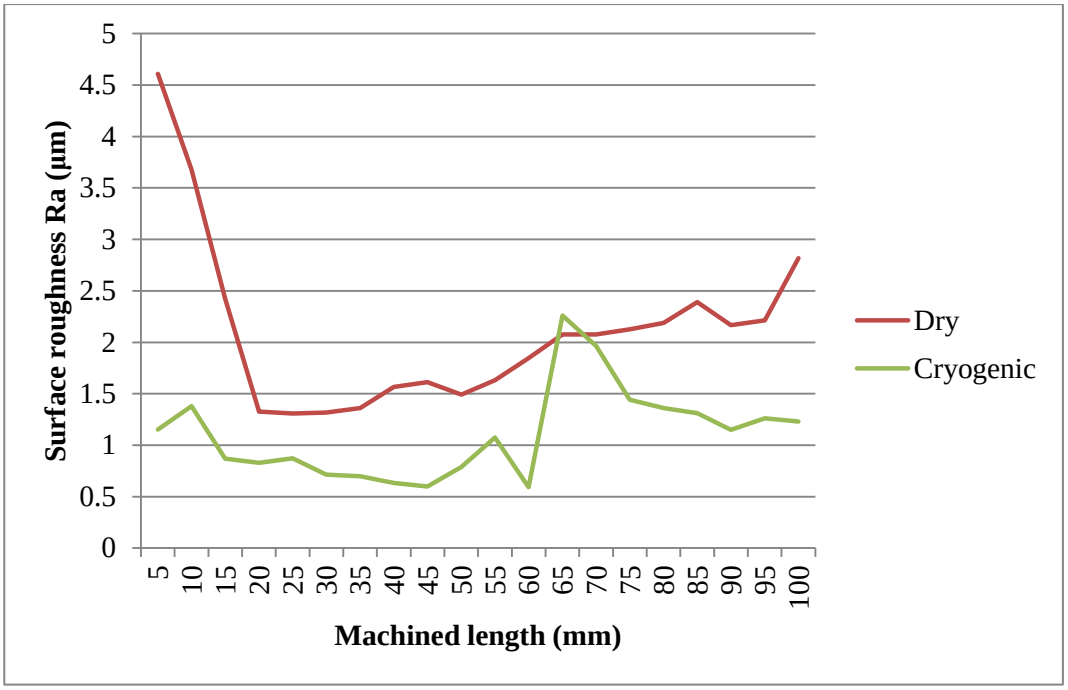

Figure 6.18 Surface roughness of machined surfaces under cryogenic and dry condition in the first machining trial

As illustrated in figure 6.19, the average power consumption showed that cryogenic cooling resulted in a 1.3% increase in the machine tool's power consumption. However, due to the short machining length, it cannot be concluded that the change in power consumption as a result of the introduction of liquid nitrogen in the process is significant.

Each cutting tool was examined after machining operations using a toolmakers microscope. It has been found that while crater and flank wear observed on the tool used for dry machining, there was no sign of flank wear on the tool used in cryogenic machining. The dominant tool failure mode was chipping of the cutting edge leading to catastrophic fracture of the cutting edges after an almost identical machining length. Figure 6.20 provides a pictorial view of the failed cutting tools used for the experiments. The effect of chipping is also clear in both power consumption and surface roughness diagrams as shown in figures 6.19 and 6.21. For instance, chipping of the tool resulted in an average of 4.6% and 5.9% increase in the power consumption of the machine tool in dry and cryogenic machining respectively. This indicates that the use of power measurement systems is a viable method to monitor tool condition irrespective of machining environment. Sudden spikes in power consumption can be attributed directly to damage of the cutting tool and in particular the cutting edges.

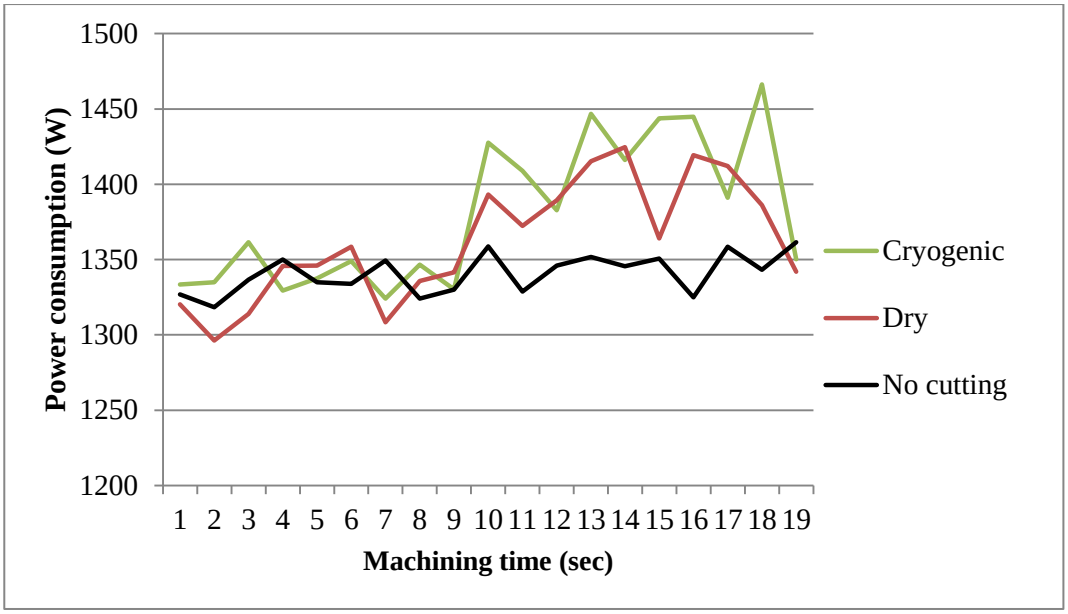

Figure 6.19 Power consumption of CNC milling machine during the first machining trial

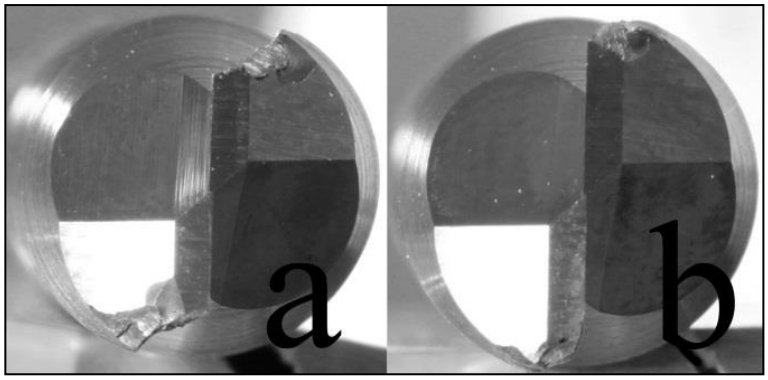

Figure 6.20 Pictorial view of the uncoated solid carbide cutting tools used in the first machining trial after machining under a) dry and b) cryogenic conditions

II. Second machining trial

II.1 Design of experiments

In order to confirm the results observed in the first machining trial and eliminate the problems that occurred due to short tool life, a set of 12mm coated tools specifically designed for machining heat resistant alloys was acquired from Sandvik®. The selected tools were of GC1630 carbide grade and had 12° rake angle, 30° helix angle, two flutes and TiAlN coating.

A one-factor-at-a-time design was used for this trial. The machining environment was the changing parameter of the DoE whilst other cutting parameters, namely cutting speed, chip load, immersion rate and depth of cut being kept constant. The cutting parameters used for this trial are provided in table 6.6. Similar to the previous trial, the cutting parameters were selected based on the tool manufacturer's recommendations for emulsion machining. Surface roughness (Ra), power consumption (W) and tool wear (mm) was selected as the monitoring parameters and the machining length was limited to 300mm (3x100mm).

Cutting Tool	TiAlN coated solid carbide end mill
Tool Diameter	12mm
Cutting Speed	70m/min
Chip Load	0.03mm/tooth
Immersion Rate	50%
Depth of Cut	1mm

Table 6.6 Cutting parameters used for the second machining trial

II.2. Results and discussion for the second machining trial

After conducting a series of machining operations and examining the cutting tools, machined surfaces and power consumption of the machine tool, it has been found that spraying liquid nitrogen into the cutting zone and using the cryogenic shower nozzle has the potential to improve machinability of Ti-6Al-4V. As shown in figure 6.21, the trial demonstrated that cryogenic cooling reduced the surface roughness by 11% and 59% as compared to dry and emulsion cooling respectively.

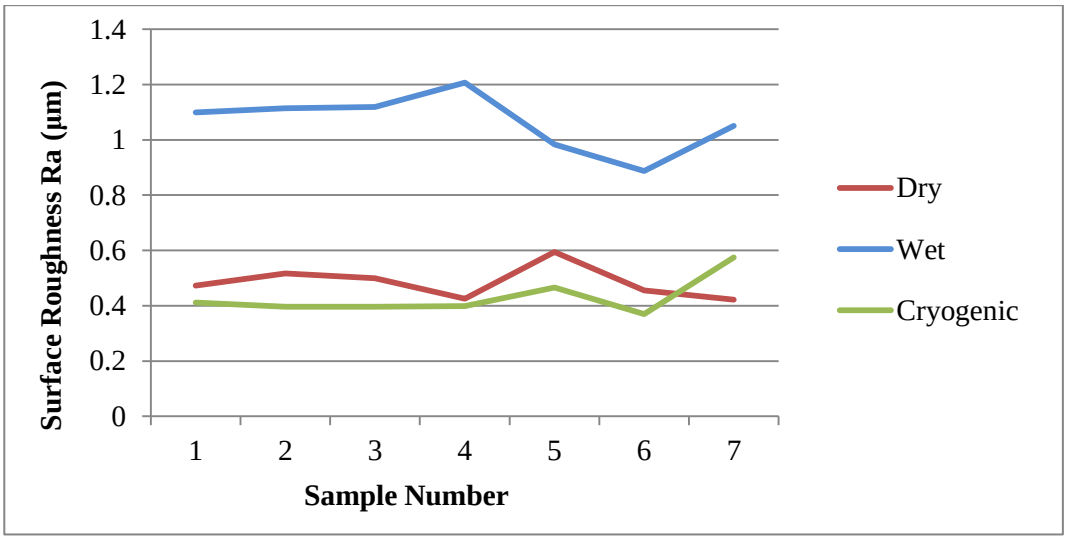

Figure 6.21 Measurement of surface roughness along the machining path for the second machining trial

Analysis of power consumption indicated that the use of liquid nitrogen has resulted in a significant reduction in the total power consumption of the machine tool as compared to emulsion cooling due to the elimination of the coolant pump (figure 6.22). Using t-test, cryogenic cooling showed slightly higher power consumption (1.3%) in comparison with dry machining. The cutting forces and consequently power consumption are dependent on a series of phenomena including but not limited to cutting speed, feed rate, depth of cut, coolant/lubricant, cutting tool geometry and the material properties of the workpiece (Astakhov, 2006). As explained in section 3.3.1, changing temperature affects the hardness and material strength of the workpiece material. In comparison with dry machining, the most significant change in machining condition was reducing the temperature of the system and thus the material properties of the workpiece. Therefore, increases in the power consumption in cryogenic machining in comparison with dry machining can be explained by the increase in the workpiece material strength and hardness as a result of cryogenic cooling.

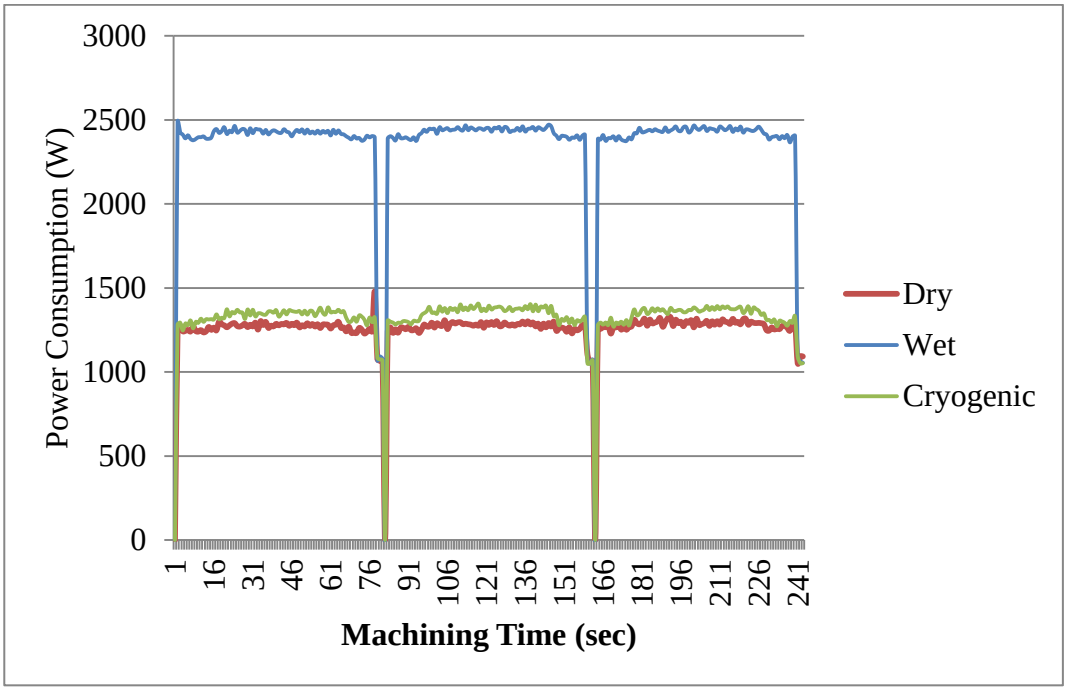

Figure 6.22 Power consumption of the machine tool during machining operation under different cutting environments in the second trial

Monitoring the tool wear during and after the machining operations has been conducted using a toolmaker's microscope. As shown in figure 6.23, cryogenic cooling has significantly reduced the flank wear growth rate on the edges of the cutting tools. In fact, using liquid nitrogen as coolant has resulted in a 70% reduction in the tool wear growth rate. This can be explained by modification of the cutting tools material properties as a result of extremely low temperatures and reductions in the cutting material interface temperature, resulting in lower chemical reactivity between the cutting tool and workpiece material.

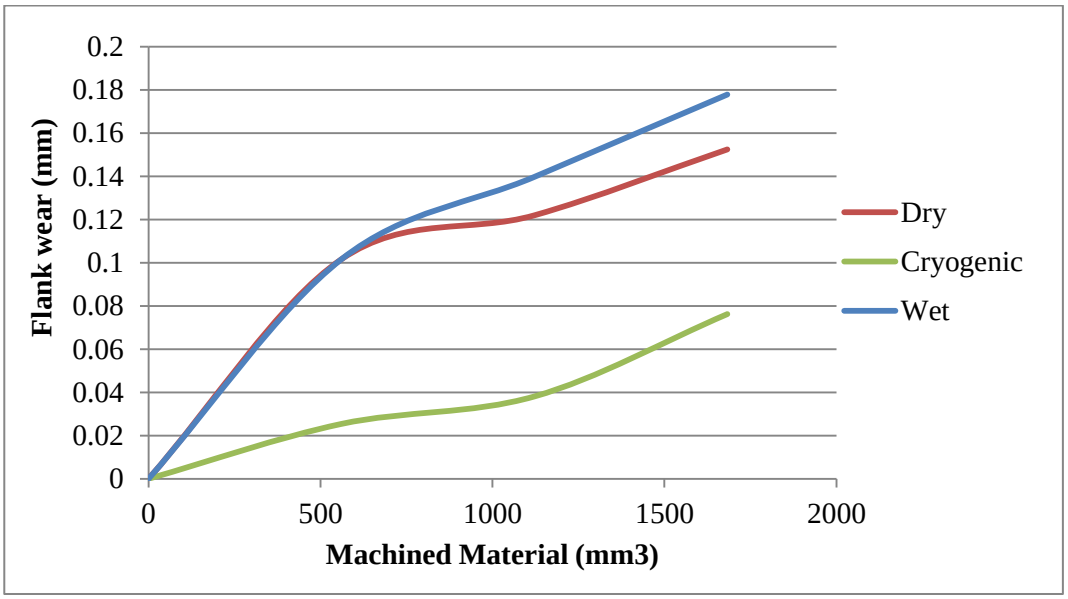

Figure 6.23 Flank wear graph of the cutting tools used for second trial

6.3.3.6. Discussion on the cryogenic cooling system based on the machining trials

High speed filming of the nozzle in action and machining trials proved that the design has the potential to improve the machinability of Ti-6Al-4V in end milling operations. However, some issues aroused during the machining trials which requires to be addressed by modifying the design. These issues can be listed as:

i- The threaded bars used for holding the ring to the C clamp are required to be stiffer.

ii- Aligning the clamping system with nozzle and cutting tool is difficult due to the design of the C clamp.

iii- The ring obscures the vision of the cutting tool.

iv- Extra material from the nozzle can be removed in order to reduce its weight.

Considering these points, the clamp design has been modified in order to make it easier to align the clamp, nozzle and cutting tool axes. Thus, the C clamp was replaced with a ring with sliding tolerance. This eliminates the requirement for aligning the clamp with spindle to a great extent. The diameter of the threaded bars has been increased to 10 mm to increase the stability of the nozzle against machining vibrations.

The design of the nozzle has also been updated and the excess material was removed making it almost 25% lighter. Figure 6.24, illustrates the updated design of the nozzle and clamping system. Main parameters for selecting material for the components of the design were low thermal conductivity, low thermal expansion coefficient, machinability and cost effectiveness. In addition, the selected material should not show ductile to brittle behaviour due to low temperatures. Thus, AISI 316 stainless steel was selected as an appropriate candidate material for the nozzle.

6.4. Detailed design and manufacture

Based on the embodiment design stage, the final design depicted in figure 6.24 has been brought to this section for detail design. In this section the tolerances required for the design and assembly of the system were added to the embodiment design and the details of design and manufacturing process were clarified. In addition, the dimensions of both nozzle and clamping system have been updated and checked according to the spindle, tool holder and system requirements.

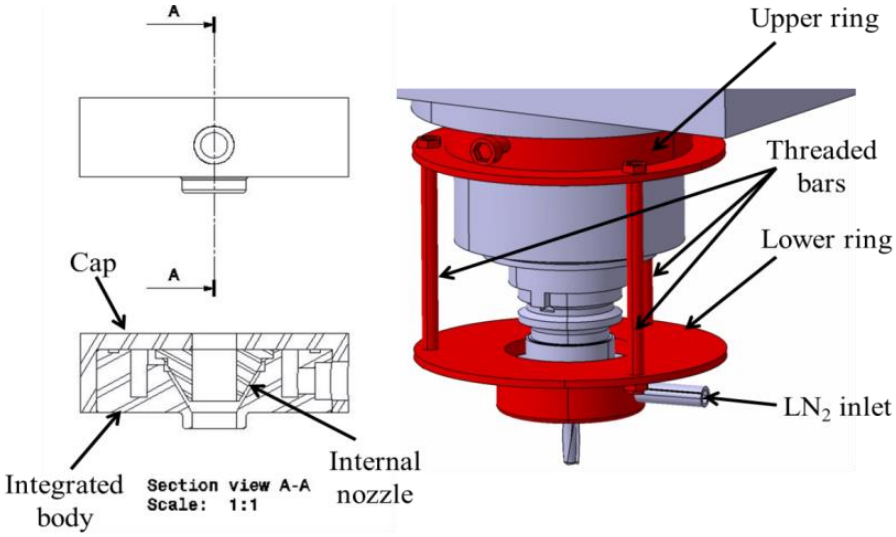

Figure 6.24 Updated design of cryogenic shower nozzle and clamping system after conducting a set of machining trials

The detailed sketches of the nozzle and clamping system parts together with assembly sketches are provided in Appendix A. In addition, the assembly sequence for the nozzle is shown in figure 6.25 whilst figure 6.26 illustrates the final assembly of the nozzle and clamping system. They also indicate the key names for each part.

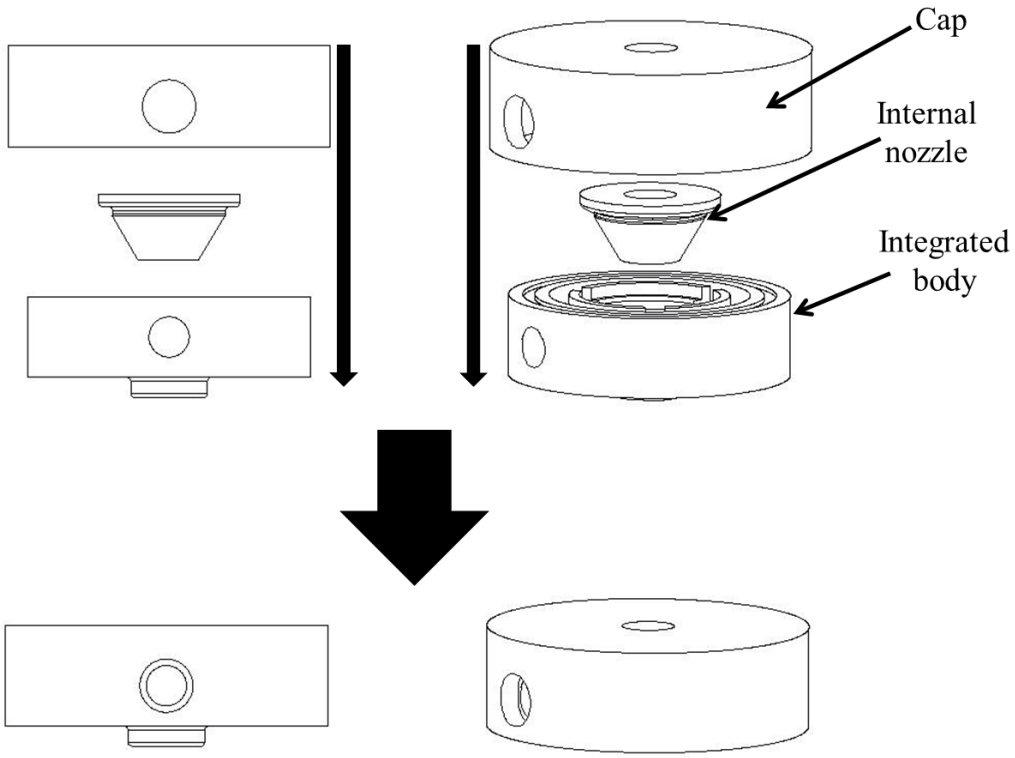

Figure 6.25 Exploded assembly sequence of the cryogenic shower nozzle

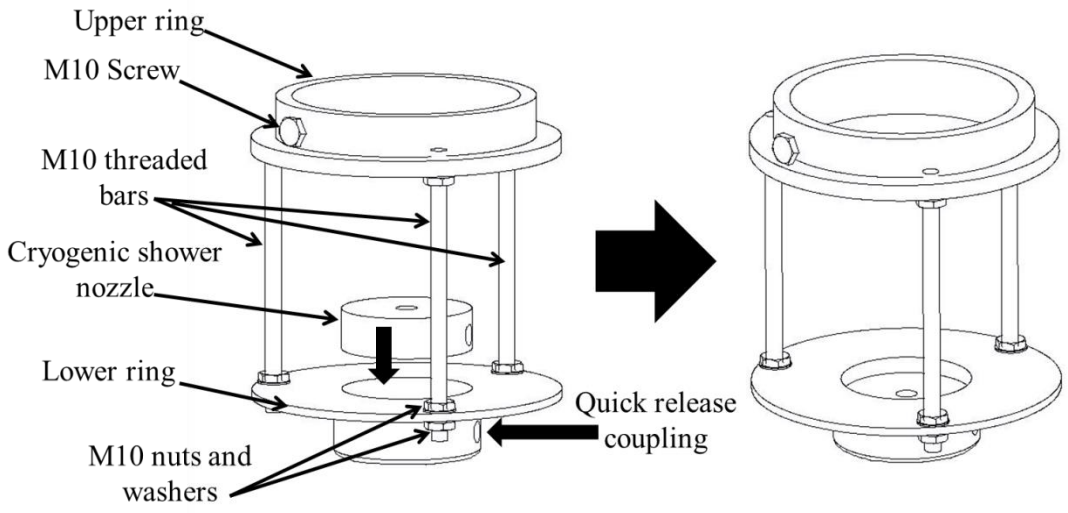

Figure 6.26 Final assembly and specifications of cryogenic shower nozzle and clamping system

All three parts of the nozzle, namely cap, internal nozzle and integrated body and the upper and lower rings of the clamping system were machined out of a bar of AISI 316 stainless steel.

The manufactured parts were assembled and silicon sealant was used for sealing the parts. Figure 6.27 shows the assembly process of the parts and the final product mounted on the Bridgeport machine's spindle.

Figure 6.27 Assembly of cryogenic shower nozzle and clamping system mounted on the Bridgeport machine tool

6.5. Summary

This chapter detailed the activities which have been conducted to design, manufacture and develop a cryogenic cooling system for end milling using a conventional CNC milling machine. The design was divided into development of the cryogenic delivery system and cryogenic nozzle and clamping system. For the development of cryogenic delivery system, expert companies were consulted and different facilities have been outsourced and assembled in house. Pahl and Beitz systematic design has been implemented for the design of cryogenic nozzle and clamping system. Three different concepts have been generated for cryogenic nozzle and the most appropriate design, namely cryogenic shower was selected. A series of computational and empirical investigations have been conducted and the concept has been updated based on their findings. The final design has been detailed and manufactured using available resources in the University. Figure 6.28 illustrates the final cryogenic shower nozzle and clamping system mounted on the spindle of the Bridgeport VMC 610 XP^2 vertical CNC milling centre together with the cryogenic delivery system. This system will be used for comparative study disclosed in chapter 7 to evaluate and identify the effects of cryogenic cooling on the machinability of Ti-6Al-4V alloy in comparison with traditional machining environment, namely dry and wet.

Figure 6.28 Final assembly of the cryogenic shower nozzle, clamping and delivery systems

Chapter 7

Comparative study of cryogenic machining with conventional machining environments

7.1. Introduction

In order to identify the effects of cryogenic cooling on the machinability of Ti-6Al-4V titanium alloy, it is necessary to compare the results with conventional machining environments, namely dry and flood cooling (wet). This chapter discloses the comparative study of cryogenic machining with dry and wet machining environments by using the cryogenic shower cryogenic cooling system. The aim of this chapter is to provide a clear understanding of the effects of cryogenic cooling in comparison with dry and wet machining environments.

As shown in figure 7.1, the methodology for the comparative study presented in this chapter is divided into four main sections, namely preparatory activities, machining experimentation, data collection and experimental results and statistical analysis. First, in the preparatory section, the effects of cryogenic cooling on material properties of titanium were studied. In addition, the geometries of the cutting tool for machining experiments were selected and a set of machining trials has been conducted to identify the boundaries of machining parameters.

A DoE technique was selected and generated based on the cutting parameters and machining boundaries defined in the preparatory section. In order to reduce the errors in experimentation, a procedure was developed for conducting machining experiments. Following the DoE and the experimental procedure, a series of machining operations were conducted and cutting tools and chips were collected for further analysis. The details of these activities are provided in section 7.3.

Power and energy consumption of the machine tool was monitored during machining operations. In addition, surface roughness, tool wear and chip morphology for each machining experiment were measured accordingly. Furthermore, as shown in figure 7.1, the machined samples were prepared and the subsurface microstructure and microhardness and surface topography were studied for each machining experiment. These activities are disclosed in section 7.4 entitled data collection.

Following the DoE, the gathered data from machining experiments for different machinability metrics were analysed using various statistical techniques. The aim of this stage is to identify the effects of cryogenic cooling on different machinability metrics as compared to conventional dry and wet machining environments.

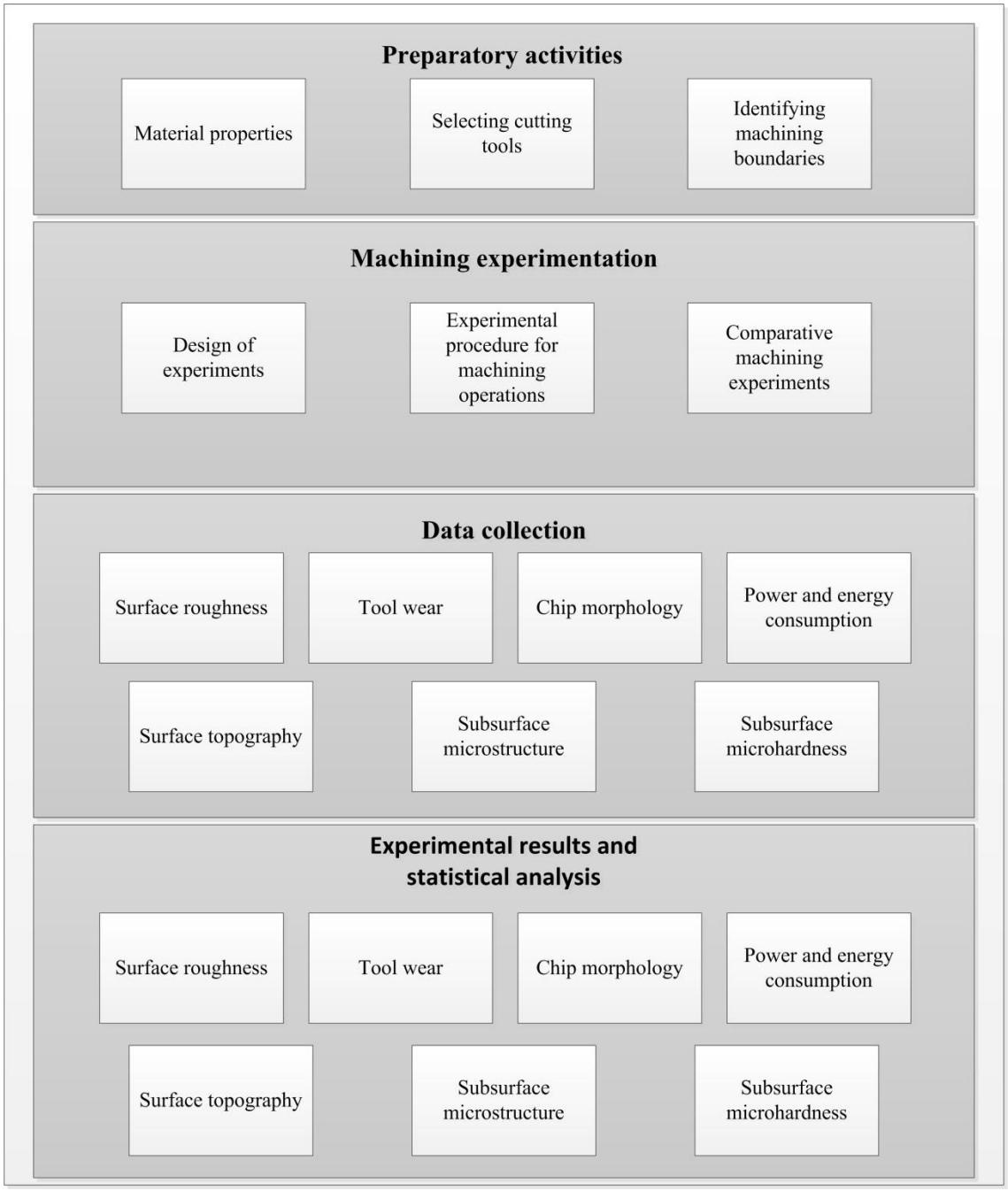

Figure 7.1 Illustration of the methodology for comparative study

7.2. Preparatory activities for comparative study

In this section, the effects of cryogenic cooling on material properties and microstructure of Ti-6Al-4V alloy are presented. In addition, the specification of the cutting tools which were used for machining experiments and the boundaries of cutting parameters are disclosed.

7.2.1. Evaluation of effects of cryogenic cooling on material properties of Ti-6Al-4V

The selected material for this experiment is annealed Ti-6Al-4V α-β titanium alloy. The microstructure of annealed Ti-6Al-4V comprises of coarse plate shaped α phases and grain boundaries of β phase (Hong et al., 2001). In order to be able to perform cryogenic machining, the effects of cryogenic cooling on material properties of Ti-6Al-4V alloy should be determined. Thus, the hardness and microstructure of the alloy were to be tested.

In order to measure the hardness of the material, a Vickers hardness tester with 20 kg load was employed. The hardness test was conducted on an annealed Ti-6Al-4V sample with the dimensions of 150mmx50mmx50mm. As shown in table 7.1 the hardness of a sample was measured at 10 randomly selected points across the sample and the average value of the hardness was calculated to present its hardness. After measuring the material hardness, LN_2 was sprayed on the sample for 10 min which is a typical machining time for cryogenic machining of a block of this size. The sample was left to warm up in room temperature. After the sample reached the ambient temperature, the hardness of the sample was measured again at 10 randomly selected points as shown in table 7.1. Comparing the average value of macro hardness for the sample, before and after cryogenic cooling shows a slight reduction of 1 VH as a result of cryogenic cooling. However, this change is significantly smaller than standard deviation of the measurement results. Thus, it cannot be concluded that cryogenic cooling has changed the material hardness.

	Vickers Hardness	
Measurement number	**Before cryogenic cooling**	**After cryogenic cooling**
1	291	321
2	317	298
3	301	289
4	310	293
5	298	291
6	293	310
7	294	296
8	310	285
9	271	291
10	296	298
Average	298.1	297.2
Standard deviation	12.8	10.8

Table 7.1 Vickers hardness of a Ti-6Al-4V sample before and after exposing to LN_2

As shown in table 7.2, a standard paired t-test with 99% confidence was performed on the collected data using Microsoft Excel® (Microsoft-Corporation, 2010) to test if there is a significant difference between the hardness before and after cryogenic cooling. Since the calculated t statistic is smaller than the critical t values for both one and two tailed, the results of the t-test (table 7.2) show that, with 99% confidence, there is no significant difference between the hardness of the sample before and after cryogenic cooling.

In addition, two samples were prepared from a single bar of Ti-6Al-4V alloy and mounted in epoxy resin for microstructural investigation. The first sample was as delivered whilst the second samples has been subjected to liquid nitrogen spray for 10 min. The samples were ground and polished according to the following procedure for microstructural analysis:

- Grind with P400 grid SiC paper until flat
- Polish with 9 μm liquid diamond using polishing cloth
- Polish with 0.05 μm alumina using micropolish cloth

A Jeol 6480LV SEM was used to study the microstructure of the samples. The Composition Backscattered Electron Imaging (BEI) mode of the SEM was used for microscopy which facilitated imaging of the microstructure of the material.

t-test statistics	Before cryogenic cooling	After cryogenic cooling
Mean	298.1	297.2
Variance	164.544	115.956
No. observations	10	10
Pearson Correlation	0.539	
Hypothesized Mean Difference	0	
Degree of freedom	9	
t statistic	-0.248	
P(T<=t) one-tail	0.405	
t Critical one-tail	2.821	
P(T<=t) two-tail	0.810	
t Critical two-tail	3.250	

Table 7.2 Paird two sample mean t-test for Vickers hardness of Ti-6Al-4V sample before and after exposing to LN_2

An image of the microstructure of each sample was taken at 500x magnification as shown in figure 7.2. The bright areas show β phase and the darker areas are α phase titanium. As shown in figure 7.2, no differences between the microstructure of the samples were recognised, therefore it can be concluded that no significant changes were imposed to the material microstructure as a result of cryogenic cooling.

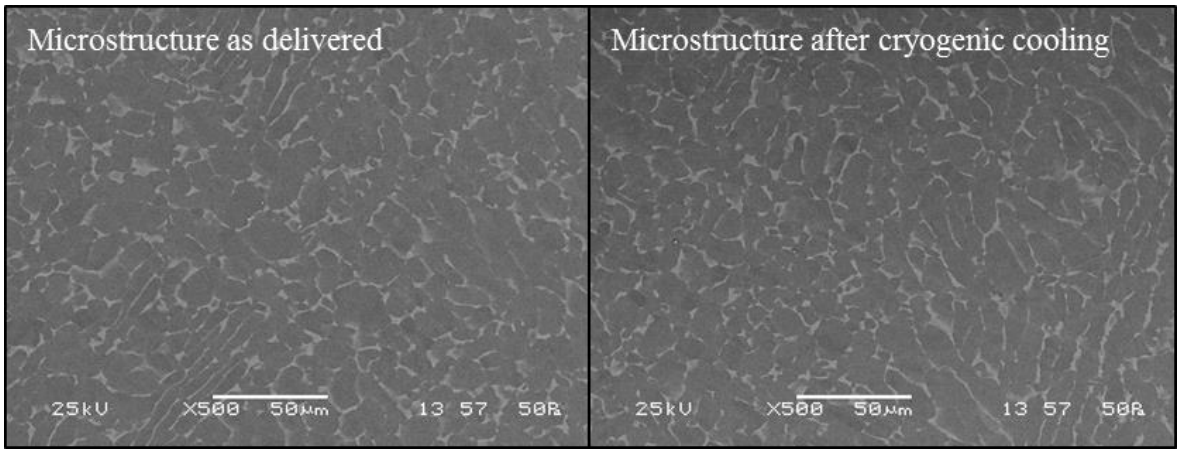

Figure 7.2 Microstructure of Ti-6Al-4V titanium alloy before and after cryogenic cooling

In addition, a high sensitivity Oxford INCA X-Act SSD X-ray detector for Energy-dispersive X-ray spectroscopy (EDS) was used to identify the material composition of the samples. Figure 7.3 illustrates an example of the results of the X-ray spectroscopy for the Ti-6Al-4V alloy used for this research.

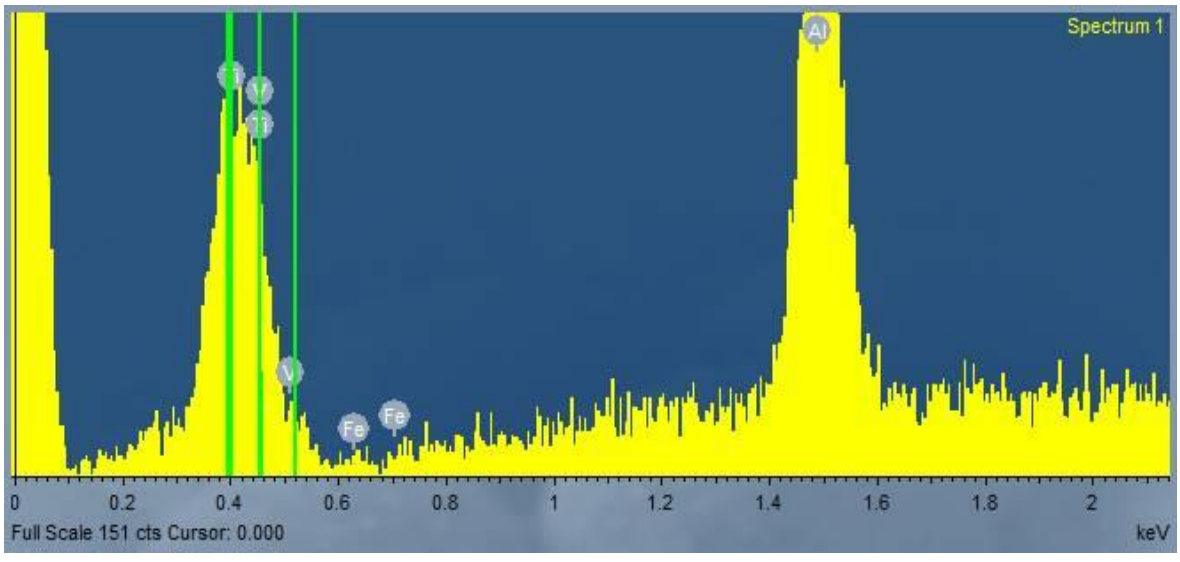

Figure 7.3 Material composition graph of X-ray spectroscopy of Ti-6Al-4V material used for this research

Nine regions with the area of approximately 40 μm^2 were selected for material composition analysis. The analysis showed that on average the samples consist of 89.37 wt% titanium, 6.57 wt% aluminium, 3.86 wt% vanadium and 0.21 wt% iron. Table 7.3 provides the details of the material composition analysis of the titanium samples. Furthermore, the analyses showed that the concentration of vanadium and iron in the β phase of the material is significantly higher than α phase and can reach up to 9% and 1.5% respectively.

Spectrum	Al	Ti	V	Fe	Total
Spectrum 1	6.55	89.53	3.88	0.04	100.00
Spectrum 2	6.80	89.83	3.28	0.08	100.00
Spectrum 3	6.17	89.69	4.02	0.12	100.00
Spectrum 4	6.54	89.09	4.10	0.27	100.00
Spectrum 5	6.20	89.03	4.46	0.31	100.00
Spectrum 6	6.45	88.68	4.42	0.44	100.00
Spectrum 7	7.24	90.28	2.33	0.15	100.00
Spectrum 8	6.74	89.15	3.91	0.20	100.00
Spectrum 9	6.40	89.02	4.32	0.25	100.00
Mean	6.57	89.37	3.86	0.21	100.00
Std. deviation	0.33	0.50	0.68	0.13	
Max.	7.24	90.28	4.46	0.44	
Min.	6.17	88.68	2.33	0.04	

Table 7.3 Detailed material composition of Ti-6Al-4V used for this research

7.2.2. Cutting tools

A special end mill cutter was designed in collaboration with Renishaw Plc, based on the existing cutting tools used for machining titanium alloys. In addition, the new design was aimed to eliminate the problems occurred during the initial machining trials outlined in section 6.3.3.5 e.g. chipping of the cutting tool. The specifications of the cutting tool are provided in table 7.4. As shown in table 7.4, the tools were made from a solid carbide bar and coated with a TiAlN PVD coating.

7.2.3. Identification of the boundaries of machining parameters

Three cutting parameters of cutting speed, chip load (feed rate) and depth of cut were identified as the most important cutting parameters affecting the machinability metrics. In addition, the machining environment needed to be considered for the design of experiments.

Blank material	Carbide
Coating	TiAlN
Blank diameter	12mm
Blank length	84mm
Flute length	26mm
Number of flutes	3
Flute depth	2.9mm
Helix angle	38°
Rake angle	12°
Eccentric o/d relief angle	9°
O/d raised land width	1.5mm
End tooth prim land width	1.2mm
End tooth primary angle	9°
End tooth secondary angle	20°
Axial rake	12°
Padded front face yes/no	No
Corner chamfer angle	45°
Corner chamfer size	0.3mm

Table 7.4 Specifications of 12mm three flute end mill cutter used for this research

In order to identify the boundaries of machining parameters, a set of machining trials were conducted. Cutting parameters based on common industrial practice (Buckingham, 2011) were selected as the starting point for the trials as presented in table 7.5. The cutting parameters were increased accordingly until the cutting tool was failed. The varying cutting parameters have been selected to be cutting speed, chip load and axial depth of cut (depth of cut) whilst radial depth of cut (immersion rate) was kept constant at 30%.

The aim of this set of trials was to find the maximum machining parameters where the cutting tool can machine a minimum of one machining pass along the workpiece material (150 mm) before catastrophic failure. Increasing the cutting parameters from starting point indicated that the cutting parameters can be increased up to 200 m/min cutting speed, 0.1mm/tooth and 5 mm depth of cut without catastrophic failure of cutting tool. Thus, the machining boundaries for this research were identified to be:

- Cutting speed: Min 30 m/min – Max 200 m/min;
- Chip load: Min 0.03 mm/tooth – Max 0.1 mm/tooth;
- Depth of cut: Min 1 mm – Max 5 mm.

It is noteworthy to mention that it has been found that the cryogen flow rate can affect the results as it changes the cooling rate of the cutting tool and workpiece materials at the cutting zone. Thus, in order to keep the results constant the flow rate was set at a maximum and was kept constant throughout the experiments.

Cutting speed	30 m/min
Chip load	0.03 mm/tooth
Depth of cut	1 mm

Table 7.5 Base cutting parameters for end milling Ti-6Al-4V (Buckingham, 2011)

7.3. Machining experimentation

In this section the details of the DoE and the procedure used for conducting machining experiments are explained in detail. In addition, the process of conducting the machining experiments is disclosed.

7.3.1. Design of experiments

The DoE refers to the process of planning for conducting activities in which meaningful data can be collected and be analysed using statistical techniques where meaningful conclusions can be drawn (Montgomery, 2013). The DoE provides instructions on how an experiment should be conducted in a valid, economical and efficient manner in order to answer to a research question. However, this does not imply that all DoE techniques are economical and/or efficient (BS ISO 3534-3, 2013). Selecting the input parameters is one of the most important stages of a DoE as it affects the number and quality of experiments. For a DoE, all main parameters affecting the output should be considered and the insignificant parameters can be discarded (Ghani et al., 2004). As mentioned previously, for this research, three cutting parameters of cutting speed, chip load and depth of cut and the machining environment are selected whilst the immersion rate will be kept constant at 30%.

It is known that full factorial DoE is the most comprehensive DoE as it considers all possible combinations of factors at all levels (Montgomery, 2013). However, the high number of experiments required for this DoE has made this uneconomical and in some cases impossible. For instance, in the case of this research, four input parameters of cutting speed, chip load, depth of cut and machining environment at three levels will require 3^4 experimental runs.

Taguchi's design of experiments is one of the most widely used and well known approaches for process optimisation which was developed by Genichi Taguchi, a Japanese engineer (Anderson and Whitcomb, 2000). His approach has had a prominent influence in the adaptation of the design of experiments in industry by introducing a low resolution orthogonal array design. Orthogonal array has been derived from fractional factorial design and significantly reduces the number of experimental runs, resulting in its popularity (Mason et al., 2003, Anderson and Whitcomb, 2000, Campbell, 2008). Taguchi's design of experiments provides a more comprehensive insight than the traditional one-factor-at-a-time DoE as it covers a combination of input parameters in case of multi-factor optimisation problems (Xin, 2011, Campbell, 2008).

Taguchi's design is based on two fundamental ideas, namely (i) quality loss function and (ii) that products can be designed so as to reduce the quality loss, thus improving robustness of the design. In his design, the quality loss is defined as deviations of the product property from a target value and is used to measure the deviations of performance characteristics from the desired value, which is then converted into a signal to noise (SN) ratio (Mason et al., 2003, Nian et al., 1999). It is known that standard deviation and mean are related to each other, thus, for optimisation, it is not easy to first reduce the standard deviation and then shift the mean to target value (Ghani et al., 2004). Instead of standard deviation, Taguchi suggests using signal-to-noise (SN) ratio as a measure for process improvement by keeping the mean on target and reducing the standard deviation (Xin, 2011). For a particular optimisation problem, the SN is usually expressed in one of the three following categories based on the optimisation characteristics using their corresponding formula (Xin, 2011).

(i) Nominal-is-best SN = $10\,log_{10}(\frac{\bar{Y}^2}{\sigma^2})$ when response mean and variance are related
or SN = $-10\log_{10}\sigma^2$ when mean and variance can be treated independently

(ii) Smaller-is-better SN = $-10\log_{10}(\frac{\sum y^2}{n})$

(iii) Larger-is-better SN = $-10\log_{10}(\frac{1}{n}\sum\frac{1}{y^2})$

Where, for a sample y, $\bar{Y}$ is the sample mean; σ^2 is the variance and n is the sample size for one experiment.

Taguchi's minimal-run technique is best suited for optimising main parameters and is particularly useful when the interactions between parameters are not important (Xin, 2011, Mason et al., 2003, Anderson and Whitcomb, 2000).

For the purpose of this research, the optimum machining parameters for cryogenic machining is unknown as low temperatures modify the material properties of both cutting tool and workpiece. Thus, a one-factor-at-a-time DoE by changing the machining environment and keeping other cutting parameters at the base level, shown in table 7.5, is not conclusive. Therefore, in order to provide an in-depth understanding of the effects of cryogenic cooling on the machinability of Ti-6Al-4V alloy in comparison with dry and wet environments, a combination of different cutting parameters at different levels should be used. To achieve this, three inputs of cutting speed, chip load and depth of cut were considered to be used at three levels, namely minimum, medium and maximum. The minimum and maximum levels of these parameters were identified in section 7.2.3 and a medium level in between of each range was also introduced. The levels and values of the cutting parameters used in this research are shown in table 7.6.

Cutting parameter	**Level**		
	Min	**Med**	**Max**
Cutting speed	30	115	200
Chip load	0.03	0.055	0.1
Depth of cut	1	3	5

Table 7.6 Levels and values of cutting parameters used for DoE

An L9 Taguchi's orthogonal array design was implemented in order to provide a meaningful combination of the cutting parameters whilst keeping the number of experiments at a minimum. The L9 design for cutting parameters is shown in table 7.7. As mentioned previously, a full factorial design is the most comprehensive DoE.

Since the effect of changing the machining environment from dry and wet to cryogenic is the main concern of this research, a hybrid DoE was developed by combining a 3^1 full factorial design with L9 Taguchi's design making an L9x3 DoE. In this design, the L9 Taguchi's orthogonal array developed for the cutting parameters (table 7.7) was repeated three times using different machining environments, namely dry, wet and cryogenic. Table 7.8 depicts the L9x3 DoE which was used to conduct the comparative machining experiments.

Number of experiment	Cutting speed	Chip load	Depth of cut
1	30	0.03	1
2	30	0.055	3
3	30	0.1	5
4	115	0.03	3
5	115	0.055	5
6	115	0.1	1
7	200	0.03	5
8	200	0.055	1
9	200	0.1	3

Table 7.7 Taguchi's L9 orthogonal array DoE for cutting parameters

Experiment ID	Number of experiment	Cutting speed	Chip load	Depth of cut	Machining environment
D1	1	30	0.03	1	Dry
D2	2	30	0.055	3	Dry
D3	3	30	0.1	5	Dry
D4	4	115	0.03	3	Dry
D5	5	115	0.055	5	Dry
D6	6	115	0.1	1	Dry
D7	7	200	0.03	5	Dry
D8	8	200	0.055	1	Dry
D9	9	200	0.1	3	Dry
W1	10	30	0.03	1	Wet
W2	11	30	0.055	3	Wet
W3	12	30	0.1	5	Wet
W4	13	115	0.03	3	Wet
W5	14	115	0.055	5	Wet
W6	15	115	0.1	1	Wet
W7	16	200	0.03	5	Wet
W8	17	200	0.055	1	Wet
W9	18	200	0.1	3	Wet
C1	19	30	0.03	1	Cryogenic
C2	20	30	0.055	3	Cryogenic
C3	21	30	0.1	5	Cryogenic
C4	22	115	0.03	3	Cryogenic
C5	23	115	0.055	5	Cryogenic
C6	24	115	0.1	1	Cryogenic
C7	25	200	0.03	5	Cryogenic
C8	26	200	0.055	1	Cryogenic
C9	27	200	0.1	3	Cryogenic

Table 7.8 Hybrid L9x3 DoE for comparative study of cryogenic machining with dry and wet environments at different cutting parameters

7.3.2. Experimental procedure for machining operations

A block of Ti-6Al-4V alloy with dimensions of 150mmx50mmx50mm was allocated for each machining experiment. The blocks were ordered in one batch and were all annealed in order to reduce the variation in material properties among samples.

The machining operation for each experiment was defined to be four slots along the length of the workpiece material. As mentioned previously, the immersion rate is 30% of the tool, thus the axial depth of cut and consequently the width of the slots will be 4mm. Figure 7.4 illustrates the machining process for each experiments. As it is shown in this figure, the top front left corner of the titanium block was selected as the machining reference point whilst the cutting tool moves from right to left providing a climb milling strategy.

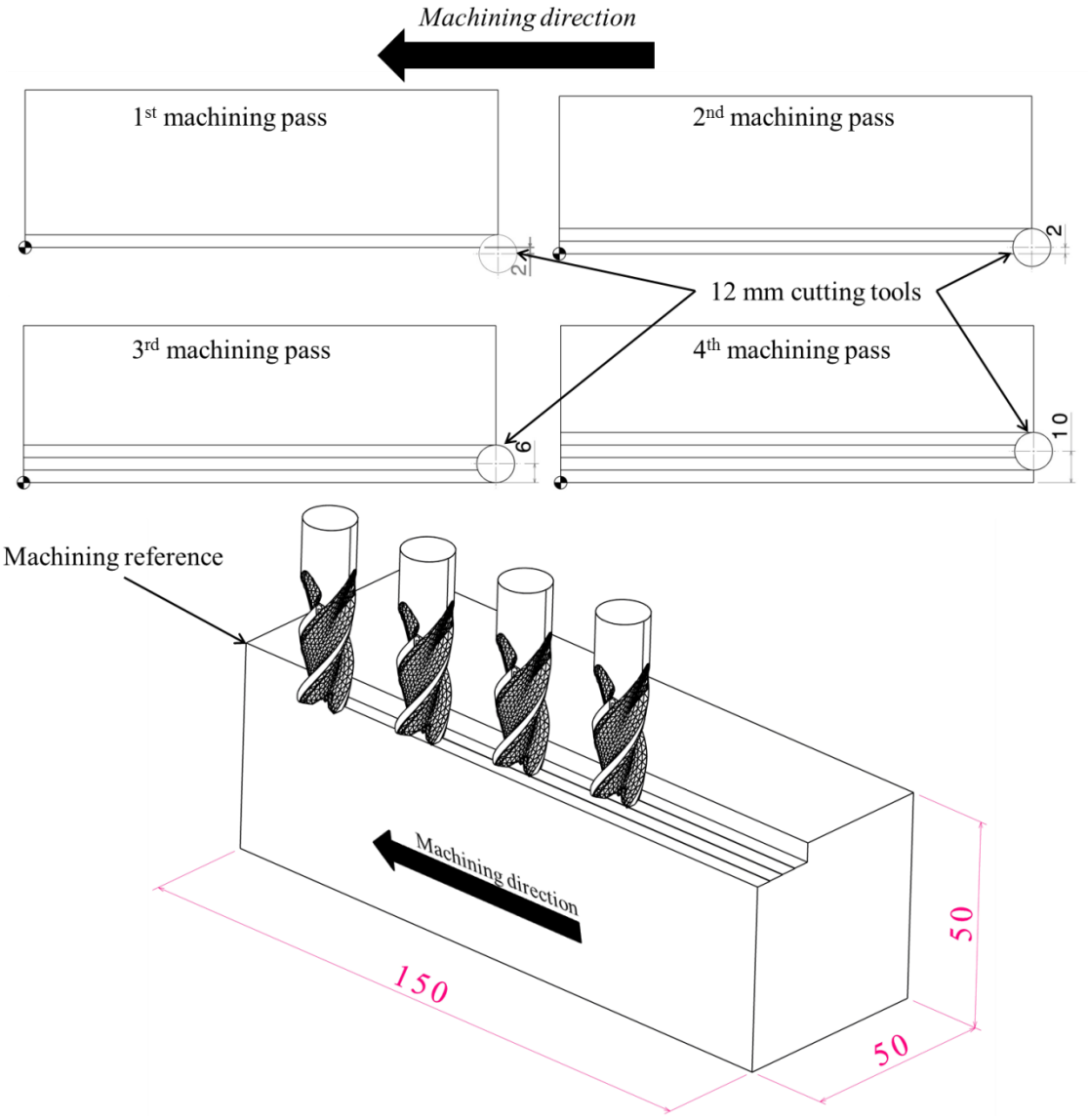

Figure 7.4 Pictorial illustration of the machining process used for each experiment

In order to reduce the effects of vibration and secure the block on the machine tool's table, the workpiece block was fixed within four MicroLoc® fixtures on each side during machining operations. In addition to compensate for the effects of acceleration and deceleration at the start and end of the machining process, the cutting tool travelled at feed speed for 100 mm before and after the workpiece.

A 12mm high precision collet with 2µm concentricity was outsourced for the machining experiments. In order to measure the tool wear for each set of machining parameters and environment, a new cutting tool was used for each machining experiment. In addition, the tool overhang was kept constant at 50mm which was measured prior to each machining operation as shown in figure 7.5. This would reduce the variations imposed to the output parameters due to the tool deflection.

Figure 7.5 Measurement of tool's overhang prior to machining operation

7.3.3. Comparative machining experiment

Following the DoE, 27 machining experiments were conducted on the Bridgeport VMC 610XP^2 vertical CNC milling centre. A machining programme was generated on the machine tool's controller to machine the previously defined slots for each experiment. A workpiece block was fixed on the machine tool's table as explained in section 7.3.2 and was measured using a touch trigger probe to define the machining reference point. In addition, a new cutting tool was defined for each machining experiment and its length was measured prior to the machining operation. The cutting parameters were updated according

to the DoE (table 7.8) and were inserted into the machine tool's controller. As the machine tool requires spindle speed and feed rate instead of cutting speed and chip load respectively, the following equations were used to calculate spindle speed and feed rate.

$$Spindle\ speed = \frac{Cutting\ speed}{\pi \times D}$$

$$Feed\ rate = Spindle\ speed\ \times Chip\ load\ \times number\ of\ teeth$$

Where spindle speed is in rpm, cutting speed in m/min, D is the tool diameter, feed rate is in mm/min and chip load is in mm/tooth. The calculated cutting parameters for each experiment are given in table 7.9.

Experiment ID	Number of experiment	Spindle speed	feed rate
D1	1	796	71.62
D2	2	796	131.30
D3	3	796	238.73
D4	4	3050	274.54
D5	5	3050	503.33
D6	6	3050	915.14
D7	7	5305	477.46
D8	8	5305	875.35
D9	9	5305	1591.55
W1	10	796	71.62
W2	11	796	131.30
W3	12	796	238.73
W4	13	3050	274.54
W5	14	3050	503.33
W6	15	3050	915.14
W7	16	5305	477.46
W8	17	5305	875.35
W9	18	5305	1591.55
C1	19	796	71.62
C2	20	796	131.30
C3	21	796	238.73
C4	22	3050	274.54
C5	23	3050	503.33
C6	24	3050	915.14
C7	25	5305	477.46
C8	26	5305	875.35
C9	27	5305	1591.55

Table 7.9 Calculated cutting parameters for machining experiments

Following the DoE, 27 machining experiments were conducted and the samples were prepared for further analysis. It is noteworthy to mention that experiment D7 was terminated after two machining passes due to the excessive heat generation where the workpiece material became red hot. Apart from this, the rest of the machining experiments were carried out successfully.

7.4. Data collection

In this section the activities conducted for collecting experimental data for each machining experiment are described. The collected data includes machine tool's power and energy consumption, surface roughness, tool wear and surface topography and surface integrity which consist of subsurface microstructure and microhardness. Furthermore, the equipment and facilities used for data collection are specified in this section.

In order to minimise the uncertainty in the collected data, according to BS ISO 5725-1 (1994), BS ISO 5725-2 and BS ISO 5725-3, same calibration, operator and equipment were used to collect the desired machinability metric. In addition, where possible, the time elapse between measurements was intended to be minimised.

7.4.1. Monitoring power consumption

A Hioki power demand analyser, shown in figure 7.6, was wired into the machine tool in order to monitor the total power consumption of the machine. The specification of the power demand analyser are given in table 7.10. The equipment has been connected to a computer via a RS-232 cable and set to give the power consumption of the machine tool at 1 sec intervals.

In order to monitor the power consumption of the machine tool for each experiment, the equipment has been run prior to the machining operation and stopped after it was finished. The gathered data was then downloaded into a computer in the form of a digital spreadsheet for further analysis.

In order to identify the average power consumption of the machine tool, the sampled data during material cutting operations were identified and a 20% truncated mean of the data was calculated. This was used to represent the average power consumption of the machine tool for a specific experiment.

Figure 7.6 Hioki Clamp-On HiTester 3169-20 power demand analyser

Manufacturer	Hioki E. E. Corporation
Model	Clamp-On HiTester 3169-20
Measurement range – Voltage	150.00 V to 600.00 V
Measurement range – Ampere	500.00 mA to 5.0000 kA
Measurement range – Power	75.000 W to 900.00 kW
Accuracy – Voltage	0.2%
Accuracy – Ampere	0.2%
Accuracy – Power	0.2%
Sampling method	Digital sampling

Table 7.10 Specification of Hioki power demand analyser

7.4.2. Tool wear measurement

After machining operations, the cutting tools were cleaned by pressured air and prepared to be examined by optical microscopy for tool wear. A Nikon tool makers' microscope was used to observe and measure the tool wear on the cutting tools. The microscope has a 60X magnification and was equipped with a digital camera as shown in figure 7.7. Prior to measuring the tool wear, the microscope and camera were calibrated and the same calibration was used for all the samples. The instructions provided by ISO 8688-2 (1989) were strictly followed in order to identify and measure the tool wear. As highlighted by the standard (ISO-8688-2, 1989), flank wear was selected as the governing type of tool wear for tool life and the maximum flank wear observed on each tooth of the cutting tool was selected for analysis.

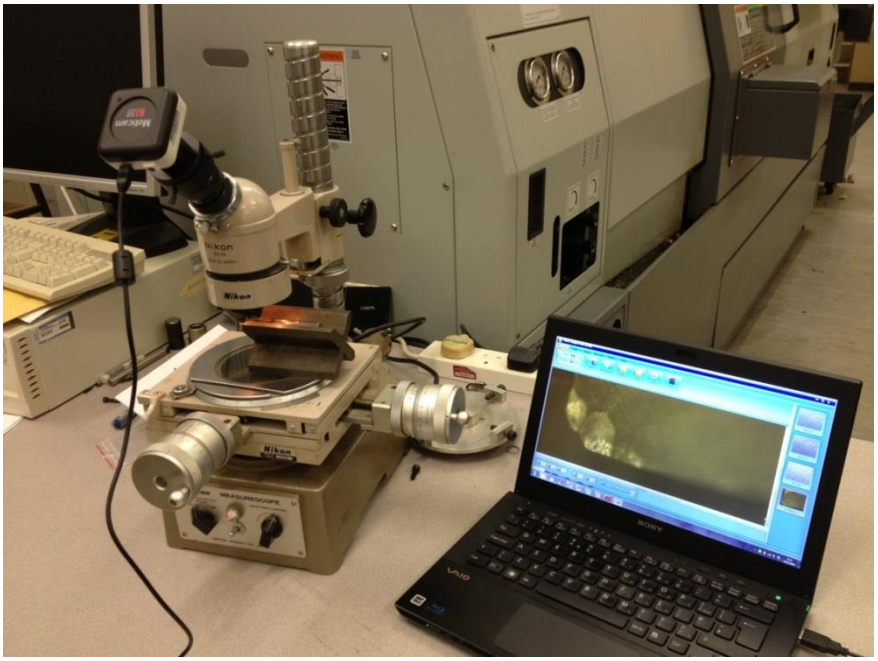

Figure 7.7 Tool makers' microscope and the setup used for tool wear measurement

7.4.3. Measurement of surface roughness

For surface roughness measurement, an optical non-contact surface profiler was employed. The apparatus is a Scantron Ltd Proscan 2000 ® equipped with a S5/03 optical sensor (figure 7.8). As given in table 7.11, the surface profiler had a 0.01 μm resolution and minimum step size of 1 μm. Further specifications of the surface profiler are provided in table 7.11.

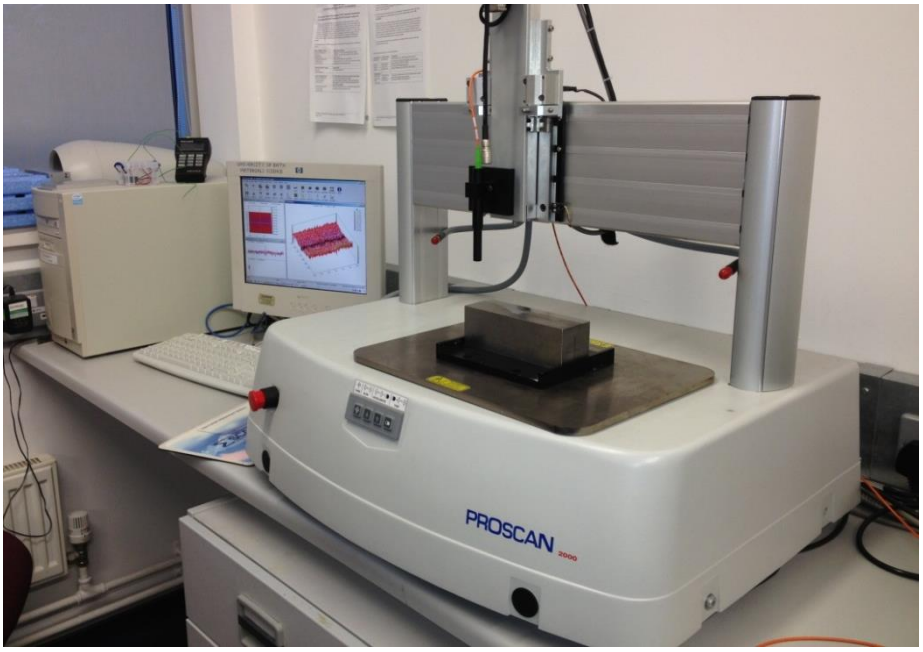

Figure 7.8 Proscan 2000 surface profiler used for this research

Manufacturer	Scantron Ltd.
Model	Proscan 2000
Type	Optical non-contact
Sensor type	S5/03 optical
Resolution	10 nm
Sensor's measuring range	300 µm
Sensor's spot size	4 µm
Linear accuracy	0.1% of range
Minimum step size	1 µm
Table size	380 mm x 280 mm
Maximum sample weight	6 kg

Table 7.11 Specifications of the surface profiler used for this research

For the purpose of this research, arithmetic surface roughness (Ra), ten point height of irregularity (Rz) and root-mean-square deviation (Rq) have been selected to present the quality of a machined surface. In order to perform a meaningful, repeatable and comparable surface roughness measurement, the instructions recommended by (BS EN ISO 4288, 1998) and the Proscan surface profiler's manufacturer were strictly followed.

The standard (BS EN ISO 4288, 1998) indicated that where the expected Ra ranges between 0.1 µm and 2 µm, the sampling length (l_r) for measurement should be 0.8 mm with 4 mm evaluation length (l_n). Furthermore, according to (BS EN ISO 3247, 1998) for this sampling length, a bandwidth of 300:1 should be used. According to (BS EN ISO 4287, 1998) sampling length is the length along the X-axis which is used for "identifying the irregularities characterising the profile under evaluation" whilst evaluation length is the "length in the direction of the X-axis used for assessing the profile under evaluation."

The standard notes that an evaluation length may consist of one or more sampling lengths. These parameters have been used to define the input parameters to setup the surface profiler. Table 7.12 provides the parameters used for measuring the surface roughness of the machined samples.

Step size X	3 µm
Step number X	1335
Step size Y	50 µm
Step number Y	40
Surface filter value	133

Table 7.12 Step size, step number and surface filter value for surface roughness measurement

As indicated by the standard, it is noteworthy to mention that surface roughness is a 2D parameter and is measured along the X-axis. Therefore, the measurements have been repeated 40 times (step number Y) with 50 µm intervals (step size Y) to identify the average surface roughness of a surface detailed in figure 7.9. Each machining pass has been measured at five points as depicted in figure 7.9 and thus each machined block has been measured at 20 points.

In order to identify the effects of cryogenic cooling on the surface roughness and minimise the effect of tool wear on the surface roughness, the average of the surface roughness of the first machining pass (row 1 in figure 7.9) was used for analysis.

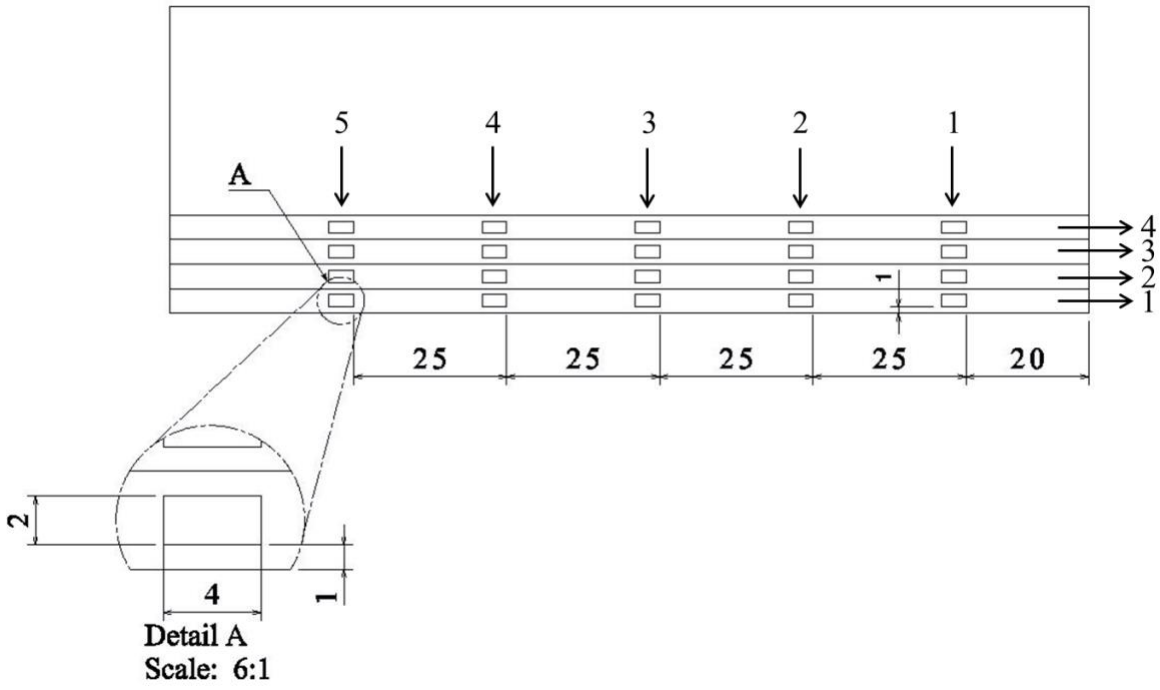

Figure 7.9 Surface roughness measurement procedure for each machining pass (rows 1 to 4) and the dimensions of the sampling rectangle (detail A)

7.4.4. Chip morphology

The cutting chips produced during machining experiments were collected to be examined. After cleaning the chips with distilled water, a low magnification image of the chips was taken for each machining experiment to present the general chip formation. In addition, a high magnification microscope and a micrometer were used to measure the chip thickness for further analysis.

7.4.5. Microscopic surface topography

In addition to surface roughness, the machined surfaces were assessed using an SEM to indicate the existence of any microscopic surface defect and provide an understanding of the cutting process. Due to the dimensional and weight limits of the SEM, a slice of material was cut from each machined block using a band saw at low speed. As shown in figure 7.10, the slices have an approximate thickness of 20 mm and were cut from the centre of each block to prevent the effects of cutting tool's instability at the start and end of each machining path.

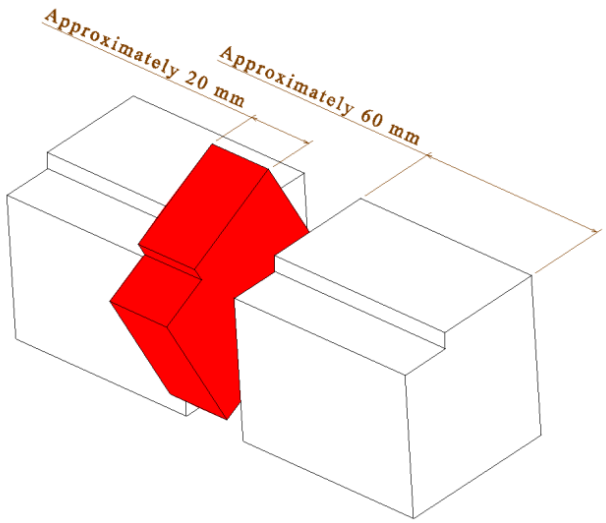

Figure 7.10 Cutting dimensions of the selected slice (red) for SEM

The samples were washed by industrial solvent and distilled water and were also cleaned using an ultrasonic cleaning tank as shown in figure 7.11. Furthermore, the samples were cleaned by propan2ol in order to remove any possible organic contamination from the surfaces. Afterwards, the samples were left in vacuum to be dried for 12 hrs prior to SEM.

A JEOL SEM6840LV SEM, depicted in figure 7.12a, was used to study the surface topography of each machining sample. As shown in figure 7.12b three images from outer side, middle and inner side of the first machining pass were taken for each sample. Two modes of backscattered electron imaging (BEI) and scanning electron imaging (SEI) at 1000X magnification were used to generate micrographs of machined surfaces. Figure 7.12, illustrates the position of the images on each sample and the SEM system used for imaging.

Figure 7.11 Samples being cleaned in ultrasonic tank using distilled water and soap

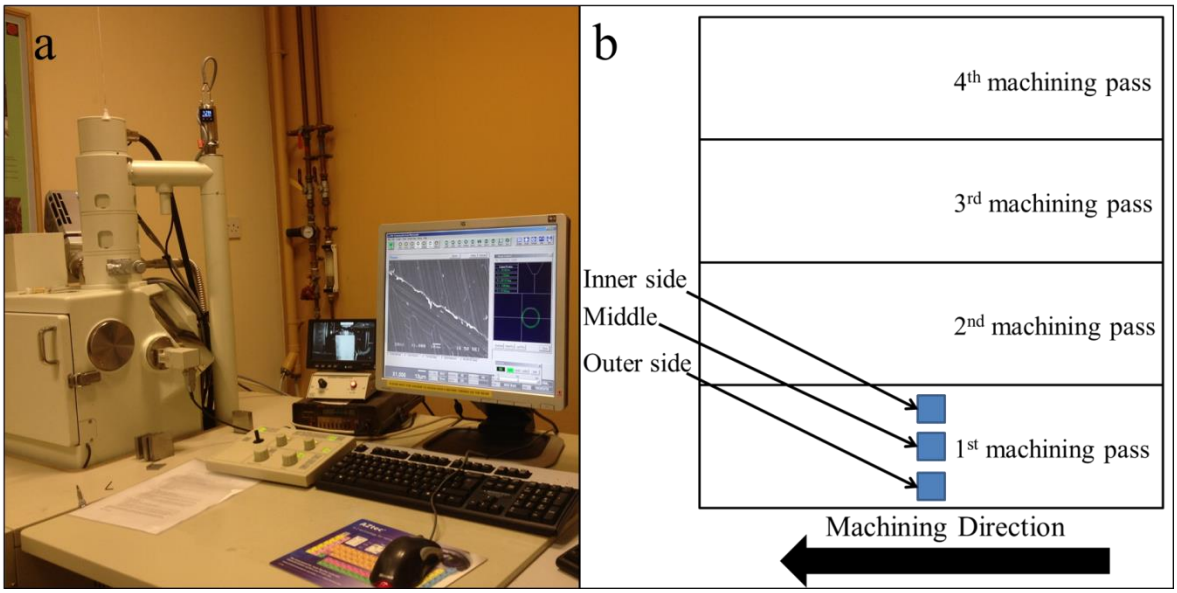

Figure 7.12 (a) SEM suit used for imaging the samples and (b) position of the images taken

7.4.6. Microstructural analysis

In order to identify the effects of cryogenic machining on the microstructure of Ti-6Al-4V alloy and measure the depth of microstructural damage due to machining, a cross-sectional image of the microstructure of the machined samples was required. Thus, a sample similar to those prepared in section 7.4.5 was cut from each machined block.

The machined area of the samples were cut using an abrasive cutter (figure 7.13a) and the samples were mounted in epoxy resin in a way that the cross-section of the machined zone, namely the red face in figure 7.13a, was facing upward as shown in figure 7.13b. In order to prepare the samples for microstructural analysis, each sample was ground and polished to 5nm. The samples were ground using P400 grit paper until plane and then polished at three stages using 9 μm and 3 μm liquid diamond and finally 0.05 μm silica.

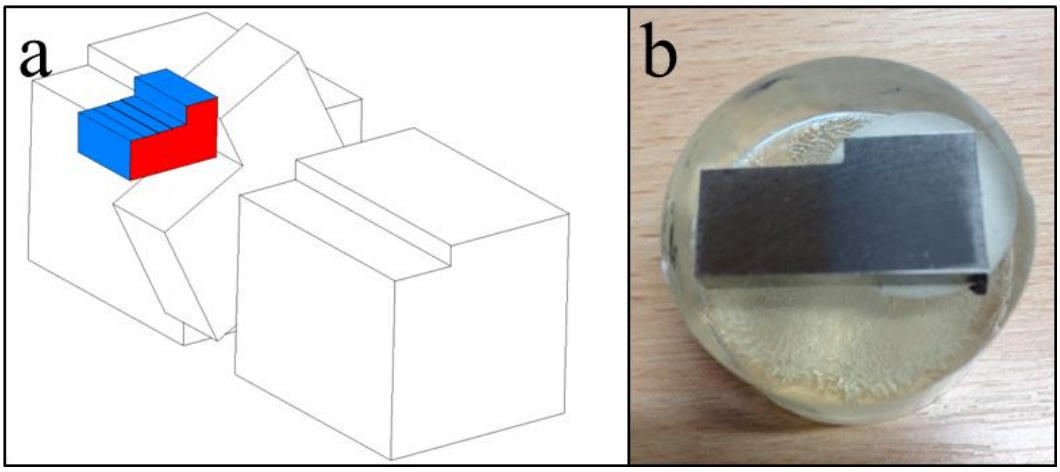

Figure7.13 (a) Cross sectional sample of machined surfaces and (b) sample mounted in resin

7.4.7. Micro hardness test

In order to indicate the effect of cryogenic machining on the micro hardness of the machined blocks in comparison with dry and wet conditions, the samples prepared in section 7.4.6 were used for microhardness testing. A Leco M400 micro hardness tester, shown in figure 7.14, was used to measure the micro hardness of the samples beneath the machined surface. The microhardness tester table has an axial movement resolution of 10 μm which indicates the minimum distance between sampling points. A Vickers pyramid indenter with 136° angle and 15 sec dwelling was used to indent the samples for microhardness.

As shown in figure 7.14, the microhardness was measured at 10 μm below the machined surface and repeated every 10 μm up to 120 μm, 100 μm intervals afterward up to 1 mm and 1000 μm intervals up to 3mm below the machining surface. 50 gr lf was used for the first indentation whilst it was increased to 100 gr lf for the rest of the indentations.

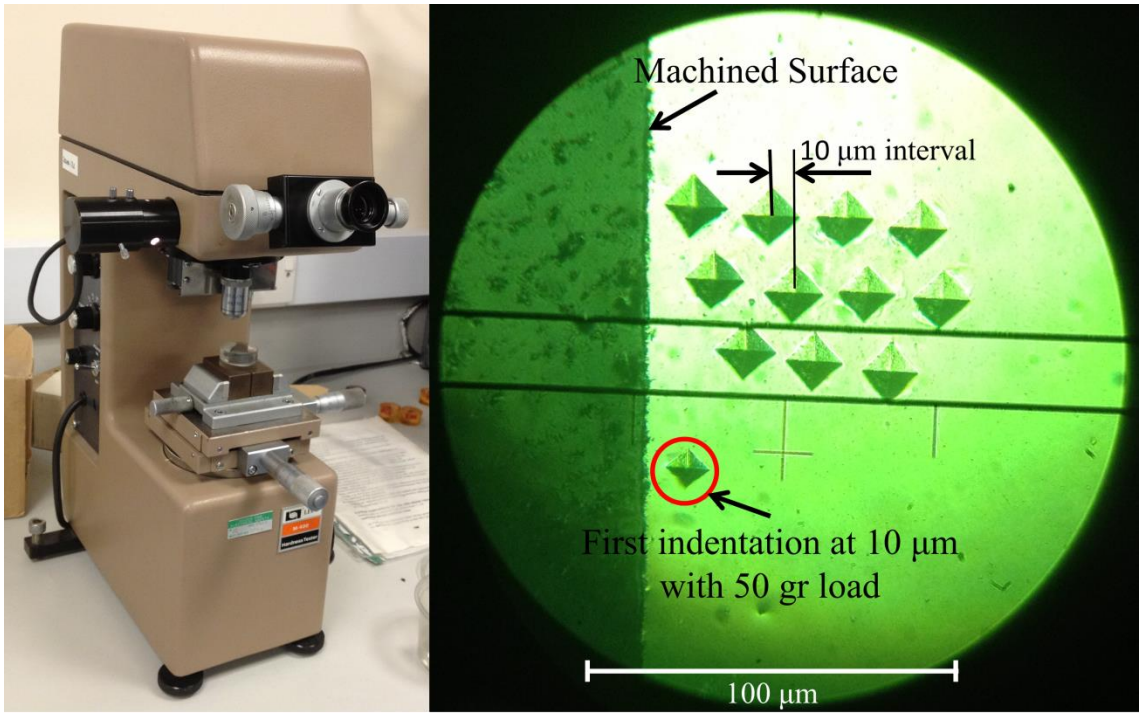

Figure 7.14 Leco M400 microhardness tester (left) and indentations below the machined surface for microhardness test (right)

7.5. Results and analysis

After conducting the machining experiments, the power consumption, surface roughness and tool's flank wear have been collected for each machining experiment. In addition, SEM images of the machined surfaces have been taken. Furthermore, the micro hardness and microstructure of three samples produced under dry, wet and cryogenic conditions at base cutting parameters have been assessed. In order to focus the results on the machining environment and bypass the effects of tool wear on different machinability metrics, the analysis for the machining environment has been limited to the results obtained for the first machining pass.

7.5.1. Power consumption

As mentioned previously in section 7.4.1, the power consumption of the machine tool was monitored during the cutting operation. The average power consumption of the machine tool for each tool pass of each machining experiment is given in table 7.13. A Gaussian filter was applied to remove the noise from the measured values and the graphs of power consumption were generated for each machining experiment. The detailed graphs of the power consumption are provided and further discussed in appendix B.

Exp. ID	Exp. No.	Power consumption (W)			
		1st pass	2nd pass	3rd pass	4th pass
D1	1	1303.792	1304.486	1305.514	1310.044
D2	2	1332.561	1341.780	1344.171	1352.195
D3	3	1423.565	1443.957	1443.000	1444.565
D4	4	1367.850	1369.650	1364.550	1381.100
D5	5	1557.200	1607.700	1621.300	1624.700
D6	6	1354.143	1392.000	1380.857	1378.429
D7	7	1742.750	1801.583	x	x
D8	8	1446.429	1493.429	1501.571	1506.429
D9	9	2015.000	2145.000	2130.000	2177.500
W1	10	2186.000	2092.958	2092.389	2086.900
W2	11	2143.561	2143.049	2144.390	2140.756
W3	12	2273.130	2253.652	2257.652	2249.609
W4	13	2246.000	2214.450	2186.500	2184.200
W5	14	2696.400	2579.400	2532.800	2605.900
W6	15	2466.000	2462.286	2461.286	2466.857
W7	16	2841.643	2823.357	2810.643	2811.357
W8	17	2567.000	2594.857	2622.286	2652.714
W9	18	3129.250	3193.250	3327.500	3405.000
C1	19	1304.944	1302.736	1302.639	1303.211
C2	20	1344.171	1346.463	1339.854	1345.659
C3	21	1432.565	1444.217	1444.565	1447.826
C4	22	1365.650	1383.850	1392.300	1394.850
C5	23	1619.700	1675.600	1675.500	1707.400
C6	24	1374.429	1403.571	1418.714	1409.857
C7	25	1723.571	1731.429	1741.429	1737.143
C8	26	1528.714	1556.571	1568.000	1567.000
C9	27	2045.250	2317.500	2650.750	3013.250

Table 7.13 Average power consumption for each machining experiment

As different depths of cut were used for each machining experiment, comparison of power consumption does not reflect the effects of all cutting parameters for calculations and it is only sufficient for the full factorial side of the DoE, namely machining environment. Thus, in addition to power consumption, the power consumption per unit volume of removed material (PC/V) was also calculated. Furthermore, since machining time is an important parameter for defining the cost of a machined product, and energy is a product of time and power, the energy consumption of the machine tool per removing a unit volume of material (EC/V) was calculated which are provided in table 7.14. This provides an understanding of the cost of machining from the energy point of view. Since it is desired to minimise the power and energy consumption for machining, the smaller-is-better equation defined in

section 7.3.1 is used to calculate the SN ratio for power consumption, PC/V and EC/V parameters for the first machining pass of each experiment.

Exp. ID	Exp. No.	Power consumption (W)		PC/V (W/mm^3)		EC/V (J/mm^3)	
		Measured	SN ratio	Measured	SN ratio	Measured	SN ratio
D1	1	1303.8	-62.304	2.173	-6.741	273.065	-48.725
D2	2	1332.6	-62.494	0.740	2.612	50.744	-34.108
D3	3	1423.6	-63.068	0.475	6.475	17.889	-25.052
D4	4	1367.9	-62.721	0.760	2.385	24.911	-27.928
D5	5	1557.2	-63.847	0.519	5.696	9.281	-19.352
D6	6	1354.1	-62.633	2.257	-7.070	22.196	-26.925
D7	7	1742.8	-64.825	0.581	4.718	10.950	-20.788
D8	8	1446.4	-63.206	2.411	-7.643	24.786	-27.884
D9	9	2015.0	-66.086	1.119	-0.980	6.330	-16.028
W1	10	2186.0	-66.793	3.643	-11.230	457.835	-53.214
W2	11	2143.6	-66.623	1.191	-1.517	81.627	-38.237
W3	12	2273.1	-67.132	0.758	2.410	28.565	-29.117
W4	13	2246.0	-67.028	1.248	-1.923	40.904	-32.235
W5	14	2696.4	-68.616	0.899	0.927	16.071	-24.121
W6	15	2466.0	-67.840	4.110	-12.277	40.420	-32.132
W7	16	2841.6	-69.071	0.947	0.471	17.855	-25.035
W8	17	2567.0	-68.189	4.278	-12.625	43.988	-32.867
W9	18	3129.3	-69.909	1.738	-4.803	9.831	-19.852
C1	19	1304.9	-62.312	2.175	-6.749	273.307	-48.733
C2	20	1344.2	-62.569	0.747	2.536	51.186	-34.183
C3	21	1432.6	-63.122	0.478	6.420	18.002	-25.106
C4	22	1365.7	-62.707	0.759	2.399	24.871	-27.914
C5	23	1619.7	-64.189	0.540	5.354	9.654	-19.694
C6	24	1374.4	-62.762	2.291	-7.199	22.528	-27.055
C7	25	1723.6	-64.729	0.575	4.814	10.830	-20.692
C8	26	1528.7	-63.687	2.548	-8.124	26.196	-28.365
C9	27	2045.3	-66.215	1.136	-1.109	6.425	-16.158

Table 7.14 Average power consumption and their corresponding SN ratio for each machining experiment

The results of the machining experiments for power consumption, PC/V and EC/V and their respective SN ratios are provided in table 7.14. In order to identify the machining effects of input parameters on the outputs, the mean SN ratio for each level of inputs should be calculated. The level with the highest mean SN ratio presents the level of the corresponding input parameter in which the output is a minimum. The mean SN ratio for each level of input parameters was calculated and represented in table 7.15. δ represents the difference between maximum and minimum mean SN ratio for each input parameter.

Environment	**Level**	**Dry**	**Wet**	**Cryogenic**	**δ**
	Power consumption	-63.465	-67.911	-63.588	4.446
	PC/V	-0.061	-4.508	-0.184	4.446
	EC/V	-27.421	-31.868	-27.544	4.446
Cutting speed	**Level**	**30**	**115**	**200**	**δ**
	Power consumption	-64.046	-64.705	-66.213	2.166
	PC/V	-0.643	-1.301	-2.809	2.166
	EC/V	-37.386	-26.373	-23.074	14.312
Chip load	**Level**	**0.03**	**0.055**	**0.1**	**δ**
	Power consumption	-64.721	-64.824	-65.419	0.698
	PC/V	-1.317	-1.421	-2.015	0.698
	EC/V	-33.918	-28.757	-24.158	9.760
Depth of cut	**Level**	**1**	**3**	**5**	**δ**
	Power consumption	-64.414	-65.150	-65.400	0.986
	PC/V	-8.851	-0.045	4.143	12.994
	EC/V	-36.211	-27.405	-23.218	12.994

Table 7.15 Mean SN ratio values of each level of input parameters for power consumption, PC/V and EC/V

Analysis of the power consumption of the machine tool for each set of experiments at equal cutting parameters reveals that a significant portion of the machine tool's power consumption is associated with coolant pump. For instance, as shown in figure 7.15, comparison of the power consumption of D1, W1 and C1 indicated that using coolant pump in wet machining increases the power consumption up to a 67%. This figure increases to almost 80% for experiment 6 where power consumption increased respectively from 1354w and 1374w in dry and cryogenic to 2466w in wet machining. Compilation of the gathered data on power consumption for all machining experiments, reveals that on average 66% and 64% higher power consumption can be expected in wet machining as compared to dry and cryogenic machining environments.

Figure 7.16 illustrates the average power consumption of the machining experiments whilst it is arranged based on the L9 DoE so as to keep different machining environments with similar cutting parameters next to each other.

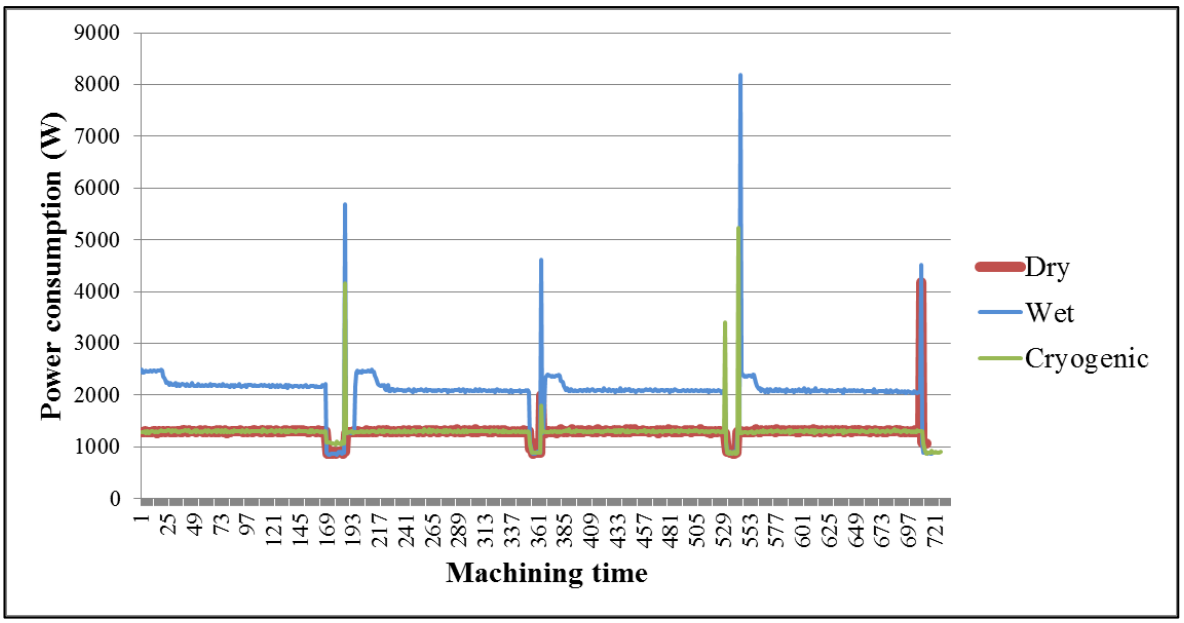

Figure 7.15 Power consumption of machine tool for experiments D1, W1 and C1

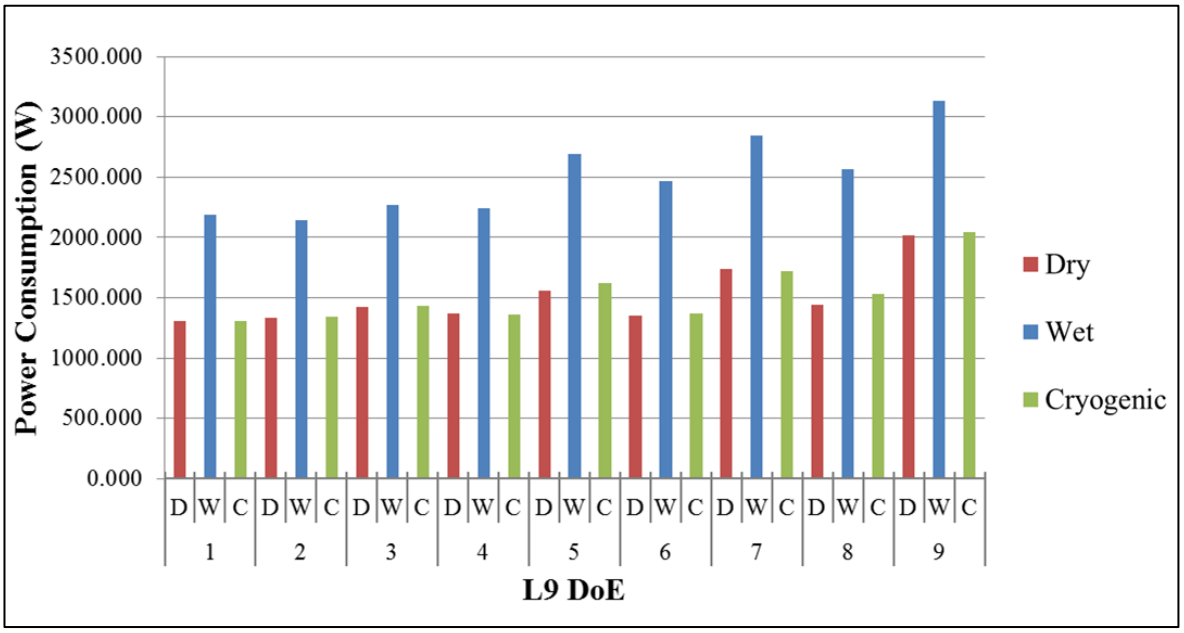

Figure 7.16 Average power consumption of machine tool for machining experiments

Comparing the average power consumption in cryogenic machining with dry machining demonstrates that cryogenic cooling has an average of 1.45% higher power consumption than dry machining. However, due to the small difference between the means and relatively larger standard deviation of 13W, comparing the means is not totally valid. Thus, one-tailed t-test for homoscedastic data was performed on the data gathered for experiments outlined in L9 DoE at two machining environments of dry and cryogenic.

Prior to t-test, all the data were tested for normality using Shapiro-Wilk (Shapiro and Wilk, 1965, Chou et al., 1998, Mason et al., 2003). The null hypothesis of the tests is that there is no significant difference between power consumption in dry and cryogenic machining. The t-test was performed using Microsoft® Excel® (Microsoft-Corporation, 2010) and the computed P-value for each set of machining experiment in L9 DoE are provided in table 7.16.

As shown in table 7.16, the results obtained from t-test shows that in most of the experiments (2, 5, 6, 7, 8 and 9) the hypothesis of equality between the mean values of power consumption in dry and cryogenic machining can be rejected. Thus, it is a valid argument to conclude that cryogenic cooling changes the power consumption of machine tool. However, as this change is very small compared to the total power consumption of the machine tool, it is negligible.

L9 ID	ID of the first dataset	ID of the second dataset	t-test's P-value
1	D1	C1	0.12
2	D2	C2	0.03
3	D3	C3	0.19
4	D4	C4	0.27
5	D5	C5	$1.2\ e^{-10}$
6	D6	C6	0.02
7	D7	C7	$7\ e^{-4}$
8	D8	C8	$1.1\ e^{-7}$
9	D9	C9	0.02

Table 7.16 t-test analysis of power consumption data for L9 DoE at dry and cryogenic environments

Similar conclusions can be derived from mean SN ratio analysis of power consumption, PC/V and EC/V (table 7.15). As shown in figures 7.17, 7.18, 7.19 and supported by the data presented in table 7.15, the difference in power consumption, PC/V and EC/V between dry and cryogenic is very small (δ=0.12) and almost negligible whilst the most undesirable machining environment is wet.

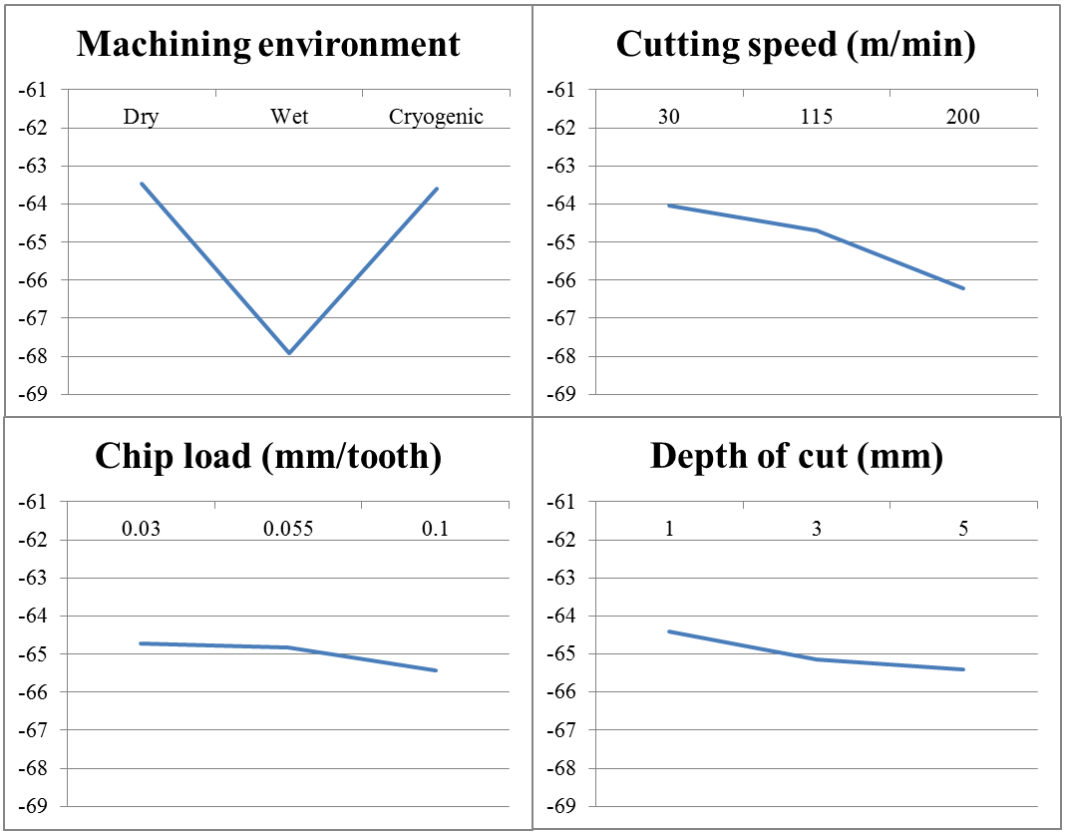

Figure 7.17 Mean SN ratio graphs for power consumption

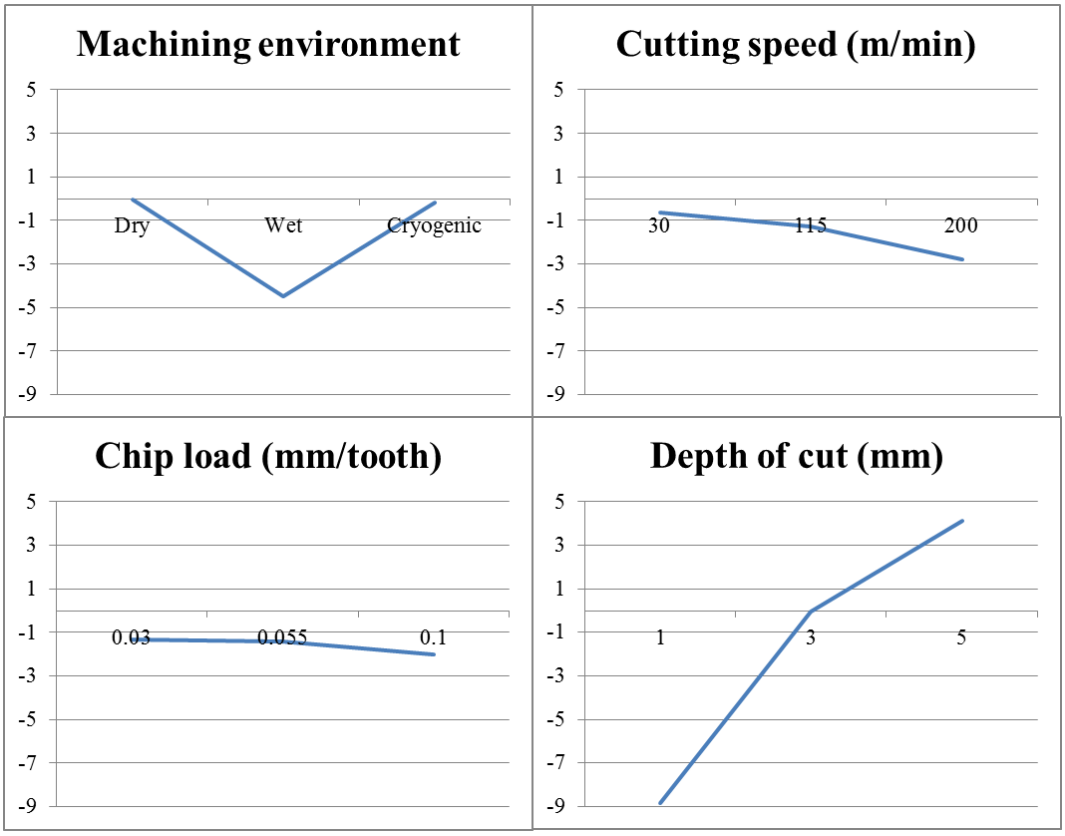

Figure 7.18 Mean SN ratio graphs for power consumption per unit volume of removed material (PC/V)

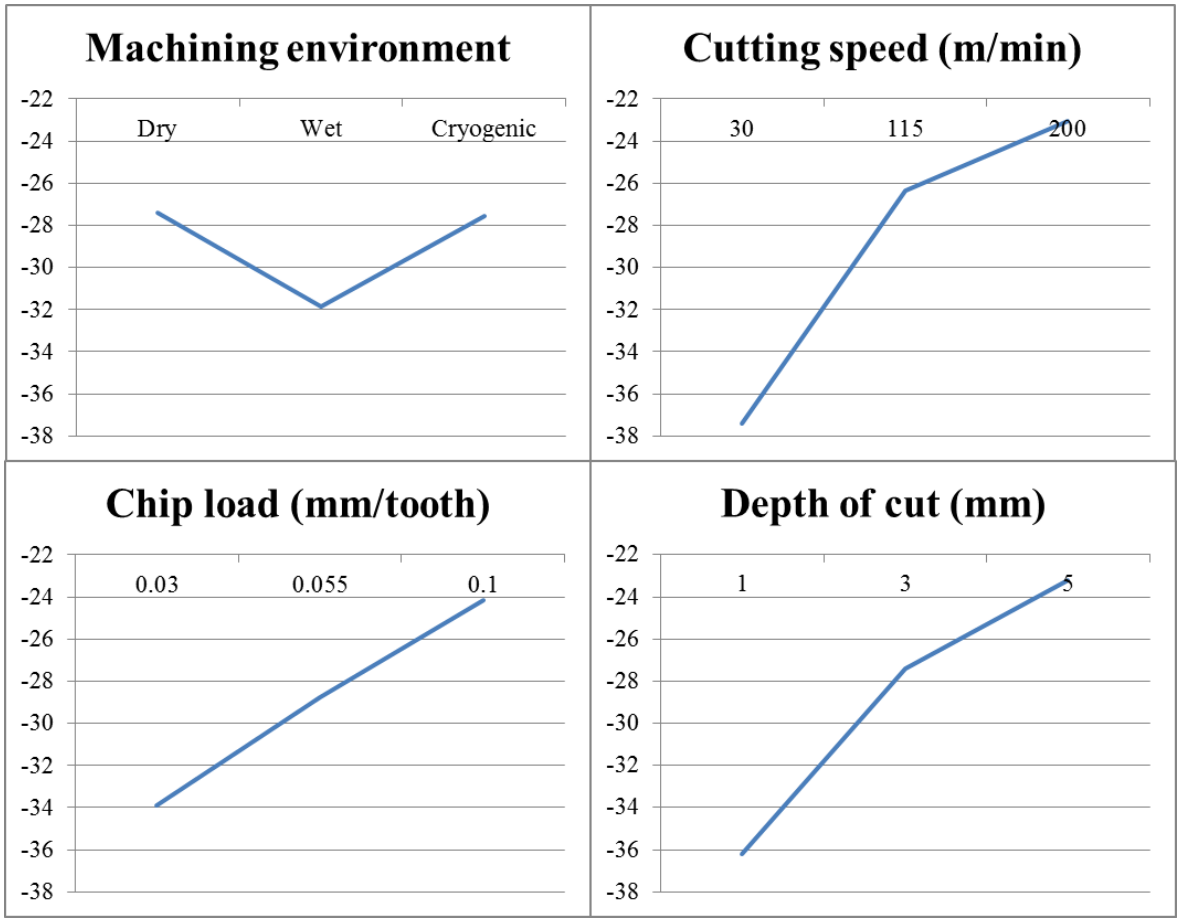

Figure 7.19 Mean SN ratio graphs for energy consumption per unit volume of removed material (EC/V)

Taguchi recommends visual examination of the mean SN ratio graphs for analysis and in order to identify the optimum level of each input parameter (Xin, 2011). From the mean SN ratio graphs, the level with highest SN ratio is considered as desired optimum level whilst the one with lowest SN ratio is the most undesirable. In addition, the input parameter with the widest SN ratio span (δ) is the most significant parameter and the one with the narrowest span is the least significant parameter.

Analysis of mean SN ratio graphs (figure 7.17) indicate that power consumption increases by increasing any of machining parameters suggesting that in order to reduce the power consumption, lowest possible cutting parameters should be considered. However, reducing cutting speed and chip load increases machining time and reduces material removal rate resulting in higher machining costs. This fact has been reflected in the SN graphs for EC/V (figure 7.19) where they suggests to choose the highest possible cutting parameters and thus increase productivity and reduce machining time in order to reduce the EC/V.

This is mainly due to the fact that the amount of energy used for running the machine tool is significantly higher than that of used for material cutting.

Observing the mean SN ratio graphs presented in figures 7.17, 7.18 and 7.19 for power consumption, PC/V and EC/V respectively and considering the value of δ calculated in table 7.15 reveals that machining environment is relatively the most significant parameter. This is mainly due to the fact that eliminating the coolant pump significantly reduces the power consumption, PC/V and EC/V making dry and cryogenic machining the most favourable machining environments. Furthermore, cutting speed has been found to be the second most significant parameter for power consumption and EC/V whilst it is depth of cut for PC/V. This can be explained by the fact that increasing depth of cut increases the volume of removed material without significant change in the machine tool's power consumption.

7.5.2. Surface roughness

For each pass of the machining experiments, five samples of surface roughness were measured and the average value of surface roughness was calculated to present the surface roughness of each machining pass for each experiment. In order to reduce the effects of tool wear, the average surface roughness of the first machining pass was used for analysis to compare the effect of cryogenic cooling as compared to dry and wet machining. For each machining experiment, three surface roughness parameters of Ra, Rz and Rq were measured. The average values of these surface roughness metrics are provided in table 7.17. The graphs of surface roughness for each machining pass of the machining experiments are given in appendix C and further discussed.

In order to minimise surface roughness, the smaller-is-better equation given in section 7.3.1 was used to calculate the SN ratio values of the surface roughness parameters for each machining experiment. The calculated SN ratio of surface roughness parameters are provided in table 7.17 next to their corresponding average measured values.

Based on the SN ratios calculated for surface roughness parameters, the mean SN ratio for each level of input parameters was calculated as disclosed in table 7.18. In addition, the difference between maximum and minimum values of mean SN ratios (δ) was calculated for each input parameter. This is be used to identify the relative importance of each machining parameter on the desired machinability metrics.

Exp. ID	Exp. No.	Surface roughness					
		Ra		Rz		Rq	
		Average	SN ratio	Average	SN ratio	Average	SN ratio
D1	1	1.037	-0.318	7.051	-16.965	1.345	-2.574
D2	2	1.102	-0.841	6.705	-16.528	1.255	-1.973
D3	3	1.281	-2.153	7.932	-17.988	1.572	-3.929
D4	4	1.169	-1.354	7.27	-17.231	1.427	-3.088
D5	5	1.094	-0.783	6.631	-16.432	1.206	-1.627
D6	6	0.987	0.114	6.098	-15.704	1.175	-1.401
D7	7	1.080	-0.671	5.308	-14.499	1.776	-4.989
D8	8	0.968	0.282	4.188	-12.440	0.782	2.136
D9	9	1.517	-3.620	7.994	-18.055	1.746	-4.841
W1	10	0.827	1.646	11.412	-21.147	2.704	-8.640
W2	11	1.080	-0.666	5.823	-15.303	1.175	-1.401
W3	12	1.789	-5.054	8.474	-18.562	1.866	-5.418
W4	13	0.860	1.313	6.495	-16.252	1.228	-1.784
W5	14	0.984	0.143	5.935	-15.468	1.156	-1.259
W6	15	1.114	-0.935	6.415	-16.144	1.272	-2.090
W7	16	0.819	1.731	4.691	-13.425	0.999	0.009
W8	17	1.098	-0.812	6.431	-16.166	1.259	-2.001
W9	18	1.240	-1.871	6.867	-16.735	1.306	-2.319
C1	19	0.664	3.557	4.044	-12.136	0.768	2.293
C2	20	1.085	-0.711	5.539	-14.869	1.024	-0.206
C3	21	1.879	-5.477	11.263	-21.033	2.086	-6.386
C4	22	0.592	4.544	3.824	-11.650	0.743	2.580
C5	23	0.756	2.430	4.301	-12.671	0.912	0.800
C6	24	0.942	0.516	13.051	-22.313	2.848	-9.091
C7	25	0.762	2.357	5.355	-14.575	0.922	0.705
C8	26	0.637	3.917	4.124	-12.306	0.783	2.125
C9	27	0.811	1.816	4.578	-13.214	0.863	1.280

Table 7.17 Average surface roughness metrics and their corresponding SN ratio

Using the values calculated for the mean SN ratios in table 7.18, the mean SN ratio graphs of different surface roughness metrics, namely Ra, Rz and Rq were generated. As shown in figure 7.20, 7.21 and 7.22, the mean SN ratio graphs demonstrated that the most favourable machining environment in order to improve surface roughness irrespective of the desired surface metrics is cryogenic cooling. Analysis of means indicated that on average, the surfaces produced by cryogenic machining have 19% and 21% lower surface roughness Ra as compared to their counterparts made by dry and wet machining.

Machining environment	**Level**	**Dry**	**Wet**	**Cryogenic**	**δ**
	Ra	-1.0382	-0.5004	1.4387	2.477
	Rz	-16.200	-16.580	-14.970	1.610
	Rq	-2.476	-2.767	-0.656	2.111
Cutting speed	**Level**	**30**	**115**	**200**	**δ**
	Ra	-1.113	0.665	0.348	1.778
	Rz	-17.170	-15.980	-14.600	2.570
	Rq	-3.137	-1.884	-0.877	2.260
Chip load	**Level**	**0.03**	**0.055**	**0.1**	**δ**
	Ra	1.423	0.329	-1.852	3.274
	Rz	-15.320	-14.690	-17.750	3.060
	Rq	-1.721	-0.378	-3.799	3.421
Depth of cut	**Level**	**1**	**3**	**5**	**δ**
	Ra	0.885	-0.154	-0.831	1.716
	Rz	-16.150	-15.540	-16.073	0.610
	Rq	-2.138	-1.306	-2.455	1.149

Table 7.18 Mean SN ratio of surface roughness parameters for each level of input parameters

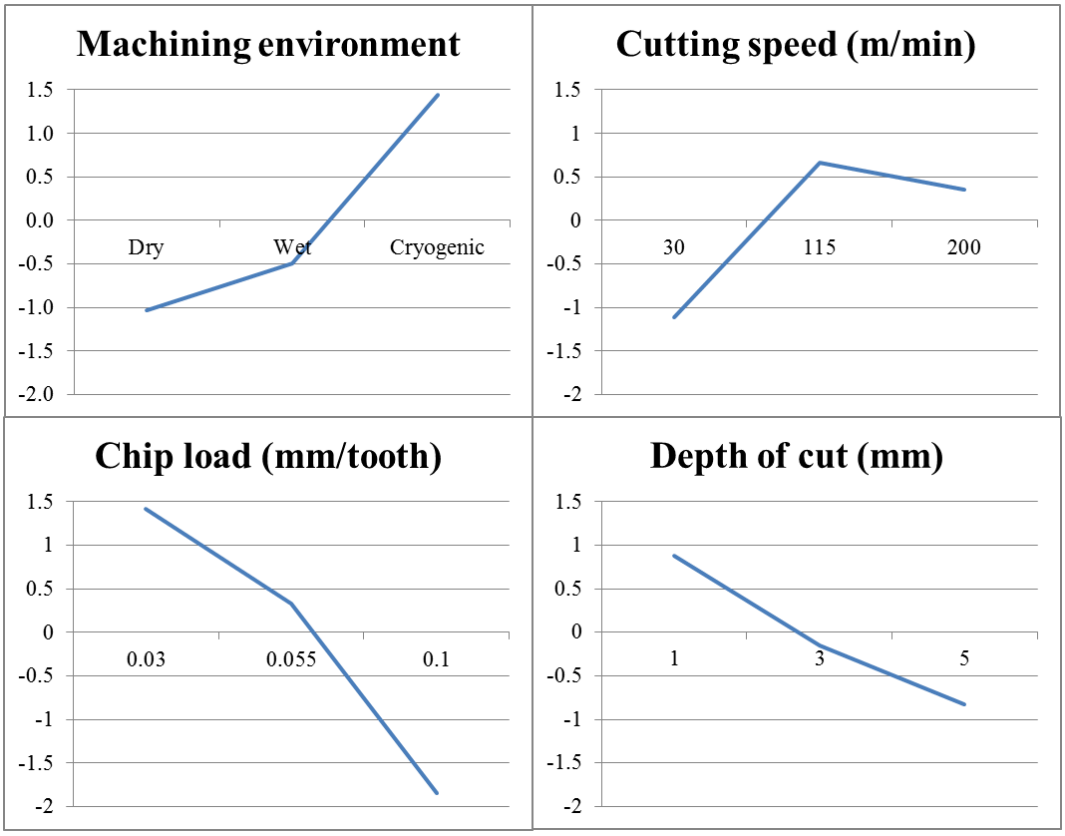

Figure 7.20 Mean SN ratio graphs for arithmetic surface roughness Ra

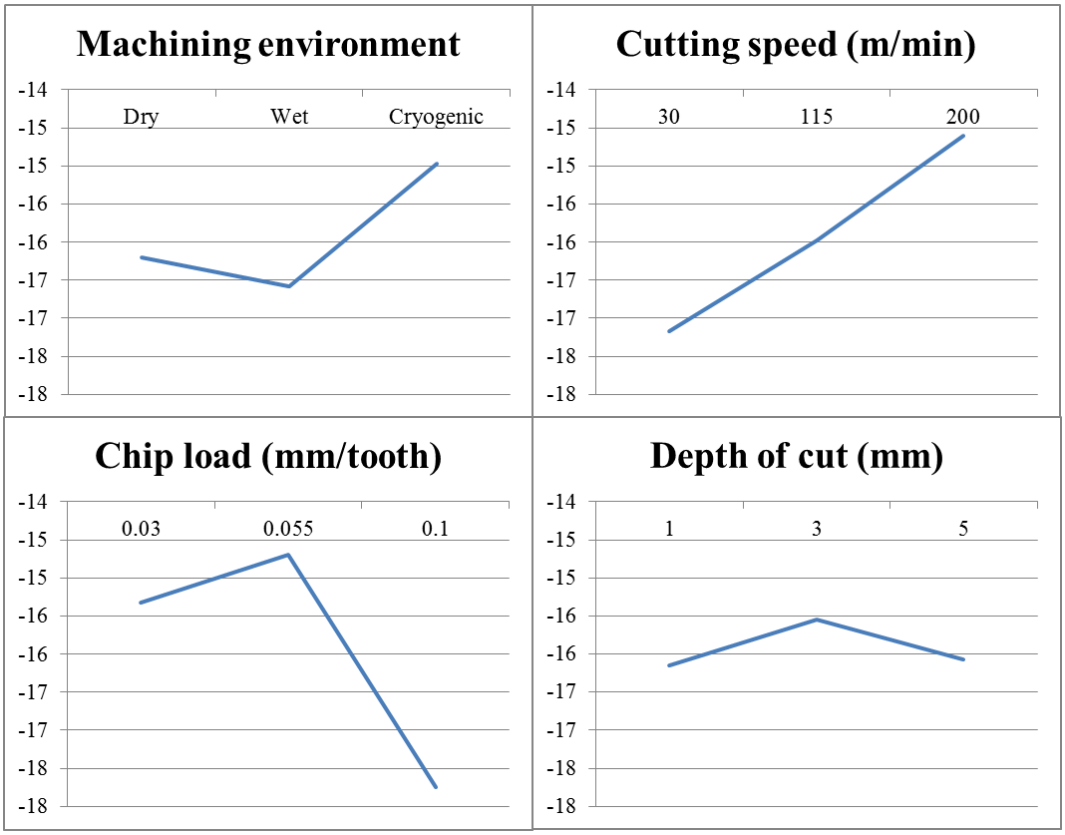

Figure 7.21 Mean SN ratio graphs for ten point height of irregularity of surface roughness Rz

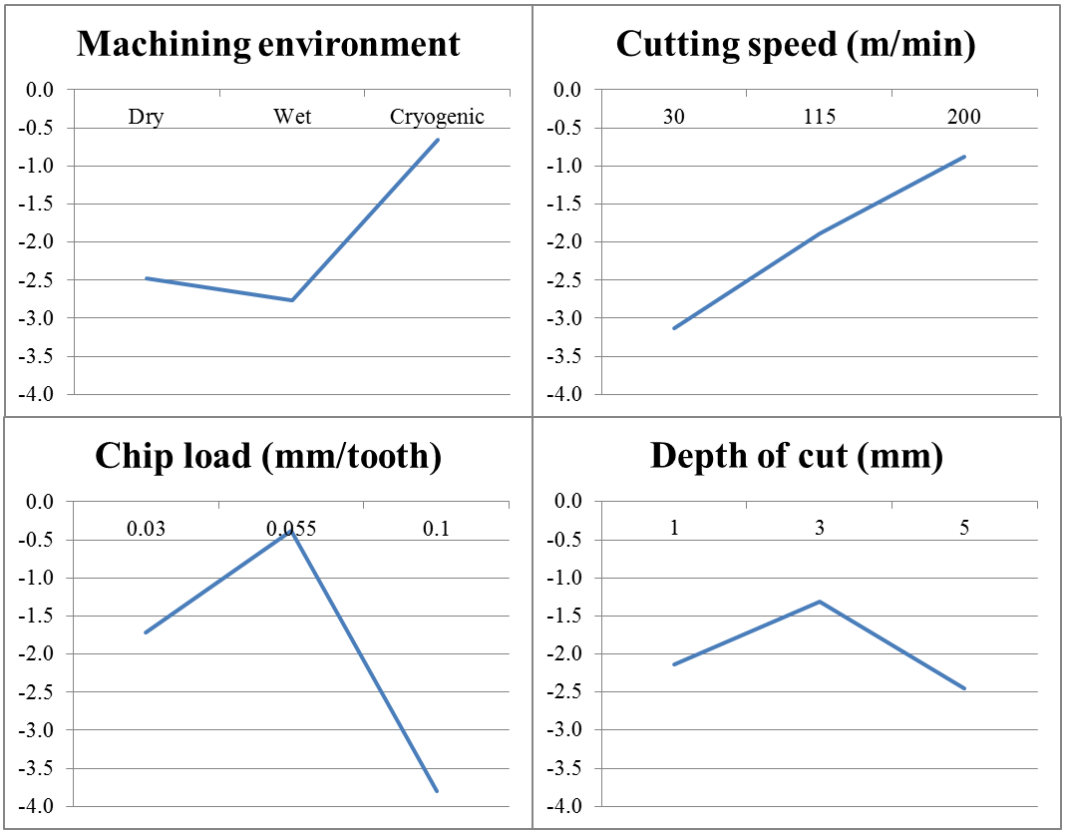

Figure 7.22 Mean SN ratio graphs for mean-root-square deviation of surface roughness Rq

Furthermore, as the machining environment side of the DoE is full factorial, the best surface roughness produced under each machining environment was identified and is shown in table 7.19. As the table demonstrates, using cryogenic cooling has resulted in a maximum 28% and 39% reduction in surface roughness Ra respectively as compared to wet and dry machining environments.

Experiment ID	Ra	Rz	Rq
D8	0.968	4.188	0.782
W7	0.819	4.691	0.999
C4	0.593	3.824	0.743

Table 7.19 Machining experiments with lowest surface roughness values for each machining environment

As shown in figure 7.20, the study of the mean SN ratio graphs for the machining environment together with table 7.18 also shows that if the arithmetic surface roughness (Ra) is desired, better results can be expected from wet machining than dry machining. However, for Rz and Rq, dry machining is more favourable than wet.

The analysis of mean SN ratio graphs, depicted in figure 7.20, 7.21 and 7.22, suggested that higher values of cutting speed (115-200 m/min) produces lower surface roughness (Ra, Rz and Rq). In addition, it has been found that low level of chip load (0.03 mm/tooth) is more desirable to improve Ra, whilst medium level (0.055 mm/tooth) gives better Rz and Rq surface roughness. Furthermore, interpreting mean SN ratio graphs indicated that low level (1mm) of depth of cut is more favourable to achieve lower surface roughness Ra whilst it is not significant for Rz and Rq surface roughness.

7.5.3. Tool wear

The cutting tools' flank wear was measured after conduction of the machining experiments. A high resolution digital image of the flank faces of each cutting tool was taken and the one with maximum flank wear was selected to present the flank wear of the respective cutting tool. Figure 7.23 illustrates the images of the flank face of the cutting tools used for each machining experiment according to DoE.

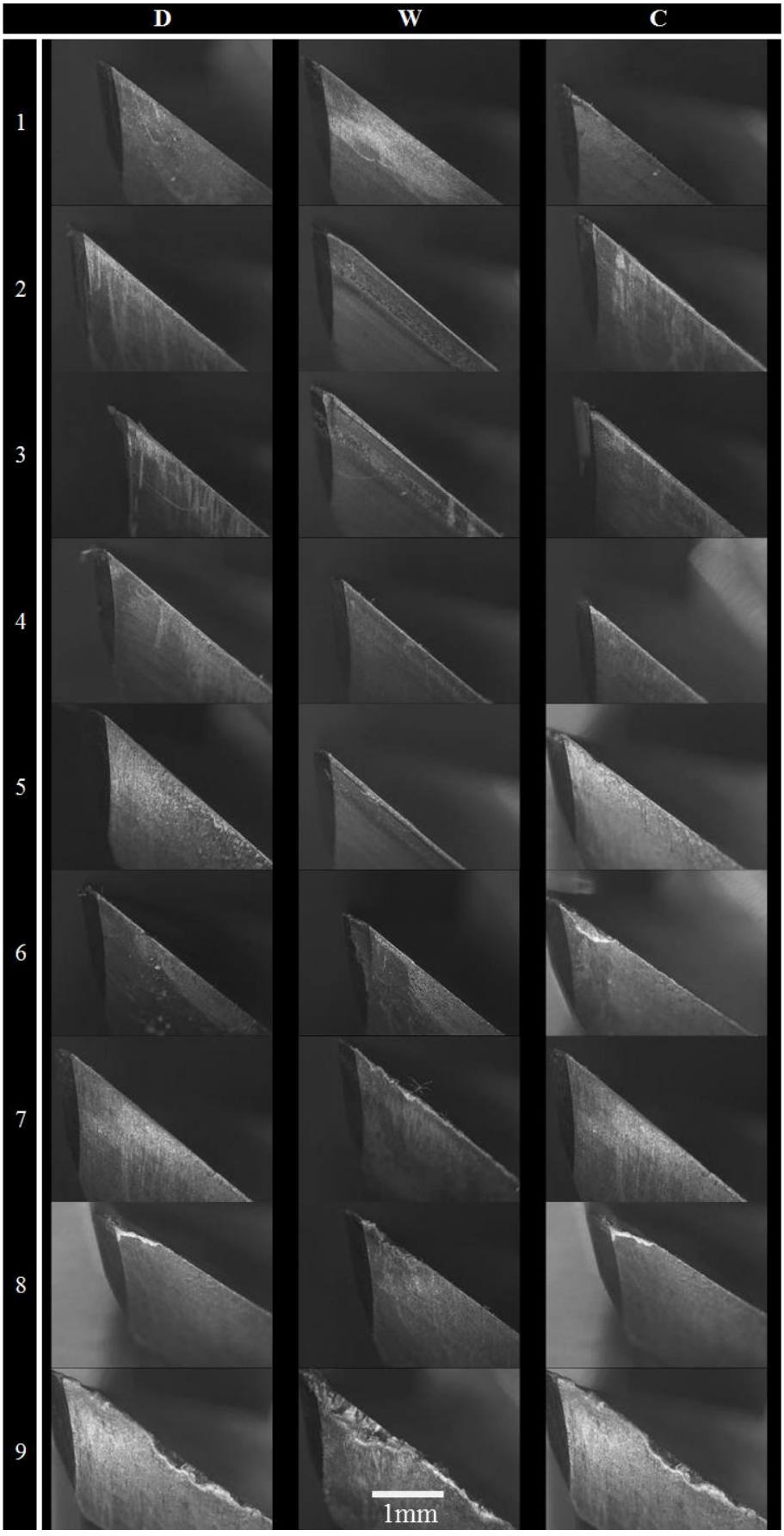

Figure 7.23 Flank face of the cutting tools used for machining experiments

From the images and following the instruction of (ISO 8688-2, 1989), the maximum flank wear of each cutting tool was measured and is provided in table 7.20. Furthermore, smaller-is-better SN ratio for each machining experiment was calculated. As previously mentioned in section 7.3.3, experiment D2 was terminated after two machining passes and the tool wear was measured to be 31.2 µm, thus for analysis purposes, a tool wear of 62 µm was assumed for this tool after four machining passes. The mean SN ratios of the SN ratios given in table 7.20 were computed for each level of input parameters and are provided in table 7.21.

Exp. ID	Exp. No	Flank wear (µm)	SN ratio
D1	1	64.7	-36.218
D2	2	53.9	-34.632
D3	3	83.8	-38.465
D4	4	29.7	-29.455
D5	5	76.2	-37.639
D6	6	36.7	-31.293
D7	7	31.1	-29.855
D8	8	135.2	-42.620
D9	9	213.9	-46.604
W1	10	16.5	-24.350
W2	11	41.4	-32.340
W3	12	78.2	-37.864
W4	13	28.9	-29.218
W5	14	46.2	-33.293
W6	15	92	-39.276
W7	16	63.4	-36.042
W8	17	116	-41.289
W9	18	347.1	-50.809
C1	19	16.8	-24.506
C2	20	40.7	-32.192
C3	21	74.6	-37.455
C4	22	27.7	-28.850
C5	23	40.1	-32.063
C6	24	232.5	-47.328
C7	25	10.4	-20.341
C8	26	86.4	-38.730
C9	27	251.2	-48.000

Table 7.20 Measured values of flank wear and their respective SN ratio

The mean SN ratio data calculated for tool flank wear, shown in table 7.21, were used to generate the mean SN ratio graphs as shown in figure 7.24. Similar to surface roughness, analysis indicated that cryogenic machining has the largest mean SN ratio and thus is the most favourable machining environment for reducing flank wear. Considering δ and as it can be seen in figure 7.24, chip load and cutting speed are the most significant parameters affecting tool wear being followed by depth of cut and machining environment respectively. In order to reduce flank wear, SN ratio analysis recommends selecting low cutting speed (30 m/min) and chipping load (0.03 mm/tooth) and high depth of cut (5 mm).

Machining environment	**Level**	**Dry**	**Wet**	**Cryogenic**	**δ**
	Mean SN ratio	-36.309	-36.053	-34.385	1.924
Cutting speed	**Level**	**30**	**115**	**200**	**δ**
	Mean SN ratio	-33.113	-34.268	-39.366	6.252
Chip load	**Level**	**0.03**	**0.055**	**0.1**	**δ**
	Mean SN ratio	-28.759	-36.089	-41.899	13.140
Depth of cut	**Level**	**1**	**3**	**5**	**δ**
	Mean SN ratio	-36.179	-36.900	-33.668	3.232

Table 7.21 Mean SN ratio of the levels of each input parameter for flank wear

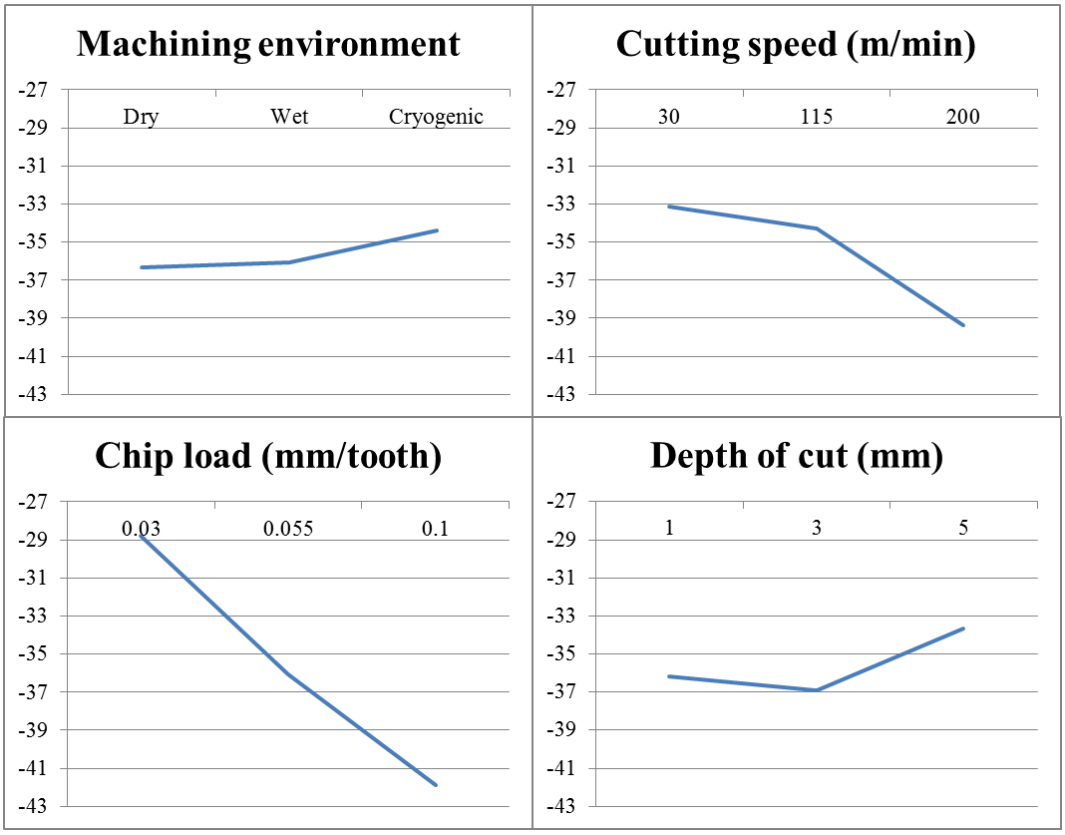

Figure 7.24 Mean SN ratio graphs for tool flank wear

As shown in figure 7.25, comparison of the measurement results for tool wear revealed that the smallest flank wear in cryogenic machining is associated with experiment C7 (10 µm), whilst they are W1 (16.5 µm) and D4 (29.7 µm) for wet and dry machining respectively. From this, it can be concluded that lower tool flank wear can be expected in cryogenic machining whilst increased productivity can be achieved as a result of higher cutting speed in comparison with dry and wet machining.

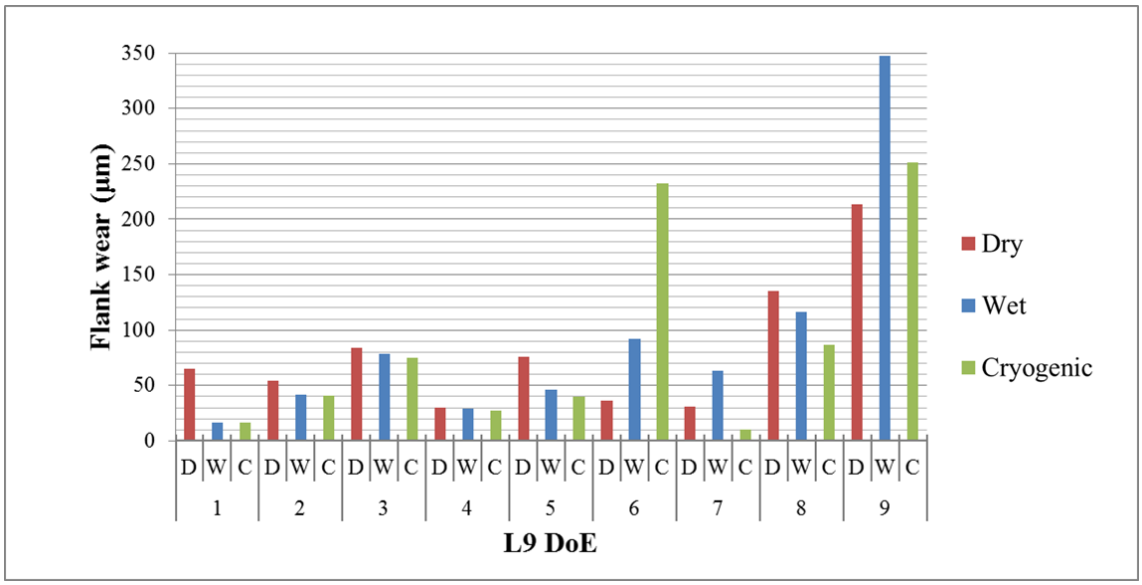

Figure 7.25 Measurement results for tool flank wear

It is noteworthy to mention that whilst the standard (ISO 8688-2, 1989) suggested flank wear as one of the indicators of tool life, there are other types of wear which can affect the tool life e.g. chipping, crater wear and catastrophic tool failure. As shown in figure 7.23, microscopic images of the cutting tools indicated that tool wear at low feed rates and cutting speeds is more in the form of a mechanical wear such as abrasive wear whereas it is more thermal and chemical at higher cutting speeds. For instance, whilst abrasion was the dominant tool wear mechanism for D1, W1 and C1 (figure 7.23), smearing, welding and diffusion can be seen for the tools D9, W9 and C9. In addition, as shown in figure 7.23, the tools used for D9, W9 and C9 suffers from crater wear which was resulted in significant chipping of the cutting edge.

Crater wear is not considered as one of the main tool failure modes as unlike flank face, the rake face is not in direct contact with machined surface. However, welding and formation of built up edge on the rake face has the potential of weakening the cutting edge by making crater wear. As shown in figure 7.26, flaking, crater wear and formation of built up edge

were dominant for all machining experiments irrespective of machining environment. It has been noticed that the crater wear formed a narrow line adjacent to the cutting edge on all the cutting tools. Constant flow of the chips over the rake face removes material from the cutting tool adjacent to the cutting edge and forms crater wear. This potentially weakens the cutting edge resulting in chipping and tool failure. As illustrated in figure 7.26, cryogenic cooling significantly reduced the severity of this phenomenon showing the potential to improve the tool life.

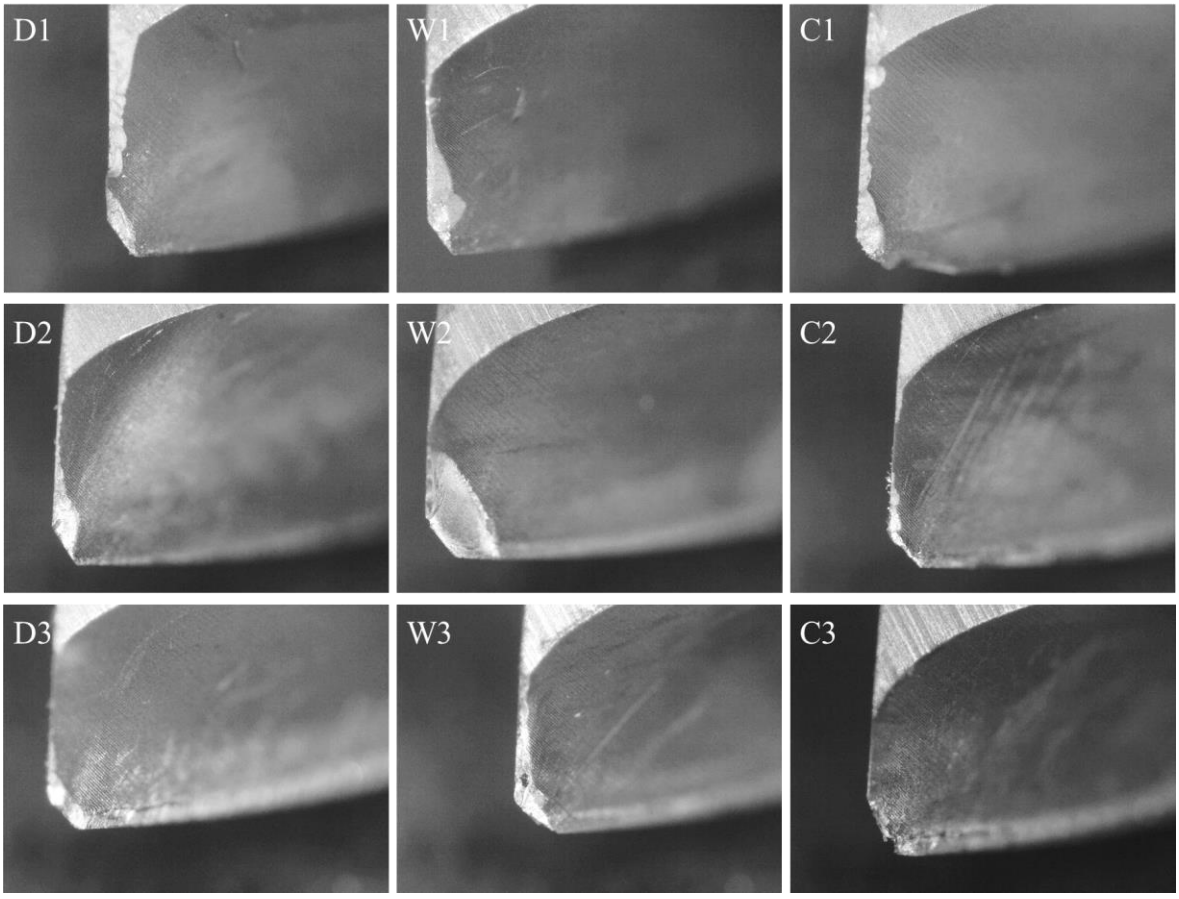

Figure 7.26 Flaking and crater wear on the tools used in machining experiments

7.5.4. Chip morphology

The machining chips produced during each experiment have been collected and cleaned for further analysis. A low magnification microscopic image was taken from the chips for each machining experiment. As shown in figure 7.27, these images present the general form of the machining chips. Moreover, a microscopic image of the internal surface of the chips was taken as shown in figure 7.28.

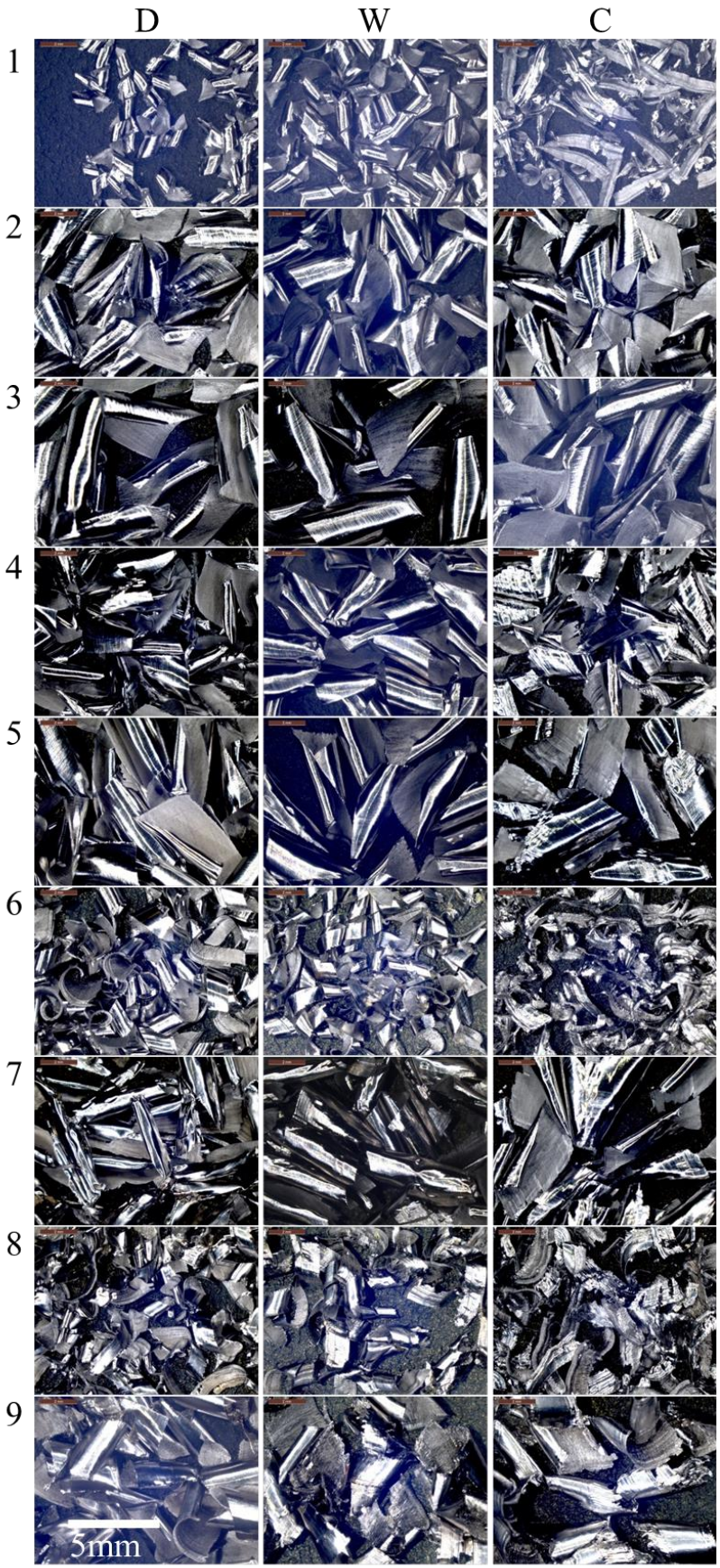

Figure 7.27 Images of the form of the machining chips for each machining experiment

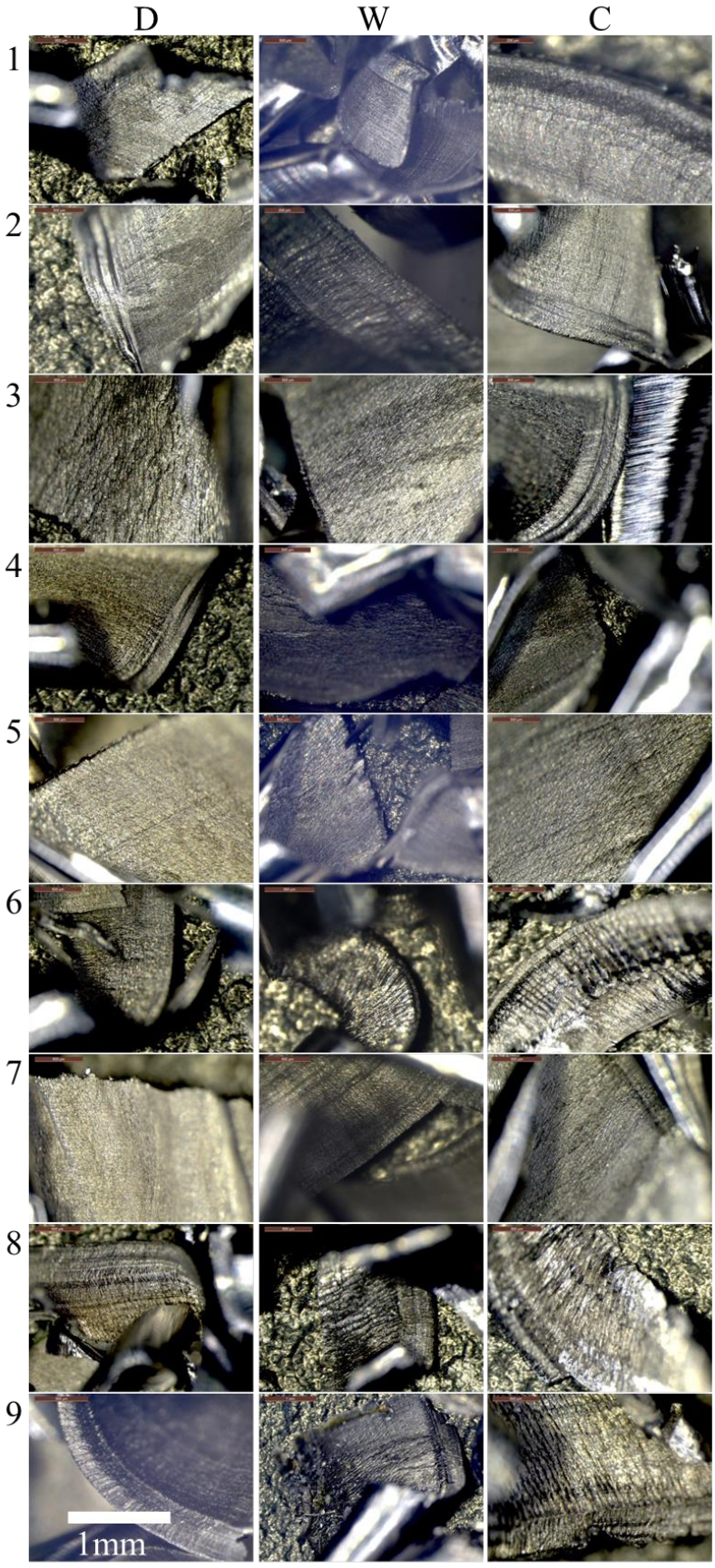

Figure 7.28 Microscopic images of the inside of the machining chips

Chip thickness is one of the parameters which can be used to study the performance of machining operations. The chip thickness, together with chip load and cutting tool's rake angle can be used to calculate chip compression ratio and shear angle.

A digital microscope and a micrometer were used to measure the thickness of the machining chips. The results of the chip thickness measurement are provided in table 7.22. These results were used to calculate the chip compression ratio (r) and thus the shear angle.

Experiment	Dry	Wet	Cryogenic
1	84	53	41
2	82	84	72
3	133	182	111
4	44	72	53
5	83	112	83
6	134	136	133
7	50	50	49
8	170	79	81
9	168	192	177

Table 7.22 Deformed chip thickness (μm) for each machining experiment

General comparison of the chips collected for machining experiments as depicted in figure 7.27, does not reveal any significant changes in the chip formation. The most noticeable change as a result of machining environment belongs to experiment 1 where the chips from experiments D1 and C1 are curl whilst it changed to sword shaped chips in cryogenic machining. This can be explained by the fact that cryogenic cooling increases the hardness and strength of the workpiece material and thus machining chips. As a result and since titanium does not show low temperature embrittlement, the chips generated in cryogenic machining are more resistant to plastic deformation than in dry and wet machining. As shown in figure 7.28, serrated chips were observed for all machining experiments irrespective of the machining environment. Figure 7.29, illustrates a detailed microscopic image of the serrated chips observed in experiment C9.

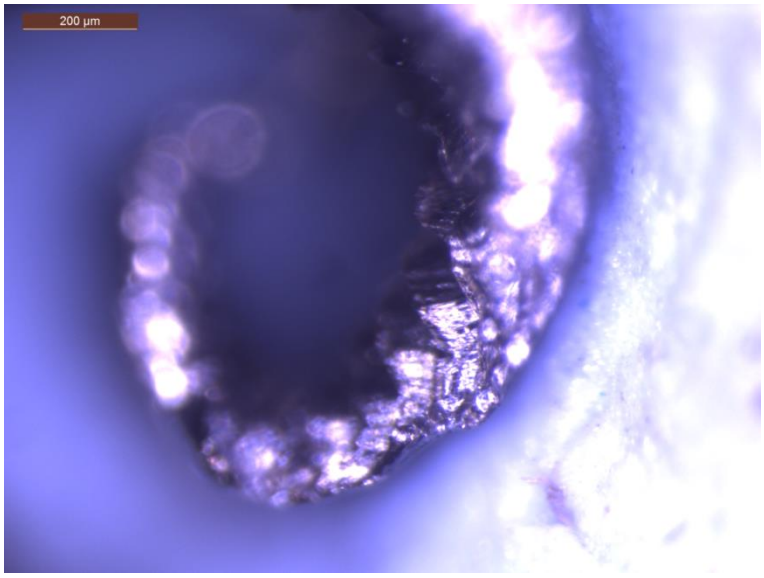

Figure 7.29 Microscopic image of serrated chip produced in experiment C9

The measured chip thickness, presented in table 7.22, was used to calculate the chip compression ratio. Furthermore, Merchant's equation (Merchant, 1945) was used to compute the shear angle for each machining experiment. The Merchant's equation is as depicted below:

$$\varphi = arctan\left(\frac{r\cos\alpha}{1 - r\sin\alpha}\right)$$

where φ is shear angle, r is chip compression ratio and α is the tool's rake angle. The chip compression ratio is the ratio of undeformed chip thickness to the deformed chip thickness.

The calculated values of chip compression ratio and shear angle for each machining experiment are provided in table 23.

Experiment	Dry		Wet		Cryogenic	
	r	Shear angle°	r	Shear angle°	r	Shear angle°
1	0.38	21.69	0.75	41.00	0.60	33.84
2	0.69	38.12	0.79	42.57	0.69	38.12
3	0.77	41.85	0.91	47.63	0.56	31.57
4	0.75	41.00	0.60	33.84	0.43	24.71
5	0.69	38.12	0.69	38.12	0.50	28.63
6	0.77	41.85	0.77	41.85	0.71	39.37
7	0.60	33.84	0.60	33.84	0.60	33.84
8	0.32	18.74	0.69	38.12	0.69	38.12
9	0.59	33.25	0.55	31.25	0.53	30.03

Table 7.23 Chip compression ratio and shear angle for each machining experiment

The calculated values for r and shear angle were tested for normality and the analysis indicated that both datasets are normally distributed. Analysis of means was performed on the data using Minitab (Minitab Inc., 2010) and the main effect plots were generated for chip compression ratio and shear angle as shown in figure 7.30 and 7.31. Since the shear angle and chip compression ratio are in direct relation, the effect of cutting parameters are identical on both shear angle and chip compression ratio.

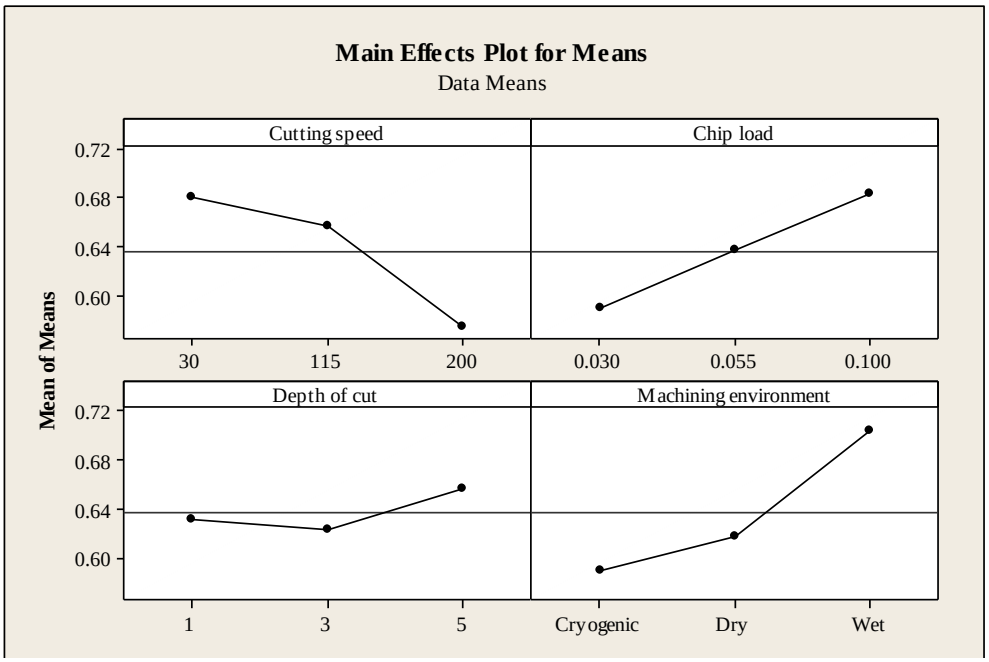

Figure 7.30 Main effects plots for chip compression ratio

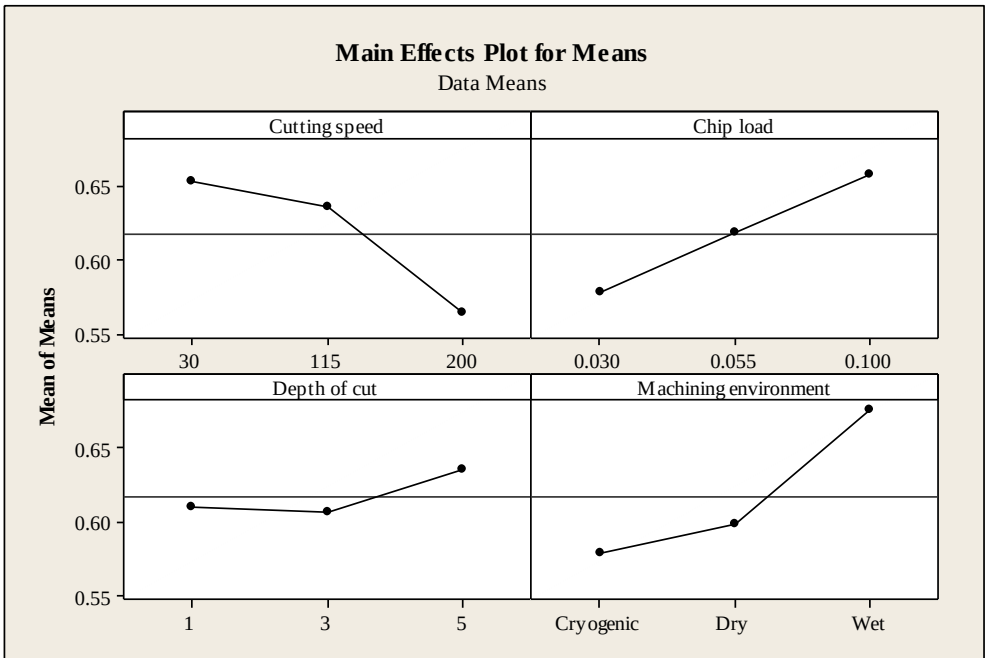

Figure 7.31 Main effects plot for shear angle

A shown in figure 7.30 and 7.31, cryogenic cooling produces lower chip compression ratio and shear angle as compared to dry and wet machining. From the analysis, it appears that both values increase linearly with an increase in chip load. In contrast, they are in adverse relation with cutting speed where lower chip compression ratio is achieved at higher cutting speeds.

7.5.5. Surface topography, microstructure and micro hardness

As mentioned in section 7.4.6, six SEM images were taken from the first machining pass for each experiment. Figure 7.32 and 7.33 illustrate the images taken for each machining experiment using BEI and SEI techniques respectively. Microscopic study of the machined surfaces indicates that deformation of feed marks, smearing and re-deposition of chips on the machined surfaces were detected for all experiments irrespective of machining environment.

Smearing and deformation of feed mark occurs where plastic deformation takes place during cutting operation which can be attributed to the formation of built up edge. On the other hand, chips re-deposition is originated from fine cutting chips which are welded onto the machined surface under high temperatures and pressures occurred during machining processes (Ezugwu et al., 2007, Ulutan and Ozel, 2011).

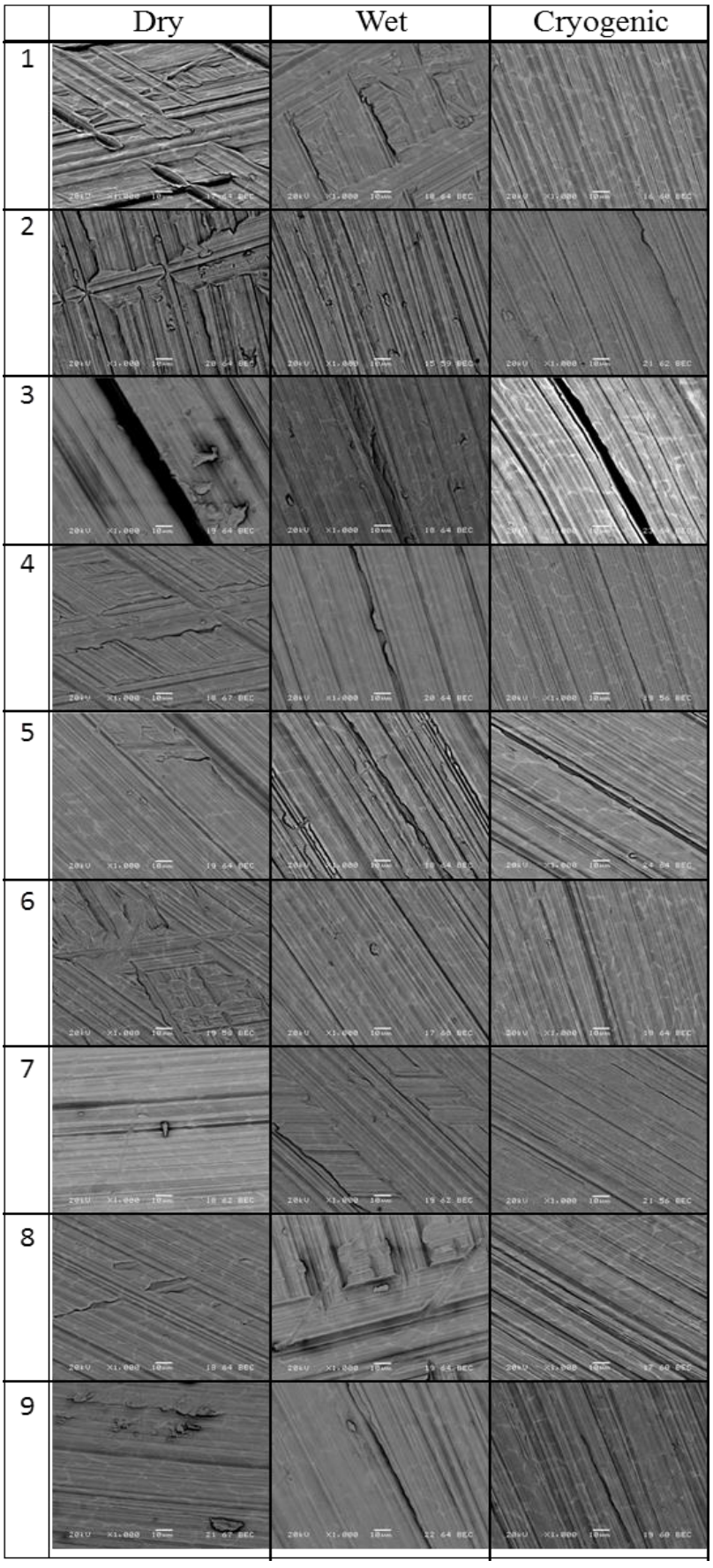

Figure 7.32 BEI micrographs of machined surfaces

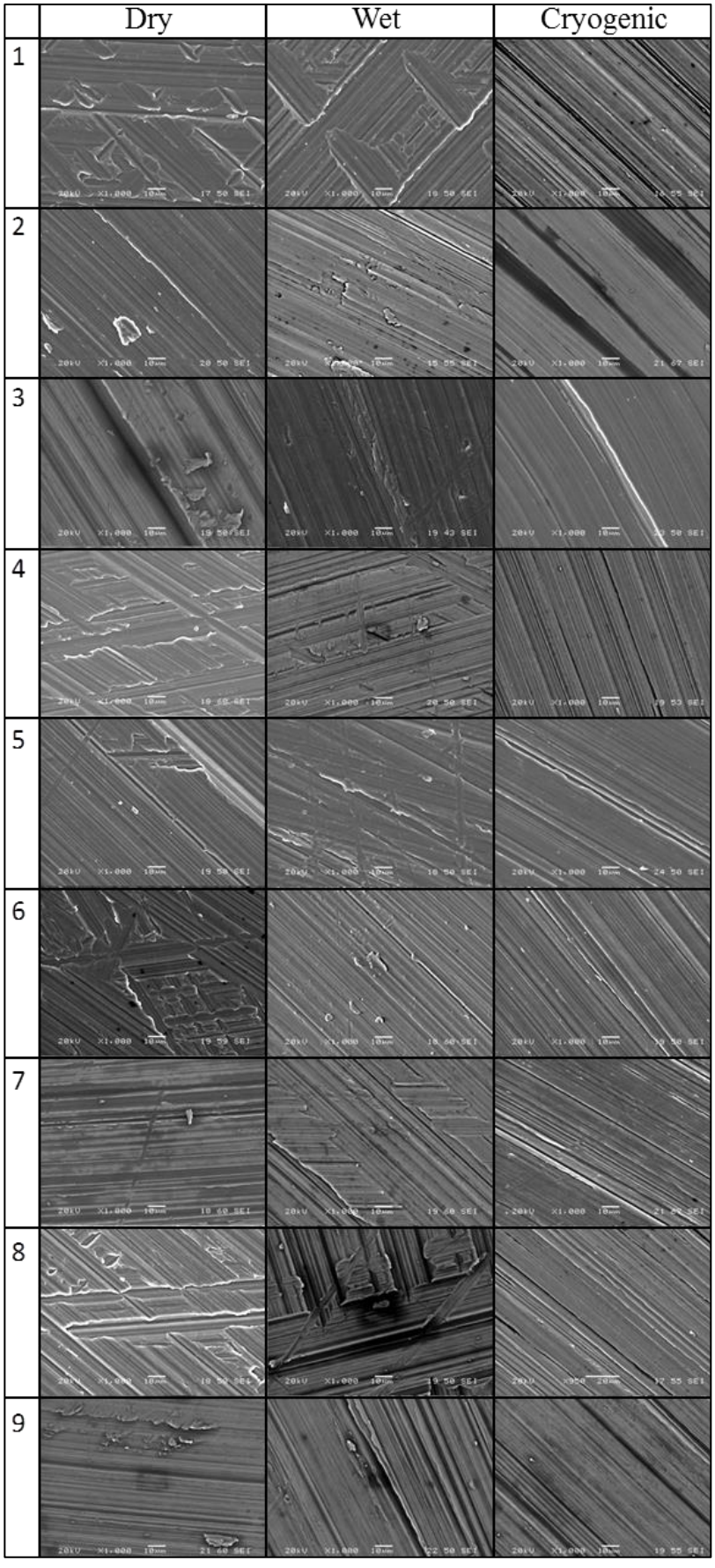

Figure 7.33 SEI micrographs of machined surfaces

Although surface defects were detected on all machined surfaces, the extent of the surface defects was different at various machining environments. For instance, as shown in figure 7.34 for the first set of machining experiments in L9 DoE (D1, W1 and C1), the highest smearing was observed in dry machining.

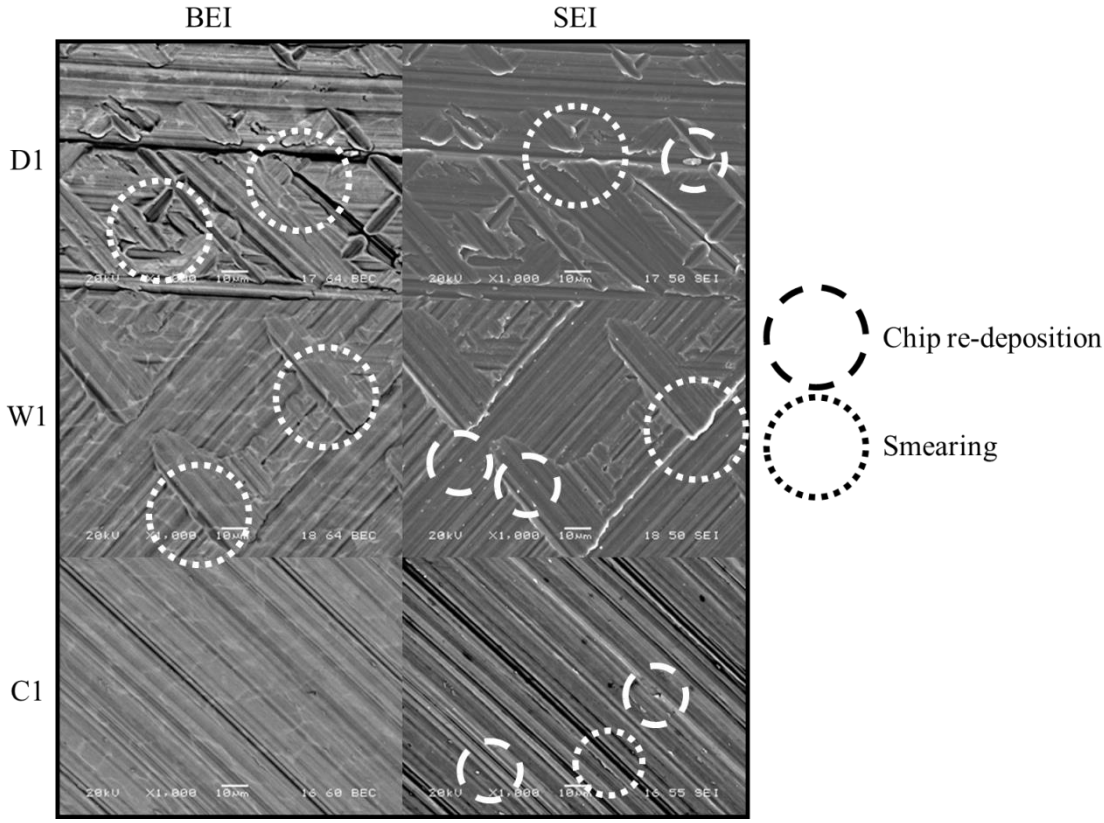

Figure 7.34 SEM images of machined surfaces for experiments D1, W1 and C1

The introduction of coolant has reduced surface defects where the best surface was made under cryogenic cooling. As illustrated in figure 7.35, microscopic images of the machined surfaces from the third set of machining experiments in L9 DoE (D3, W3 and C3) demonstrated severe surface damage and deformation for dry and wet machining whilst the best surface was made by cryogenic machining. As shown in figure 7.35, the existence of micro cracks was detected on the surface made by dry machining, whilst severe plastic deformation and smearing were observed for wet machining. Slight smearing and chip re-deposition were found on the surface of the sample from C3 experiment.

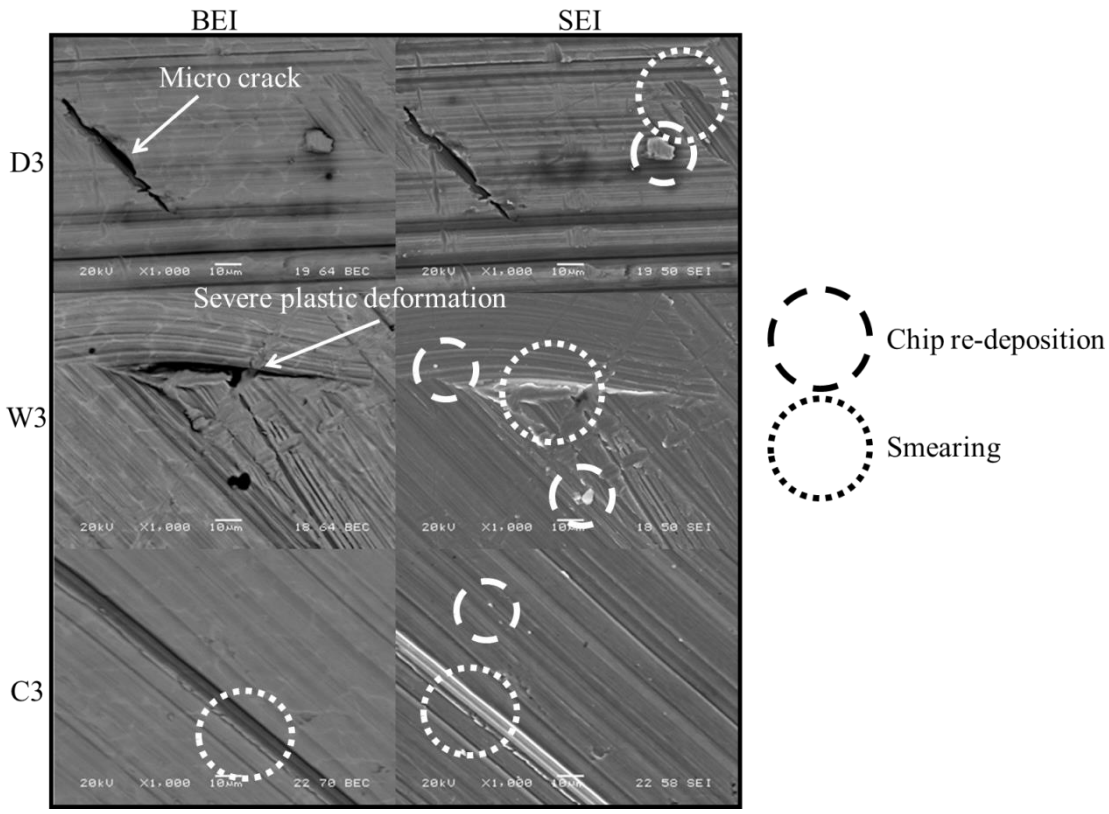

Figure 7.35 SEM images of machined surfaces for experiments D3, W3 and C3

A composition BEI of the microstructure of the workpiece in experiment D7, demonstrated in figure 7.36, indicates that the material grains were stretched along the machining direction. This can be explained by the fact that the workpiece and cutting tool became red hot during the experimentation and machining operation was stopped after second machining pass. This is particularly important considering the fact that titanium ignites at temperatures above 400°C making machining operations dangerous. As shown in figure 7.36, studying the images of the machined samples for experiments W7 and C7 clearly demonstrates that using coolants has reduced this phenomenon.

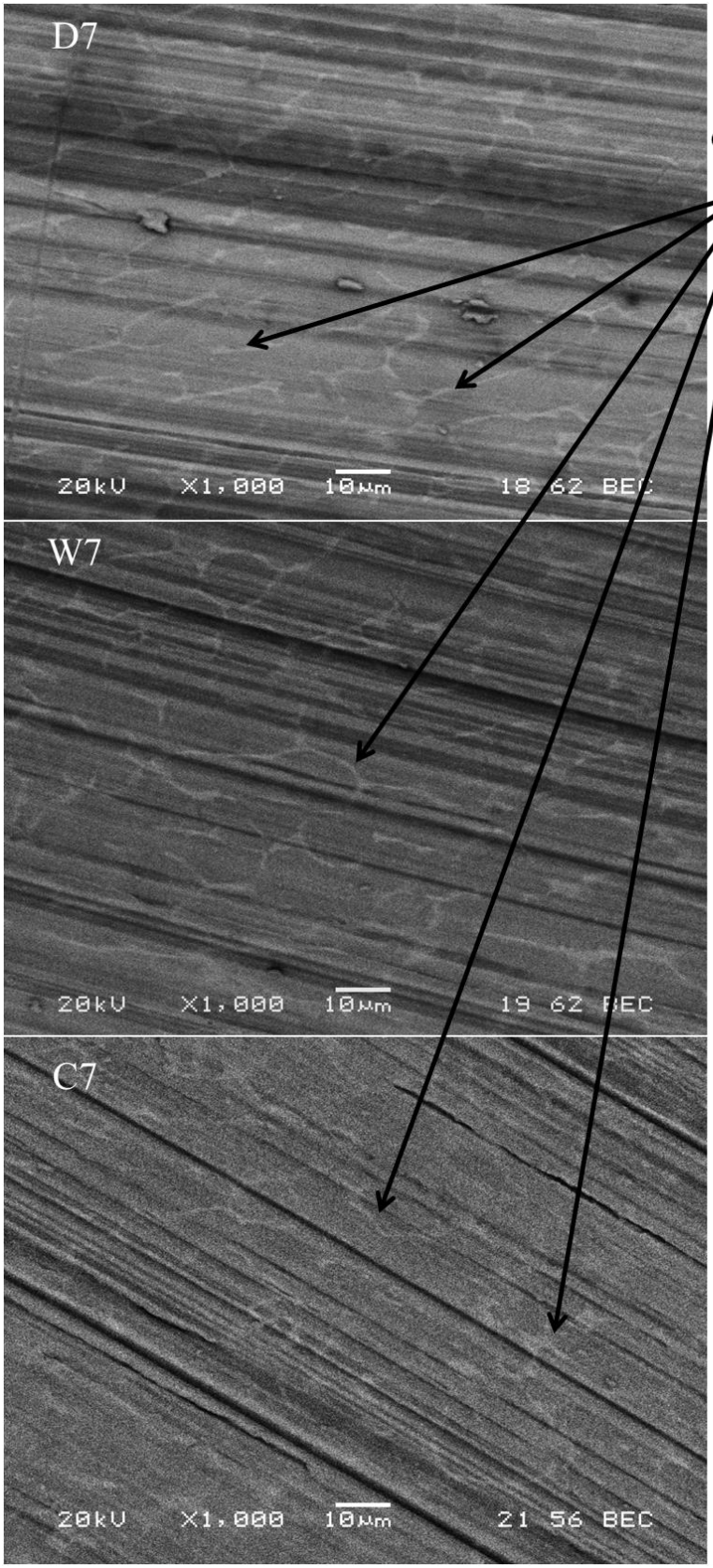

Figure 7.36 Composition BEI images of machined surfaces for experiments D7, W7 and C7 at 1000x magnification

One of the possibilities in cryogenic machining of titanium with LN_2 is chemical reaction between nitrogen and the workpiece material. Thus, the machined surfaces under cryogenic condition were randomly tested for material composition using EDS and the following elements were detected.

- Titanium
- Aluminium
- Vanadium
- Iron
- Carbon
- Oxygen

The first four elements are known to exist in the material composition of Ti-6Al-4V alloy which were confirmed initially as explained in section 7.2.1. In addition, the presence of carbon and oxygen is mainly due to organic contamination of the samples which were not removed during washing. Oxygen was only detected in one spectrum. This spectrum and the results of analysis are shown in figure 7.37. It is noteworthy to mention that according to Donachie (2000), a total maximum of 4 weight% impurities such as nitrogen, oxygen, carbon, hydrogen and iron are allowed in the material composition of Ti-6Al-4V. However, no traces of nitrogen were detected on the surface of the machined material.

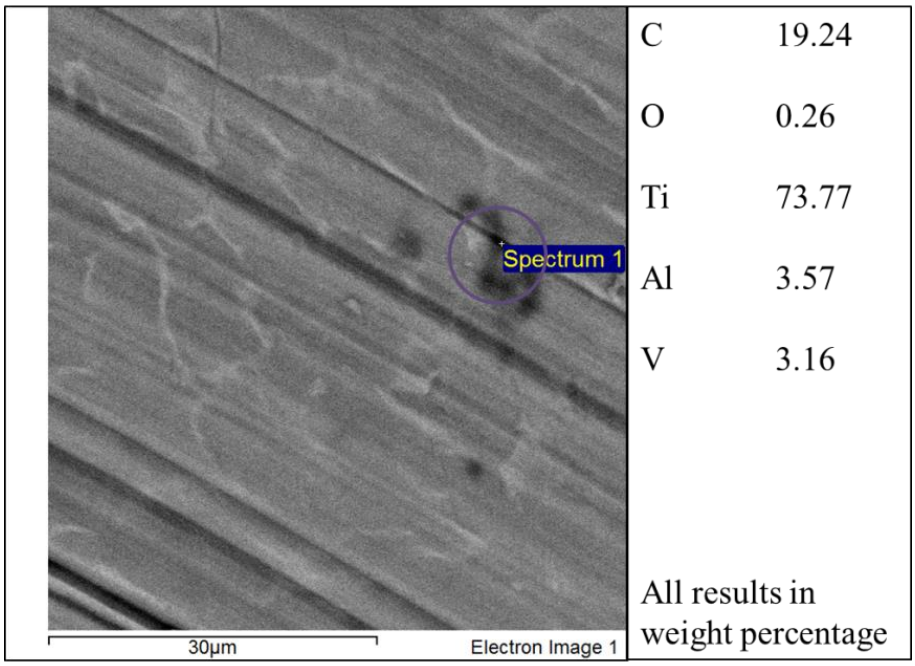

Figure 7.37 EDS Spectrum and the material composition of a cryogenically machined surface

Figure 7.38 illustrates the micrographs of the cross section of the machined samples depicting the microstructure of the material below the machined surface. As the figure shows, due to the variations in crystal formation within samples, no noticeable changes can be seen in the microstructure of the material as a result of changes in the machining environment. Furthermore, visual investigation of the images does not reveal any change detectable by eye on the material structure below the machined surfaces.

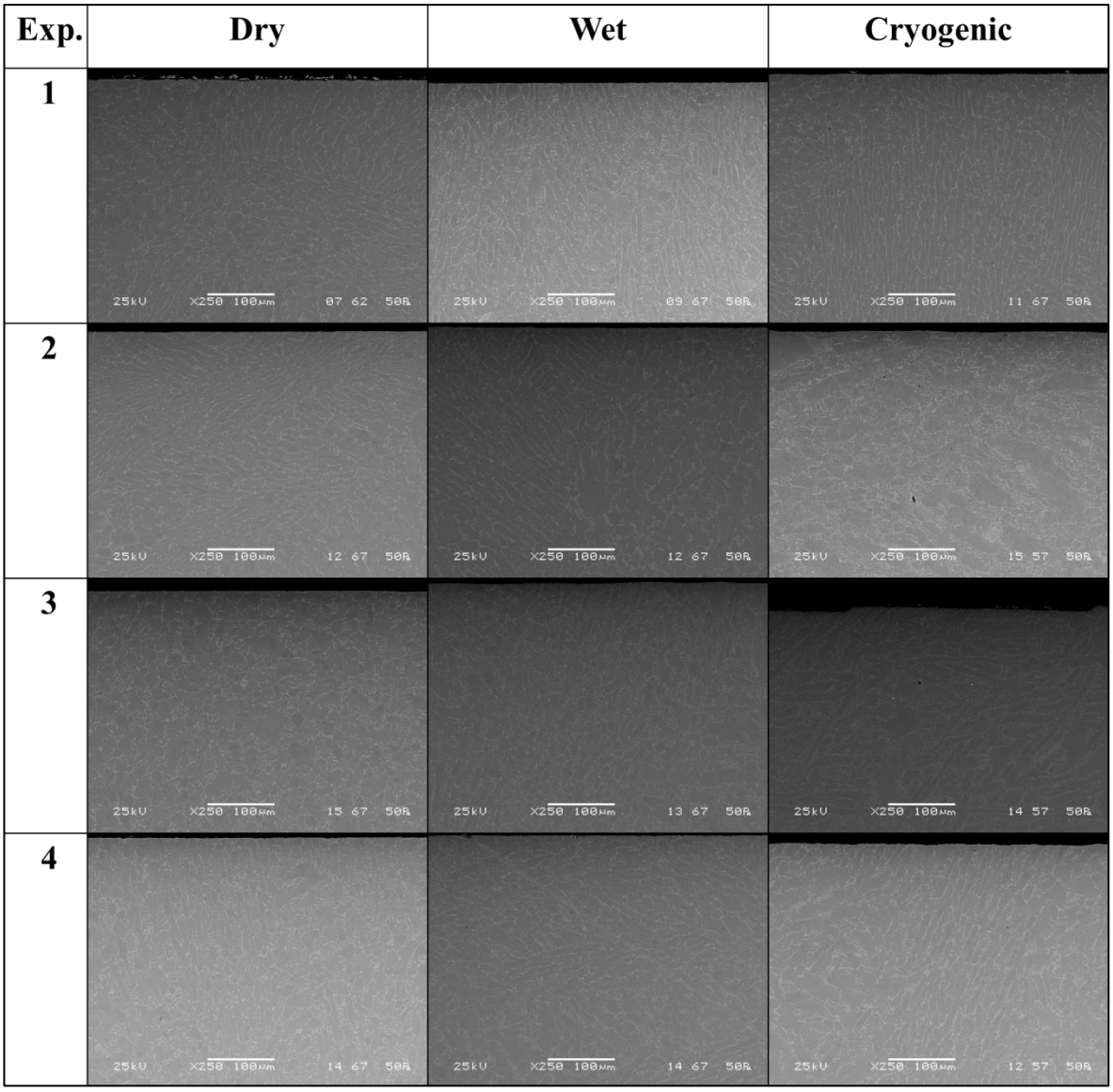

a) Experiments 1-4

Figure 7.38 Micrographs of the microstructure below the machined surface

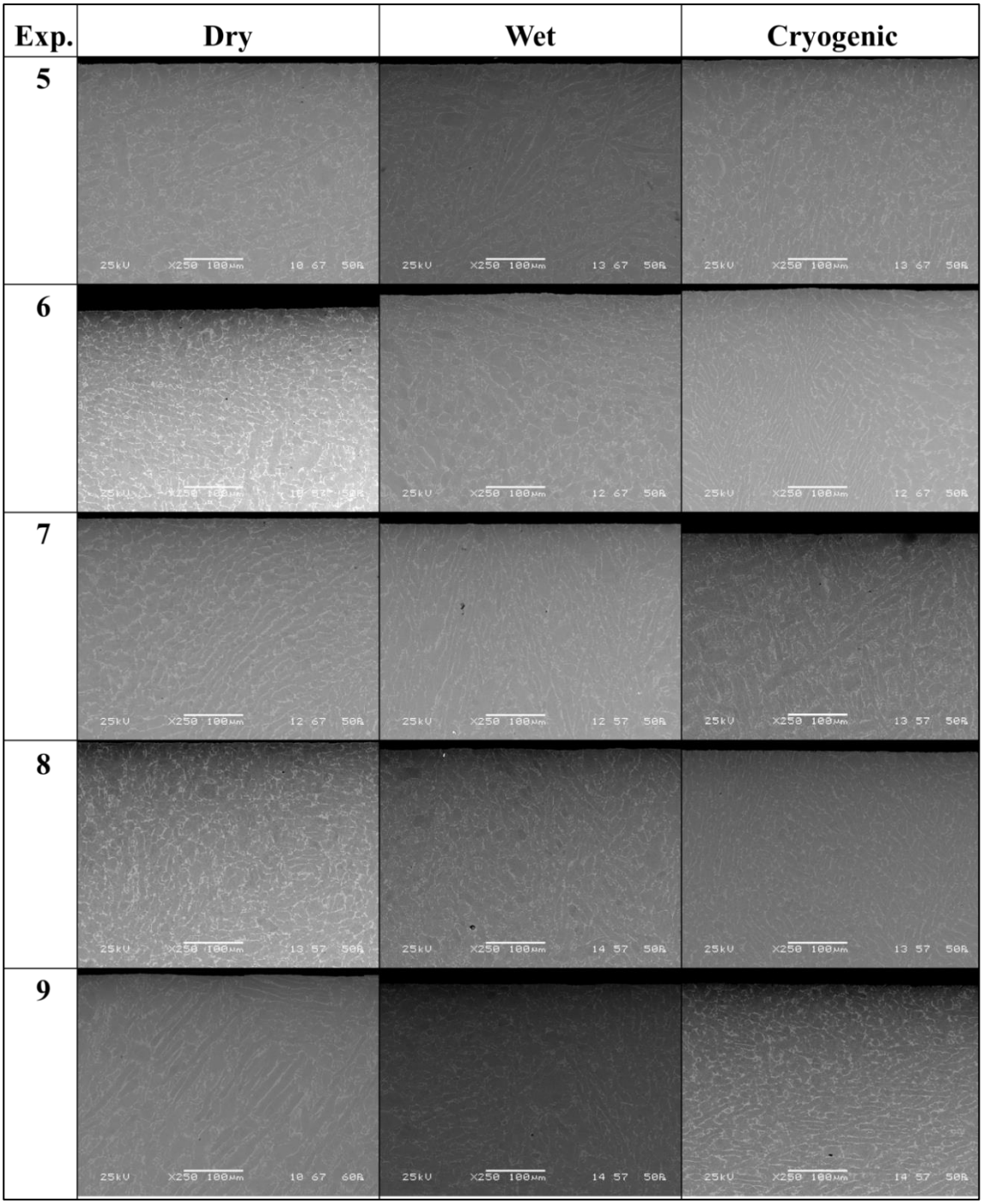

b) Experiments 5-9

Figure 7.38 Micrographs of the microstructure below the machined surface

According to the methodology described in section 7.4.7, 23 micro indentations were produced for each machining sample at various lengths below the machined surface. In order to calculate the microhardness at each point, the length of horizontal and vertical diagonals of the pyramid indentations for microhardness was measured. The average length of the diagonals was used to calculate the Vickers microhardness below the

machining surface for each sample. The measured values of microhardness are shown in figure 7.39.

a) Experiments 1-4

Figure 7.39 Logarithmic graphs of micro hardness of machined samples under different machining environments

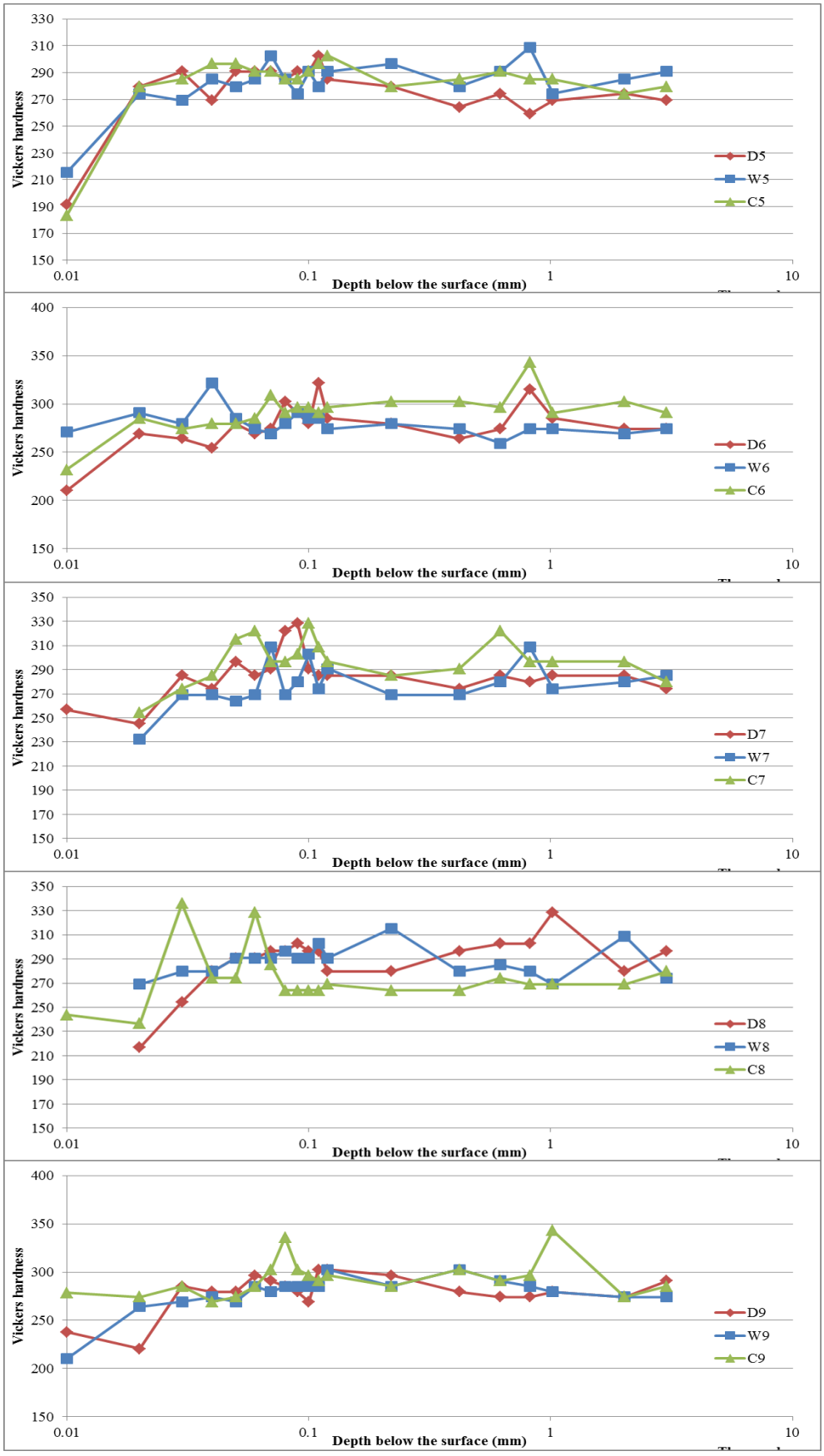

b) Experiments 5-9

Figure 7.39 Logarithmic graphs of micro hardness of machined samples under different machining environments

Analysis of microhardness of the samples beneath the machining surface indicated that the hardness of the material has been changed up to 100 μm below the surface irrespective of machining environment. However, the most noticeable change has taken place in the first 20 μm below the machined surface. This is mainly due to the local heat treatment at cutting temperatures and strain hardening as a result of cutting forces. However, as mentioned previously, these phenomena were not detectable by eye inspection of the micrographs of the cross sectional microstructure.

As a result, an image processing technique was implemented using Matlab (MathWorks, 2013) in order to compare the concentration of β phase beneath the machined surface. Since the β phase appeared brighter than the α phase, a binary image of the cross section can help identifying the changes in the microstructure.

The 250X magnification BEI was used for image processing. Figure 7.40 demonstrates the stages conducted for image processing and depicts the image from sample C1 as an exemplar. Initially, the images were translated in Matlab (MathWorks, 2013) into a matrix and cropped in order to remove the areas which do not present the cross section e.g. resin (stage 1). A low pass Gaussian filter was applied on the images in order to reduce the noise of the image (stage 2). In order to put an emphasis on the β phase in the images, Canny's edge detection filter was applied with various sigma values as shown in stage 3 in figure 7.40. The Canny method seeks local maxima of gradient using two thresholds to detect strong and weak edges (MathWorks, 2013).

The generated image of the edges was merged into the image from the second stage to form an image with extra emphasis on the β phase of the material (stage 4). In SEM imaging, any tilt or slope of the sample results in a change in the contrast and brightness across of an image as shown in figure 7.40(1). In order to eliminate the adverse effect of various contrast and brightness, contrast limited adaptive histogram equalisation technique was performed on the merged image to uniform the contrast and brightness across the image (stage 5). A binary filter was then applied to the normalised image (stage 6) to represent the image in two colours of black and white. In this image, the β phase is presented in white whilst α is black.

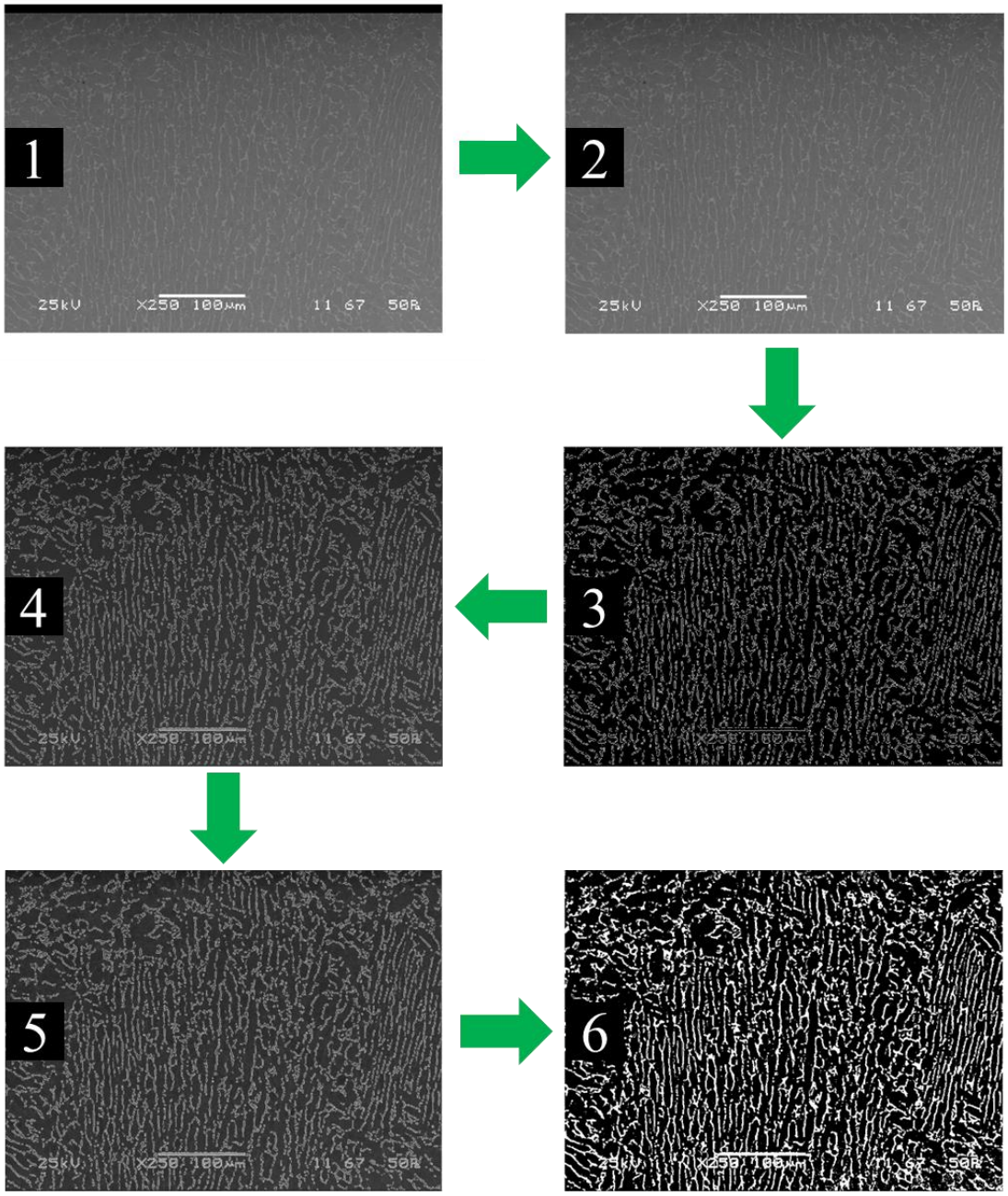

Figure 7.40 Image processing sequence for analysing microstructure below machined surface

As shown in figure 7.40(6), the annotations in the image are also in white colour which has been transformed into the binary image at the end of the stage 6. Thus, in order to prevent them affecting the analysis, the lower side of the images was cropped as illustrated in figure 7.41(7). In Matlab (MathWorks, 2013), images are presented in the form of an intensity matrix where each member of the matrix represents the intensity value of its corresponding pixel in the image. Since the image from stage 6 is a binary image, the members of the representing matrix are either 0 or 1. Each member of the matrix represents a 1 μm x 1 μm square of the material.

In stage 8, the average white pixel concentration (AWPC) for each 1 μm beneath the machined surface was calculated and plotted using the intensity matrix. As shown in figure 7.41, stage 8, the plotted data corresponding to AWPC indicated a highly noisy data. Thus, a moving average filter with span of 10 has been applied in order to smooth the data for AWPC (stage 9). Furthermore, a curve has been fitted to the filtered data to represent the trend of the AWPC beneath the machined surface (stage 10). Visual comparison of the curve generated for AWPC with microhardness below the machined surface implies that a reduction in the AWPC and therefore β phase has resulted in reduced microhardness below the machined surface. Figure 7.42 illustrates a comparison between the graph generated for microhardness with the curve fitted for AWPC for sample C1.

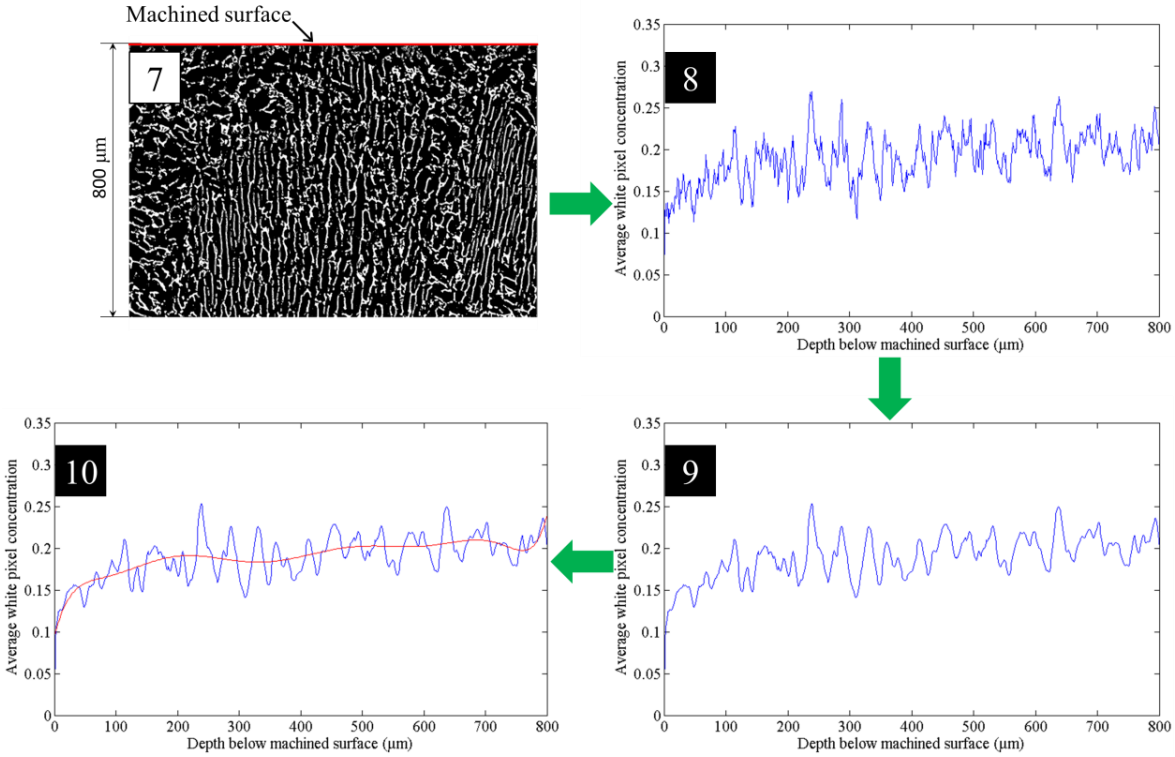

Figure 7.41 Sequence of analysis of processed images for microstructure below machined surface for experiment C1

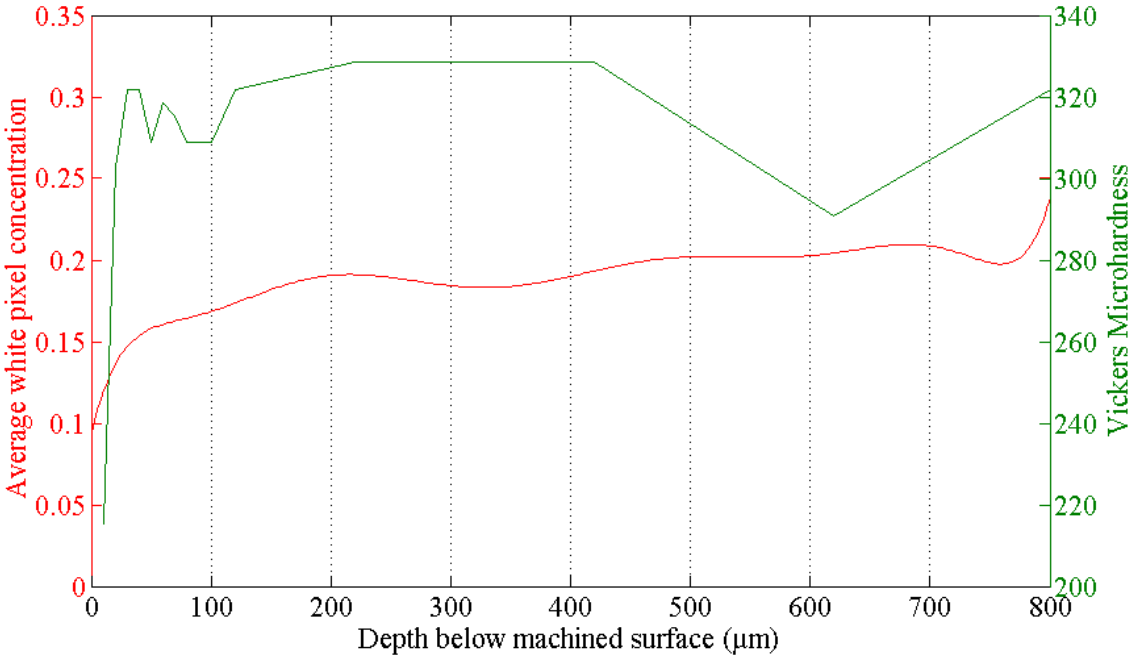

Figure 7.42 Graph of microhardness and average white pixel concentration in SEM images against depth below machined surface for experiment C1

Studying the graphs generated for AWPC against depth below the machined surface in figure 7.43, demonstrates that the AWPC and consequently β phase titanium increases as the depth below the machined surface increases. This indicates that cutting operation affects the concentration of β phase titanium irrespective of machining environment. As shown in figure 7.43, examining the AWPC graphs indicated that apart from the samples for experiment 6, the effect of machining on the microstructure of the material is shallower under cryogenic cooling as compared to dry and wet conditions. The depth of machining affected zones for different machining environments is shown with vertical lines in figure 7.43.

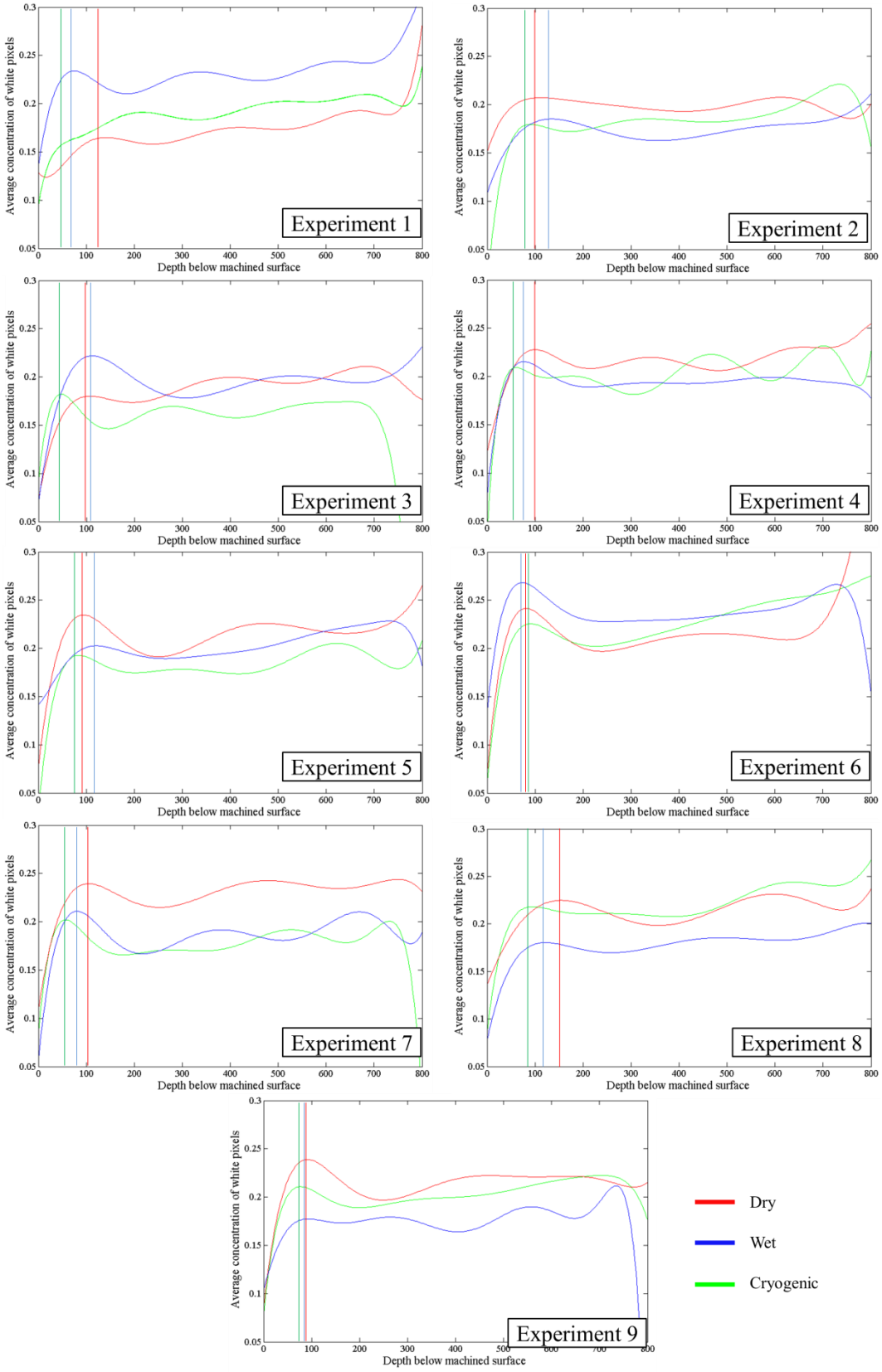

Figure 7.43 Results of image processing of SEM micrographs of material microstructure for each machining sample

7.6. Summary

In order to identify the boundaries of machining parameters, namely cutting speed, chip load and depth of cut, a set of machining trials were conducted. As a result, the minimum and maximum values of each parameter have been defined. As the optimum cutting parameters for cryogenic machining is unknown, these values together with a medium value were then used for the DoE. A Taguchi's L9 orthogonal array was used to generate a set of experiments which include a meaningful combination of cutting parameters. As the aim of this chapter is to evaluate the effect of cryogenic cooling on the machinability of Ti-6Al-4V alloy in comparison with dry and wet machining environments, the L9 design was repeated for each machining environment.

Three machinability metrics of surface roughness, power consumption and tool wear were selected to be analysed for each machining experiment. From the power consumption, PC/V and EC/V were calculated and three surface roughness parameters of Ra, Rz and Rq were measured. The cutting tools used for machining experiments were also examined microscopically and their flank wear was measured for further analysis. In addition, SEM images of machined surfaces were taken for surface integrity analysis. Furthermore, a cross sectional sample were prepared for each machining experiment for subsurface microstructural and microhardness analysis.

In order to analyse the results obtained from the machining experiments, Taguchi's SN ratio analysis was performed and the mean SN ratio graphs for each machining parameter were generated. The analysis indicated that eliminating the power consumption of coolant pump has a significant effect on reducing the power consumption, PC/V and EC/V making dry and cryogenic conditions the most favourable machining environments. A comparison between dry and cryogenic machining environments demonstrated that cryogenic cooling can increase the power consumption of the machine tool by an average of 1.45%, however this is not always statistically significant.

Analysis of mean SN ratio revealed that cryogenic cooling is the most favourable machining environment in order to achieve the lowest Ra, Rz and Rq surface roughness parameters. A similar conclusion was drawn from the analysis of the mean SN ratio for tool flank wear. However, although the tool flank wear is defined as the main tool life indicator, it cannot be directly concluded that cryogenic cooling increases tool life. Nevertheless, study of the flank wear and crater wear of the tools used for cryogenic

machining provides significant evidence that longer tool life can be achieved using cryogenic cooling in comparison with dry and wet machining.

In addition, study of SEM images of the machined surfaces, microstructure of the material and micro hardness suggested that cryogenic cooling potentially improves the surface integrity in end milling Ti-6Al-4V alloy. As mentioned previously, this study was performed using a range of machining parameters in the absence of knowledge on the optimum value of the cutting parameters. Thus, it is important to identify the specific cutting parameters where the desired machinability metrics is optimum. The next chapter will explain the activities to optimise these cutting parameters in cryogenic end milling of Ti-6Al-4V alloy.

Chapter 8

Optimisation of cutting parameters in cryogenic machining

8.1. Introduction

The comparative study of cryogenic cooling, provided in chapter 7, indicates that cryogenic cooling has significantly improved the machinability of Ti-6Al-4V as compared to dry and wet environments. As mentioned in chapter 6, cryogenic temperatures modify the material properties of the cutting tool and workpiece, thus the optimum cutting parameters are unknown. The aim of this chapter is to identify the optimum level of cutting parameters for cryogenic end milling. Two parameters of surface roughness and tool wear have been selected for optimisation. The optimisation process for surface roughness is limited to Ra. This is mainly due to the fact that Ra covers most of the surface characteristics required in industry (Petropoulos et al., 2009). In addition, it is the most known surface roughness parameter in industry and is particularly used in machining operations (Petropoulos et al., 2009).

The analysis of SN ratio for surface roughness and tool wear using the L9 DoE were both in agreement to suggest using 0.03 mm/tooth chip load to achieve lower tool wear and surface roughness. Furthermore, it is a common knowledge among machinists that increasing chip load has an adverse effect on both surface roughness and tool wear (Kirby, 2010). In this chapter, two input parameters of cutting speed and depth of cut are used for a DoE whilst keeping the chip load constant at 0.03 mm/tooth. Response surface methodology (RSM) is used to optimise the input parameters in order to minimise surface roughness and tool wear. RSM is a multi-disciplinary method using statistical and mathematical techniques to generate a graphical model between output and input parameters of a design (Montgomery, 2013).

In this chapter, a central composite DoE is generated to enable the optimisation of cutting speed and depth of cut and surface roughness and tool wear are identified as desirable outputs. A set of machining operations were conducted according to the DoE and the surface roughness and tool wear were measured for each machining experiment. The experimental data were modelled using RSM and regression. In order to identify the optimum value of the input parameters, simulated annealing was performed on the generated models. Finally, the computed values for optimisation were tested empirically.

The Ra and tool flank wear are referred to as surface roughness and tool wear in this chapter.

8.2. Design of experiments for optimisation

Central Composite Design (CCD) is the most prevalent type of DoE used for RSM optimisation which is known to be efficient for fitting quadratic models (Montgomery, 2013, Mason et al., 2003). CCD consists of a 2^k full factorial design, 2k axial or star points and n replications of a centre point. Since a 2^k full factorial design is included in a CCD, it provides a good approximation of the interactions between input parameters.

For the purpose of this research, a Face Centred Central Composite Design (FCCCD) with three centre points has been generated with two input parameters. Matlab's Model Based Optimisation toolbox (MathWorks, 2013) has been used to generate the DoE. A FCCCD has been generated by specifying two parameters of cutting speed (X_1) and depth of cut (X_2) with their respective boundaries. Figure 8.1 shows the position of the experimental points within the machining boundaries and the details of each machining experiment for the FCCCD are provided in table 8.1. As shown in figure 8.1 and detailed in table 8.1, the FCCCD used for this experiment consists of four points on the boundaries, four star points with $\alpha = 1$ and three replications at the centre which make 11 machining experiments altogether.

8.3. Methodology and data collection for Response Surface Methodology

Identical procedure used for comparative study, described in section 7.3, has been implemented for conducting the machining experiments following the DoE outlined in table 8.1. Eleven blocks of Ti-6Al-4V were prepared and similar cutting tools presented in section 7.2.2 were used for this set of experiments. Similar to comparative study and as outlined in section 7.3, 4 machining passes of 150 mm length were executed for each experiment. The immersion rate and tool's overhang were kept constant to 30% and 50 mm respectively for all the experiments.

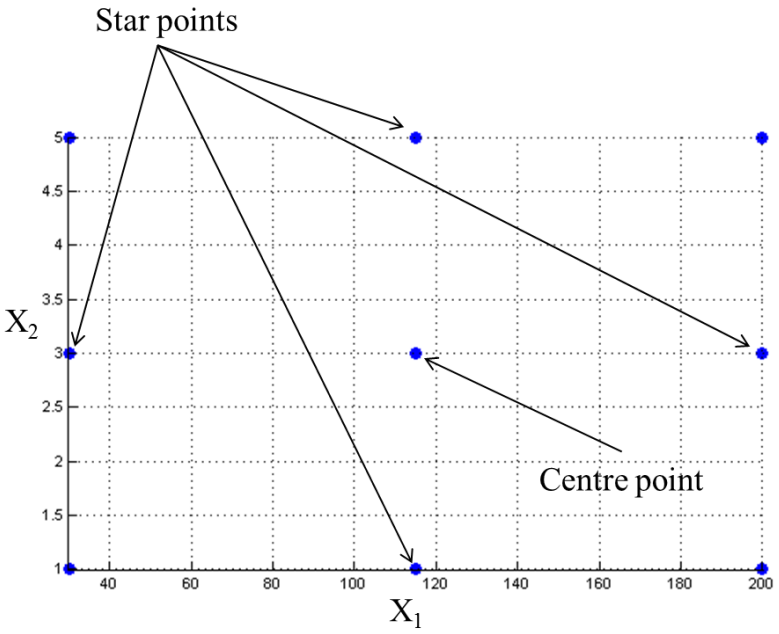

Figure 8.1 Visual presentation of the FCCCD generated for optimisation

Experiment	Cutting speed (m/min)	Depth of cut (mm)
1	30	1
2	200	1
3	30	5
4	200	5
5	30	3
6	200	3
7	115	1
8	115	5
9	115	3
10	115	3
11	115	3

Table 8.1 FCCCD for two input parameters of cutting speed and depth of cut

After the machining experiments, the tool wear and surface roughness for each machining experiment were measured as specified in sections 7.4.2 and 7.4.3 respectively. The arithmetic surface roughness (Ra) was selected to present the surface roughness for each machining experiment and was used for optimisation. The collected data for each machining experiment is presented in table 8.2.

Experiment	Surface roughness Ra (µm)	Tool flank wear (µm)
1	0.639	16.8
2	0.463	60.4
3	0.871	22
4	0.574	10.4
5	0.794	18.9
6	0.613	34.3
7	0.495	40.9
8	0.663	18.7
9	0.593	27.7
10	0.605	25.3
11	0.563	26

Table 8.2 Surface roughness and tool wear of the optimisation experiments

8.4. Data Evaluation

One of the assumptions for most of statistical analysis techniques such as ANOVA and regression is that the data is normally distributed. Shapiro-Wilk test is one of the most powerful methods of checking data for normality (Mason et al., 2003). Thus, Shapiro-Wilk statistic (W) for surface roughness and tool wear was calculated. As shown in table 8.3, W for both surface roughness and tool wear is larger than Shapiro-Wilk critical value at 5% and 1% significance level. In addition, the normal probability plots for surface roughness and tool wear were generated as provided in figures 8.2 and figure 8.3 respectively. Considering the result of Shapiro-Wilk test and visual inspection of the normal probability plots depicted in figures 8.2 and 8.3, the hypothesis of normally distributed data cannot be rejected and it can be concluded that the data for both surface roughness and tool wear are normally distributed.

Data	W	Shapiro-Wilk critical value	
		5%	1%
Surface roughness (Ra)	0.9182	0.8500	0.7920
Tool wear	0.8854	0.8500	0.7920

Table 8.3 Shapiro-Wilk analysis for normality of the data for surface roughness and tool wear

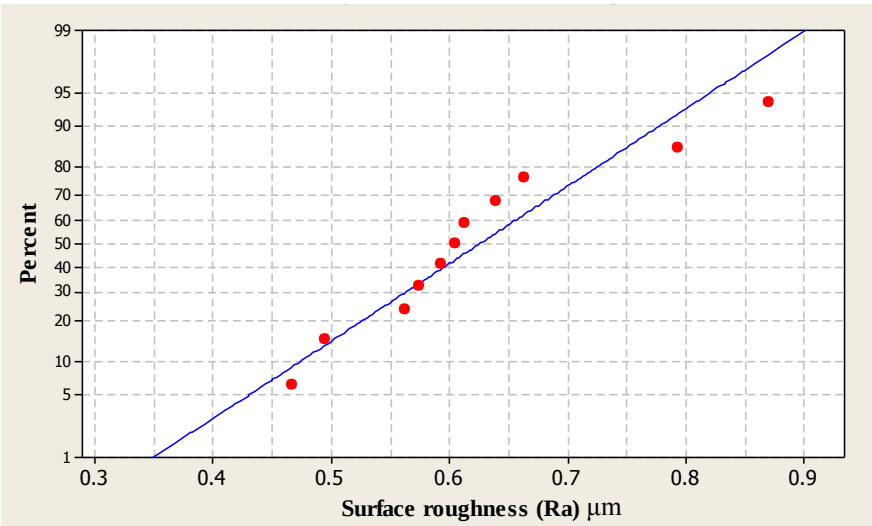

Figure 8.2 Normal probability plot of surface roughness

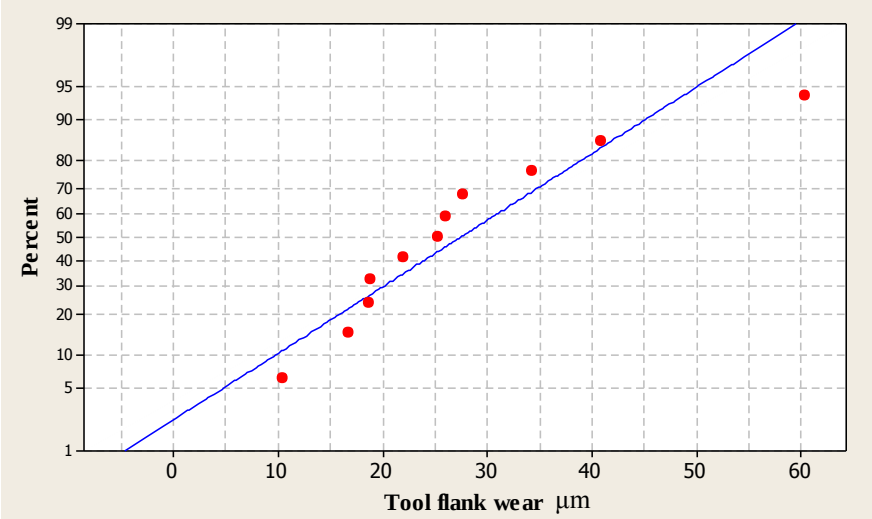

Figure 8.3 Normal probability plot of tool flank wear

In addition to normality, both datasets were tested for outliers. Grubbs test for outliers (Mason et al., 2003) was performed on the data and the Z value was calculated for each measured value of surface roughness and tool wear. The results of the Grubbs test are provided in table 8.4. From the tables (Mason et al., 2003), the critical Z value for 11 samples is 2.3547 at 5% significance level and 2.5641 at 1% significance level. Therefore, any Z value larger than critical Z indicates the presence of an outlier. Considering the values given in table 8.4, the Z value for the tool wear of experiment 2 indicates an outlier at 5% significance level. Since there is not enough evidence at 1% significance level, the tool wear in experiment 2 needs to be treated cautiously for regression modelling using instructions provided by Mason et al. (2003).

Experiment ID	Surface roughness		Tool wear	
	Measured (µm)	Z	Measured (µm)	Z
1	0.639	0.078	16.8	0.768
2	0.463	1.288	60.4	2.392
3	0.871	2.066	22	0.391
4	0.574	0.426	10.4	1.232
5	0.794	1.282	18.9	0.616
6	0.613	0.124	34.3	0.5
7	0.495	1.040	40.9	0.978
8	0.663	0.265	18.7	0.631
9	0.593	0.279	27.7	0.022
10	0.605	0.186	25.3	0.152
11	0.563	0.512	26	0.101

Table 8.4 Results of the Grubbs test for outliers for surface roughness and tool wear datasets

8.5. RSM analysis for surface roughness and tool wear in cryogenic end milling

RSM is a combination of mathematical and statistical techniques where an output variable known as response is affected by one or a combination of factors known as input parameters. The objective of RSM is to optimise the response by varying the input parameters (Montgomery, 2013).

In RSM, the response is modelled mathematically and defined as a function of input parameters and an error. For the purpose of this research, the responses can be expressed as:

$$y_1 = f_{(x_1,x_2)} + \epsilon_1$$

$$y_2 = f_{(x_1,x_2)} + \epsilon_2$$

where y_1 is surface roughness, y_2 is tool wear, x_1 is cutting speed, x_2 is depth of cut and ϵ_1 and ϵ_2 represent the error observed in response as compared to the measured results.

Consequently, $\mu_1 = f_{(x_1,x_2,x_3)}$ and $\mu_2 = g_{(x_1,x_2,x_3)}$ represent the response surfaces for surface roughness and tool wear. Since in most cases, the form of the relation between response and input parameters are unknown, usually a low order polynomial function is employed for approximation (Montgomery, 2013). Since the FCCCD used for this research consists of nine different combinations of input parameters and three replications, a full-quadratic model as shown below is used for mathematical modelling to represent the responses as a function of the input parameters.

$$y = a_1x_1 + a_2x_2 + b_1{x_1}^2 + b_2{x_2}^2 + cx_1x_2 + d$$

where a_1, a_2, b_1, b_2 and c are coefficients and d is a constant.

The Minitab statistical software package (Minitab Inc., 2010) was used to calculate the models' coefficients and constants. Table 8.5 illustrates the values of coefficients and constants for surface roughness and tool wear models. As shown in figure 8.4 and 8.5, the normal probability plots of the residuals were generated for surface roughness and tool wear models respectively. The plots indicate that the residuals are normally distributed for both tool wear and surface roughness, however the residuals for tool wear are slightly skewed from the centre.

Coefficient	Surface roughness	Tool wear
a_1	-0.00346	0.372661
a_2	0.120982	0.657224
b_1	1.19E-05	-0.000157
b_2	-0.0096	0.515789
C	-1.83824E-04	-0.0811765
D	0.626781	7.51179

Table 8.5 Coefficients of the models for surface roughness and tool wear

In addition, the graphs of observed vs fitted values were generated for surface roughness and tool wear as depicted in figures 8.6 and 8.7 respectively. Visual examination of the figures does not imply any pattern in the residuals.

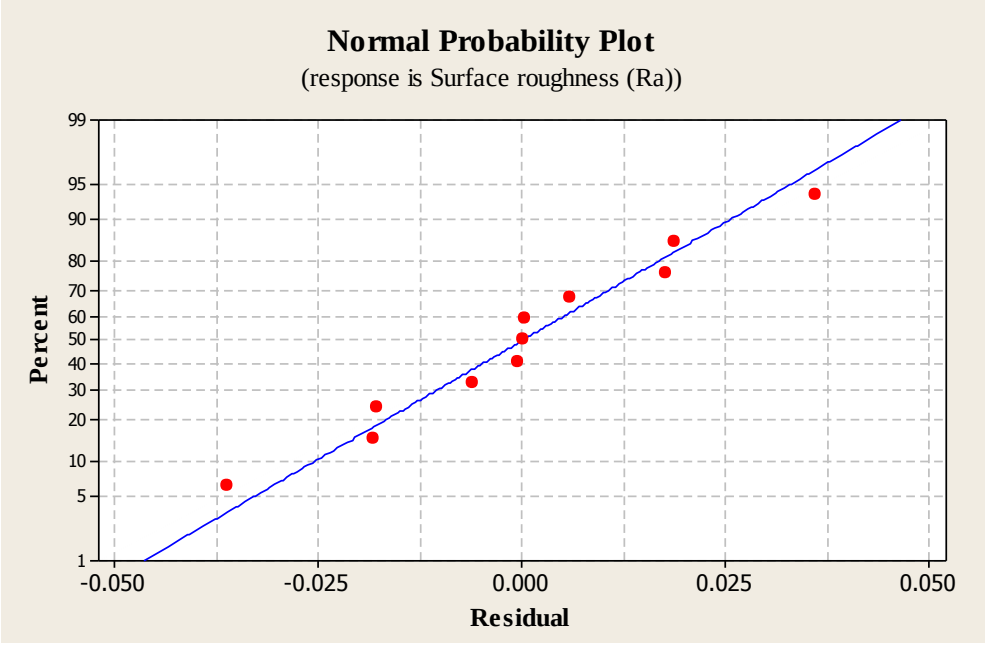

Figure 8.4 Normal probability plot of the residuals of the model for surface roughness

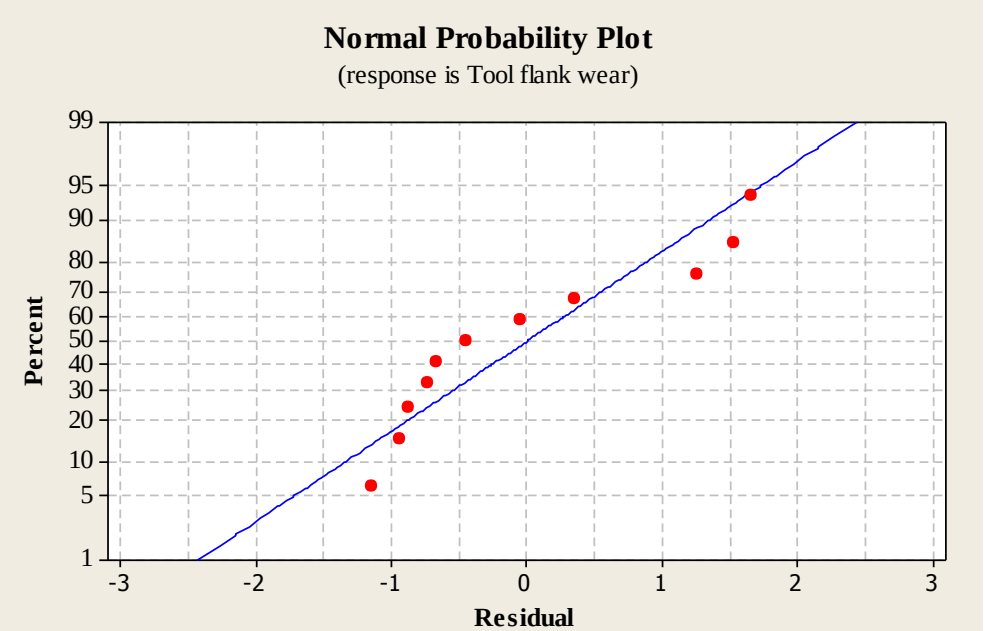

Figure 8.5 Normal probability plot of the residuals of the model for tool wear

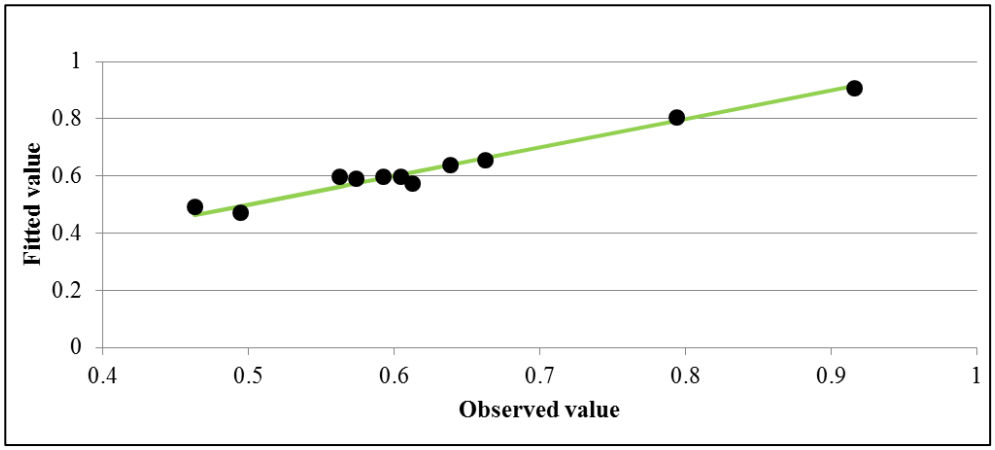

Figure 8.6 Observed vs fitted values graph for surface roughness

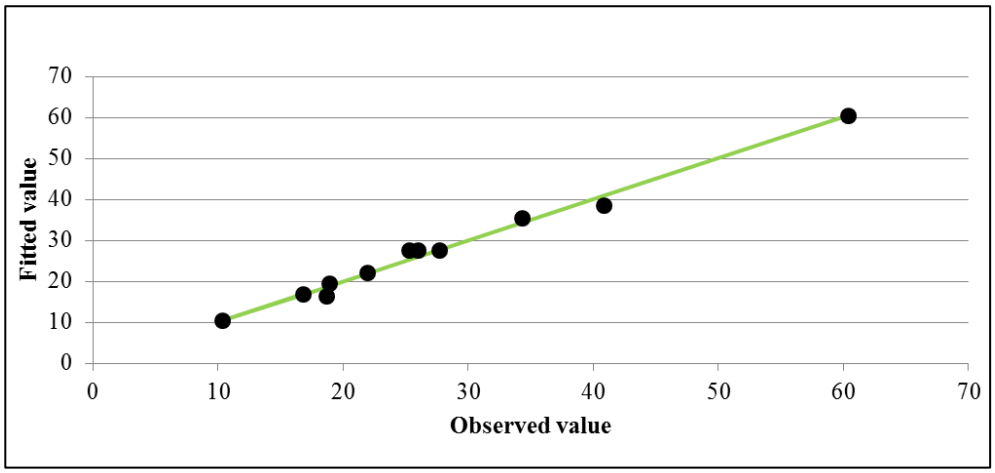

Figure 8.7 Observed vs fitted values graph for tool wear

Furthermore, the coefficient of determination (R^2) and predicted coefficient of determination (predicted R^2) values were computed for both models. R^2 is calculated by dividing the sum of squares of the regression model by the total sum of squares whilst predicted R^2 is calculated from predicted sum of squares (Minitab Inc., 2010). The results of the computations are provided in table 8.6. R^2 shows how a model fits the observed data whilst the predicted R^2 indicates the predicting ability of a model. As shown in table 8.6, both models for surface roughness and tool wear reasonably fit the data. In addition, predicted R^2 shows that the models are capable of predicting surface roughness and tool wear to 81% and 98% respectively. The analysis demonstrates that since there is a close agreement between the R^2 and predicted R^2 for both models, the models are not over-fitting the data.

R^2	**Surface roughness**	**Tool wear**
Actual	97.16%	99.60%
Predicted	81.50%	98.05%

Table 8.6 Model evaluation statistics for surface roughness and tool wear

ANOVA was performed on the data to identify the significance of each input parameters and their interactions for modelling. As the ANOVA for surface roughness (Table 8.7) shows, the P-value of the regression model is significantly less than 0.01 which indicates that there is not enough evidence to reject the validity of the model by 99% confidence. Furthermore, the calculated P-value for the second order of depth of cut and interaction between cutting speed and depth of cut is higher than 0.05 and less than 0.1. Thus, the effects of these interactions on surface roughness are not as significant as the main effects and the second order of cutting speed.

Pareto ANOVA is a simplified ANOVA, which does not require the F-test to be performed and has previously been used by researchers (Ghani et al., 2004, Palanikumar, 2006) to identify the contribution percentage of parameters on the desired quality measures. In this method the sum of squares of the results obtained for each parameter is used to identify its contribution percentage.

As shown in figure 8.8, the Pareto ANOVA of the results for surface roughness reveals that cutting speed, depth of cut and the second order of cutting speed contribute to more than 90% of the surface roughness.

	DF	SS	MS	F	P
Regression	5	0.136596	0.027319	34.17	0.001
Linear	2	0.113258	0.056629	70.84	0.000
Cutting speed	1	0.070417	0.070417	88.08	0.000
Depth of cut	1	0.042841	0.042841	53.59	0.001
Square	2	0.019432	0.009716	12.15	0.012
Cutting speed^2	1	0.015698	0.018782	23.49	0.005
Depth of cut^2	1	0.003735	0.003735	4.67	0.083
Interaction	1	0.003906	0.003906	4.89	0.078
Cutting speed*Depth of cut	1	0.003906	0.003906	4.89	0.078
Residual errors	5	0.003997	0.000799		
Lack of fit	3	0.003061	0.001020	2.18	0.330
Pure error	2	0.000936	0.000468		
Total	10	0.140594			

Table 8.7 Results of ANOVA for surface roughness

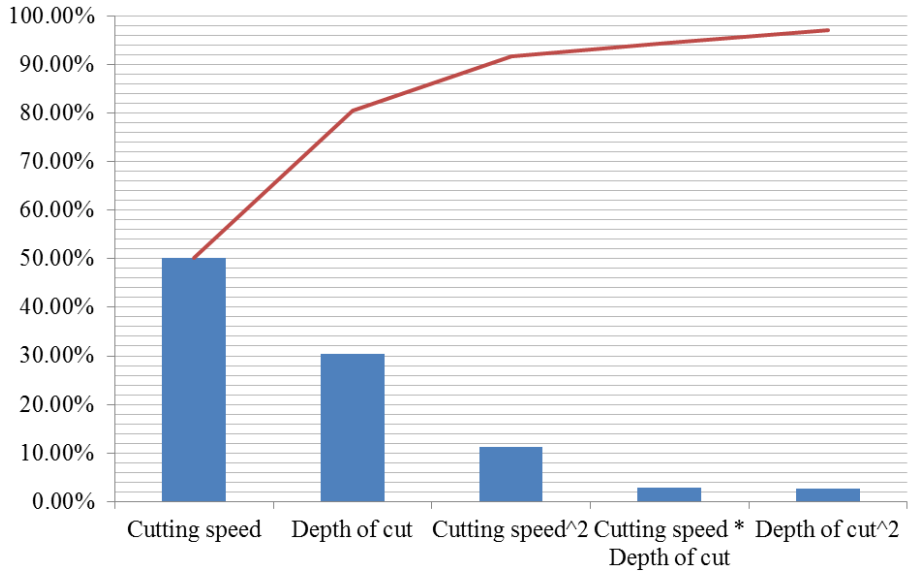

Figure 8.8 Pareto ANOVA graph of the data collected for surface roughness

Similar to surface roughness, ANOVA was performed on the data collected for tool wear. As shown in table 8.8, the analysis indicates that there is no evidence to reject the validity of the developed model for tool wear within the selected range of input parameters. The ANOVA for tool wear, given in table 8.8, shows that the P-value for the second order of cutting speed is significantly higher than 0.05 and thus its effects on the tool wear is very small. The Pareto ANOVA graph for tool wear, illustrated in figure 8.9, indicates that the interaction between cutting speed and depth of cut is the most significant parameter affecting tool wear being followed closely by depth of cut. Altogether, these parameters and cutting speed contribute to almost 98% of tool wear.

	DF	SS	MS	F	P
Regression	5	1896.11	379.222	247.17	0.000
Linear	2	1122.63	561.313	365.86	0.000
Cutting speed	1	374.46	374.460	244.07	0.000
Depth of cut	1	748.17	748.167	487.64	0.000
Square	2	11.72	5.861	3.82	0.098
Cutting speed^2	1	0.94	3.274	2.13	0.204
Depth of cut^2	1	10.78	10.783	7.03	0.045
Interaction	1	761.76	761.760	496.50	0.000
Cutting speed*Depth of cut	1	761.76	761.760	496.50	0.000
Residual errors	5	7.67	1.534		
Lack of fit	3	4.62	1.542	1.01	0.532
Pure error	2	3.05	1.523		
Total	10	1903.78			

Table 8.8 Results of ANOVA for tool wear

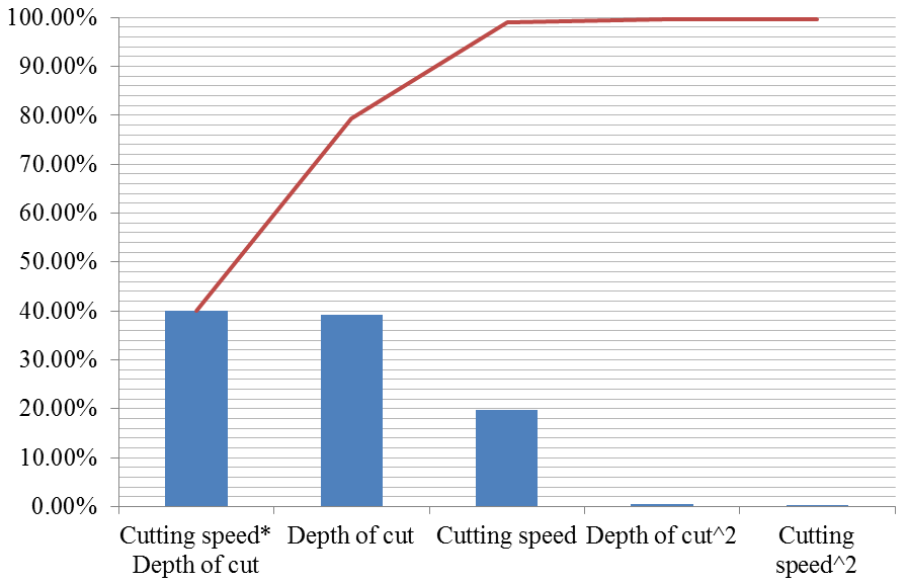

Figure 8.9 Pareto ANOVA graph of the data collected for tool wear

In order to improve predicted R^2 for both models and following the recommendations from ANOVA, the inputs with the least significance were removed from the models and R^2 and predicted R^2 were calculated for new models. This analysis revealed that in order to achieve the highest fitting and prediction of quality for both models, full quadratic model with all interactions should be considered. As a result, the final models for surface roughness and tool wear are:

$$Surface\ roughness = -0.00346\,X_1 + 0.120982\,X_2 + 0.0000119\,{X_1}^2 - 0.0096\,{X_2}^2 - 0.000183824\,X_1X_2 + 0.626781$$

$$Tool\ wear = 0.372661\,X_1 + 0.657224\,X_2 - 0.000157348\,{X_1}^2 + 0.515789\,{X_2}^2 - 0.0811765\,X_1X_2 + 7.51179$$

where $X_1$is cutting speed and X_2 is depth of cut.

8.6. Optimisation of cutting parameters for cryogenic end milling

As mentioned previously, the aim of RSM is to generate a graphical representation of an output based on the input parameters. Thus, Matlab (MathWorks, 2013) was employed to generate 3-dimensional graphs of surface roughness and tool wear based on input parameters of cutting speed and depth of cut. As shown in figure 8.10, the generated models for surface roughness and tool wear were defined as functions in Matlab (MathWorks, 2013). In addition, the response surfaces representing the functions for surface roughness and tool wear were generated within the machining boundaries using Matlab's surface generator (MathWorks, 2013) as shown in figures 8.11 and 8.12 respectively.

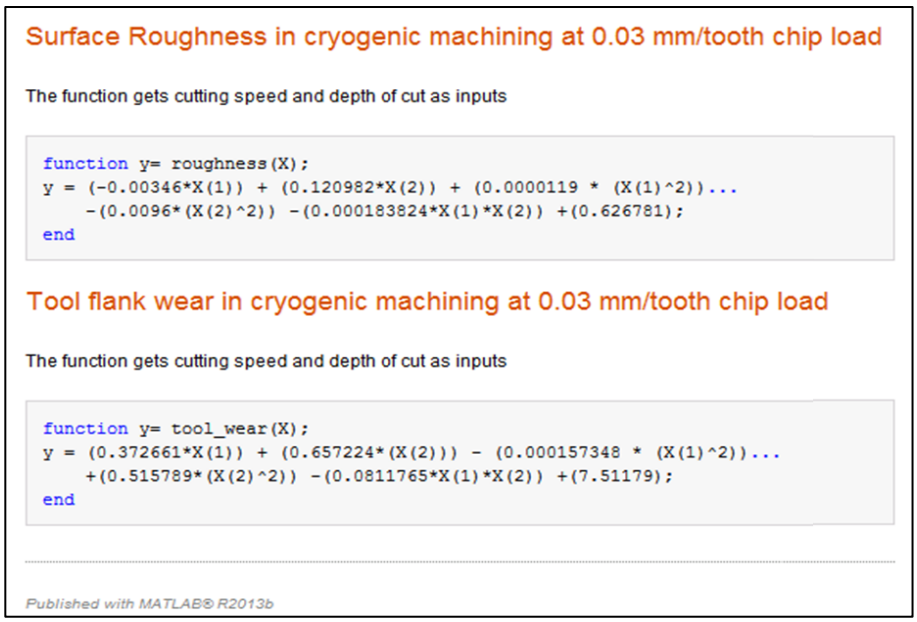

Surface Roughness in cryogenic machining at 0.03 mm/tooth chip load

The function gets cutting speed and depth of cut as inputs

```
function y= roughness(X);
y = (-0.00346*X(1)) + (0.120982*X(2)) + (0.0000119 * (X(1)^2))...
    -(0.0096*(X(2)^2)) -(0.000183824*X(1)*X(2)) +(0.626781);
end
```

Tool flank wear in cryogenic machining at 0.03 mm/tooth chip load

The function gets cutting speed and depth of cut as inputs

```
function y= tool_wear(X);
y = (0.372661*X(1)) + (0.657224*(X(2))) - (0.000157348 * (X(1)^2))...
    +(0.515789*(X(2)^2)) -(0.0811765*X(1)*X(2)) +(7.51179);
end
```

Published with MATLAB® R2013b

Figure 8.10 Generated functions in Matlab (MathWorks, 2013) for surface roughness and tool wear

As shown in figure 8.11, the highest surface roughness is produced at low cutting speed (30 m/min) and 5 mm depth of cut. Reducing the depth of cut results in reduction in surface roughness whilst better surface roughness is produced at higher cutting speeds.

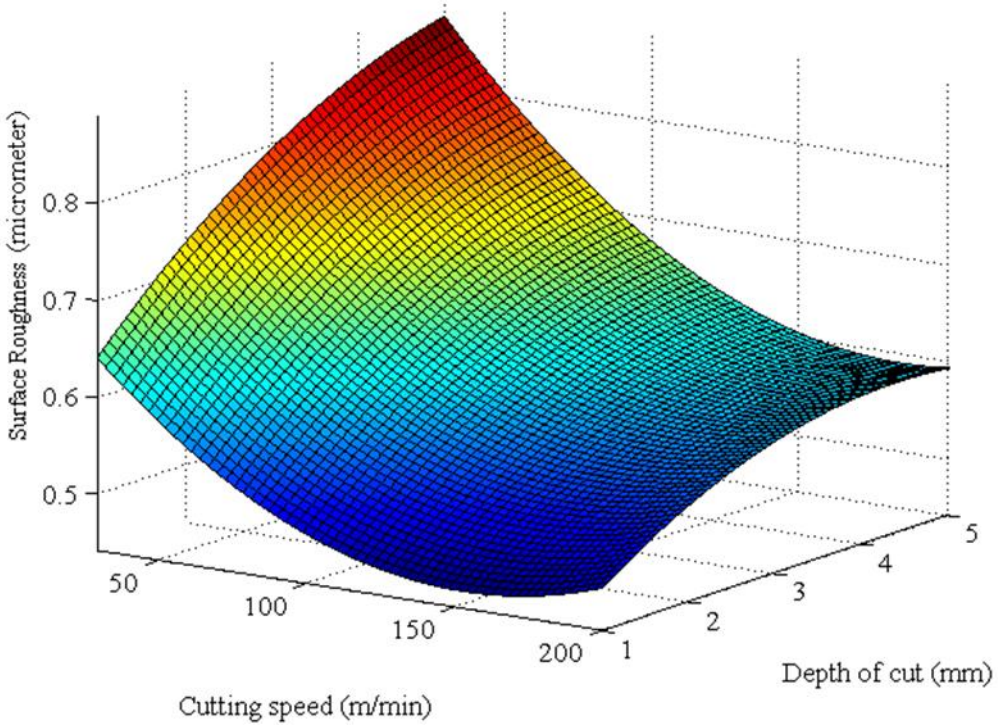

Figure 8.11 Response surface of surface roughness as a function of cutting speed and depth of cut

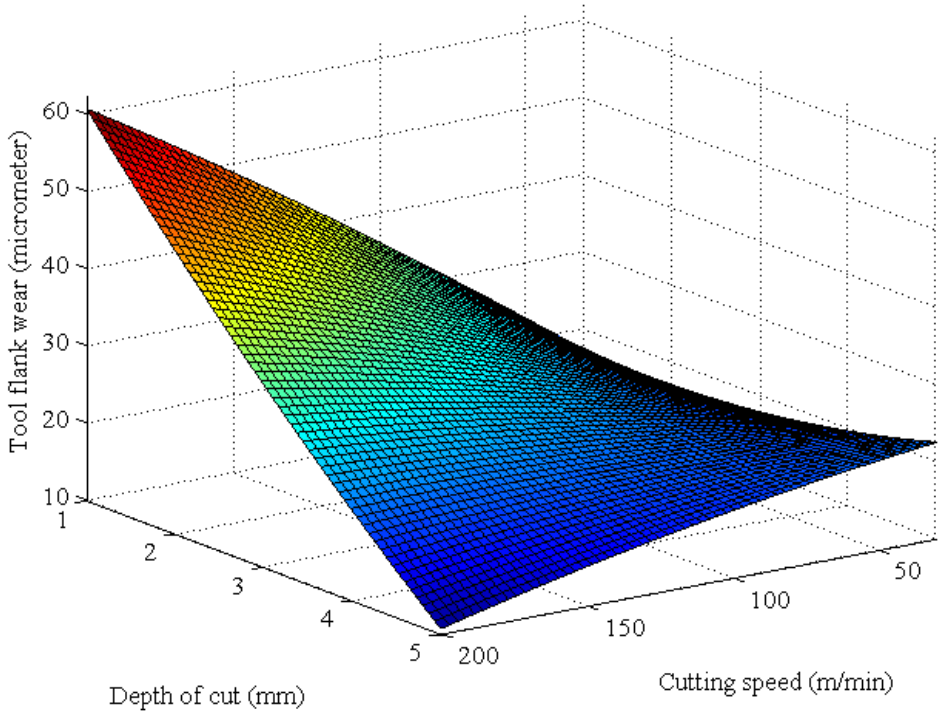

Figure 8.12 Response surface of tool wear as a function of cutting speed and depth of cut

Analysing the response surface graph generated for tool wear shows that lower tool wear is produced where cutting speed and depth of cut both are either minimum or maximum. This reflects the importance of interaction between cutting speed and depth of cut as outlined in chapter 8.6. Since recognising more precise values of optimum cutting parameters is difficult from the graphs, Simulated annealing (SA) was used to identify the values of cutting speed and depth of cut where surface roughness and tool wear are minimum.

Simulated annealing technique is a probabilistic metaheuristic method for optimisation which resembles the cooling of metals in annealing processes to find the minimum value of a given function (Asokan et al., 2003, Mukherjee and Ray, 2006, Chandrasekaran et al., 2010). SA uses a temperature parameter using the concept of Boltzmann probability distribution for energy (Yang et al., 2009). According to this, the energy of a thermal equilibrium at a given temperature (T) is probabilistically distributed as:

$$P(E) = \exp(-\frac{E}{KT})$$

Where E is energy and K is Boltzmann constant (Yang et al., 2009)

SA uses a single point search method and has been used extensively in machining operation optimisation problems (Mukherjee and Ray, 2006, Yang et al., 2009, Khan et al., 1997, Asokan et al., 2003, Wang et al., 2005, Venkata Rao and Pawar, 2010, Chandrasekaran et al., 2010). In SA, the algorithm starts with an initial starting point (x_1) and assumes a high temperature for the process (T). A Gaussian distribution is then used to randomly produce the second point (x_2) in the vicinity of the starting point and thus the value of the function is calculated. The difference between the values of the function between these points is computed and it is assumed that this difference is analogous to the difference in energy level (ΔE). If the function value of the second point is smaller than the initial value, the second point replaces the initial point. On the other hand if the second point has a larger function value than the initial point, it replaces the initial point with a probability of $\exp(-\Delta E/T)$. This process is repeated until a sufficiently small temperature has been found or the changes in the function value become insignificant (Chandrasekaran et al., 2010, Yang et al., 2009, Asokan et al., 2003).

In order to proceed with SA optimisiation for surface roughness, a SA function was generated using Matlab's Optimisation Tool (MathWorks, 2013) as shown in figure 8.13. The SA function requires three 2-dimensional row vector inputs of (i) starting point, (ii) lower boundaries and (iii) upper boundaries. The first member of each vector represents cutting speed whilst the secnd member represnts the depth of cut.

In order to perform the SA for surface roughness the a combination of cutting speed and depth of cut were used as the starting point for optimisation. The optimisation process stops when the average change in the value of surface roughness function becomes less than $1e^{-6}$ in 1000 iterations. The SA optimisation was performed and the function value was plotted for each iteration as illustrated in figure 8.14. The optimisation process was repeated 9 times using different starting points. As shown in table 8.9, the minimum surface roughness is predicted to be 0.459 at the cutting speed of 152 m/min and 1 mm depth of cut.

Simulated annealing code for minimising surafce roughness

The programme requires (i) an starting point, (ii) lower limit of the cutting speed and depth of cut and (iii) the upper limit of cutting speed and depth of cut as inputs.

```
function [x,fval,exitflag,output] = SA_roughness(Start,Lower_bound,Upper_bound)
% Deffult options
options = saoptimset;
% Set Boltzmann anealing function
options = saoptimset(options,'AnnealingFcn', @annealingboltz);
% No hybrid function
options = saoptimset(options,'HybridInterval', 'end');
% Plot surface roughness value
options = saoptimset(options,'PlotFcns', { @saplotf });
[x,fval,exitflag,output] = ...
    simulannealbnd(@roughness,Start,Lower_bound,Upper_bound,options);
```

Figure 8.13 Matlab code for SA of surface roughness

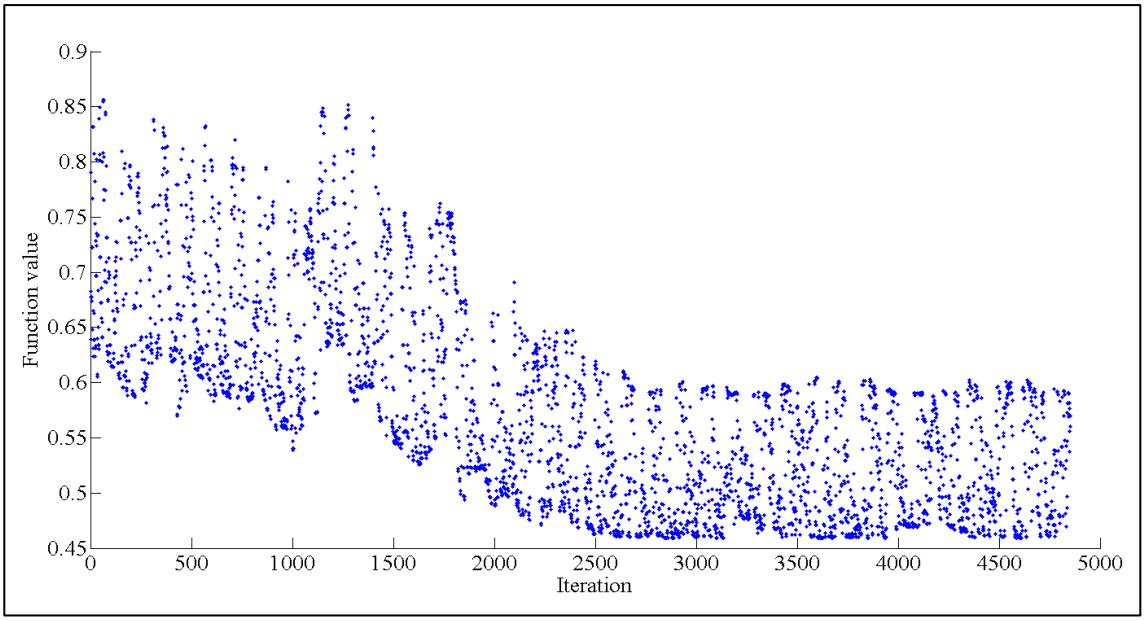

Figure 8.14 Surface roughness for each iteration during SA optimisation

A similar procedure to surface roughness was used to optimise the cutting parameters for tool wear using SA. Figure 8.15 illustrates the calculated values of tool wear at different iterations during optimisation process. Different starting points were used and the optimisation process was repeated 9 times. As shown in table 8.10, the optimisation process recommended using 200 m/min cutting speed and 5 mm depth of cut in order to achieve the lowest tool wear of 10.75 μm.

Starting point	Iterations	Calculated Ra	Cutting speed	Depth of cut
[30 1]	4852	0.45923	152.49	1.00
[200 1]	4902	0.45928	151.57	1.00
[30 3]	4206	0.45923	152.87	1.00
[200 3]	2378	0.45961	147.74	1.00
[30 5]	3231	0.45940	149.59	1.00
[200 5]	1717	0.45923	152.53	1.00
[115 1]	2483	0.47946	111.87	1.00
[115 3]	2932	0.45923	153.01	1.00
[115 5]	1853	0.46403	133.02	1.00

Table 8.9 Results of SA optimisation for surface roughness at different starting points

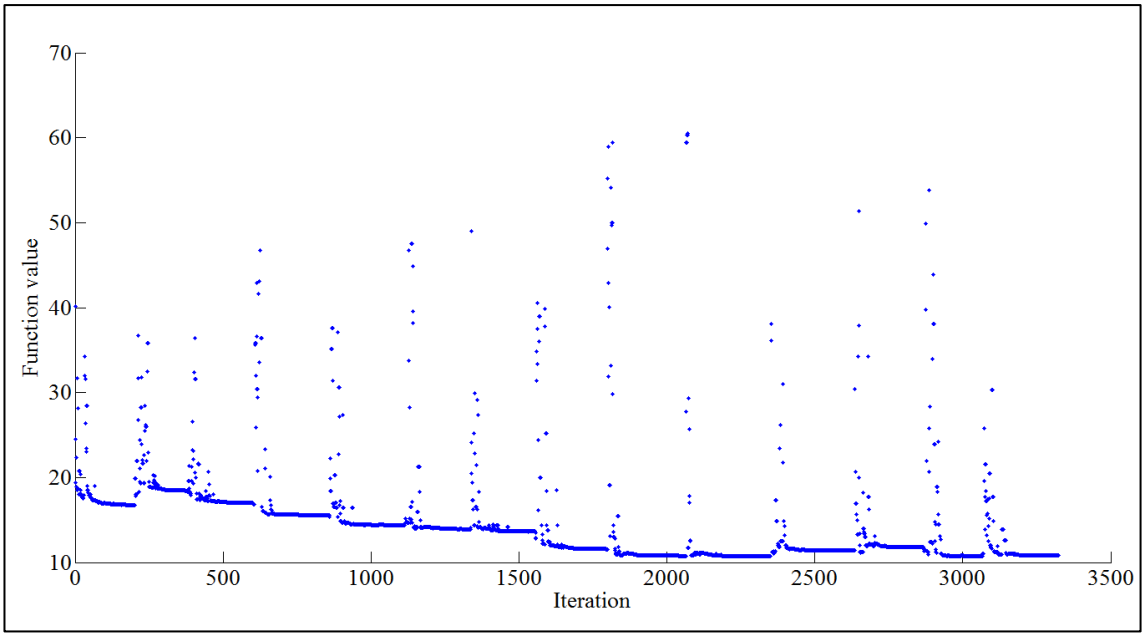

Figure 8.15 Tool wear for each iteration during SA optimisation

Starting point	Number of iterations	Tool wear	Cutting speed	Depth of cut
[30 1]	1972	17.02	30.00	1.72
[200 1]	1121	10.75	200.00	5.00
[30 3]	3317	12.47	181.59	5.00
[200 3]	1121	10.75	200.00	5.00
[30 5]	1155	17.02	30.00	1.68
[200 5]	1000	10.75	200.00	5.00
[115 1]	3323	10.75	200.00	5.00
[115 3]	3323	10.75	200.00	5.00
[115 5]	3311	12.88	177.09	5.00

Table 8.10 Results of SA optimisation for tool wear at different starting points

In addition to individual RSM graphs for each of the machinability metrics, an overlaid counter plot of surface roughness and tool wear was generated by defining the boundaries of accepted values for surface roughness and tool wear. According to the funding body of the project, the desired surface roughness (Ra) is to be less than 0.8µm. Thus, the boundaries of machining were defined as:

- Surface roughness

  Min: 0.4 µm; Max: 0.8 µm;

- Tool wear

  Min: 10 µm; Max: 15 µm.

The overlaid contour plot for surface roughness and tool wear illustrated in figure 8.16 and considering the results of optimisation for surface roughness and tool wear showed that in order to achive minimum tool wear whilst the surface roughness is kept below 0.8 μm, cutting speed of 200 mm/min and 5 mm depth of cut are optimum.

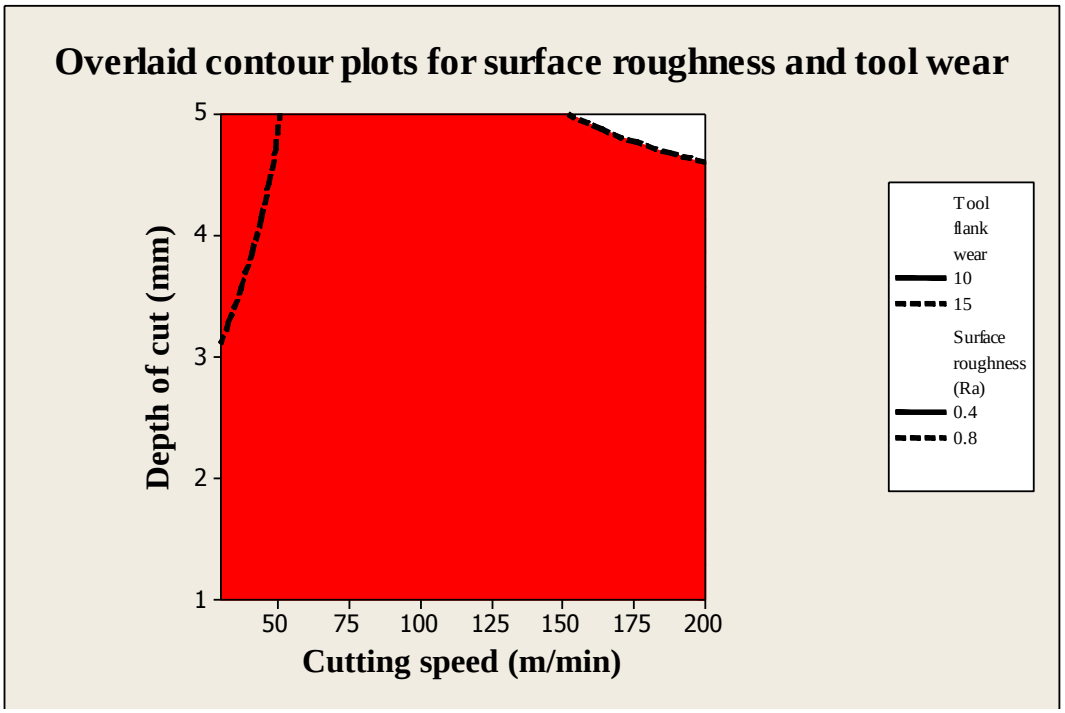

Figure 8.16 Overlaid contour plot of surface roughness and tool wear

8.7. Confirmation experiments of the optimised machining parameters

In order to confirm the correctness of the optimised value of cutting parameters for surface roughness and tool wear, the parameters should be tested empirically. The recommended values of cutting parameters for surface roughness and tool wear based RSM and SA are summarised in table 8.11. Based on these cutting parameters, two machining experiments were conducted to examine the correctness of the predicted values.

	First experiment	Second experiment
Optimisation objective	Surface roughness Ra	Tool flank wear
Cutting speed (m/min)	152	200
Spindle speed (rpm)	4032	5305
Chip load (mm/tooth)	0.03	0.03
Feed rate (mm/min)	362.87	477.46
Depth of cut (mm)	1	5

Table 8.11 Cutting parameters of the machining experiments for optimisation

8.7.1. Machining experiment for surface roughness

Following the methodology described in sections 7.3.2, a block of Ti-6Al-4V titanium was prepared and set up for machining experiment. The cutting parameters for the first machining experiment, shown in table 8.11, were used to machine four machining passes using a new unworn cutting tool with the specifications defined in section 7.2.2.

The machined block was cleaned using distilled water and acetone and the surface roughness of the machined passes was measured following the prescriptions given in section 7.4.3. The average surface roughness was calculated for each machining pass which are provided in table 8.12.

Machining pass	Surface roughness Ra
1	0.449
2	0.469
3	0.489
4	0.495

Table 8.12 Average surface roughness Ra for each machining pass of the first machining experiment

The predicted value of surface roughness for the first machining pass was 0.459 μm using the model developed for surface roughness. The machining experiment for surface roughness indicated that the average surface roughness for the first machining pass using the optimised cutting parameters is 0.449 μm. This reveals that the predicted values are offset from the measured value by 2.2%.

In addition, the cutting tool used for the experiment was examined using a tool makers' microscope. The tool wear was measured to be 45.8 μm which is 7% less than the predicted value.

8.7.2. Machining experiment for tool wear

The procedures provided in sections 7.3.2 was followed using the cutting parameters for second machining experiment (table 8.11) to conduct the machining experiment for tool wear. In addition, after the first four machining passes, the machining operations was continued in order to define the tool life. The machining process was interrupted at different intervals in order to measure the tool wear. The images of the cutting tool are illustrated in figure 8.17 and the number of machining passes when the image was taken is

provided on the corresponding picture. In addition, the tool wear was measured during the machining and is plotted against machining length as shown in figure 8.18.

In addition to tool wear, the surface roughness of the first four machining passes was measured and is plotted in figure 8.19. As figure 8.19 demonstrates, the surface roughness has slightly increased from the first machining pass to the fourth machining pass.

Comparison of the measured and predicted values for tool wear and surface roughness showed that the measured tool wear and surface roughness are 6.9% and 3% less than the predicted values respectively.

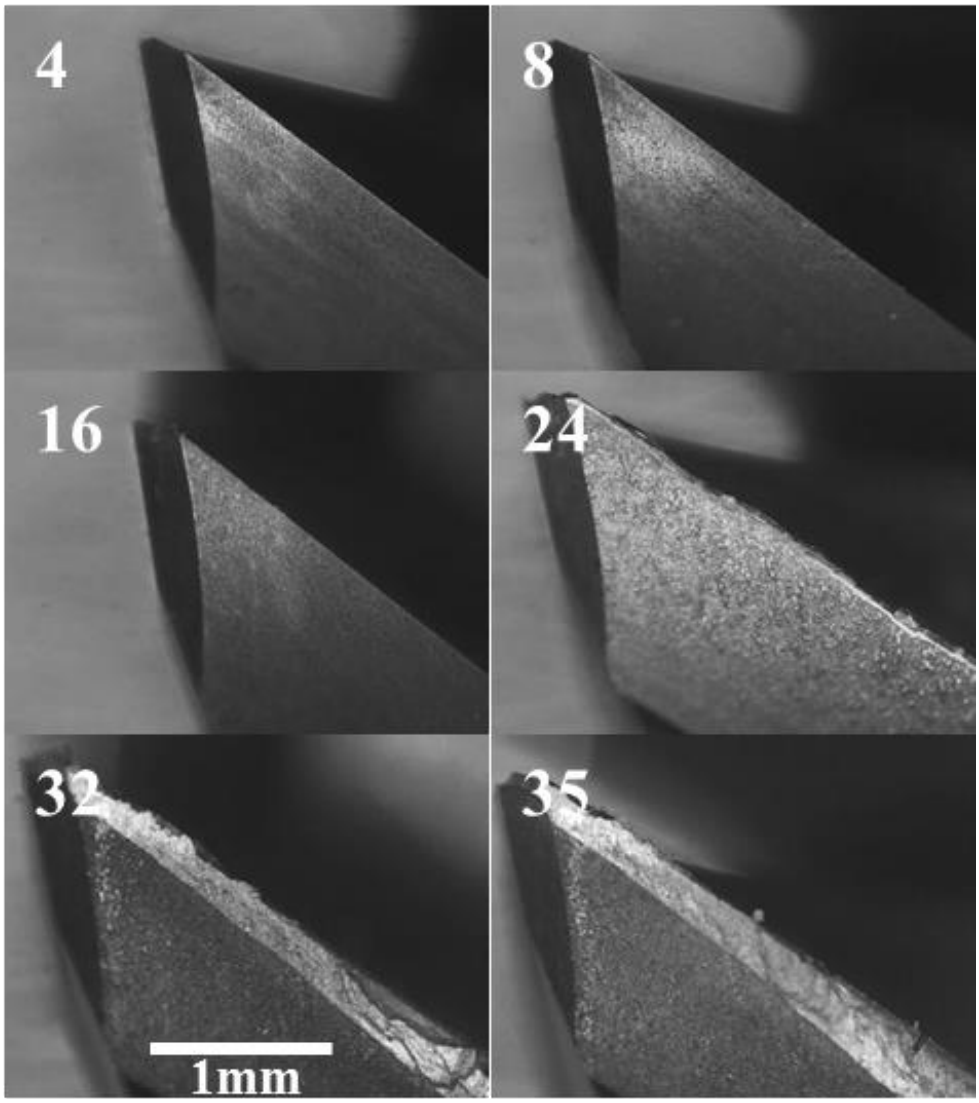

Figure 8.17 Microscopic images of the cutting tool used for confirmation experiment for tool wear

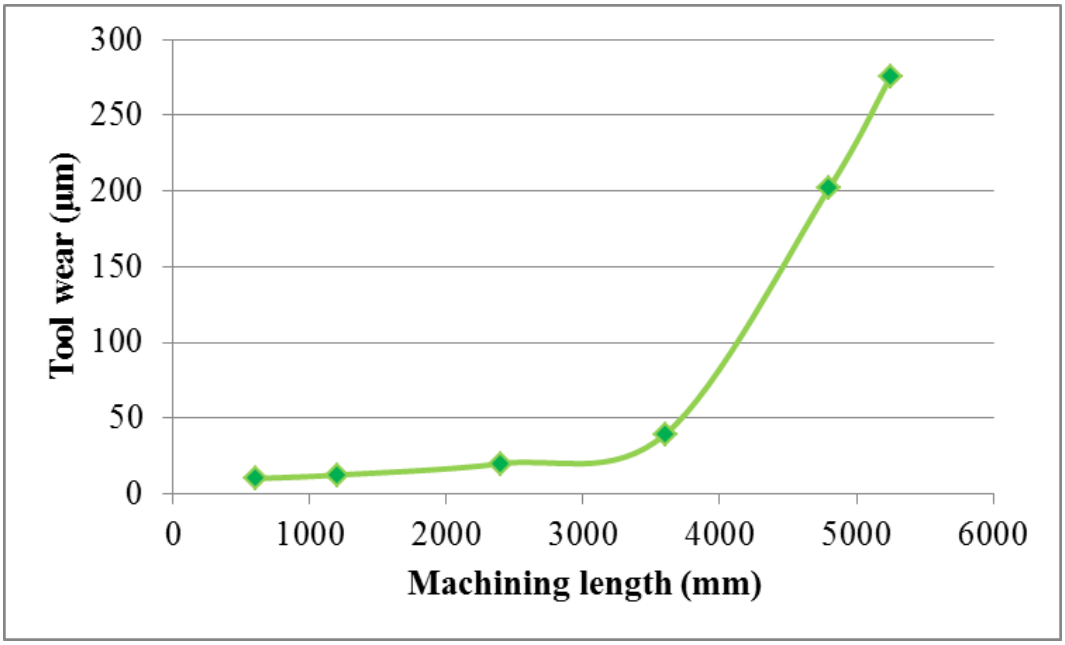

Figure 8.18 Measured tool wear of the cutting tool used for confirmation experiment for tool wear

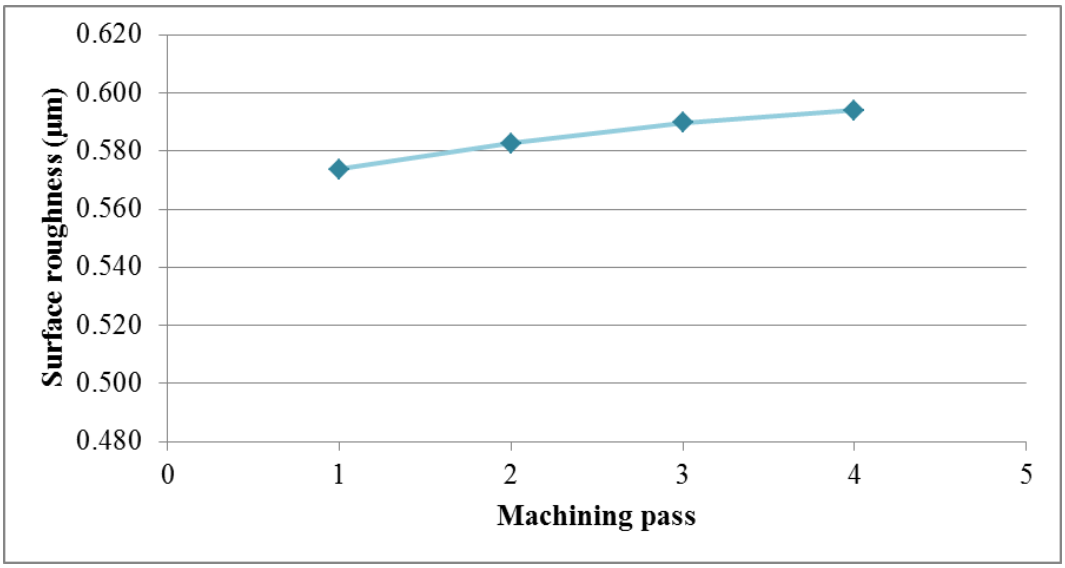

Figure 8.19 Average surface roughness of the first four machining passes of the second machining experiment

8.8. Summary

The results from comparative study in chapter 7 supported that cryogenic cooling has the potential to improve machinability of Ti-6Al-4V alloy. In this chapter, a DoE was generated and used to conduct a set of machining experiments to optimise machinability of Ti-6Al-4V alloy in end milling operations. Surface roughness and tool flank wear were selected as desired performance factors.

Following the DoE, a series of machining experiments were conducted and surface roughness and tool wear were measured for each experiment. The collected data were analysed and the regression models representing the relation between the performance factors and cutting parameters were developed. ANOVA of the models indicated that both models for surface roughness and tool wear fit the measured data and have high prediction ability.

In order to optimise the cutting parameters, the RSM graphs of surface roughness and tool wear were generated and SA was performed on the developed models. The models showed that minimum surface roughness is produced at cutting speed of 152 m/min and 1 mm depth of cut whilst tool wear is minimum at 200 m/min cutting speed and 5 mm depth of cut. Two machining trials were conducted to examine the results of optimisation process. The machining experiments confirmed that the predicted values for the surface roughness and tool wear are maximum 7% offset from the measured values.

Chapter 9

Discussion

9.1. Introduction

In this chapter, the activities conducted for this research and the observations and results of the experimental works are critically discussed in order to formulate the conclusions.

9.2. Design, manufacture and development of a cryogenic cooling system

A novel cryogenic nozzle for milling operations was designed and manufactured. The nozzle is easy to use and is retrofit-able to the majority of the conventional CNC machining centres as an external attachment to the spindle. The only available cryogenic machining system is the Cryo Advantage® by MAG IAS GmbH (MAG, 2012) which uses coolant through the spindle of the machine tool and since it requires complete change of the machine tool's spindle, it is not comparable with this design.

Computer modelling and experimental investigations have shown that cryogenic cooling using the shower nozzle configuration (chapter 6) has the potential to improve machinability thus validating the design. High speed filming of the nozzle revealed that the nozzle effectively sprays LN_2 through the tool's flute directly into the cutting zone. The design of the nozzle is unique and there is no similar concept for cryogenic milling operations.

On the other hand, the design of the nozzle at present limits the tool changing capabilities since the nozzle must be removed from the spindle in order to perform the tool changing routine. In addition, a limited number of tool diameters can be used on a single nozzle as the cutting tools need to pass through the hole in the centre of the nozzle. Therefore, a range of nozzles for different diameters of cutting tools is required. Furthermore, the length of the tools and tool overhang are dictated by the thickness of the nozzle (30 mm). The nozzle requires being manual assembly and disassembly on the machine tool's spindle. Considering the weight of the nozzle's assembly together with the clamping system which makes it difficult and cumbersome for technicians, there is a need for automation of the clamping system, so as to minimise manual assembling and disassembling.

9.3. Comparative study of cryogenic machining with conventional machining environments

In this section the activities and results of the comparative study presented in chapter 7 are discussed based on the methodology shown in figure 7.1.

9.3.1. Preparatory activities

Initial analysis of Ti-6Al-4V alloy indicated that exposing the material to extremely low temperatures during cryogenic machining has no or limited effects on the hardness and microstructure of the material. This has confirmed that cryogenic machining can be performed on Ti-6Al-4V workpiece material with no changes in the material properties and microstructure due to the low temperatures. In addition, in the absence of knowledge with regards to cutting parameters and tool geometry required for cryogenic machining of titanium, a series of machining experiments were conducted in order to identify the boundaries of machining parameters. Moreover, the cutting tool's geometries were selected based on existing cutting tools used for machining Ti-6Al-4V and initial machining experiments conducted in chapter 6. The geometries of the cutting tool e.g. rake angle, helix angle, etc. are important parameters affecting the quality of the machining operations. However, since the scope of this research was to evaluate the effects of cryogenic cooling as compared to dry and wet machining, identifying the optimum cutting tool's geometry was outside the scope of this research.

9.3.2. Machining experimentation

In the absence of optimum cutting parameters, a hybrid L9x3 DoE was generated for the comparative studies (chapter 7). This design was based on the fact that each machining environment should be compared to other environments when the specific optimum cutting parameters for that environment is selected. Using a traditional one-factor-at-a-time design using cutting parameters recommended for one specific machining environment does not provide meaningful comparison between different machining environments. This is mainly due to the fact that selecting the values of cutting parameters is related to the material properties which are dependent to temperature. Thus, applying different cooling methods at different temperatures changes the material properties and therefore different cutting parameters are required.

The experimental design used for this research consists of a L9 Taguchi's orthogonal array design which was repeated three times under different machining environments. Performing Taguchi's optimisation technique on each L9 design provides the optimum machining parameter for that machining environment whilst Taguchi analysis of the L9x3 design indicates the most desired machining environment. It is known that full factorial DoE is the best approach for identifying the effects of input parameters on outputs as it

includes all possible combinations of input parameters. However, full factorial designs require significant resources due to the high number of experimental runs. For instance, this research required 3^4 experiments in a full factorial design. In addition, since the machining environment is an intermittent qualitative parameter, more advanced statistical/mathematical based DoEs such as Box-Behnken and Central Composite cannot be used. The generated L9x3 DoE reduced the number of required experiments from 81 to 27 and is a low resolution DoE which assumes no significant interaction between the first three input parameters of cutting speed, chip load and depth of cut. Since, the aim of this research is to identify the effects of cryogenic cooling in comparison with other machining environments and not modelling of the data, this is considered to be a valid assumption to neglect the interactions between input parameters.

As explained in sections 7.3.2 and 7.4, a series of instructions were generated in order to reduce the uncertainty and uncontrolled variations in the results of machining experiments and data collection. According to BS ISO 5725-1 (1994) and BS ISO 7525-3 (1994), the four parameters of time, calibration, operator and equipment are the most important parameters affecting precision of a series of defined measurements. Thus, it was ensured that the time elapse between machining experiments was kept to a minimum whilst the same calibration, operator and equipment with identical setups were used. Similarly, the apparatuses used for data collection were calibrated prior to measurement and same calibration was used for all measurements. In addition, the same operator and equipment were used for the measurement of the each machinability metric whilst keeping the time elapsed between measurements to a minimum.

9.3.3. Statistical analysis of experimental results

In this section the effects of cryogenic cooling on the machinability of Ti-6Al-4V is discussed in four categories of (I) power and energy consumption, (II) surface roughness, (III) tool wear and (IV) surface topography and surface integrity.

I. Power and energy consumption

Through performing comparative machining experiments, a range of machinability metrics were measured and analysed. The analysis of the machine tool's power consumption indicated that using the coolant pump in wet machining increases power consumption of the machine tool by 55% to 80% as opposed to dry and cryogenic machining. As presented

in section 7.5.1, the analysis of EC/V showed that in order to reduce the amount of energy required for removing a unit volume of material the highest possible values of cutting speed, chip load and depth of cut are desirable. The mean SN ratio graphs for EC/V shows an almost linear relation between SN ratios of cutting parameters and EC/V. This is mainly due to the fact that the amount of energy required for running the machine tool is significant as compared to the amount of energy required for cutting. Thus, increasing the material removal rate by selecting higher cutting parameters reduces the proportion of the energy required for running the machine tool for a unit volume of removed material.

Comparing the power and energy consumption of the machine tool in dry and cryogenic machining showed that cryogenic cooling slightly increases the power and energy required for machining. Hong et al (2001a) and Uehara and Kumagai (1968) reported that in turning operations, cryogenic cooling has produced higher cutting forces than dry machining. The researchers (Hong et al., 2001a) attributed this increase to the cold strengthening of titanium material as a result of cryogenic cooling. Since cutting forces and power consumption are related, it can be concluded that higher power consumption is expected in cryogenic machining which is similar to the observations of this research. However, these results are contradictory to the results reported by Kalyan Kumar and Choudhury (2008) that almost 15% lower cutting forces have been achieved in cryogenic machining as opposed to dry cutting.

II. Surface roughness

Analysis of the results for surface roughness concluded that cryogenic cooling produced the lowest surface roughness in comparison to other machining environments. The analysis was limited to the data collected for the first machining pass in order to reduce the effect of tool wear on surface roughness. As disclosed in section 7.5.2, the analysis indicated that cryogenic cooling has reduced the surface roughness by an average 13% and by a maximum of 22% in comparison with wet machining which is similar to the results reported by different researchers in turning operations (Dhananchezian and Kumar, 2011, Wang and Rajurkar, 2000). In contradiction, an early study in cryogenic turning of titanium (Uehara and Kumagai, 1968) stated that cryogenic cooling has adverse effects on surface roughness. This statement can be explained by different cooling approaches used by researchers as they used internal freezing of the workpiece during turning operations

whilst others along with this research (Dhananchezian and Kumar, 2011, Wang and Rajurkar, 2000) used LN_2 spray jet.

III. Tool wear

After the machining experiments, microscopic images of the cutting tools have were taken and the tool flank wear measured. Measuring the tool wear in order to map the tool wear against machining length or time was not possible as it involved interrupting the machining operation for measurement which prevents accumulation of cutting heat which occurs in machining practices. This would prevent high cutting temperatures and induce thermal shock to the tool as a result of constant interruption of the machining operation. Therefore, tool wear was only measured at the end of each machining experiment.

The SN ratio analysis of the tool flank wear indicated that cryogenic cooling is the best machining environment when tool wear is of interest. Flank and crater wear were observed on all cutting tools irrespective of cutting parameters and machining environment. The severity of the wear increased at higher cutting speeds and chip loads. Microscopy of the tools also showed that whilst at lower levels of cutting speed and chip load the tool wear is mechanical it changes to more thermal and chemical wear at higher levels of cutting speed and chip load.

The analysis also revealed that tool wear in cryogenic machining is more mechanical by flank wear and chipping, whereas it is more thermally induced in dry and wet machining. This phenomenon was particularly evident at higher cutting speeds and chip loads where higher cutting temperatures result in melting of the chips, smearing of the workpiece material on the flank face and formation of BUE on the rake face of the cutting tool as illustrated in figures 7.23 and 7.26. Due to the stochastic nature of the DoE, vis-à-vis comparison of the tool wear phenomenon for cutting parameters is not possible. In addition, the collected data for tool wear for all machining environments was highly skewed and thus statistical comparison for defining the improvement percentage is not meaningful.

Apart from experiments D6 and D9 where dry machining outperformed cryogenic machining, cryogenic cooling reduced flank wear by 7%-74% in comparison with dry machining. Similarly, apart from experiment W6, cryogenic cooling reduced flank wear by 2%-84% as opposed to wet machining. Comparing the minimum tool wear for each

machining environment demonstrates that cryogenic cooling has the capability to reduce tool flank wear by 65% and 37% in comparison with dry and wet machining environments, respectively.

Whilst cryogenic cooling showed lower tool wear in comparison with other machining environments, analysis showed that the effect of cutting parameters on tool wear is significantly higher. Similar improvements were reported in turning operations of Ti-6Al-4V alloy (Dhananchezian and Kumar, 2011, Hong et al., 2001b, Paul and Chattopadhyay, 2006, Wang and Rajurkar, 2000, Venugopal et al., 2007). Birmingham et al (2011) stated that 43% to 58% improvement in tool life was achieved as a result of cryogenic machining. Since the longest tool life was achieved at low feed rates and depths of cut, they concluded that controlling the heat generation by precise selection of cutting parameters is more important than removing the heat by cryogenic cooling.

IV. Surface topography and surface integrity

Micrographs of the machined surfaces showed that cryogenic cooling has significantly reduced the surface defects of smearing, plastic deformation and welding. Generally the surface topography of the machined samples has been improved through cryogenic cooling. Visual examination of the cross section images of the microstructure below the machined surface did not indicate any significant change in the microstructure of the material. Similar observations were reported by Ezugwu et al. (2007) in turning Ti-6Al-4V alloy.

Analysis of the workpieces showed that the microhardness of the material below the machined surface has been changed up to 100 μm below the machined surface as shown in figure 7.39. The major part of this change has taken place at the first 20 μm below the surface. For most of the samples, the material hardness at this depth has been found to be lower than the material substrate which can be due to over-aging of the material at the cutting temperature (Che-Haron and Jawaid, 2005). The change in microhardness of materials has been observed on all samples irrespective of machining environment.

Due to the low resolution of the microhardness tester equipment, measuring microhardness closer than 10 μm to the surface was not applicable as explained in section 7.4.4. Thus, no significant difference between the samples of cryogenic and wet machining was observed. Visual examination of micrographs of the subsurface microstructure of the samples

indicated that no significant changes in the microstructure took place in cryogenic machining as compared to wet and dry machining. Similar observations were reported by Ezugwu et al (2007) in turning of Ti-6Al-4V using high pressure and conventional coolants and by Dandekar et al. (2010) in hybrid turning.

Since visual examination of the subsurface microstructure micrographs was not in agreement with the data from microhardness, the image processing technique was implemented to analyse the images quantitatively. This technique has previously been used by researchers (Ducato et al., 2013, Chrapoński and Szkliniarz, 2001) to enhance the visual difference between different phases of material microstructure. In addition, Christodoulou (2013) used image processing to quantify the grain density and grain size in cast steel. However, to the best of the author's knowledge using average white pixel concentration (AWPC) has not been reported previously.

The quality of this technique is dependent on the quality and size of the image. Sharper images with higher resolutions and wider area can improve the quality of the analysis. In addition, the comparison between the AWPC graphs and microhardness is considered subjective due to the low resolution of the microhardness tester.

The analysis of the AWPC graphs has indicated that machining has changed the microstructure of the material below the machined surface by reducing the concentration of β phase. This change appears to take place up to almost 100 μm beneath the machined surface. This can explain the reduction in microhardness of the material below the machined surface. Examining the AWPC graphs showed that cryogenic cooling slightly reduced the depth of this change.

9.4. Optimisation of cutting parameters in cryogenic machining

The comparative study of cryogenic machining with dry and wet machining revealed that cryogenic cooling has significantly improved the machinability of Ti-6Al-4V in end milling operations. As explained in section 8.2, a FCCC DoE was generated to optimise machining parameters for surface roughness (Ra) and tool flank wear. It is known that generally increasing chip load has an adverse effect on tool wear and surface roughness (Astakhov, 2006, Dhar et al., 2006). Thus, the lower chip load of 0.03 mm/tooth was kept constant and two input parameters of cutting speed and depth of cut were used for the DoE. This reduces the number of experiments required for optimisation. The DoE consists of 4

experiments on the boundaries, 4 star points and 3 replications in the centre. The replications indicate the repeatability and errors of the process.

Eleven machining experiments were conducted and surface roughness and tool flank wear were measured for each machining experiment. Since the majority of statistical methods require a normally distributed data, the normality of the data was evaluated. The analysis indicated that there is not enough evidence to reject the hypothesis of normally distributed data and thus both datasets are normally distributed.

ANOVA of the data indicated that both input parameters and their interaction have significant effect on the surface roughness and tool wear. As shown in figure 8.8 and 8.9, Pareto ANOVA diagrams of surface roughness and tool wear were generated which show the contribution percentage of each input parameter and their interactions on the desired output parameter. This is a commonly used method by many researchers (Ghani et al., 2004, Palanikumar, 2006, Hayajneh et al., 2007, Hamdan et al., 2012) to optimise cutting parameters in machining operations.

Based on the collected data two quadratic models were generated for surface roughness and tool wear. Evaluation of the models indicated that the models of surface roughness and tool wear fit the data by 97% and 99% respectively and provide a high predictability of 81% and 98%. High fit value raises the suspicion for over-fitting of the data thus step method was used by removing parameters from the models and checking the predictability value. This indicated that full-quadratic model provides the best agreement between fit and predictability.

The RSM graphs of generated models for surface roughness and tool wear were plotted and SA was used to identify the optimum values of input parameters for surface roughness and tool wear. As explained in section 8.7, two confirmatory machining experiments indicated that the predicted values for optimisation are within 7% of the measured values. This shows that the optimisation procedure was successfully conducted.

The optimisation procedure used in this research is based on RSM which used only three levels of each input parameter for modelling. Optimisation is an ongoing procedure and whilst the predicted values for input parameters are optimum amongst the values used in the DoE, they do not necessarily reflect global optimum values. In addition, chip load was assumed to be optimum at 0.03 mm/tooth and was not considered in the DoE in order to

minimise the number of experiments. However, the effects of interactions between chip load and other input parameters are unknown.

Chapter 10

Conclusions and further work

10.1. Introduction

In this chapter the conclusions drawn from this research together with further areas of investigation are presented.

10.2. Conclusion

- Based on the findings of the literature, the best cooling approach for cryogenic machining of titanium was found to be spraying LN_2 into the cutting zone and freezing both cutting tool and workpiece material at the point of cut.
- A cryogenic cooling system has been designed and developed by the author for CNC milling of Ti-6Al-4V alloy which is retrofitable to an existing CNC milling machine. Initial machining experiments proved the effectiveness of the system in improving machinability of the alloy as compared to dry and wet machining environments.
- A hybrid DoE was developed for three machining environments of dry, wet and cryogenic using different combinations of cutting speed, chip load and depth of cut as input parameters. In the absence of knowledge with regards to the optimum cutting parameters for different machining environments, the methodology for comparative study proved to be an effective and efficient way for comparing the effects of different machining environments on machinability.
- Comparing the results for power consumption showed that the coolant pump represent 55% to 80% of the overall machine tool power consumption. This percentage depends on the power consumption of other components of the machine tool which are determined by cutting parameters e.g. cutting speed, chip load and depth of cut.
- Comparing the power consumption in dry machining with cryogenic machining demonstrated that cryogenic cooling increases the power consumption by an average of 1.45%.
- Using cryogenic cooling has reduced surface roughness by an average of 19% and 21% in comparison to wet and dry machining respectively.
- Analysis of the cutting tools used for machining experiments showed that cryogenic cooling has significantly reduced tool flank wear and crater wear as compared to dry and wet machining operations.

- Microscopic analysis of the machined surfaces showed that lower surface defects and improved topography can be expected in cryogenic machining. Cryogenic cooling has reduced chip re-deposition and smearing as compared to dry and wet machining environments.
- Subsurface microstructural and microhardness analysis showed that there is no significant difference between the samples produced under different machining environments. Nevertheless, analysis of the subsurface microstructure showed shallower damage under cryogenic machining.
- RSM optimisation method and a FCCC DoE was used to enable optimisation of cutting speed and depth of cut whilst keeping the chip load constant at 0.03 mm/min, aiming to minimise surface roughness and tool wear. The analysis indicated that this is a suitable method for fitting a full quadratic model. The analysis and confirmatory experiments indicated that the optimisation procedure for cutting parameters has significant potential for identifying the optimum values of cutting parameters.
- ANOVA of the data showed that both cutting speed and depth of cut are the most significant parameters for surface roughness. Furthermore, ANOVA indicated that the interaction between cutting speed and depth of cut is the most significant for tool wear. Moreover, cutting speed and depth of cut ranked second and third for affecting the tool wear.
- SA was used to define the optimum values of input parameters for surface roughness and tool wear. Two confirmatory experiments have been conducted to testify the correctness of the optimisation process. Both experiments confirmed the predicted values of the optimisation procedure are within a close proximity (7%) to the measured values.
- It can be concluded that the application of LN_2 in cryogenic machining using the cryogenic shower nozzle has significantly improved the machinability of Ti-6Al-4V. In addition, by adopting cryogenic cooling, a minimum seven fold increase in material removal rate through realisation of higher cutting speeds has been achieved.

10.3. Contribution to knowledge

This research has contributed to knowledge by providing information on the effects of cryogenic cooling in CNC end milling of Ti-6Al-4V alloy in comparison with traditional dry and wet machining environments. Though there are papers on cryogenic turning of titanium, to the best of the author's knowledge no previous publication exists in the area of cryogenic CNC milling of Ti-6Al-4V. In addition, there is a limited publication on the surface integrity and surface topography of cryogenically machined titanium workpieces. Furthermore, no previously published data exist on the power consumption, PC/V and EC/V in cryogenic machining operations.

10.4. Further work

Apart from the research gaps recognised in the literature review, during the course of this research, a number of research areas have been identified as an opportunity for further investigation. These areas can be summarised as:

I. Expanding the vision of this research to other milling operations

This research was focused on cryogenic end milling using solid carbide tools, however other milling operations such as face milling, sculptured surface milling using ball nose cutters and drilling have been neglected. Furthermore, using indexable inserts of different materials is becoming more prevalent in milling operations. Similarly, different coatings and carbide grades can be explored for solid carbide tools in cryogenic end milling.

II. Optimising the cryogenic cooling nozzle design

The design of the cryogen shower nozzle used in this research limits the size of the cutting tools and automatic tool changing. Further work is required to optimise the design and automate the tool changing operation during machining.

In addition, the CFD modelling used in this research was limited to the cryogen flow inside the material with a fixed cutting tool. There is a significant research opportunity to model the flow of cryogen during cutting operations and modelling the material cutting process and chip formation in cryogenic machining.

III. Further machining experiments for comparative study

The effects of interaction between cutting parameters has been neglected in the L9 Taguchi's DoE used in this research in order to reduce the number of experiments. However, as shown in chapter 8, the interactions have significant effect on both tool wear and surface roughness. Further investigations can identify the effects of interactions between machining parameters under different machining environments. In addition, some parameters such as tool overhang and immersion rate, cryogen flow rate and cryogen pressure have been kept constant which can be considered for future DoEs.

IV. Study of tool life and tool failure mode

Due to the limited resources, this research was limited to the study of tool wear after machining 4x150mm machining length. As explained in chapter 7, flank wear is not the only indicator of tool life as the cutting tool may fail catastrophically by chipping and crater wear. Thus, further research is necessary to identify the effects of cryogenic cooling on tool life and define the tool failure mode.

V. Identifying the effects of cryogenic cooling on material properties of Ti-6Al-4V

In this research the effect of subjecting workpiece material to LN_2 for 10 min on hardness and microstructure were studied. In many industrial cases, the machining time exceeds 10 min and can reach up to a few hours. There is a potential area of investigation to study the effects of cryogenic cooling on the material properties such as hardness, strength, fatigue, etc. of Ti-6Al-4V.

VI. Studying the effects of cryogenic cooling on the geometrical accuracy of final products

Although Ti-6Al-4V has a very low coefficient of thermal expansion, subjecting the workpiece to cryogenic temperatures during cryogenic machining can affect the geometrical accuracy of the final product. Thus, the effect of cryogenic cooling on the dimensions of final products is required to be considered during design and process planning for manufacturing. This raises the requirements for further investigations on the geometrical accuracy of the products which are manufactured by cryogenic machining.

VII. Studying the correlation between subsurface microhardness and microstructure

In this research a subjective relation between subsurface microhardness and microstructure has been found. However, due to the limited resources and low resolution of the equipment, the microhardness of the samples is not exactly taken from where the images of microstructure are produced. Thus, further research is required to identify the relation between the AWPC and microhardness and the effects of different machining environments on subsurface microhardness and microstructure.

VIII. Modelling the relation between cutting parameters and desired machinability metrics and optimisation

In this research, surface roughness and tool wear were modelled based on cutting speed and depth of cut whilst keeping other cutting parameters such as chip load, immersion rate and cryogen pressure constant. Further research is required to model the relation between different cutting parameters involved in cryogenic machining. Similarly, further investigation is necessary to identify the optimum value of each input parameter.

References

Abele, E. & Fröhlich, B. 2008. High speed milling of titanium alloys. Advances in Production Engineering & Management, 3, pp.131-140.

Abele, E. & Schramm, B. 2008. Using PCD for machining CGI with a CO_2 coolant system. Production Engineering, 2(2), pp.165-169.

Abukhshim, N., Mativenga, P. & Sheikh, M. 2006. Heat generation and temperature prediction in metal cutting: A review and implications for high speed machining. International Journal of Machine Tools and Manufacture, 46(7-8), pp.782-800.

Aggarwal, A., Singh, H., Kumar, P. & Singh, M. 2008a. Optimization of multiple quality characteristics for CNC turning under cryogenic cutting environment using desirability function. Journal of Materials Processing Technology, 205(1-3), pp.42-50.

Aggarwal, A., Singh, H., Kumar, P. & Singh, M. 2008b. Optimizing power consumption for CNC turned parts using response surface methodology and Taguchi's technique—A comparative analysis. Journal of Materials Processing Technology, 200(1-3), pp.373-384.

Aggarwal, A., Singh, H., Kumar, P. & Singh, M. 2009. Optimizing feed and radial forces in CNC machining of P-20 tool steel through Taguchi's parameter design approach. Indian Journal of Engineering & Materials Sciences, 16, pp.23-32.

Ahmed, M., Ismail, A., Abakr, Y. & Amin, A. 2007. Effectiveness of cryogenic machining with modified tool holder. Journal of Materials Processing Technology, 185(1-3), pp.91-96.

Air Products. 2011. ICEFLY® Cryogen Delivery System [Online]. Allentown, PA. Available: http://airproducts.com/en/company/technology-partnerships/technology-licensing/gases/gases-icefly-cryogen-delivery-system.aspx [Accessed 6 Jan 2012].

Alauddin, M., El Baradie, M. & Hashmi, M. 1996. Optimization of surface finish in end milling Inconel 718. Journal of Materials Processing Technology, 56(1-4), pp.54-65.

Alauddin, M., Mazid, M., El Baradi, M. & Hashmi, M. 1998. Cutting forces in the end milling of Inconel 718. Journal of Materials Processing Technology, 77(1-3), pp.153-159.

Anderson, M. J. & Whitcomb, P. J. 2000. Design of Experiments. Kirk-Othmer Encyclopedia of Chemical Technology. Hoboken, New Jersey: John Wiley & Sons, Inc.

Arunachalam, R. & Mannan, M. 2000. Machinability of nickel-based high temperature alloys. Machining Science and Technology, 4(1), pp.127-168.

Asokan, P., Saravanan, R. & Vijayakumar, K. 2003. Machining parameters optimisation for turning cylindrical stock into a continuous finished profile using genetic algorithm (GA) and simulated annealing (SA). The International Journal of Advanced Manufacturing Technology, 21(1), pp.1-9.

Astakhov, V. P. 2006. Tribology of Metal Cutting, Rochester Hills, Michigan, Elsevier Science.

Axer, H. 1954. Zur Physik des Werkzeugverschleisses. In: Shaw, M.C. and Smith, P.A, 1956. Methods of applying cutting fluids, ASTE Paper No. RR-3, pp.

Aykut, S., Gölcü, M., Semiz, S. & Ergür, H. S. 2007. Modeling of cutting forces as function of cutting parameters for face milling of satellite 6 using an artificial neural network. Journal of Materials Processing Technology, 190(1-3), pp.199-203.

Bagci, E. & Aykut, Ş. 2006. A study of Taguchi optimization method for identifying optimum surface roughness in CNC face milling of cobalt-based alloy (stellite 6). The International Journal of Advanced Manufacturing Technology, 29(9), pp.940-947.

Benfredj, N. & Sidhom, H. 2006. Effects of the cryogenic cooling on the fatigue strength of the AISI 304 stainless steel ground components. Cryogenics, 46(6), pp.439-448.

Benfredj, N., Sidhom, H. & Braham, C. 2006. Ground surface improvement of the austenitic stainless steel AISI 304 using cryogenic cooling. Surface and Coatings Technology, 200(16-17), pp.4846-4860.

Bermingham, M., Palanisamy, S., Kent, D. & Dargusch, M. 2011a. A comparison of cryogenic and high pressure emulsion cooling technologies on tool life and chip morphology in Ti-6Al-4V cutting. Journal of Materials Processing Technology, 212(4), pp.752–765.

Bermingham, M. J., Kirsch, J., Sun, S., Palanisamy, S. & Dargusch, M. S. 2011b. New observations on tool life, cutting forces and chip morphology in cryogenic machining Ti-6Al-4V. International Journal of Machine Tools and Manufacture, 51(6), pp.500-511.

Bhattacharyya, D. & Horrigan, D. 1998. A study of hole drilling in Kevlar composites. Composites science and technology, 58(2), pp.267-283.

Bian, R., Ferraris, E., He, N. & Reynaerts, D. 2014. Process investigation on meso-scale hard milling of ZrO_2 by diamond coated tools. Precision Engineering, 38(1), pp.82-91.

Biermann, D. & Heilmann, M. 2010. Improvement of workpiece quality in face milling of aluminum alloys. Journal of Materials Processing Technology, 210(14), pp.1968-1975.

Boyer, R., Welsch, G. & Collings, E. W. 1994. Materials Properties Handbook - Titanium Alloys, Matrials Park, OH, ASM International.

Brandao, L., Coelho, R. & Rodrigues, A. 2008. Experimental and theoretical study of workpiece temperature when end milling hardened steels using (TiAl)N-coated and PcBN-tipped tools. Journal of Materials Processing Technology, 199(1-3), pp.234-244.

Brinksmeier, E. & Glabe, R. 2001. Advances in Precision Machining of Steel. CIRP Annals - Manufacturing Technology, 50(1), pp.385-388.

BS EN ISO 3274:1998. Geometric Product Specification (GPS) Surface texture: Profile method — Nominal characteristics of contact (stylus) instruments —. London: British Standard Institute.

BS EN ISO 4287:1998. Geometric Product Specification (GPS) Surface texture —Profile method: Terms, definitions and surface texture parameters. London: British Standard Institute.

BS EN ISO 4288:1998. Geometric Product Specification (GPS) Surface texture —Profile method: Rules and procedures for the assessment of surface texture. London: British Standard Institute.

BS ISO 3534-3:2013. Statistics - Vocabulary and Symbols. Part 3: Design of Experiments. London: British Standard Institution

BS ISO 5725-1:1994. Accuracy (Trueness and Precision) of Measurement Methods and Results. Part 1: General Principles and Definitions. London: British Standard Institute.

BS ISO 5725-2:1994. Accuracy (Trueness and Precision) of Measurement Methods and Results. Part 2: Basic Methods for the Determination of Repeatability and Reproducibility of a Standard Measurement Method. London: British Standard Institute.

BS ISO 5725-3:1994. Accuracy (Trueness and Precision) of Measurement Methods and Results. Part 3: Intermediate Measures of the Precision of a Standard Measurement Method. London: British Standard Institute.

Buckingham, M. 2011, Personal Communication: Technical Meeting. Renishaw Plc, Wotton-under-edge.

Busch, W. S. 1969. Introduction to Cryogenics. ASTME Technical Paper, CM69-252.

Byrne, G. & Scholta, E. 1993. Environmentally Clean Machining Processes -- A Strategic Approach. CIRP Annals - Manufacturing Technology, 42(1), pp.471-474.

Campbell, S. A. 2008. Fabrication Engineering at the Micro- and Nanoscale (3rd Edition), Oxford, Oxford University Press.

Chandrasekaran, M., Muralidhar, M., Krishna, C. M. & Dixit, U. S. 2010. Application of soft computing techniques in machining performance prediction and optimization: a literature review. The International Journal of Advanced Manufacturing Technology, 46(5-8), pp.445-464.

Che-Haron, C. H. & Jawaid, A. 2005. The effect of machining on surface integrity of titanium alloy Ti–6% Al–4% V. Journal of Materials Processing Technology, 166(2), pp.188-192.

Chen, H. & Alpas, A. T. 2000. Sliding wear map for the magnesium alloy Mg-9Al-0.9 Zn (AZ91). Wear, 246(1-2), pp.106-116.

Childs, T. H. C., Maekawa, K., Obikawa, T. & yamane, Y. 2000. Metal Machining - Theory and Applications. Elsevier.

Choragudi, A., Kuttolamadom, M. A., Jones, J. J., Mears, M. L. & Kurfess, T. 2010. Investigation of the machining of titanium components in lightweight vehicles. SAE International Congress. Detroit, MI, USA.

Chou, Y.-M., Polansky, A. M. & Mason, R. L. 1998. Transforming non-normal data to normality in statistical process control. Journal of Quality Technology, 30(2), pp.133-141.

Chrapoński, J. & Szkliniarz, W. 2001. Quantitative metallography of two-phase titanium alloys. Materials Characterization, 46(2), pp.149-154.

Christodoulou, P. 2013. Planar Spatial Arrangement of Precipitates in 0.3 C-30Ni 18Cr-0.9 Ti Austenitic Cast Steel Aged at 600° C for 10 h. Journal of Materials Engineering and Performance, 22(5), pp.1490-1504.

Coshh. 2011. COSHH essentials for machining with metalworking fluids [Online]. Health and Safety Executive. Available: http://www.hse.gov.uk/metalworking/ecoshh.htm [Accessed 01 Nov 2011].

Courbon, C., Pusavec, F., Dumont, F., Rech, J. & Kopac, J. 2014. Influence of cryogenic lubrication on the tribological properties of Ti6Al4V and Inconel 718 alloys under extreme contact conditions. Lubrication Science, pp.n/a-n/a.

Dandekar, C. R., Shin, Y. C. & Barnes, J. 2010. Machinability improvement of titanium alloy (Ti–6Al–4V) via LAM and hybrid machining. International Journal of Machine Tools and Manufacture, 50(2), pp.174-182.

Das, D., Dutta, A. K., Toppo, V. & Ray, K. K. 2007. Effect of Deep Cryogenic Treatment on the Carbide Precipitation and Tribological Behavior of D2 Steel. Materials and Manufacturing Processes, 22(4), pp.474 - 480.

Dasilva, F., Franco, S., Machado, A., Ezugwu, E. & Souzajr, A. 2006. Performance of cryogenically treated HSS tools. Wear, 261(5-6), pp.674-685.

Davim, J. P. 2002. Diamond tool performance in machining metal-matrix composites. Journal of Materials Processing Technology, 128(1-3), pp.100-105.

Davim, J. P. 2013. Machining Composites Materials, London, John Wiley & Sons.

De Chiffre, L., Andreasen, J. L., Lagerberg, S. & Thesken, I. B. 2007. Performance Testing of Cryogenic CO_2 as Cutting Fluid in Parting/Grooving and Threading Austenitic Stainless Steel. CIRP Annals - Manufacturing Technology, 56(1), pp.101-104.

Dearnley, P. & Grearson, A. 1986. Evaluation of principal wear mechanisms of cemented carbides and ceramics used for machining titanium alloy IMI 318. Materials Science and Technology, 2(1), pp.47-58.

Denkena, B., Witte, F., Podolsky, C. & Lucas, A. 2005. Degradable implants made of magnesium alloys. France: Montpellier, pp.

Devillez, A., Schneider, F., Dominiak, S., Dudzinski, D. & Larrouquere, D. 2007. Cutting forces and wear in dry machining of Inconel 718 with coated carbide tools. Wear, 262(7-8), pp.931-942.

Dhananchezian, M. & Kumar, M. P. 2011. Cryogenic turning of the Ti–6Al–4V alloy with modified cutting tool inserts. Cryogenics, 51(1), pp.34-40.

Dhananchezian, M., Kumar, M. P. & Rajaduari, A. 2009. Experimental investigation of cryogenic cooling by liquid nitrogen in the orthogonal machining process. International Journal of Recent Trend in Engineering, 1(5), pp.55-59.

Dhar, N., Islam, M., Islam, S. & Mithu, M. 2006a. The influence of minimum quantity of lubrication (MQL) on cutting temperature, chip and dimensional accuracy in turning AISI-1040 steel. Journal of Materials Processing Technology, 171(1), pp.93-99.

Dhar, N. & Kamruzzaman, M. 2007. Cutting temperature, tool wear, surface roughness and dimensional deviation in turning AISI-4037 steel under cryogenic condition. International Journal of Machine Tools and Manufacture, 47(5), pp.754-759.

Dhar, N., Nanda Kishore, S., Paul, S. & Chattopadhyay, A. 2002a. The effects of cryogenic cooling on chips and cutting forces in turning AISI 1040 and AISI 4320 steels. Proceedings of the Institution of Mechanical Engineers, Part B: Journal of Engineering Manufacture, 216(5), pp.713-724.

Dhar, N. R., Islam, S., Kamruzzaman, M. & Paul, S. 2006b. Wear behavior of uncoated carbide inserts under dry, wet and cryogenic cooling conditions in turning C-60 steel. Journal of the Brazilian Society of Mechanical Sciences and Engineering, 28, pp.146-152.

Dhar, N. R., Kamruzzaman, M. & Ahmed, M. 2006c. Effect of minimum quantity lubrication (MQL) on tool wear and surface roughness in turning AISI-4340 steel. Journal of Materials Processing Technology, 172(2), pp.299-304.

Dhar, N. R., Paul, S. & Chattopadhyay, A. B. 2002b. The influence of cryogenic cooling on tool wear, dimensional accuracy and surface finish in turning AISI 1040 and E4340C steels. Wear, 249(10-11), pp.932-942.

Dhar, N. R., Paul, S. & Chattopadhyay, A. B. 2002c. Machining of AISI 4140 steel under cryogenic cooling--tool wear, surface roughness and dimensional deviation. Journal of Materials Processing Technology, 123(3), pp.483-489.

Dhar, N. R., Paul, S. & Chattopadhyay, A. B. 2002d. Role of Cryogenic Cooling on Cutting Temperature in Turning Steel. Journal of Manufacturing Science and Engineering, 124(1), pp.146.

Dhokia, V., Newman, S., Crabtree, P. & Ansell, M. 2011. Adiabatic shear band formation as a result of cryogenic CNC machining of elastomers. Proceedings of the Institution of Mechanical Engineers, Part B: Journal of Engineering Manufacture, 225(9), pp.1482-1492.

Dhokia, V., Shokrani, A. & Newman, S. T. 2012a. Study of Cryogenics in CNC Milling of Metal Alloys (Keynote). International Chemnitz Manufacturing Colloquium in association with the 2nd International Colloquium of the Cluster of Excellenz eniPROD. Chemnitz.

Dhokia, V., Shokrani, A., Newman, S. T. & Safdari, G. 2012b. Cryogenic Machining of Carbon Fibre. 12th Euspen International Conference. Stockholm.

Dhokia, V. G. 2009. The Cryogenic Sculpture Surface Machining of Elastomers. PhD, University of Bath.

Dhokia, V. G., Newman, S. T., Crabtree, P. & Ansell, M. P. 2010. A methodology for the determination of foamed polymer contraction rates as a result of cryogenic CNC machining. Robotics and Computer-Integrated Manufacturing, 26(6), pp.665-670.

Dogra, M., Sharma, V. S., Sachdeva, A., Suri, N. M. & Dureja, J. S. 2010. Tool wear, chip formation and workpiece surface issues in CBN hard turning: A review. International Journal of Precision Engineering and Manufacturing, 11(2), pp.341-358.

Dolinšek, S. 2003. Work-hardening in the drilling of austenitic stainless steels. Journal of Materials Processing Technology, 133(1), pp.63-70.

Donachie, J. M. J. 2000. Titanium - A Technical Guide (2nd Edition). ASM International.

Ducato, A., Fratini, L., La Cascia, M. & Mazzola, G. An Automated Visual Inspection System for the Classification of the Phases of Ti-6Al-4V Titanium Alloy. Computer Analysis of Images and Patterns, 2013. Springer, 362-369.

Dudzinski, D. 2004. A review of developments towards dry and high speed machining of Inconel 718 alloy. International Journal of Machine Tools and Manufacture, 44(4), pp.439-456.

Dutra Xavier, S. E., Delijaicov, S. & De Farias, A. Investigation on the surface integrity and tool wear in cryogenic machining. International Conference on Advances in Material and Processing Technologies, 2011. American Institute of Physics, 1199-1204.

Edwards, T. 2003. Liquid fuels and propellants for aerospace propulsion: 1903-2003. Journal of propulsion and power, 19(6), pp.1089-1107.

El-Gallab, M. & Sklad, M. 1998. Machining of Al/SiC particulate metal-matrix composites: Part I: Tool performance. Journal of Materials Processing Technology, 83(1-3), pp.151-158.

El-Tayeb, N. S. M., Yap, T. C. & Brevern, P. V. 2010. Wear characteristics of titanium alloy Ti54 for cryogenic sliding applications. Tribology International, 43(12), pp.2345-2354.

El-Tayeb, N. S. M., Yap, T. C., Venkatesh, V. C. & Brevern, P. V. 2009. Modeling of cryogenic frictional behaviour of titanium alloys using Response Surface Methodology approach. Materials & Design, 30(10), pp.4023-4034.

El Baradie, M. 1996. Cutting fluids: Part I. characterisation. Journal of Materials Processing Technology, 56(1-4), pp.786-797.

Endrino, J. L., Fox-Rabinovich, G. S. & Gey, C. 2006. Hard AlTiN, AlCrN PVD coatings for machining of austenitic stainless steel. Surface and Coatings Technology, 200(24), pp.6840-6845.

Evans, C. & Bryan, J. B. 1991. Cryogenic Diamond Turning of Stainless Steel. CIRP Annals - Manufacturing Technology, 40(1), pp.571-575.

Evans, C. & Marshall, D. B. 1980. Wear mechanisms in ceramics In: Wang, Z.Y., Rajurkar, K.P. and Murugappan, M., 1996. Cryogenic PCBN turning of ceramic (Si3N4). Wear, 195, pp.1-6.

Ezugwu, E. 2005. Key improvements in the machining of difficult-to-cut aerospace superalloys. International Journal of Machine Tools and Manufacture, 45(12-13), pp.1353-1367.

Ezugwu, E., Bonney, J. & Yamane, Y. 2003. An overview of the machinability of aeroengine alloys. Journal of Materials Processing Technology, 134(2), pp.233-253.

Ezugwu, E. O., Bonney, J., Da Silva, R. B. & Cakir, O. 2007. Surface integrity of finished turned Ti–6Al–4V alloy with PCD tools using conventional and high pressure coolant supplies. International Journal of Machine Tools and Manufacture, 47(6), pp.884-891.

Ezugwu, E. O., Da Silva, R. B., Bonney, J. & Machado, Á. 2005. The Effect of Argon-Enriched Environment in High-Speed Machining of Titanium Alloy. Tribology Transactions, 48(1), pp.18-23.

Feng, S. C. & Hattori, M. Cost and Process Information Modeling for Dry Machining. Proceedings of the International Workshop on Environment and Manufacturing, 2000. National Institute of Standards and Technology.

Fernández-Abia, A., Barreiro, J., Lacalle, L. N. L. & Martínez, S. 2011. Effect of very high cutting speeds on shearing, cutting forces and roughness in dry turning of austenitic stainless steels. The International Journal of Advanced Manufacturing Technology, pp.1-11.

Firouzdor, V., Nejati, E. & Khomamizadeh, F. 2008. Effect of deep cryogenic treatment on wear resistance and tool life of M2 HSS drill. Journal of Materials Processing Technology, 206(1-3), pp.467-472.

Froes, F., Eliezer, D. & Aghion, E. 1998. The science, technology, and applications of magnesium. JOM Journal of the Minerals, Metals and Materials Society, 50(9), pp.30-34.

Gariboldi, E. 2003. Drilling a magnesium alloy using PVD coated twist drills. Journal of Materials Processing Technology, 134(3), pp.287-295.

Ghani, A. J., Che Haron, C. H., Hamdan, S. H., Md Said, A. Y. & Tomadi, S. H. 2013. Failure mode analysis of carbide cutting tools used for machining titanium alloy. Ceramics International, 39(4), pp.4449-4456.

Ghani, J. A., Choudhury, I. A. & Hassan, H. H. 2004. Application of Taguchi method in the optimization of end milling parameters. Journal of Materials Processing Technology, 145(1), pp.84-92.

Ghosh, R., Zurecki, Z. & Frey, J. H. Cryogenic Machining with Brittle Tools and Effects on Tool Life. Proceedings of ASME International Mechanical Engineering Congress and Exposition, 2003 Washington, D.C.: ASME.

Gill, S. S., Singh, H., Singh, R. & Singh, J. 2009. Cryoprocessing of cutting tool materials—a review. The International Journal of Advanced Manufacturing Technology, 48(1-4), pp.175-192.

Gill, S. S., Singh, J., Singh, R. & Singh, H. 2011. Metallurgical principles of cryogenically treated tool steels—a review on the current state of science. The International Journal of Advanced Manufacturing Technology, 54, pp.59-82.

Ginting, A. & Nouari, M. 2006. Experimental and numerical studies on the performance of alloyed carbide tool in dry milling of aerospace material. International Journal of Machine Tools and Manufacture, 46(7-8), pp.758-768.

Gisip, J., Gazo, R. & Stewart, H. A. 2009. Effects of cryogenic treatment and refrigerated air on tool wear when machining medium density fiberboard. Journal of Materials Processing Technology, 209(11), pp.5117-5122.

Grzesik, W. 2008. Advanced machining processes of metallic materials: theory, modelling and applications, Oxford, Elsevier Science.

Grzesik, W. & Zalisz, Z. 2008. Wear phenomenon in the hard steel machining using ceramic tools. Tribology International, 41(8), pp.802-812.

Gulyaev, A. 1937. Improved methods of heat treating high speed steels to improve the cutting properties. Metallurgy, 12, pp.65-77.

Hamdan, A., Sarhan, A. D. & Hamdi, M. 2012. An optimization method of the machining parameters in high-speed machining of stainless steel using coated carbide tool for best surface finish. The International Journal of Advanced Manufacturing Technology, 58(1-4), pp.81-91.

Harris, D. 1970. Another big step forward in modern metalworking. Society of Manufacturing Engineers, TECH Paper No. AD70-734, 4 P, pp.

Hayajneh, M. T., Tahat, M. S. & Bluhm, J. 2007. A study of the effects of machining parameters on the surface roughness in the end-milling process. Jordan Journal of Mechanical and Industrial Engineering, pp.1-5.

Hong, H., Riga, A. T., Gahoon, J. M. & Scott, C. G. 1993. Machinability of steels and titanium alloys under lubrication. Wear, 162–164, Part A(0), pp.34-39.

Hong, S. 2006. Lubrication Mechanisms of Ln2 in Ecological Cryogenic Machining. Machining Science and Technology, 10(1), pp.133-155.

Hong, S., Ding, Y. & Jeong, J. 2002. Experimental Evaluation of Friction Coefficient and Liquid Nitrogen Lubrication Effect in Cryogenic Machining. Machining Science and Technology, 6(2), pp.235-250.

Hong, S. Y. 1999. Cryogenic Machining. US patent application 5,901,623, May 11, 1999

Hong, S. Y. 2001. Economical and Ecological Cryogenic Machining. Journal of Manufacturing Science and Engineering, 123(2), pp.331.

Hong, S. Y. & Broomer, M. 2000. Economical and ecological cryogenic machining of AISI 304 austenitic stainless steel. Clean Technologies and Environmental Policy, 2(3), pp.157-166.

Hong, S. Y. & Ding, Y. 2001a. Cooling approaches and cutting temperatures in cryogenic machining of Ti-6Al-4V. International Journal of Machine Tools and Manufacture, 41(10), pp.1417-1437.

Hong, S. Y. & Ding, Y. 2001b. Micro-temperature manipulation in cryogenic machining of low carbon steel. Journal of Materials Processing Technology, 116(1), pp.22-30.

Hong, S. Y., Ding, Y. & Ekkens, R. G. 1999. Improving low carbon steel chip breakability by cryogenic chip cooling. International Journal of Machine Tools and Manufacture, 39(7), pp.1065-1085.

Hong, S. Y., Ding, Y. & Jeong, W. 2001a. Friction and cutting forces in cryogenic machining of Ti-6Al-4V. International Journal of Machine Tools and Manufacture, 41(15), pp.2271-2285.

Hong, S. Y., Markus, I. & Jeong, W. 2001b. New cooling approach and tool life improvement in cryogenic machining of titanium alloy Ti-6Al-4V. International Journal of Machine Tools and Manufacture, 41(15), pp.2245-2260.

Hong, S. Y. & Zhao, Z. 1999. Thermal aspects, material considerations and cooling strategies in cryogenic machining. Clean Technologies and Environmental Policy, 1(2), pp.107-116.

Hübner, W., Gradt, T., Schneider, T. & Börner, H. 1998. Tribological behaviour of materials at cryogenic temperatures. Wear, 216(2), pp.150-159.

Islam, M. N., Anggono, J. M., Pramanik, A. & Boswell, B. 2013. Effect of cooling methods on dimensional accuracy and surface finish of a turned titanium part. The International Journal of Advanced Manufacturing Technology, 69(9-12), pp.2711-2722.

ISO 8688-2 1989. Tool life testing in milling -- Part 2: End milling. Geneva: International-Organization-for-Standardization.

Jaffery, S. I. & Mativenga, P. T. 2008. Assessment of the machinability of Ti-6Al-4V alloy using the wear map approach. The International Journal of Advanced Manufacturing Technology, 40(7-8), pp.687-696.

Jainbajranglal, J. R. & Chattopadhyay, A. 1984. Role of cryogenics in metal cutting industry. Indian Journal of Cryogenics, 9(1), pp.42-46.

Jawahir, I., Brinksmeier, E., M'saoubi, R., Aspinwall, D., Outeiro, J., Meyer, D., Umbrello, D. & Jayal, A. 2011. Surface integrity in material removal processes: Recent advances. CIRP Annals-Manufacturing Technology, pp.

Jayal, A. D., Badurdeen, F., Dillon Jr, O. W. & Jawahir, I. S. 2010. Sustainable manufacturing: Modeling and optimization challenges at the product, process and system levels. CIRP Journal of Manufacturing Science and Technology, 2(3), pp.144-152.

Jen, T., Gutierrez, G., Eapen, S., Barber, G., Zhao, H., Szuba, P., Labataille, J. & Manjunathaiah, J. 2002. Investigation of heat pipe cooling in drilling applications.:: part I: preliminary numerical analysis and verification. International Journal of Machine Tools and Manufacture, 42(5), pp.643-652.

Jia, Y., Kim, B., Hu, D. & Ni, J. 2010. Experimental investigations into near-dry milling EDM of Stellite alloys. International Journal of Machining and Machinability of Materials, 7(1), pp.96-111.

Jianxin, D., Tongkun, C. & Lili, L. 2005. Self-lubricating behaviors of AlO/TiB ceramic tools in dry high-speed machining of hardened steel. Journal of the European Ceramic Society, 25(7), pp.1073-1079.

Jun, S. C. 2005. Lubrication effect of liquid nitrogen in cryogenic machining friction on the tool-chip interface. Journal of Mechanical Science and Technology, 19(4), pp.936-946.

Kakinuma, Y., Kidani, S. & Aoyama, T. 2012. Ultra-precision cryogenic machining of viscoelastic polymers. CIRP Annals - Manufacturing Technology, 61(1), pp.79-82.

Kakinuma, Y., Yasuda, N. & Aoyama, T. 2008. Micromachining of Soft Polymer Material applying Cryogenic Cooling. Journal of Advanced Mechanical Design, Systems, and Manufacturing, 2(4), pp.560-569.

Kaladhar, M., Subbaiah, K. V. & Rao, C. 2012. Parametric optimization during machining of AISI 304 Austenitic Stainless Steel using CVD coated DURATOMIC™ cutting insert. International Journal of Industrial Engineering Computations, 3(4), pp.

Kalia, S. 2009. Cryogenic Processing: A Study of Materials at Low Temperatures. Journal of Low Temperature Physics, 158(5-6), pp.934-945.

Kalyankumar, K. & Choudhury, S. 2008. Investigation of tool wear and cutting force in cryogenic machining using design of experiments. Journal of Materials Processing Technology, 203(1-3), pp.95-101.

Kamata, Y. & Obikawa, T. 2007. High speed MQL finish-turning of Inconel 718 with different coated tools. Journal of Materials Processing Technology, 192-193, pp.281-286.

Kamody, D. J. 1999. Cryogenics Process Update. Advanced Materials & Processes, 155(6), pp.H67-H69.

Kara, H. 2009. Carbon Impact of Remanufactured Products- End Mill Cutting Tools. Alesbury: Centre for Remanufacturing and Reuse.

Karadzic, I., Masui, A. & Fujiwara, N. 2004. Purification and characterization of a protease from Pseudomonas aeruginosa grown in cutting oil. Journal of Bioscience and Bioengineering, 98(3), pp.145-152.

Karassik, I. J., Messina, J. P., Cooper, P. & Heald, C. C. 2008. Pump Handbook (4th Edition). McGraw-Hill.

Kaya, B., Oysu, C. & Ertunc, H. M. 2011. Force-torque based on-line tool wear estimation system for CNC milling of Inconel 718 using neural networks. Advances in Engineering Software, 42(3), pp.76-84.

Kaynak, Y. 2014. Evaluation of machining performance in cryogenic machining of Inconel 718 and comparison with dry and MQL machining. The International Journal of Advanced Manufacturing Technology, pp.1-15.

Ke, Y.-L., Dong, H.-Y., Liu, G. & Zhang, M. 2009. Use of nitrogen gas in high-speed milling of Ti-6Al-4V. Transactions of Nonferrous Metals Society of China, 19(3), pp.530-534.

Kenda, J., Pusavec, F. & Kopac, J. 2011. Analysis of Residual Stresses in Sustainable Cryogenic Machining of Nickel Based Alloy—Inconel 718. Journal of Manufacturing Science and Engineering, 133, pp.041009-7.

Khan, A. & Ahmed, M. 2008. Improving tool life using cryogenic cooling. Journal of Materials Processing Technology, 196(1-3), pp.149-154.

Khan, A. A., Ali, M. Y. & Haque, M. 2010. A new approach of applying cryogenic coolant in turning AISI 304 stainless steel. International Journal of Mechanical and Materials Engineering (IJMME), 5(2), pp.171-174.

Khan, Z., Prasad, B. & Singh, T. 1997. Machining condition optimization by genetic algorithms and simulated annealing. Computers & Operations Research, 24(7), pp.647-657.

Khidhir, B. A. & Mohamed, B. Analyzing the effect of cutting parameters on surface roughness and tool wear when machining nickel based hastelloy–276. 2011. IOP Publishing, 012043.

Kim, S., Lee, D., Kang, M. & Kim, J. 2001. Evaluation of machinability by cutting environments in high-speed milling of difficult-to-cut materials. Journal of Materials Processing Technology, 111(1-3), pp.256-260.

Kirby, E. D. 2010. Optimizing the Turning Process Toward an Ideal Surface Roughness Target. Journal of Industrial Technology, 26(1), pp.1-11.

Kitagawa, T., Kubo, A. & Maekawa, K. 1997. Temperature and wear of cutting tools in high-speed machining of Inconel 718 and Ti-6Al-6V-2Sn. Wear, 202(2), pp.142-148.

Klocke, F. & Eisenblätter, G. 1997. Dry Cutting. CIRP Annals - Manufacturing Technology, 46(2), pp.519-526.

Klocke, F., Krämer, A., Sangermann, H. & Lung, D. Thermo-Mechanical Tool Load during High Performance Cutting of Hard-to-Cut Materials. In: WEGENER, K., ed. 5th CIRP Conference on High Performance Cutting, 2012 Zürich. Elsevier, 312-317.

Klocke, F., Lung, D., Eisenblätter, G., Müller-Hummel, P., Pröll, H. & Rehbein, W. 2004. Minimalmengenkühlschmierung- Systeme, Werkzeuge und Medien, (1998). K. Weinert, I. Inasaki, J.W. Sutherland, T. Wakabayashi, Dry machining and minimum lubrication, Cirp Annals - Manufacturing Technology, 53(2), pp.511-537.

Koh, D. & Goh, C. L. 1998. Occupational dermatology. Clinics in Dermatology, 16(1), pp.113-118.

Komanduri, R. & Von Turkovich, B. 1981. New observations on the mechanism of chip formation when machining titanium alloys. Wear, 69(2), pp.179-188.

Koneshlou, M., Meshinchi Asl, K. & Khomamizadeh, F. 2011. Effect of cryogenic treatment on microstructure, mechanical and wear behaviors of AISI H13 hot work tool steel. Cryogenics, 51(1), pp.55-61.

Kopac, J. 2009. Achievements of sustainable manufacturing by machining. Manufacturing Engineering, 34(2), pp.180-187.

Koplev, A., Lystrup, A. & Vorm, T. 1983. The cutting process, chips, and cutting forces in machining CFRP. Composites, 14(4), pp.371-376.

Korkut, I., Kasap, M., Ciftci, I. & Seker, U. 2004. Determination of optimum cutting parameters during machining of AISI 304 austenitic stainless steel. Materials & Design, 25(4), pp.303-305.

Krain, H., Sharman, A. & Ridgway, K. 2007. Optimisation of tool life and productivity when end milling Inconel 718TM. Journal of Materials Processing Technology, 189(1-3), pp.153-161.

Kustas, F. M., Fehrehnbacher, L. L. & Komanduri, R. 1997. Nanocoatings on Cutting Tools For Dry Machining. CIRP Annals - Manufacturing Technology, 46(1), pp.39-42.

Lasri, L., Nouari, M. & Mansori, M. E. 2011. Wear resistance and induced cutting damage of aeronautical FRP components obtained by machining. Wear, 271(9–10), pp.2542-2548.

Leshock, C. E. & Kim, J. N. 2001. Plasma enhanced machining of Inconel 718: modeling of workpiece temperature with plasma heating and experimental results. International Journal of Machine Tools and Manufacture, 41(6), pp.877-897.

Leskovsek, V., Kalin, M. & Vizintin, J. 2006. Influence of deep-cryogenic treatment on wear resistance of vacuum heat-treated HSS. Vacuum, 80(6), pp.507-518.

Li, K.-M. & Liang, S. Y. 2006. Modeling of Cutting Temperature in Near Dry Machining. Journal of Manufacturing Science and Engineering, 128(2), pp.416.

Li, K.-M. & Liang, S. Y. 2007. Modeling of cutting forces in near dry machining under tool wear effect. International Journal of Machine Tools and Manufacture, 47(7-8), pp.1292-1301.

Li, S., Xie, Y. & Wu, X. 2010. Hardness and toughness investigations of deep cryogenic treated cold work die steel. Cryogenics, 50(2), pp.89-92.

Liao, Y., Lin, H. & Wang, J. 2008. Behaviors of end milling Inconel 718 superalloy by cemented carbide tools. Journal of Materials Processing Technology, 201(1-3), pp.460-465.

Lin, C., Hung, Y., Liu, W. C. & Kang, S. W. 2001. Machining and fluidity of 356Al/SiC (p) composites. Journal of Materials Processing Technology, 110(2), pp.152-159.

Lingard, D. 2011. Technical Meeting. Renishaw Plc, Stonehouse.

Liu, J. & Kevinchou, Y. 2007. On temperatures and tool wear in machining hypereutectic Al–Si alloys with vortex-tube cooling. International Journal of Machine Tools and Manufacture, 47(3-4), pp.635-645.

Liu, J., Yamazaki, K., Ueda, H., Narutaki, N. & Yamane, Y. 2002. Machinability of Pearlitic Cast Iron With Cubic Boron Nitride (CBN) Cutting Tools. Journal of Manufacturing Science and Engineering, 124(4), pp.820.

Lockheed Martin Co. 2011. New Titanium Machining Process Supports Affordability of Lockheed Martin F-35 [Online]. Bethesda, MD: Lockheed Martin Co. Official Website. Available: http://www.lockheedmartin.com/news/press_releases/2011/110915ae_f35_newtitanium.html [Accessed 6 Jan 2012].

López De Lacalle, L., Perez-Bilbatua, J., Sanchez, J., Llorente, J., Gutierrez, A. & Alboniga, J. 2000. Using high pressure coolant in the drilling and turning of low machinability alloys. The International Journal of Advanced Manufacturing Technology, 16(2), pp.85-91.

López De Lacalle, L. N., Angulo, C., Lamikiz, A. & Sánchez, J. A. 2006. Experimental and numerical investigation of the effect of spray cutting fluids in high speed milling. Journal of Materials Processing Technology, 172(1), pp.11-15.

Machado, A. R., Wallbank, J., Pashby, I. R. & Ezugwu, E. O. 1998. Tool Performance and Chip Control When Machining Ti6A14V and Inconel 901 Using High Pressure Coolant Supply. Machining Science and Technology, 2(1), pp.1-12.

Machai, C. & Biermann, D. 2011. Machining of β-titanium-alloy Ti–10V–2Fe–3Al under cryogenic conditions: Cooling with carbon dioxide snow. Journal of Materials Processing Technology, pp.

MAG. 2012. Cryogenics [Online]. New York. Available: http://www.mag-ias.com/en/mag/technologies/cryogenics.html [Accessed 15 Jan 2012].

Manimaran, G., Pradeep Kumar, M. & Venkatasamy, R. 2014. Influence of cryogenic cooling on surface grinding of stainless steel 316. Cryogenics, 59(0), pp.76-83.

Marquardt, E., Le, J. & Radebaugh, R. 2002. Cryogenic material properties database. Cryocoolers 11, pp.681-687.

Mason, R. L., Gunst, R. F. & Hess, J. L. 2003. Statistical Design and Analysis of Experiments - With Applications to Engineering and Science (2nd Edition). Hoboken, New Jersey: John Wiley & Sons.

Mathworks 2013. MATLAB R2013b. Natick, MA, USA: The MathWorks Inc.

Mattsby-Baltzer, I., Sandin, M., Ahlstrom, B., Allenmark, S., Edebo, M., Falsen, E., Pedersen, K., Rodin, N., Thompson, R. A. & Edebo, L. 1989. Microbial growth and accumulation in industrial metal-working fluids. Applied and Environmental Microbiology, 55(10), pp.2681-2689.

Merchant, M. E. 1945. Mechanics of the Metal Cutting Process. I. Orthogonal Cutting and a Type 2 Chip. Journal of Applied Physics, 16(5), pp.267-275.

Meza, F., Chen, L. & Hudson, N. 2013. Investigation of respiratory and dermal symptoms associated with metal working fluids at an aircraft engine manufacturing facility. American journal of industrial medicine, 56(12), pp.1394-1401.

Microsoft Corporation 2010. Microsoft Excel. Redmond, Washington: Microsoft Corporation.

Miller, S. 1996. Advanced materials mean advanced engines. Interdisciplinary Science Reviews, 21(2), pp.117-129.

Minitab Inc. 2010. Minitab 16 statistical software. State College, PA.

Mirer, F. E. 2010. New evidence on the health hazards and control of metalworking fluids since completion of the OSHA advisory committee report. American journal of industrial medicine, 53(8), pp.792-801.

Mishima, K., Kakinuma, Y. & Aoyama, T. 2010. Pre-Deformation-Assisted Cryogenic Micromachining for Fabrication of Three-dimensional Unique Micro Channels. Journal of Advanced Mechanical Design, Systems and Manufacturing, 4(5), pp.936-947.

Molinari, A., Pellizzari, M., Gialanella, S., Straffelini, G. & Stiasny, K. H. 2001. Effect of deep cryogenic treatment on the mechanical properties of tool steels. Journal of Materials Processing Technology, 118(1-3), pp.350-355.

Montgomery, D. C. 2013. Design and Analysis of Experiments (8th Edition), New York, John Wiley & Sons.

Mukherjee, I. & Ray, P. K. 2006. A review of optimization techniques in metal cutting processes. Computers & Industrial Engineering, 50(1), pp.15-34.

Nabhani, F. 2001. Machining of aerospace titanium alloys. Robotics and Computer-Integrated Manufacturing, 17(1-2), pp.99-106.

Nalbant, M., Gökkaya, H. & Sur, G. 2007. Application of Taguchi method in the optimization of cutting parameters for surface roughness in turning. Materials & Design, 28(4), pp.1379-1385.

Nalbant, M. & Yildiz, Y. 2011. Effect of cryogenic cooling in milling process of AISI 304 stainless steel. Transactions of Nonferrous Metals Society of China, 21(1), pp.72-79.

Nath, C., Kapoor, S. G., Srivastava, A. K. & Iverson, J. 2014. Study of Droplet Spray Behavior of an Atomization-Based Cutting Fluid Spray System for Machining Titanium Alloys. Journal of Manufacturing Science and Engineering, 136(2), pp.021004-021004.

Naves, V. T. G., Da Silva, M. B. & Da Silva, F. J. 2013. Evaluation of the effect of application of cutting fluid at high pressure on tool wear during turning operation of AISI 316 austenitic stainless steel. Wear, 302(1–2), pp.1201-1208.

Newkirk, J. & Hawk, J. A. 2001. Abrasive wear properties of Cr–Cr_3Si composites. Wear, 251(1), pp.1361-1371.

Nian, C. Y., Yang, W. H. & Tarng, Y. S. 1999. Optimization of turning operations with multiple performance characteristics. Journal of Materials Processing Technology, 95(1–3), pp.90-96.

Nisa. 2011. NISA [Online]. Troy, MI: Cranes Software International Limited. Available: http://nisasoftware.com [Accessed 13 Oct 2011].

Noorul Haq, A. & Tamizharasan, T. 2005. Investigation of the effects of cooling in hard turning operations. The International Journal of Advanced Manufacturing Technology, 30(9-10), pp.808-816.

Nor Khairusshima, M. K., Che Hassan, C. H., Jaharah, A. G., Amin, A. K. M. & Md Idriss, A. N. 2013. Effect of chilled air on tool wear and workpiece quality during milling of carbon fibre-reinforced plastic. Wear, 302(1–2), pp.1113-1123.

Oberg, E., Jones, F. D., Horton, H. L. & Ryffel, H. H. (eds.) 2004. Machinery's Handbook (27th Edition) & Guide to Machinery's Handbook: Industrial Press.

Ohkubo, C., Hosoi, T., Ford, J. P. & Watanabe, I. 2006. Effect of surface reaction layer on grindability of cast titanium alloys. Dental Materials, 22(3), pp.268-274.

Ohmori, H., Katahira, K., Akinou, Y., Komotori, J. & Mizutani, M. 2006. Investigation on Grinding Characteristics and Surface-Modifying Effects of Biocompatible Co-Cr Alloy. CIRP Annals - Manufacturing Technology, 55(1), pp.597-600.

Olofson, C. 1961. Machining of Superalloys and Refractory Metals. DTIC Document.

Ostrovskaya, Y. L., Strel'nitskij, V., Kuleba, V. & Gamulya, G. 2001. Friction and wear behaviour of hard and superhard coatings at cryogenic temperatures. Tribology International, 34(4), pp.255-263.

Pahl, G., Wallace, K. & Blessing, L. 2007. Engineering design: a systematic approach, London, Springer.

Pahlitzsch, G. 1953. Gases are good cutting coolants. American Machinist 97(1953), 196, pp.

Palanikumar, K. 2006. Cutting parameters optimization for surface roughness in machining of GFRP composites using Taguchi's method. Journal of reinforced plastics and composites, 25(16), pp.1739-1751.

Paro, J., Hänninen, H. & Kauppinen, V. 2001. Tool wear and machinability of HIPed P/M and conventional cast duplex stainless steels. Wear, 249(3-4), pp.279-284.

Paul, S. & Chattopadhyay, A. 1995. Effects of cryogenic cooling by liquid nitrogen jet on forces, temperature and surface residual stresses in grinding steels. Cryogenics, 35(8), pp.515-523.

Paul, S. & Chattopadhyay, A. 1996a. Determination and control of grinding zone temperature under cryogenic cooling. International Journal of Machine Tools and Manufacture, 36(4), pp.491-501.

Paul, S. & Chattopadhyay, A. 1996b. The effect of cryogenic cooling on grinding forces. International Journal of Machine Tools and Manufacture, 36(1), pp.63-72.

Paul, S. & Chattopadhyay, A. B. 2006. Environmentally Conscious Machining and Grinding with Cryogenic Cooling. Machining Science and Technology, 10(1), pp.87-131.

Paul, S., Dhar, N. & Chattopadhyay, A. 2001. Beneficial effects of cryogenic cooling over dry and wet machining on tool wear and surface finish in turning AISI 1060 steel. Journal of Materials Processing Technology, 116(1), pp.44-48.

Peter, C., Steven, C. & David, L. 1996. Evaporation of Polydisperse Multi Component Oil Droplets. In: Dhar, N.R, et al., Wear behaviour of uncoated carbide insertsunder dry, wet and cryogenic cooling conditions in turning C60 steel. Journal of the Barzilian Society of Mechanical Sciences and Engineering, 2006, 28, pp.146-152.

Petropoulos, G. P., Pandazaras, C. N. & Davim, J. P. 2009. Surface integrity in machining, Springer.

Pittalà, G. M. & Monno, M. 2011. A new approach to the prediction of temperature of the workpiece of face milling operations of Ti-6Al-4V. Applied Thermal Engineering, 31(2-3), pp.173-180.

Polmear, I. 1994. Magnesium alloys and applications. Materials Science and Technology, 10(1), pp.1-16.

Preciado, M., Bravo, P. M. & Alegre, J. M. 2006. Effect of low temperature tempering prior cryogenic treatment on carburized steels. Journal of Materials Processing Technology, 176(1-3), pp.41-44.

Pu, Z., Caruso, S., Umbrello, D., Dillon Jr, O. W., Puleo, D. A. & Jawahir, I. S. 2011a. Analysis of surface integrity in dry and cryogenic machining of AZ31B Mg alloy. Advanced Material Research, 223, pp.439-448.

Pu, Z., Dillon Jr, O. W., Jawahir, I. S. & Puleo, D. A. Microstructural Changes of AZ31 Magnesium Alloys Induced by Cryogenic Machining and Its Influence on Corrosion Resistance in Simulated Body Fluid for Biomedical Applications. Proceedings of the 2010 ASME Int MSEC, 2010.

Pu, Z., Puleo, D. A., Dillon Jr, O. W. & Jawahir, I. S. Controlling the biodegradation rate of magnesium-based implants through surface nanocrystallization induced by cryogenic machining. Proceeding of Magnesium Technology, 2011b. The Minerals, Metals & Material Society.

Pu, Z., Yang, S., Song, G. L., Dillon Jr, O., Puleo, D. & Jawahir, I. 2011c. Ultrafine-grained surface layer on Mg-Al-Zn alloy produced by cryogenic burnishing for enhanced corrosion resistance. Scripta Materialia, 65, pp.520-523.

Pusavec, F. 2012. Porous tungsten machining under cryogenic conditions. International Journal of Refractory Metals and Hard Materials, (In Press), (0), pp.

Pusavec, F., Hamdi, H., Kopac, J. & Jawahir, I. S. 2011. Surface integrity in cryogenic machining of nickel based alloy—Inconel 718. Journal of Materials Processing Technology, 211(4), pp.773-783.

Pusavec, F. & Kopac, J. 2009. Achieving and Implementation of Sustainability Principles in Machining Processes. Journal of Advances in Production Engineering and Management, 3-4, pp.58-69.

Pusavec, F., Kramar, D., Krajnik, P. & Kopac, J. 2010. Transitioning to sustainable production – part II: evaluation of sustainable machining technologies. Journal of Cleaner Production, 18(12), pp.1211-1221.

Rahim, E. A., Sasahara, H., 2011. A study of the effect of palm oil as MQL lubricant on high speed drilling of titanium. Tribology International, 44(3), pp.309-317.

Rahman, M., Kumar, A. S., Salam, M. U. & Ling, M. 2003a. Effect of chilled air on machining performance in end milling. The International Journal of Advanced Manufacturing Technology, 21(10), pp.787-795.

Rahman, M., Wong, Y. S. & Zareena, A. R. 2003b. Machinability of titanium alloys. JSME International Journal Series C, 46(1), pp.107-115.

Ramji, B. R., Murthy, H. N. N., Krishna, M. & Raghu, M. J. 2010. Performance Study of Cryogenically Treated HSS Drills in Drillilg Gray Cast Iron Using Orthogonal Array Technique. Research Journal of Applied Sciences, Engineering and Technology, 2(5), pp.487-491.

Ravi, S. & Kumar, M. P. 2011. Experimental investigations on cryogenic cooling by liquid nitrogen in the end milling of hardened steel. Cryogenics, 51(9), pp.509-515.

Rech, J. & Moisan, A. 2003. Surface integrity in finish hard turning of case-hardened steels. International Journal of Machine Tools and Manufacture, 43(5), pp.543-550.

Reitz, P. 1919. In: Shaw, M.C. and Smith, P.A, 1956. Methods of applying cutting fluids, American Society for Tool and Manufacturing Engineers (ASTME), Paper No. MR56-154, RR-3.

Rivero, A., Aramendi, G., Herranz, S. & López De Lacalle, L. 2006. An experimental investigation of the effect of coatings and cutting parameters on the dry drilling performance of aluminium alloys. The International Journal of Advanced Manufacturing Technology, 28(1), pp.1-11.

Roskill, 2013. Titanium Metal: Market Outlook to 2018 [online]. London, Roskill Information Services Limited. Available: http://www.roskill.com/reports/minor-and-light-metals/titanium-metal/leaflet [Accessed 3 Mar 2014]

Rozzi, J. C., Sanders, J. K. & Chen, W. 2011. The Experimental and Theoretical Evaluation of an Indirect Cooling System for Machining. Journal of Heat Transfer, 133(3), pp.031006.

Sales, W., Becker, M., Barcellos, C. S., Jr, J. L., Bonney, J. & Ezugwu, E. O. 2009. Tribological behaviour when face milling AISI 4140 steel with minimum quantity fluid application. Industrial Lubrication and Tribology, 61(2), pp.84-90.

Sarma, D. & Dixit, U. 2007. A comparison of dry and air-cooled turning of grey cast iron with mixed oxide ceramic tool. Journal of Materials Processing Technology, 190(1-3), pp.160-172.

Schulz, H. & Moriwaki, T. 1992. High-speed Machining. CIRP Annals - Manufacturing Technology, 41(2), pp.637-643.

Seah, K. H. W., Rahman, M. & Yong, K. H. 2003. Performance evaluation of cryogenically treated tungsten carbide cutting tool inserts. Proceedings of the Institution of Mechanical Engineers- Part B Journal of Engineering Manufacture, 217(1), pp.29-43.

Seong, S., Younossi, O., Goldsmith, B. W., 2009. Titanium: Base, Price Trends and Technology Initiatives. Santa Monica, RAND Corporation.

Shapiro, S. S. & Wilk, M. B. 1965. An analysis of variance test for normality (complete samples). Biometrika, 52(3/4), pp.591-611.

Sharma, J. & Sidhu, B. S. 2014. Investigation of effects of dry and near dry machining on AISI D2 steel using vegetable oil. Journal of Cleaner Production, 66(0), pp.619-623.

Sharma, V. S., Dogra, M. & Suri, N. M. 2009. Cooling techniques for improved productivity in turning. International Journal of Machine Tools and Manufacture, 49(6), pp.435-453.

Sharman, A., Dewes, R. C. & Aspinwall, D. K. 2001. Tool life when high speed ball nose end milling Inconel 718 (TM). Journal of Materials Processing Technology, 118(1-3), pp.29-35.

Shaw, M. C. 1986. Metal cutting principles, Oxford, Oxford University Press.

Shih, A. J., Lewis, M. A. & Strenkowski, J. S. 2004a. End Milling of Elastomers—Fixture Design and Tool Effectiveness for Material Removal. Journal of Manufacturing Science and Engineering, 126(1), pp.115-123.

Shih, A. J., Luo, J., Lewis, M. A. & Strenkowski, J. S. 2004b. Chip Morphology and Forces in End Milling of Elastomers. Journal of Manufacturing Science and Engineering, 126(1), pp.124-130.

Shokrani, A., Dhokia, V., Imani-Asrai, R. & Newman, S. T. 2012a. An Initial Study of the Effect of Using Liquid Nitrogen Coolant on the Surface Roughness of Inconel 718 Nickel-Based Alloy in CNC Milling. 45th CIRP Conference on Manufacturing Systems. Athenes: Elsevier.

Shokrani, A., Dhokia, V., Munoz-Escalona, P. & Newman, S. 2013. State-of-the-art cryogenic machining and processing. International Journal of Computer Integrated Manufacturing, 26(7), pp.616-648.

Shokrani, A., Dhokia, V. & Newman, S. T. 2012b. Environmentally conscious machining of difficult-to-machine materials with regard to cutting fluids. International Journal of Machine Tools and Manufacture, 57, pp.83-101.

Shokrani, A., Dhokia, V. & Newman, S. T. 2012c. Evaluation of Cryogenic CNC Milling of Ti-6Al-4V Titanium Alloy. 22nd International Conference on Flexible Automation and Intelligent Manufacturing. Helsinki-Stockholm.

Shokrani, A., Dhokia, V. & Newman, S. T. 2012d. Study of the Effects of Cryogenic Machining on the Machinability of Ti-6Al-4V Titanium Alloy. 12th Euspen International Conference. Stockholm.

Song, Y., Park, C.-H. & Moriwaki, T. 2010. Mirror finishing of Co-Cr-Mo alloy using elliptical vibration cutting. Precision Engineering, 34(4), pp.784-789.

Sreejith, P. & Ngoi, B. 2000. Dry machining: machining of the future. Journal of Materials Processing Technology, 101(1-3), pp.287-291.

Sreeramareddy, T., Sornakumar, T., Venkataramareddy, M. & Venkatram, R. 2009. Machinability of C45 steel with deep cryogenic treated tungsten carbide cutting tool inserts. International Journal of Refractory Metals and Hard Materials, 27(1), pp.181-185.

Staiger, M. P., Pietak, A. M., Huadmai, J. & Dias, G. 2006. Magnesium and its alloys as orthopedic biomaterials: A review. Biomaterials, 27(9), pp.1728-1734.

Stewart, H. A. 2004. Cryogenic treatment of tungsten carbide reduces tool wear when machining medium density fiberboard. Forest products journal, 54(2), pp.53-56.

Strano, M., Chiappini, E., Tirelli, S., Albertelli, P. & Monno, M. 2013. Comparison of Ti6Al4V machining forces and tool life for cryogenic versus conventional cooling. Proceedings of the Institution of Mechanical Engineers, Part B: Journal of Engineering Manufacture, 227(9), pp.1403-1408.

Su, Y., He, N., Li, L., Iqbal, A., Xiao, M., Xu, S. & Qiu, B. 2007. Refrigerated cooling air cutting of difficult-to-cut materials. International Journal of Machine Tools and Manufacture, 47(6), pp.927-933.

Su, Y., He, N., Li, L. & Li, X. 2006. An experimental investigation of effects of cooling/lubrication conditions on tool wear in high-speed end milling of Ti-6Al-4V. Wear, 261(7-8), pp.760-766.

Sun, S., Brandt, M. & Dargusch, M. S. 2010. Machining Ti–6Al–4V alloy with cryogenic compressed air cooling. International Journal of Machine Tools and Manufacture, 50(11), pp.933-942.

Sutherland, J. W., Kulur, V. N., King, N. C. & Von Turkovich, B. F. 2000. An Experimental Investigation of Air Quality in Wet and Dry Turning. CIRP Annals - Manufacturing Technology, 49(1), pp.61-64.

Tanaka, T. & Akasawa, T. 1999. Machinability of hypereutectic silicon-aluminum alloys. Journal of Materials Engineering and Performance, 8(4), pp.463-468.

Tarter, J. O., Effgen, M., Pusavec, F. & Jawahir, I. Cryogenic machining of porous tungsten for dispenser cathode applications. Vacuum Electronics Conference, 2008. IVEC 2008. IEEE International, 2008. IEEE, 293-294.

Taylor, F. W. 1907. On the art of cutting metals, New York, American Society of Mechanical Engineers.

Thiele, J. D. & Melkote, S. N. 1999. Effect of cutting edge geometry and workpiece hardness on surface generation in the finish hard turning of AISI 52100 steel. Journal of Materials Processing Technology, 94(2-3), pp.216-226.

Timmerhaus, K. D. & Reed, R. P. 2007. Cryogenic engineering: fifty years of progress, Springer Verlag.

Trent, E. M. & Wright, P. K. 2000. Metal Cutting, Oxford, Butterworth-Heinemann.

Truesdale, S. & Shin, Y. 2009. Microstructural Analysis and Machinability Improvement of Udimet 720 Via Cryogenic Milling. Machining Science and Technology, 13(1), pp.1-19.

Tsai, H. & Hocheng, H. 1998. Investigation of the transient thermal deflection and stresses of the workpiece in surface grinding with the application of a cryogenic magnetic chuck. Journal of Materials Processing Technology, 79(1-3), pp.177-184.

Tsao, C. C. & Hocheng, H. 2004. Taguchi analysis of delamination associated with various drill bits in drilling of composite material. International Journal of Machine Tools and Manufacture, 44(10), pp.1085-1090.

Uehara, K. & Kumagai, S. 1968. Chip formation, surface roughness and cutting force in cryogenic machining. Annals of CIRP, 17(1), pp.409-416.

Uehara, K. & Kumagai, S. 1970. Characteristics of tool wear in cryogenic machining. Annals of CIRP, 18, pp.273-277.

Ulutan, D. & Ozel, T. 2011. Machining induced surface integrity in titanium and nickel alloys: A review. International Journal of Machine Tools and Manufacture, 51(3), pp.250-280.

Umbrello, D. 2013. Investigation of surface integrity in dry machining of Inconel 718. The International Journal of Advanced Manufacturing Technology, 69(9-12), pp.2183-2190.

Umbrello, D., Caruso, S., Yang, S., Crea, F., Dillon Jr, O. & Jawahir, I. The Effect of Cryogenic Cooling on White Layer Formation in Hard Machining. Proceedings of the ASME 2011 International Mechanical Engineering Congress & Exposition, 2011 Colorado, USA.

Umbrello, D., Micari, F. & Jawahir, I. S. 2012. The effects of cryogenic cooling on surface integrity in hard machining: A comparison with dry machining. CIRP Annals - Manufacturing Technology, 61(1), pp.103-106.

Unist. 2012. UNIST, Inc. Official Website [Online]. Available: http://www.unist.com/aboutus.htm [Accessed 5 Jan 2012].

Venkata Rao, R. & Pawar, P. J. 2010. Parameter optimization of a multi-pass milling process using non-traditional optimization algorithms. Applied Soft Computing, 10(2), pp.445-456.

Venugopal, K., Paul, S. & Chattopadhyay, A. 2007a. Growth of tool wear in turning of Ti-6Al-4V alloy under cryogenic cooling. Wear, 262(9-10), pp.1071-1078.

Venugopal, K., Paul, S. & Chattopadhyay, A. 2007b. Tool wear in cryogenic turning of Ti-6Al-4V alloy. Cryogenics, 47(1), pp.12-18.

Venugopal, K., Tawade, R., Prashanth, P., Paul, S. & Chattopadhyay, A. 2003. Turning of titanium alloy with TiB 2-coated carbides under cryogenic cooling. Proceedings of the Institution of Mechanical Engineers, Part B: Journal of Engineering Manufacture, 217(12), pp.1697-1707.

Wang, Z. 2005. High-speed milling of titanium alloys using binderless CBN tools. International Journal of Machine Tools and Manufacture, 45(1), pp.105-114.

Wang, Z. & Rajurkar, K. 1997. Wear of CBN tool in turning of silicon nitride with cryogenic cooling. International Journal of Machine Tools and Manufacture, 37(3), pp.319-326.

Wang, Z. & Rajurkar, K. 2000. Cryogenic machining of hard-to-cut materials. Wear, 239(2), pp.168-175.

Wang, Z., Rajurkar, K., Fan, J. & Petrescu, G. 2002. Cryogenic Machining of Tantalum. Journal of Manufacturing Processes, 4(2), pp.122-127.

Wang, Z., Rajurkar, K. & Murugappan, M. 1996. Cryogenic PCBN turning of ceramic (Si3N4). Wear, 195(1-2), pp.1-6.

Wang, Z. G., Rahman, M., Wong, Y. S. & Sun, J. 2005. Optimization of multi-pass milling using parallel genetic algorithm and parallel genetic simulated annealing. International Journal of Machine Tools and Manufacture, 45(15), pp.1726-1734.

Wang, Z. Y., Rajurkar, K., Fan, J., Lei, S., Shin, Y. C. & Petrescu, G. 2003. Hybrid machining of Inconel 718. International Journal of Machine Tools and Manufacture, 43(13), pp.1391-1396.

Watanabe, I., Ohkubo, C., Ford, J. P., Atsuta, M. & Okabe, T. 2000. Cutting efficiency of air-turbine burs on cast titanium and dental casting alloys. Dental Materials, 16(6), pp.420-425.

Watch-Commitee 2007. Metal Working Fluids, a potential 'new and emerging issue'. In: Gregg, N. (ed.). Health and Safeftey Executive (HSE).

Weinert, K., Inasaki, I., Sutherland, J. W. & Wakabayashi, T. 2004. Dry Machining and Minimum Quantity Lubrication. CIRP Annals - Manufacturing Technology, 53(2), pp.511-537.

Witte, F., Kaese, V., Haferkamp, H., Switzer, E., Meyer-Lindenberg, A., Wirth, C. J. & Windhagen, H. 2005. In vivo corrosion of four magnesium alloys and the associated bone response. Biomaterials, 26(17), pp.3557-3563.

Xin, Q. 2011. Diesel Engine System Design, Cambridge, Woodhead Publishing.

Yalcin, B., Ozgur, A. & Koru, M. 2009. The effects of various cooling strategies on surface roughness and tool wear during soft materials milling. Materials & Design, 30(3), pp.896-899.

Yang, S.-H., Srinivas, J., Mohan, S., Lee, D.-M. & Balaji, S. 2009. Optimization of electric discharge machining using simulated annealing. Journal of Materials Processing Technology, 209(9), pp.4471-4475.

Yang, S., Pu, Z., Puleo, D. A., Dillon, O. W. & Jawahir, I. S. 2011. Cryogenic Processing of Biomaterials for Improved Surface Integrity and Product Sustainability. In: SELIGER, G., KHRAISHEH, M. M. K. & JAWAHIR, I. S. (eds.) Advances in Sustainable Manufacturing. Springer Berlin Heidelberg.

Yap, T. C., El-Tayeb, N. & Von Brevern, P. 2013. Cutting forces, friction coefficient and surface roughness in machining Ti-5Al-4V-0.6 Mo-0.4 Fe using carbide tool K313 under low pressure liquid nitrogen. Journal of the Brazilian Society of Mechanical Sciences and Engineering, 35(1), pp.11-15.

Yildiz, Y. & Nalbant, M. 2008. A review of cryogenic cooling in machining processes. International Journal of Machine Tools and Manufacture, 48(9), pp.947-964.

Yong, A. Y. L., Seah, K. H. W. & Rahman, M. 2006. Performance of cryogenically treated tungsten carbide tools in milling operations. The International Journal of Advanced Manufacturing Technology, 32(7-8), pp.638-643.

Yuan, S. M., Yan, L. T., Liu, W. D. & Liu, Q. 2011. Effects of cooling air temperature on cryogenic machining of Ti–6Al–4V alloy. Journal of Materials Processing Technology, 211(3), pp.356-362.

Zhang, S., Li, J. F., Sun, J. & Jiang, F. 2009. Tool wear and cutting forces variation in high-speed end-milling Ti-6Al-4V alloy. The International Journal of Advanced Manufacturing Technology, 46(1-4), pp.69-78.

Zhao, Z. & Hong, S. 1992. Cooling strategies for cryogenic machining from a materials viewpoint. Journal of Materials Engineering and Performance, 1(5), pp.669-678.

Zurecki, Z., Ghosh, R. & Frey, J. H. Investigation of White Layers Formed in Conventional and Cryogenic Hard Turning of Steels. Proceedings of IMechE'03, 2003 Washington D.C.: ASME.

Zurecki, Z., Ghosh, R. & Frey, J. H. 2004. Finish-turning of hardened powder metallurgy steel using cryogenic cooling. International journal of powder metallurgy, 40(1), pp.19-31.

Appendices

Appendix A

Manufacturing sketches of cryogenic cooling system

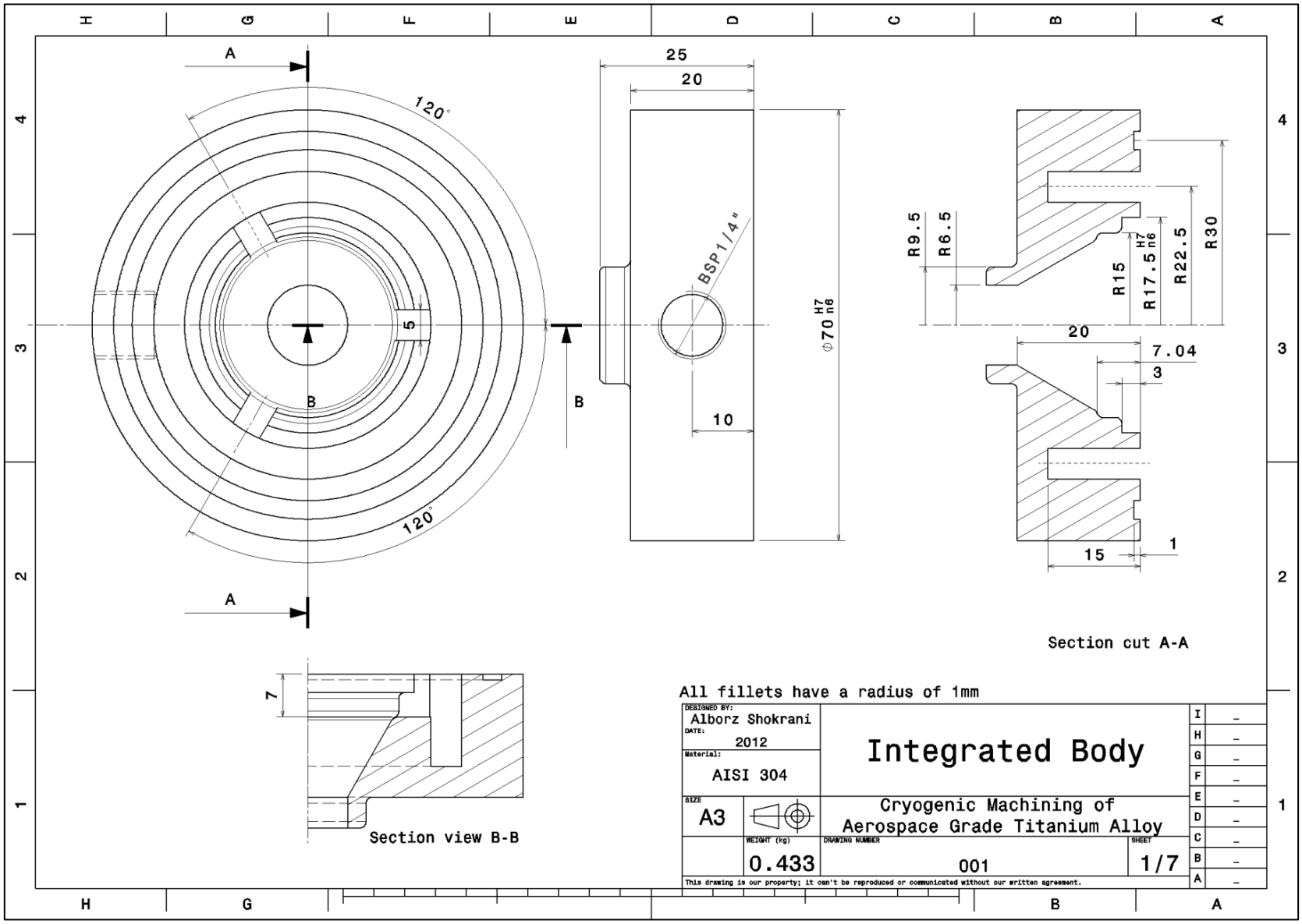
A
120°
120°
A
B
5
B
25
20
BSP1/4"
10
Ø70 H7 n6
R9.5
R6.5
R15
R17.5 H7 n6
R22.5
R30
20
7.04
3
15
1
Section cut A-A
7
Section view B-B
All fillets have a radius of 1mm
DESIGNED BY:
Alborz Shokrani
DATE:
2012
Material:
AISI 304
SIZE
A3
WEIGHT (kg)
0.433
Integrated Body
Cryogenic Machining of
Aerospace Grade Titanium Alloy
DRAWING NUMBER
001
SHEET
1/7
This drawing is our property; it can't be reproduced or communicated without our written agreement.
I
H
G
F
E
D
C
B
A

A2

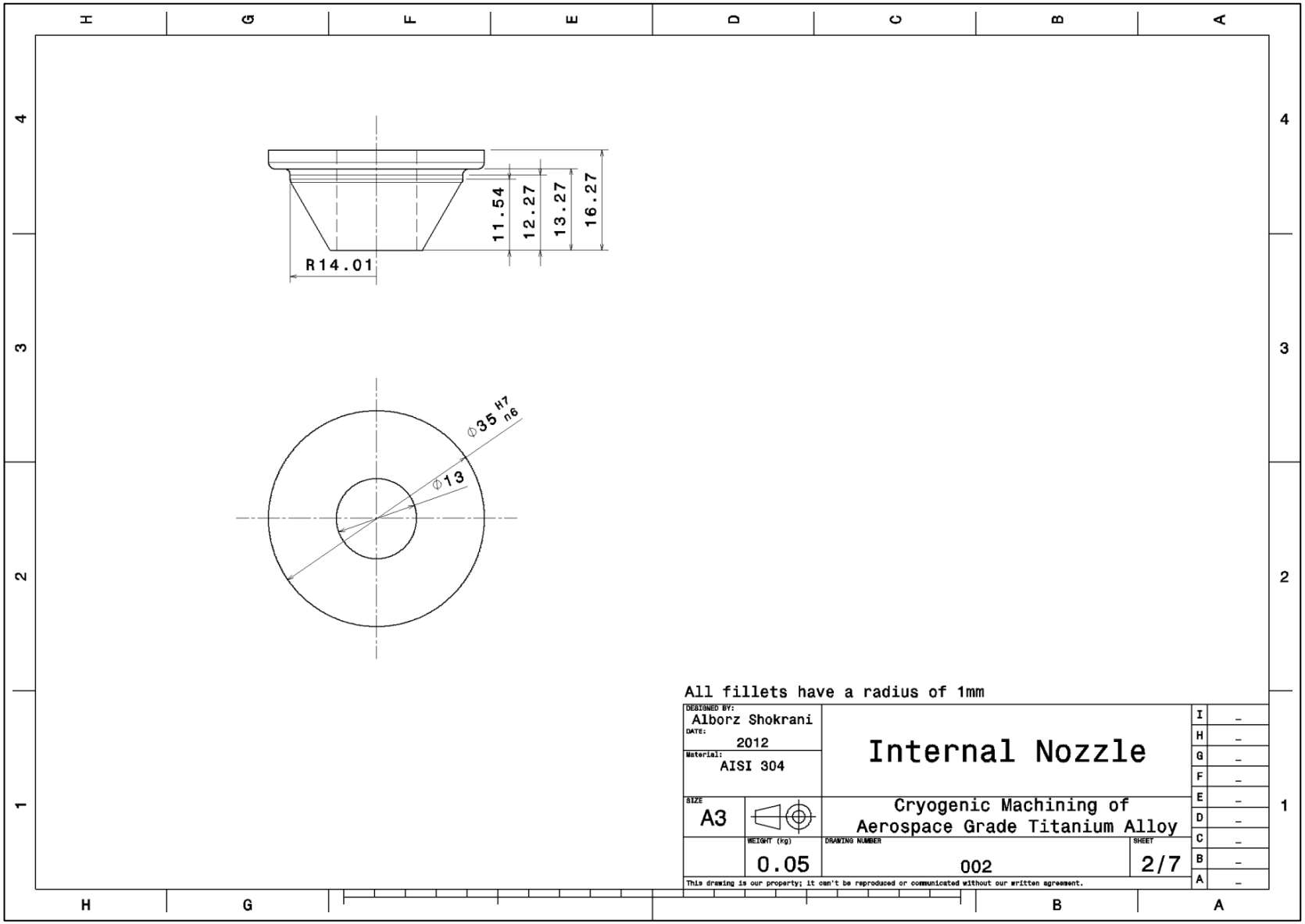
H
G
F
E
D
C
B
A
4
3
2
1
11.54
12.27
13.27
16.27
R14.01
Ø35 H7 n6
Ø13
All fillets have a radius of 1mm
DESIGNED BY:
Alborz Shokrani
DATE:
2012
Material:
AISI 304
SIZE
A3
WEIGHT (kg)
0.05
Internal Nozzle
Cryogenic Machining of
Aerospace Grade Titanium Alloy
DRAWING NUMBER
002
SHEET
2/7
This drawing is our property; it can't be reproduced or communicated without our written agreement.
I
H
G
F
E
D
C
B
A

A3

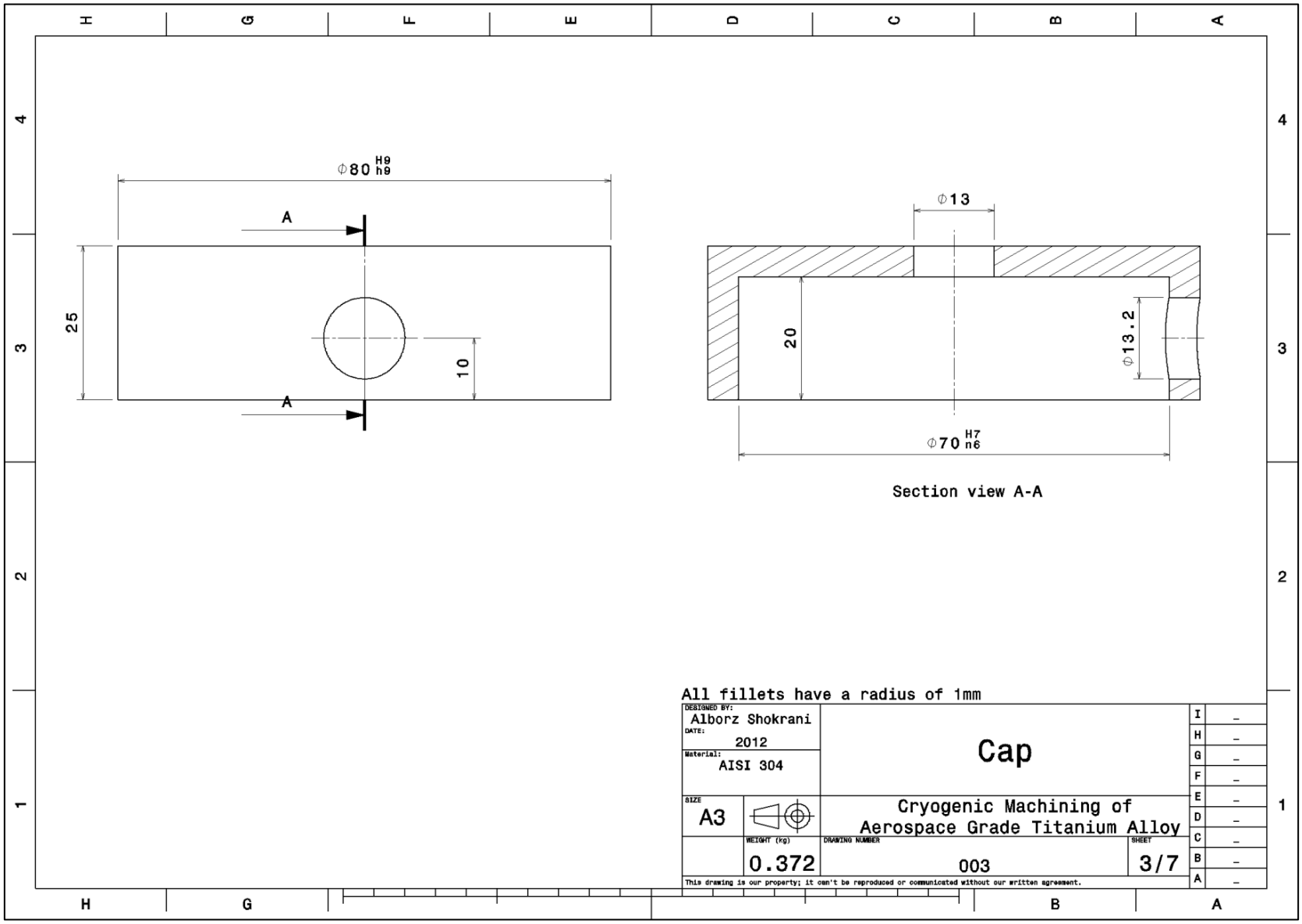
H
G
F
E
D
C
B
A
4
3
2
1
Φ80 H9 h9
A
25
10
A
Φ13
20
Φ13.2
Φ70 H7 n6
Section view A-A
All fillets have a radius of 1mm
DESIGNED BY:
Alborz Shokrani
DATE:
2012
Material:
AISI 304
Cap
SIZE
A3
Cryogenic Machining of
Aerospace Grade Titanium Alloy
WEIGHT (kg)
0.372
DRAWING NUMBER
003
SHEET
3/7
This drawing is our property; it can't be reproduced or communicated without our written agreement.
I
H
G
F
E
D
C
B
A

A4

Quantity	Part Number	Material	Nomenclature	Make/Buy
1	Integrated Body	AISI 304	A	M
1	Internal Nozzle	AISI 304	B	M
1	Cap	AISI 304	C	M

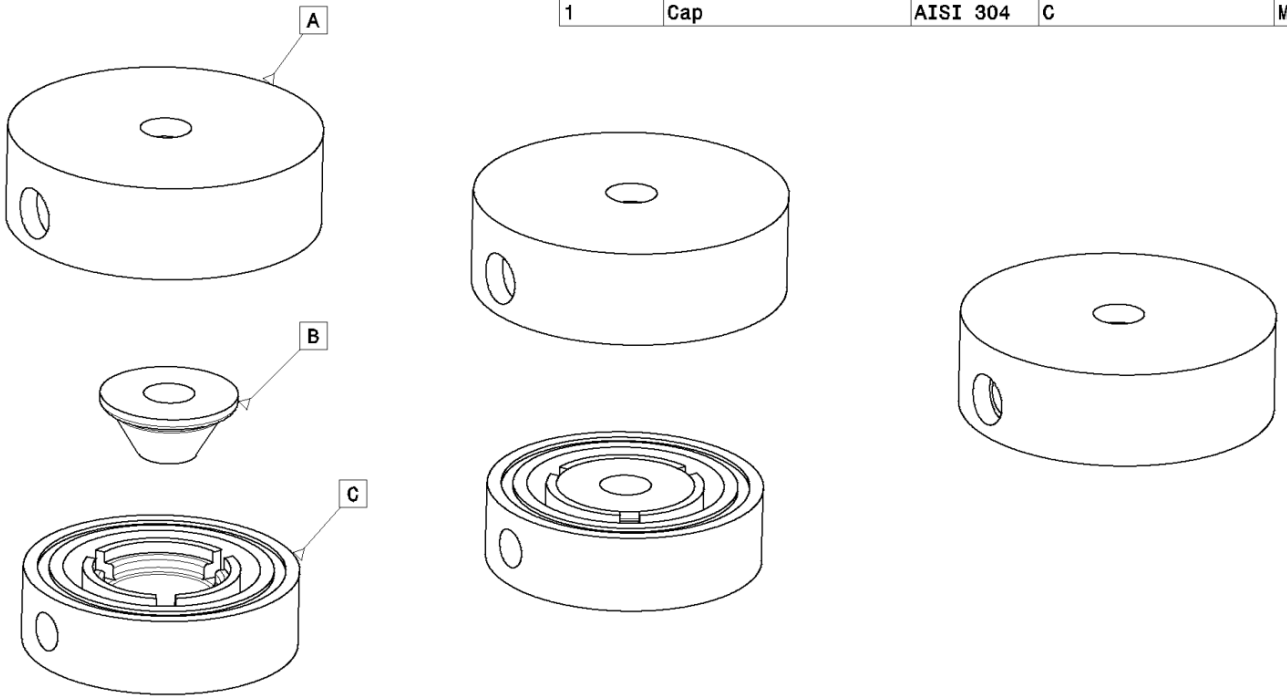

DESIGNED BY: Alborz Shokrani
DATE: 2012

Cryogenic Shower Nozzle

Cryogenic Machining of Aerospace Grade Titanium Alloy

SIZE A3

WEIGHT (kg)

DRAWING NUMBER 100

SHEET 4/7

I	–
H	–
G	–
F	–
E	–
D	–
C	–
B	–
A	–

A5

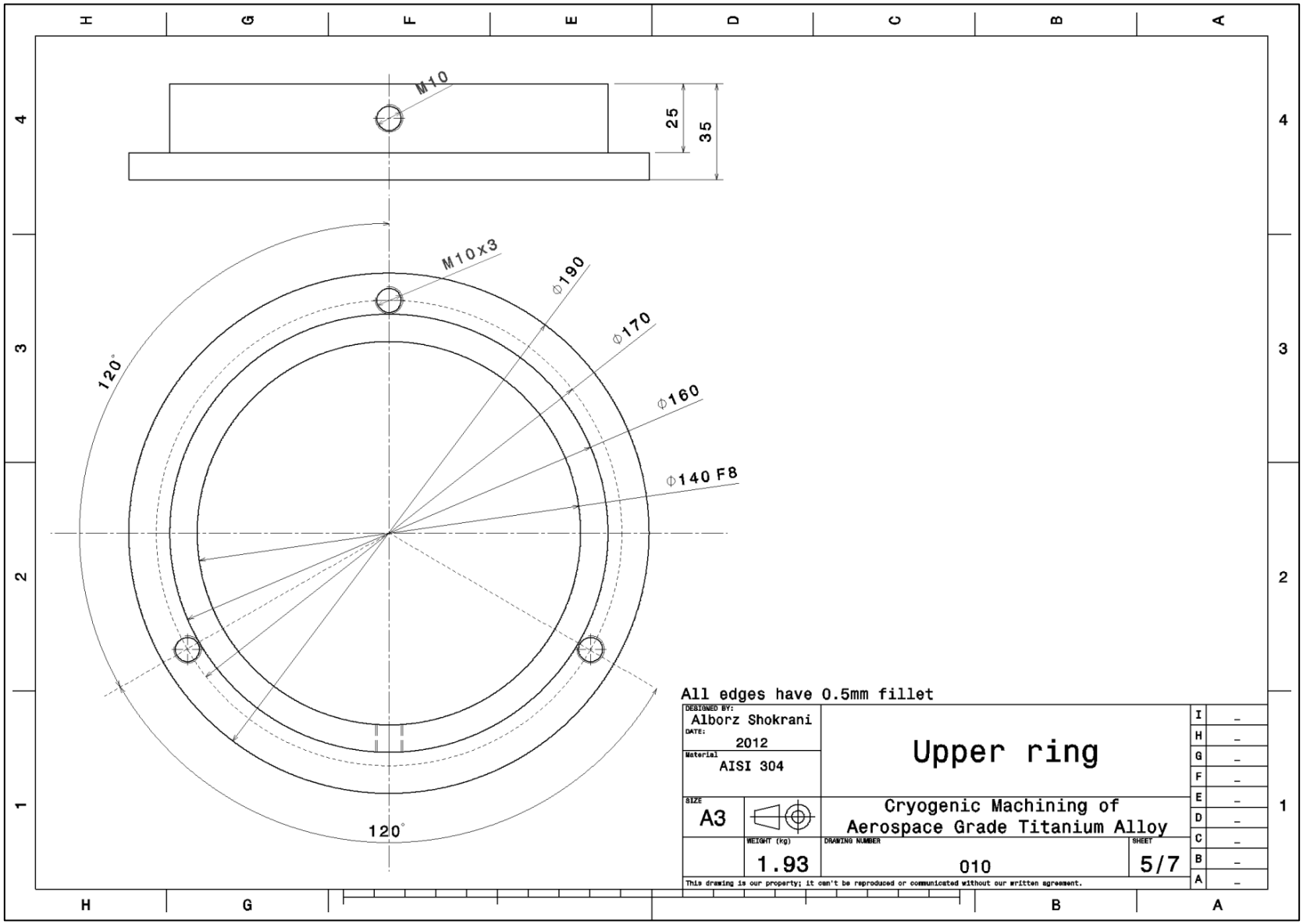
M10
25
35
M10x3
ϕ190
ϕ170
ϕ160
ϕ140 F8
120°
120°
All edges have 0.5mm fillet
DESIGNED BY:
Alborz Shokrani
DATE:
2012
Material
AISI 304
SIZE
A3
WEIGHT (kg)
1.93
Upper ring
Cryogenic Machining of
Aerospace Grade Titanium Alloy
DRAWING NUMBER
010
SHEET
5/7
This drawing is our property; it can't be reproduced or communicated without our written agreement.

A6

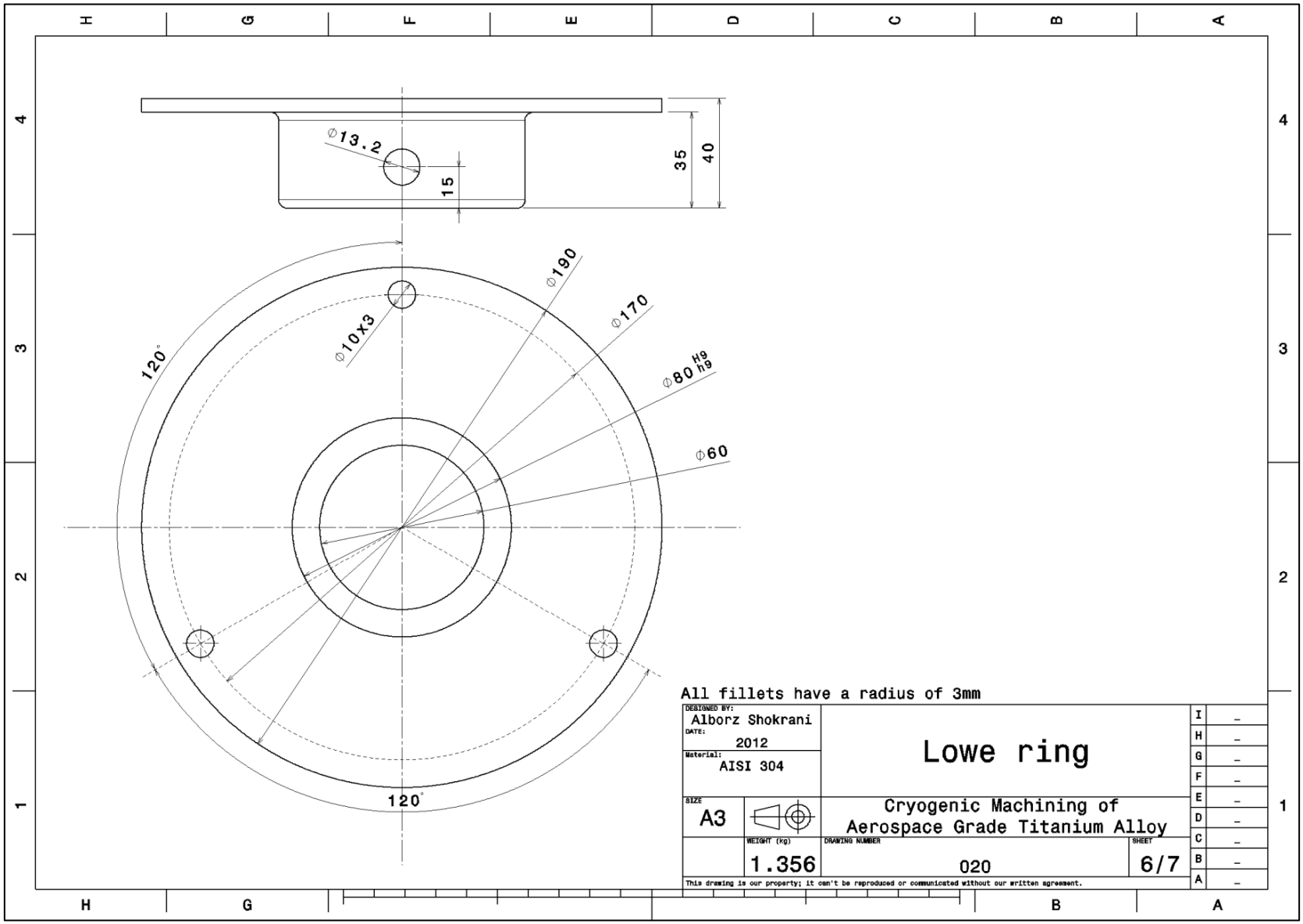
H
G
F
E
D
C
B
A
4
3
2
1
∅13.2
15
35
40
∅190
∅170
∅80 H9/h9
∅60
∅10X3
120°
120°
All fillets have a radius of 3mm
DESIGNED BY:
Alborz Shokrani
DATE:
2012
Material:
AISI 304
SIZE
A3
WEIGHT (kg)
1.356
Lowe ring
Cryogenic Machining of
Aerospace Grade Titanium Alloy
DRAWING NUMBER
020
SHEET
6/7
This drawing is our property; it can't be reproduced or communicated without our written agreement.
I
H
G
F
E
D
C
B
A

A7

Bill of Material: Total assembly

Quantity	Part Number	Material	Nomenclature	Made/Buy
1	Lower ring	AISI 304	A	M
1	Final Nozzle	Assembly	B	M
1	Upper ring	AISI 304	C	M
3	M10bar	AISI 1037	D	M
9	M10 washer	AISI 1037	E	B
9	M10Nut	AISI 1037	F	B
1	M10screw	AISI 1037	G	B

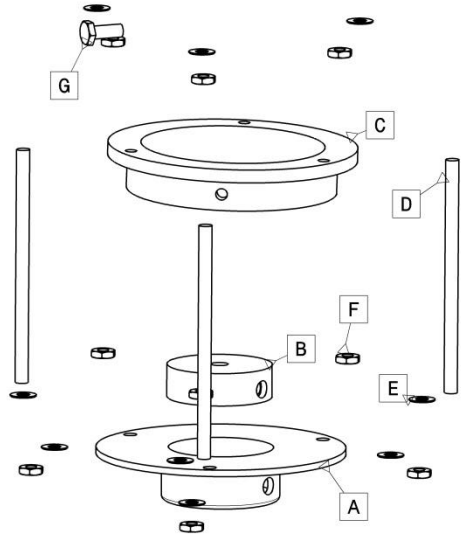

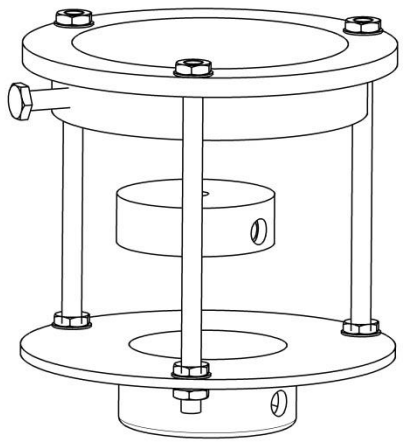

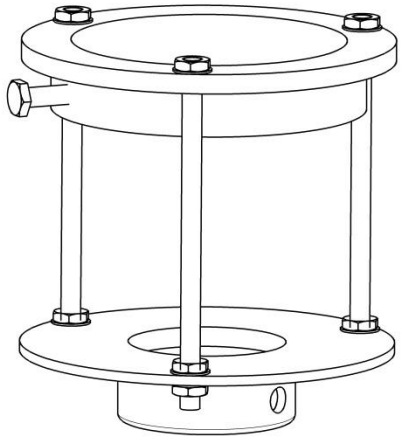

DESIGNED BY: Alborz shokrani	Cryogenic Shower Cooling System Total Assembly		
DATE: 2012			
CHECKED BY:			
DATE:			
SIZE A3	Cryogenic Machining of Aerospace Grade Titanium Alloy		
SCALE	WEIGHT (kg)	DRAWING NUMBER 200	SHEET 7/7

I	_
H	_
G	_
F	_
E	_
D	_
C	_
B	_
A	_

A8

Appendix B

Detailed graphs of power consumption

B.1. Introduction

In this appendix, the graphs of power consumption measured during comparative studies outlined in chapter 7 are presented and discussed.

B.2. Discussion of the power measurements results

In section 6.3.3.3.3, it was found that there is a correlation between power consumption and tool wear. The experimental results in section 6.3.3.3.3 indicated that power consumption of the machine tool has increased noticeably by the growth of tool wear and the highest peak took place where the cutting tool failed catastrophically.

However, studying the total power consumption graphs of machine tool during four machining passes indicated that although power consumption changes whilst machining length increases, it is not always ascending. For instance, whilst the power consumption in experiments D2,W2,C2, D5, C5, D7, W8, D9, W9 and C9 increases by the number of machining passes, it reduces for experiments D1, W1, C1, W5, D6, W6, C6, W7 and C7. Moreover, no significant change was observed in power consumption of machining passes in experiments D3, W3, C3, D4, W4, C4, D8 and C8. Comparing these with the results of tool wear presented in table 7.18 shows that there is no significant correlation between total power consumption of the machine tool and tool wear. For instance whilst the tool wear for experiments D8 and C8 were 135.2 μm and 86.4 μm respectively, no significant change in the power consumption was detected. On the other hand, whilst the tool wear for experiments W7 and C7 were respectively 63.4 μm and 10.4 μm, the power consumption descended from the first machining pass to the last.

Possible explanations for these phenomena are:

- Total power consumption of machine tool and the fluctuations in power supply is significantly more than the effect of tool wear on power consumptions to be detected by the current power monitoring system.
- The changes in the cutting tool geometry as a result of tool wear is in favour of the cutting operation and thus it has resulted in no change or a reduction in the power consumption.
- The cutting temperature affects the material strength and hardness of the workpiece which has resulted in an unexpected change in the power consumption of the machine tool during machining passes.

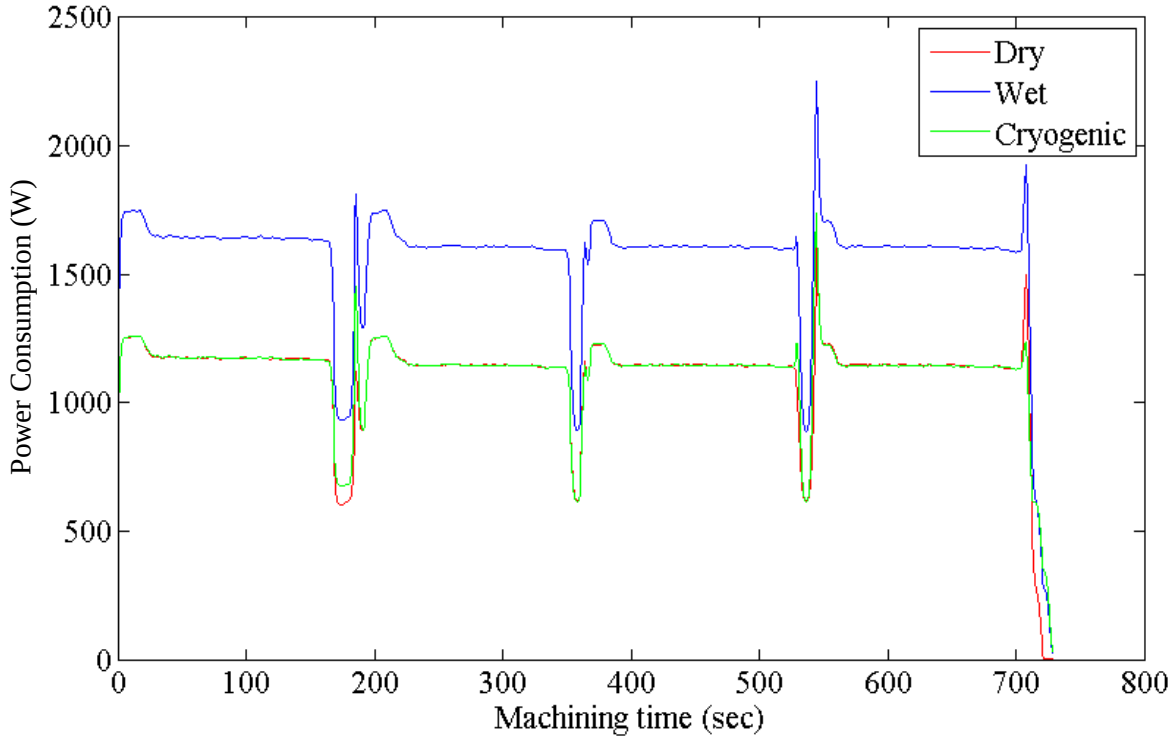

Figure B.1 Power consumption of machine tool during experiments D1, W1 and C1

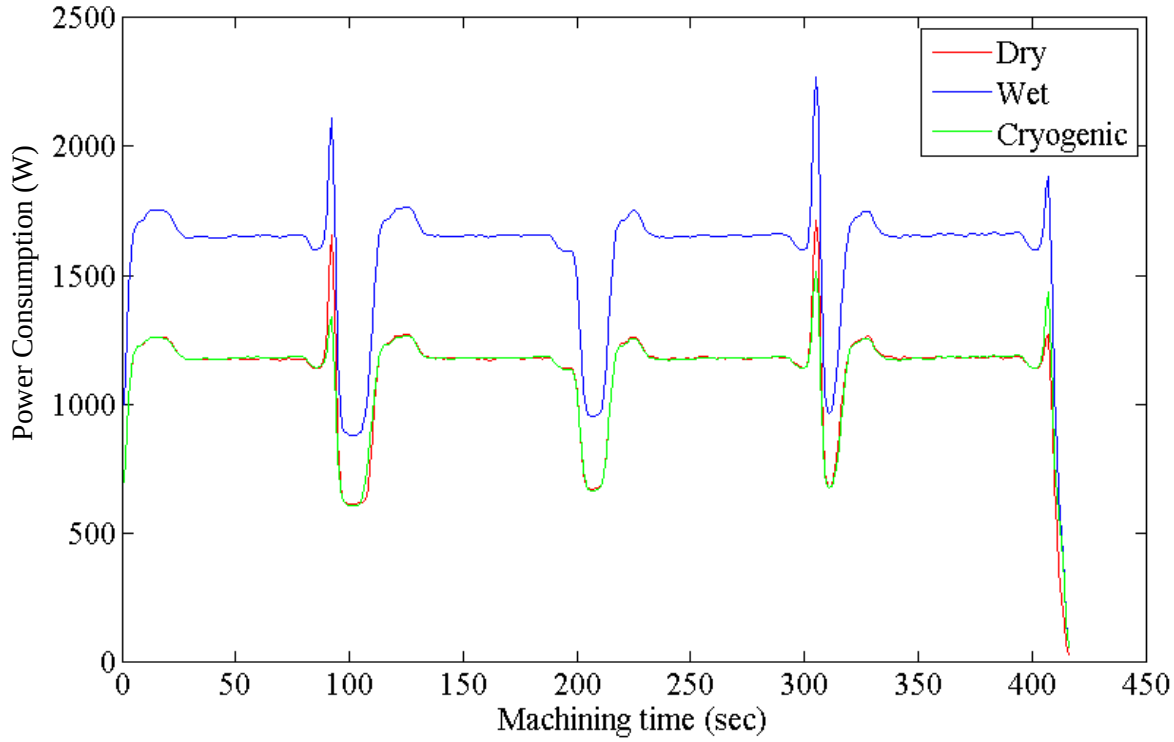

Figure B.2 Power consumption of machine tool during experiments D2, W2 and C2

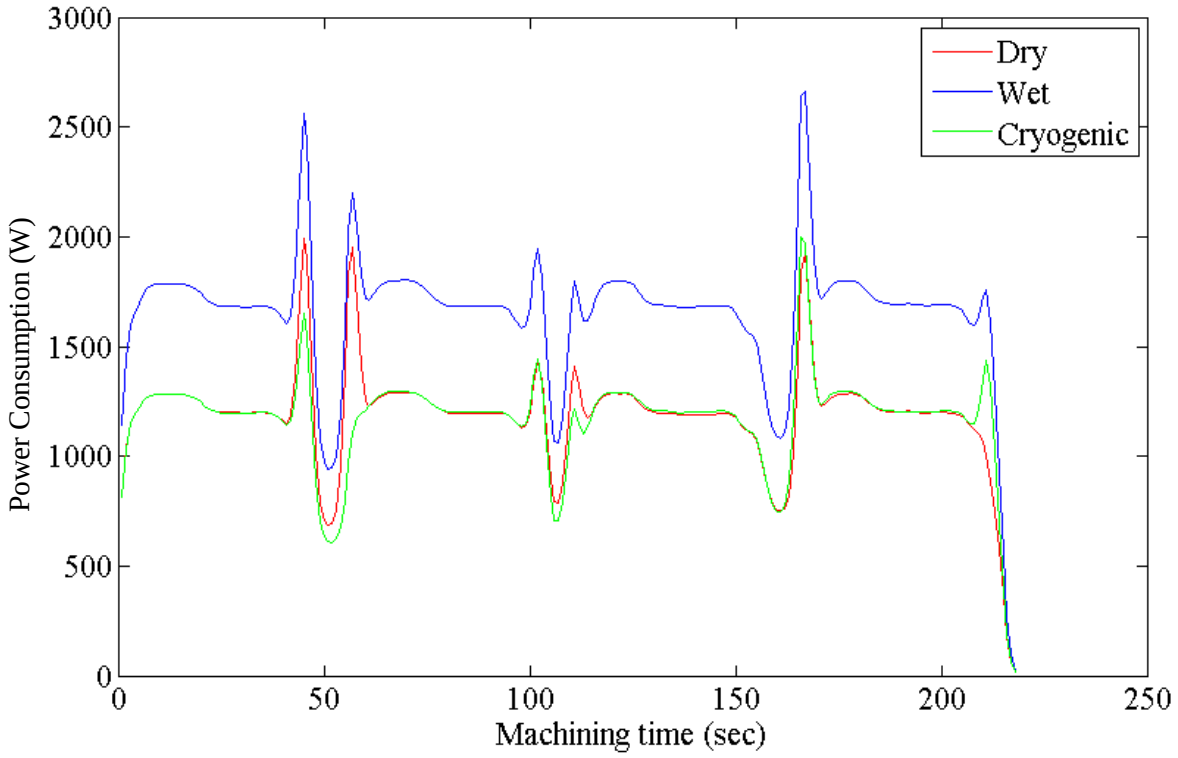

Figure B.3 Power consumption of machine tool during experiments D3, W3 and C3

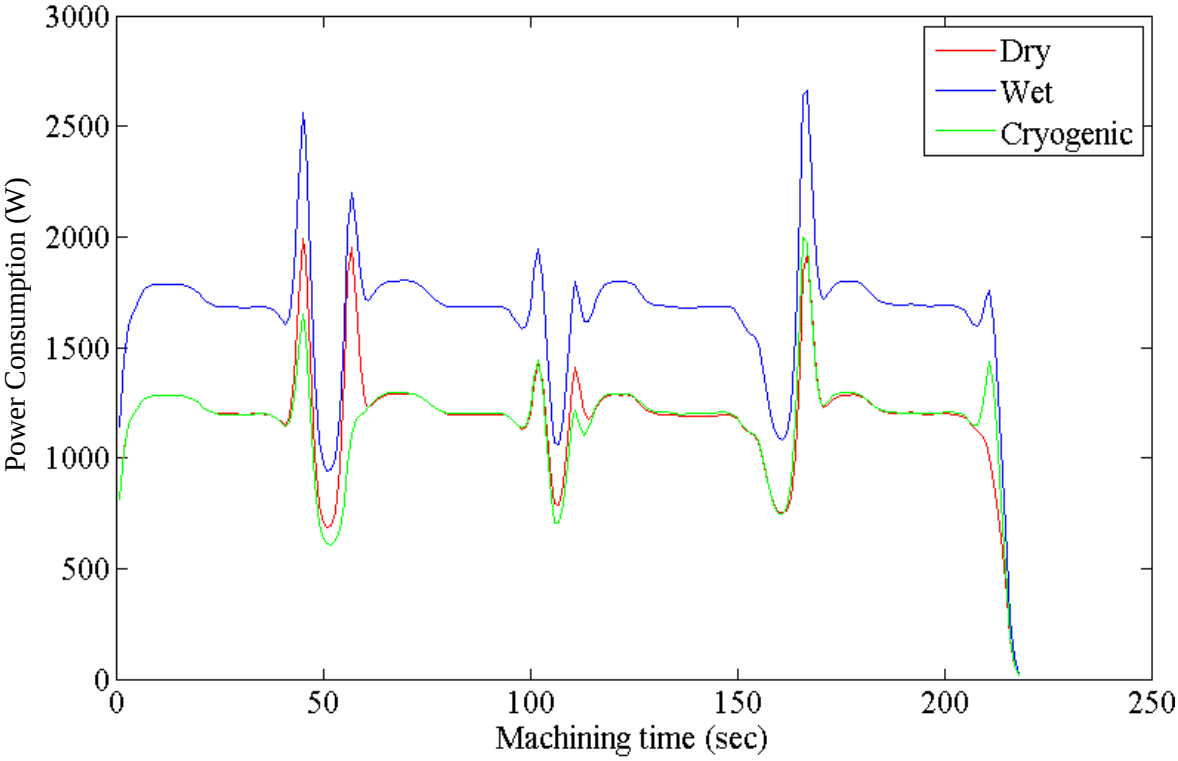

Figure B.4 Power consumption of machine tool during experiments D4, W4 and C4

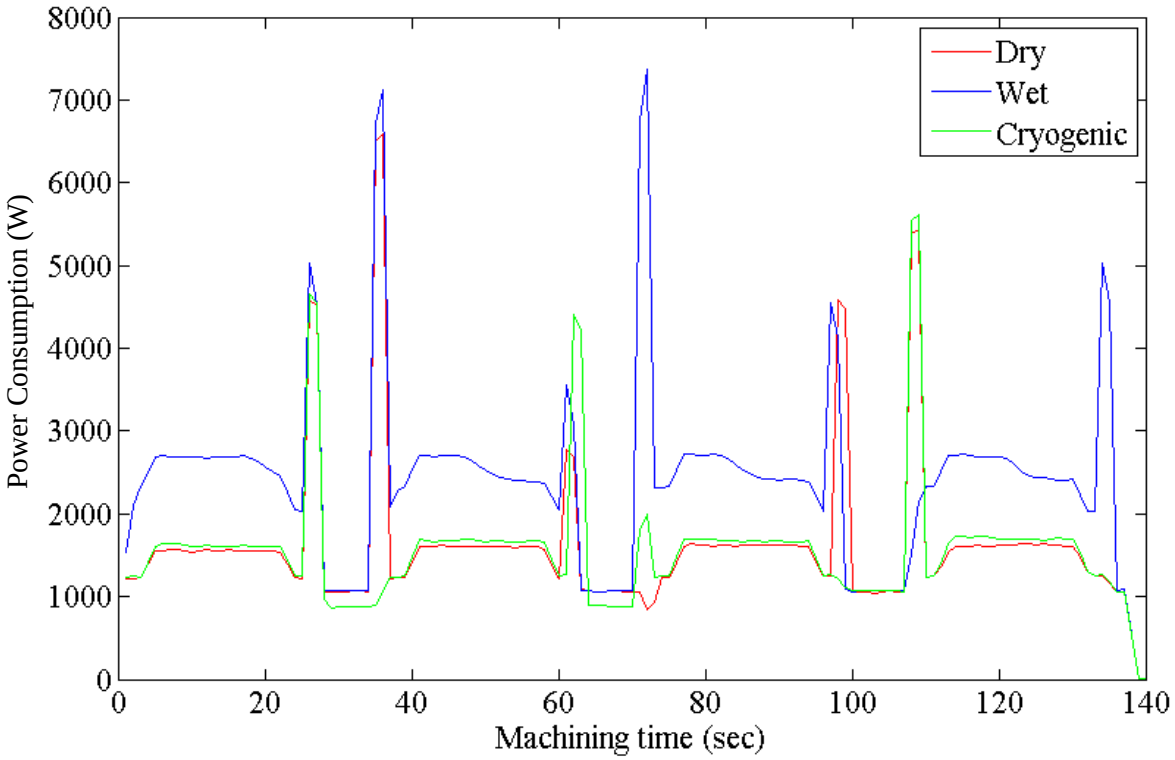

Figure B.5 Power consumption of machine tool during experiments D5, W5 and C5

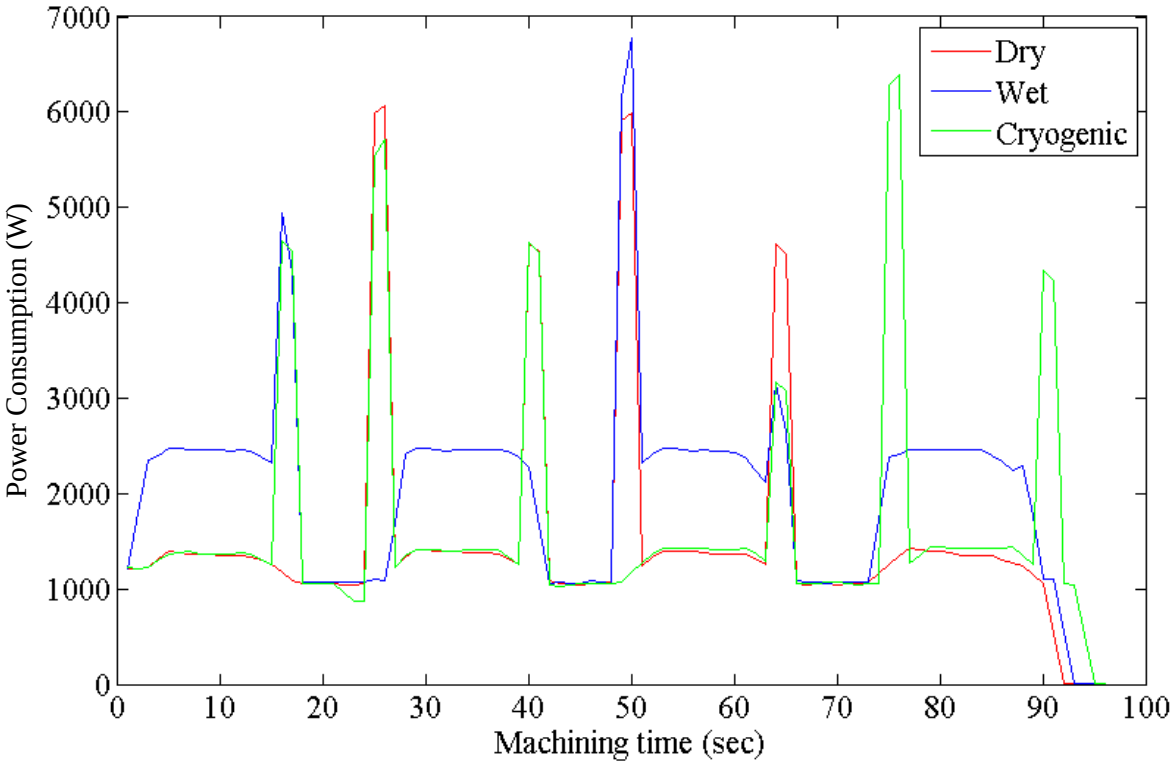

Figure B.6 Power consumption of machine tool during experiments D6, W6 and C6

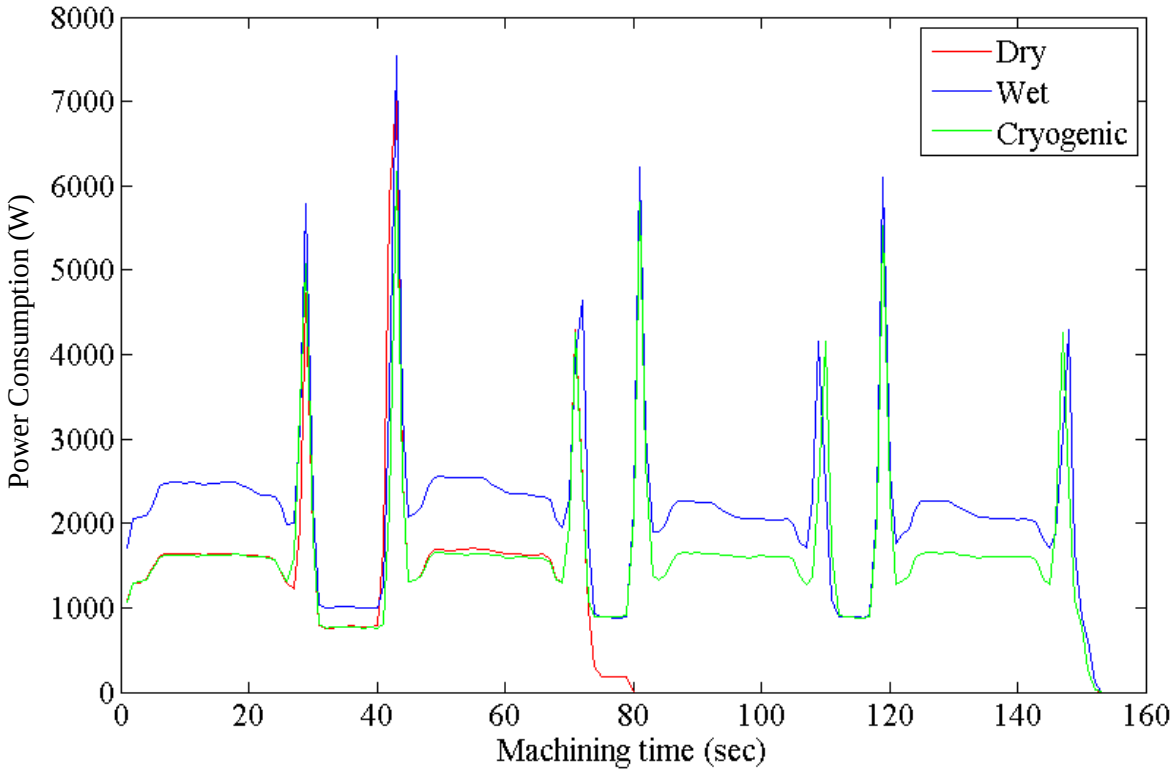

Figure B.7 Power consumption of machine tool during experiments D7, W7 and C7

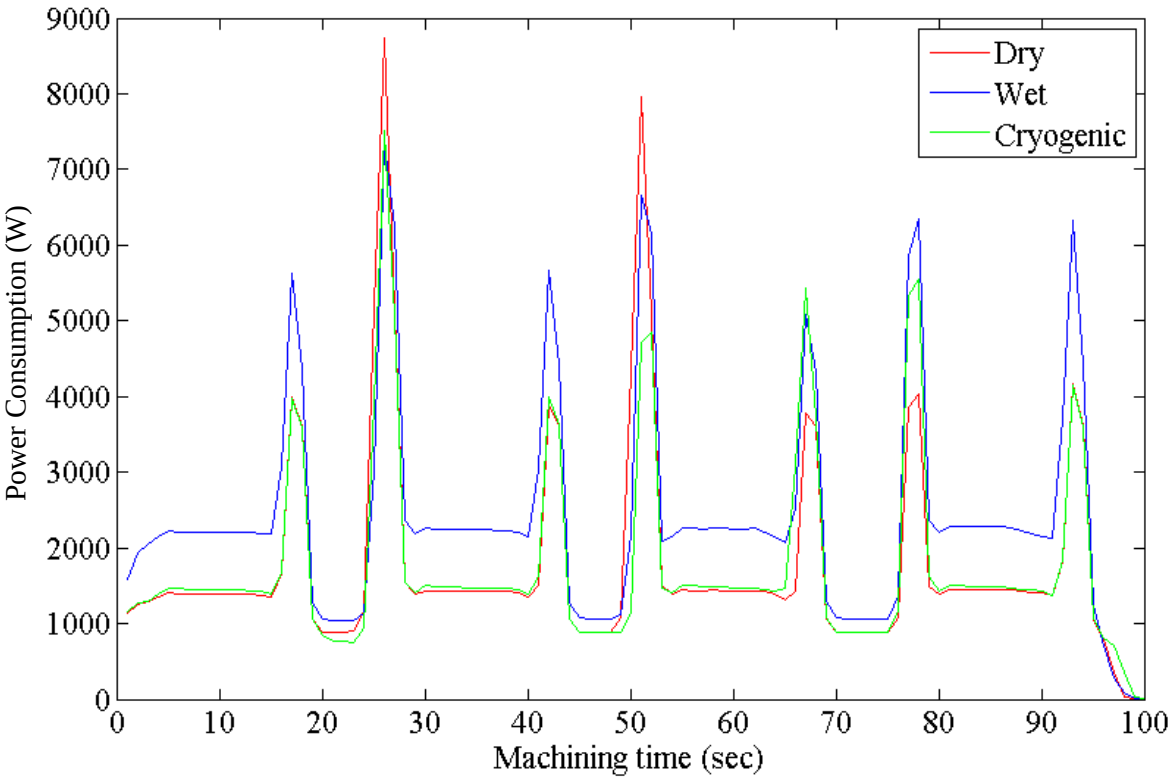

Figure B.8 Power consumption of machine tool during experiments D8, W8 and C8

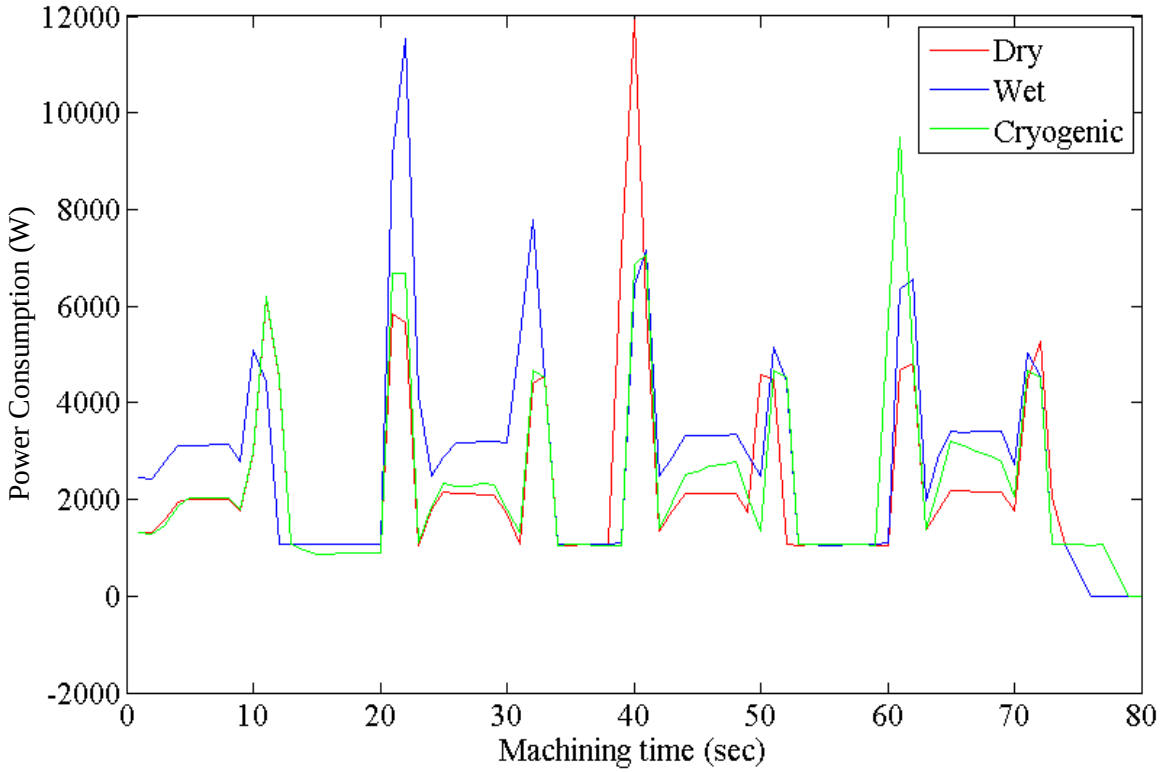

Figure B.9 Power consumption of machine tool during experiments D9, W9 and C9

Appendix C

Detailed graphs of surface roughness

C.1. Introduction

In this appendix the graphs of surface roughness for each machining pass of the experiment from comparative study are illustrated and discussed.

C.2. Discussion

It is generally accepted that tool wear has an adverse effect on the surface roughness and worn tools produce higher surface roughness. The study of surface roughness for each machining pass of the comparative machining experiments showed that in general the surface roughness increases by increased machining pass. However, in some cases such as experiments W3 and D4, lower surface roughness was measured for higher machining passes. As illustrated in following figure, this phenomenon was more dominant in dry machining as compared to wet and cryogenic machining environments.

Possible explanation for this occurrence is that worn tools tend to produce more smeared surfaces than tools with sharp cutting edges. As supported by topographical study of the machined surfaces outlined in chapter 7, plastic deformation of the machined surface can fill the valleys of tool marks which results in lower measurements for surface roughness. In particular, in dry machining, the cutting temperature softens the workpiece material which facilitates plastic deformation and smearing.

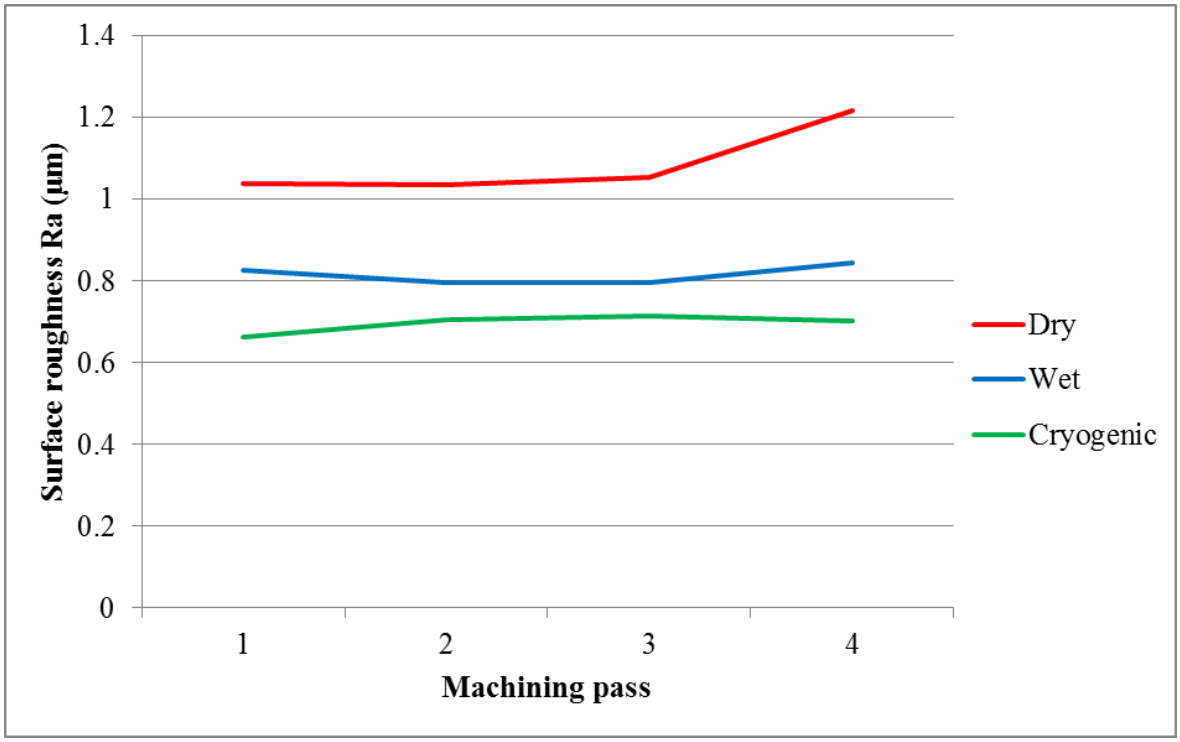

Figure C.1 Average surface roughness of each machining pass for experiments D1, W1 and C1

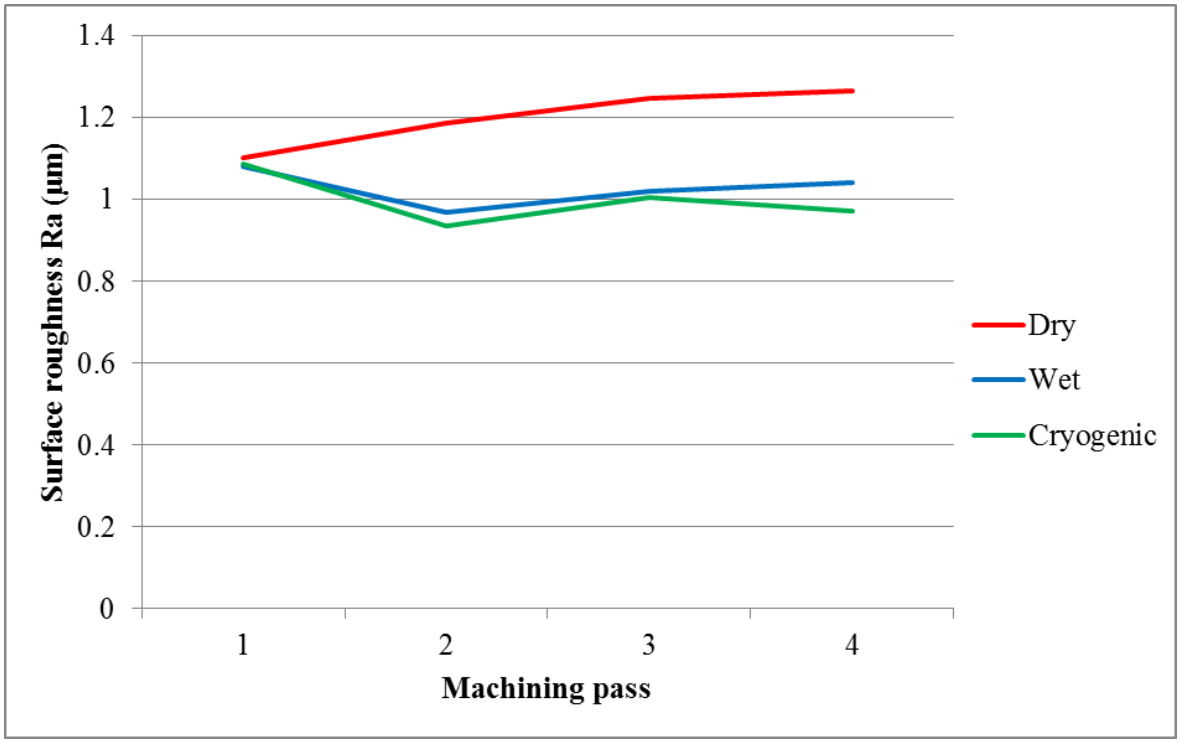

Figure C.2 Average surface roughness of each machining pass for experiments D2, W2 and C2

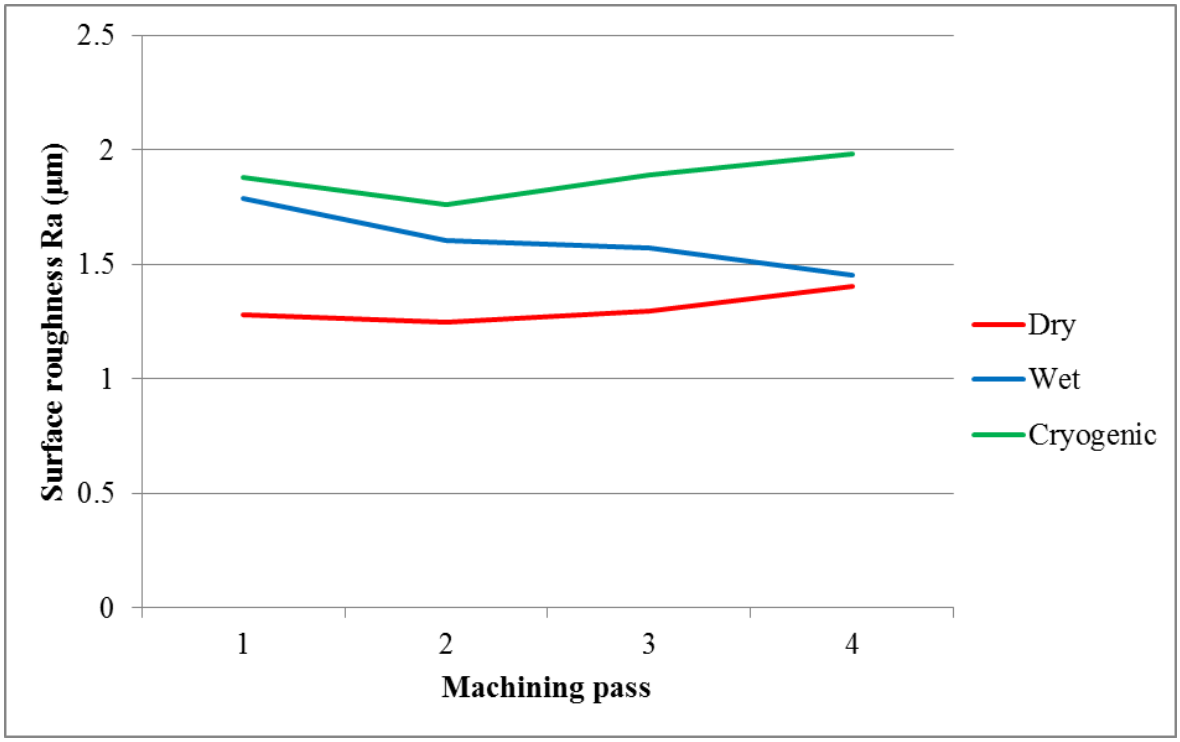

Figure C.3 Average surface roughness of each machining pass for experiments D3, W3 and C3

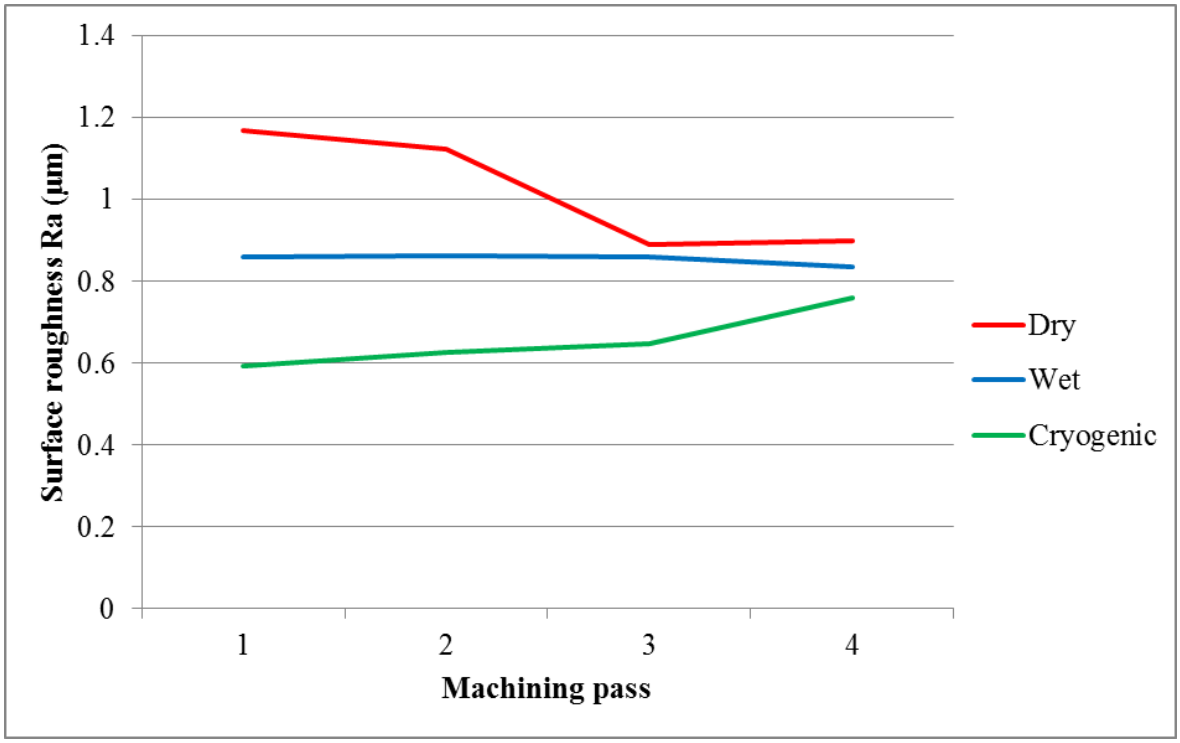

Figure C.4 Average surface roughness of each machining pass for experiments D4, W4 and C4

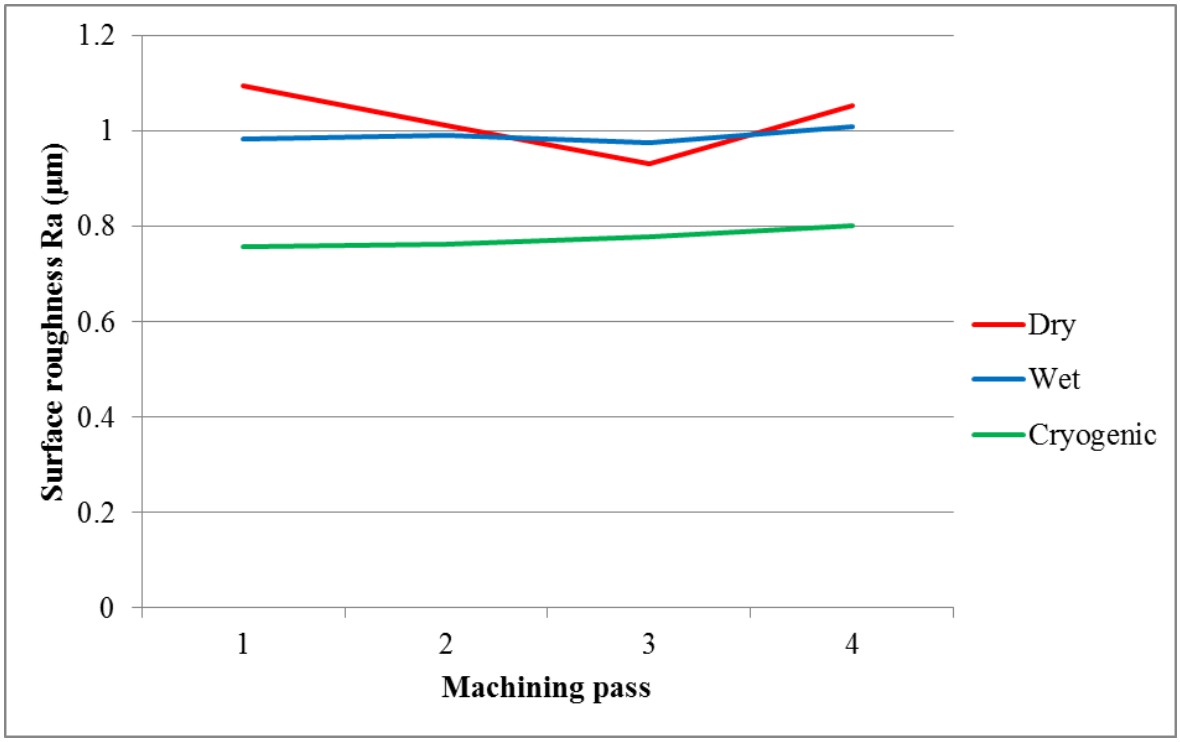

Figure C.5 Average surface roughness of each machining pass for experiments D5, W5 and C5

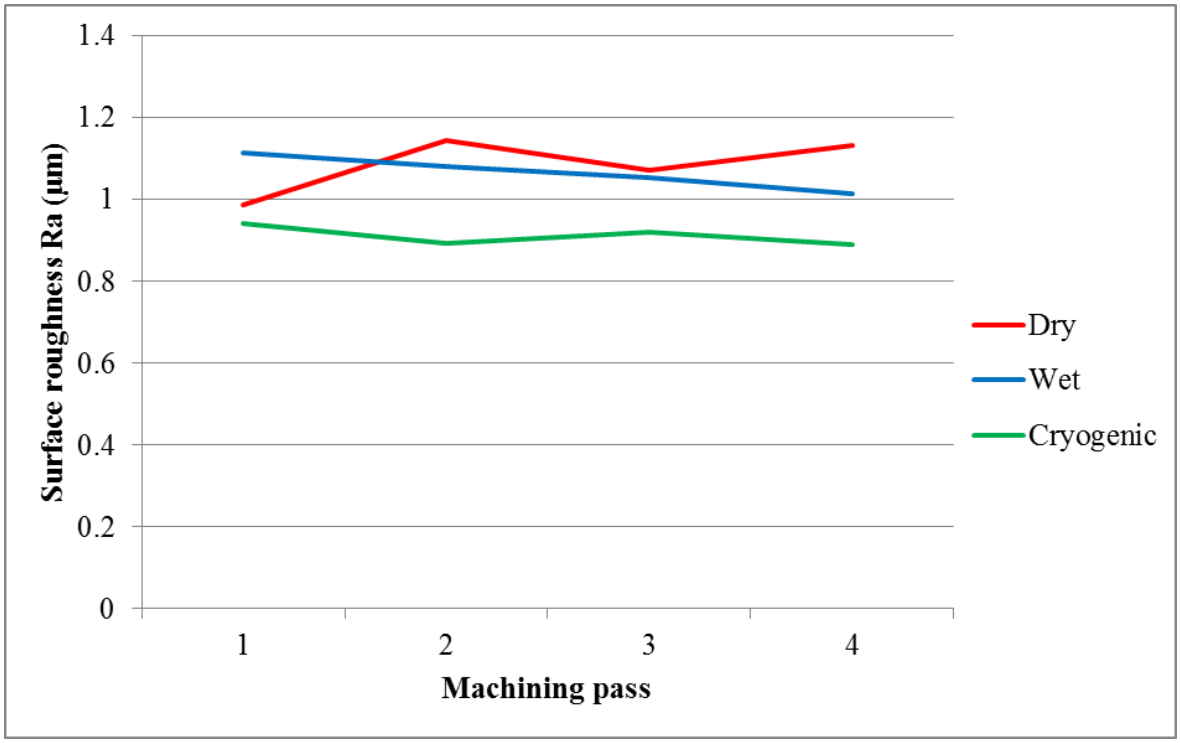

Figure C.6 Average surface roughness of each machining pass for experiments D6, W6 and C6

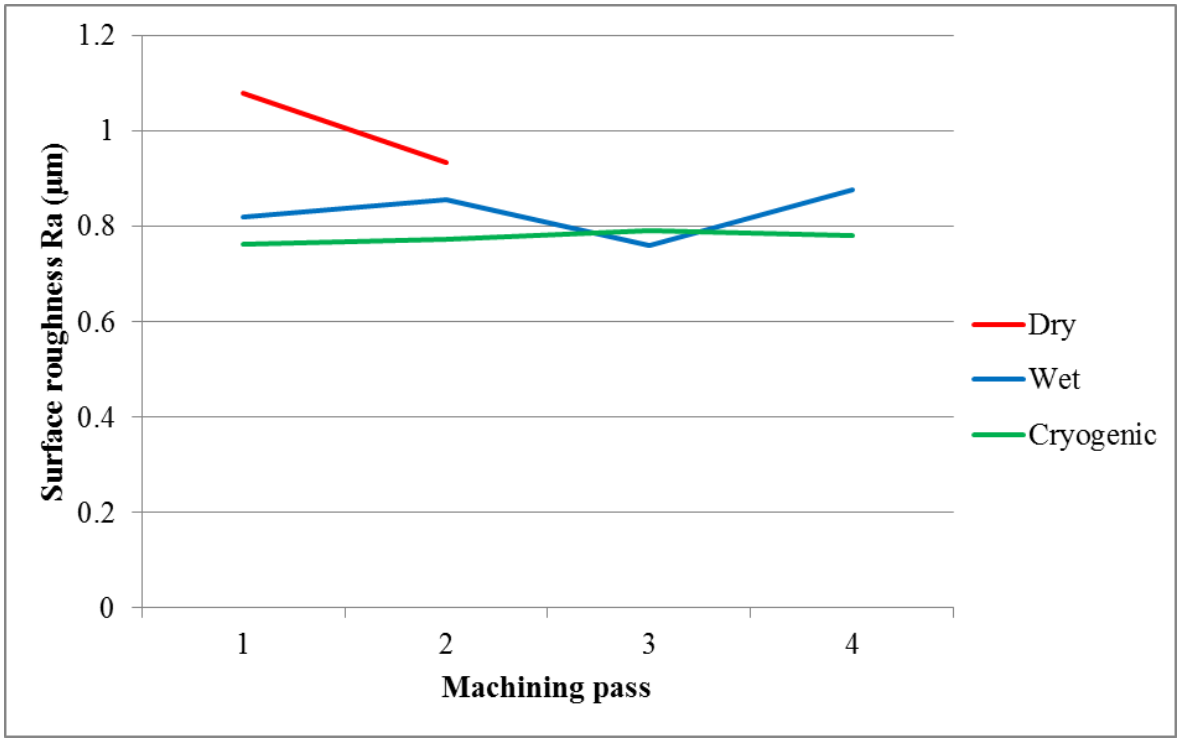

Figure C.7 Average surface roughness of each machining pass for experiments D7, W7 and C7

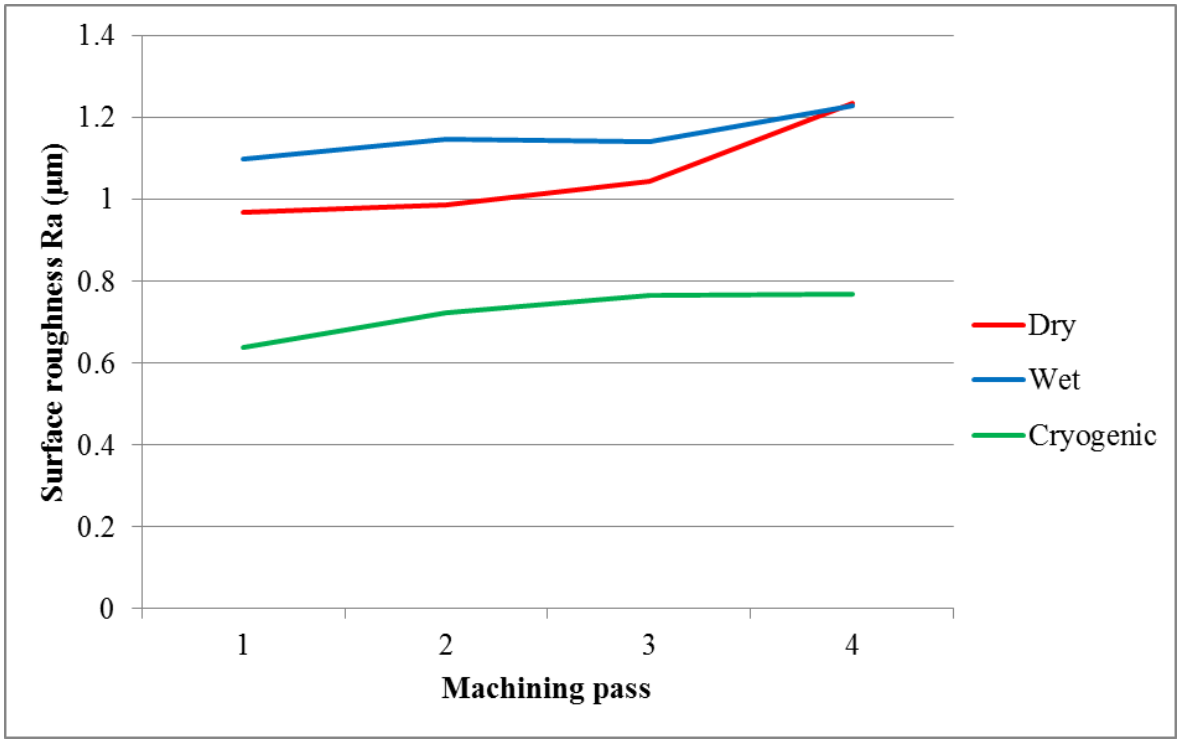

Figure C.8 Average surface roughness of each machining pass for experiments D8, W8 and C8

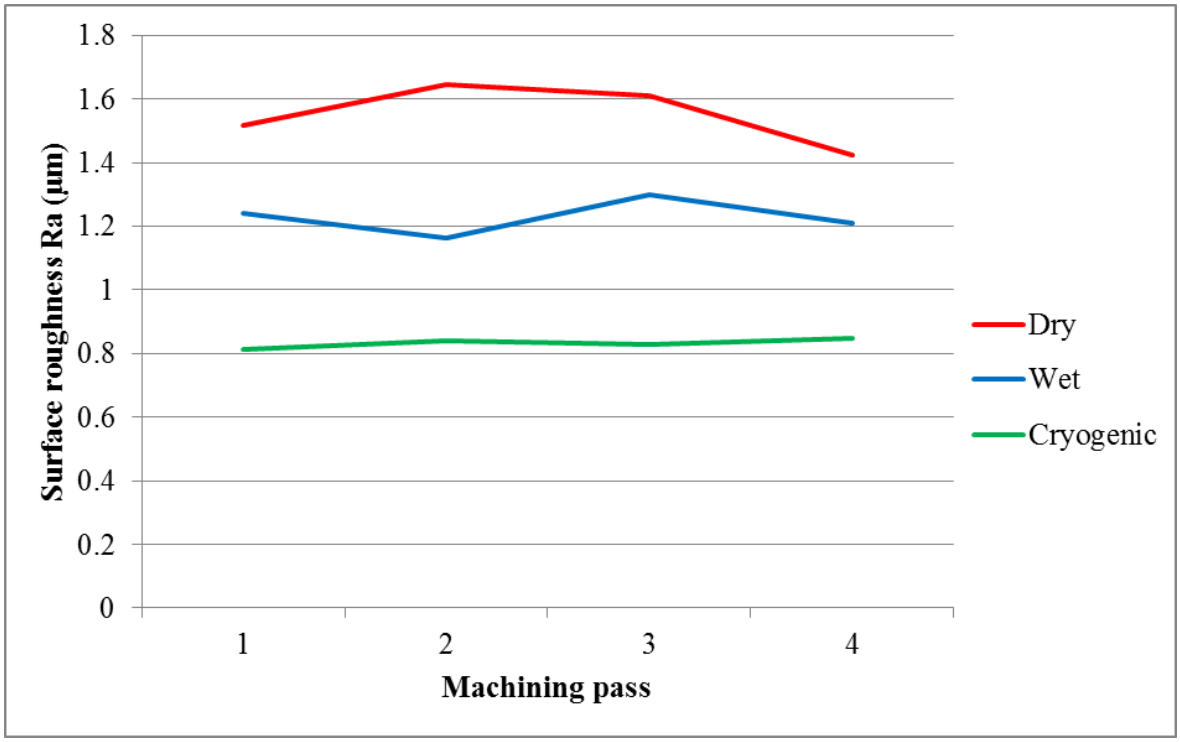

Figure C.9 Average surface roughness of each machining pass for experiments D9, W9 and C9